INFORMATION TO USERS

This manuscript has been reproduced from the microfilm master. UMI films the text directly from the original or copy submitted. Thus, some thesis and dissertation copies are in typewriter face, while others may be from any type of computer printer.

The quality of this reproduction is dependent upon the quality of the copy submitted. Broken or indistinct print, colored or poor quality illustrations and photographs, print bleedthrough, substandard margins, and improper alignment can adversely affect reproduction.

In the unlikely event that the author did not send UMI a complete manuscript and there are missing pages, these will be noted. Also, if unauthorized copyright material had to be removed, a note will indicate the deletion.

Oversize materials (e.g., maps, drawings, charts) are reproduced by sectioning the original, beginning at the upper left-hand corner and continuing from left to right in equal sections with small overlaps.

Photographs included in the original manuscript have been reproduced xerographically in this copy. Higher quality 6" x 9" black and white photographic prints are available for any photographs or illustrations appearing in this copy for an additional charge. Contact UMI directly to order.

Bell & Howell Information and Learning
300 North Zeeb Road, Ann Arbor, MI 48106-1346 USA
800-521-0600

NOTE TO USERS

This reproduction is the best copy available.

UMI

FUNCTIONAL AND BIOCHEMICAL CHARACTERIZATION OF CENTRAL ATP-GATED P_{2X} CHANNELS

KHANH-TUOC LÊ

DEPARTMENT OF NEUROLOGY AND NEUROSURGERY
MONTREAL NEUROLOGICAL INSTITUTE

MCGILL UNIVERSITY
MONTREAL, QUEBEC, CANADA

AUGUST 20th, 1999

THESIS SUBMITTED TO
THE FACULTY OF GRADUATE STUDIES AND RESEARCH
IN PARTIAL FULFILLMENT OF THE REQUIREMENTS
FOR THE DEGREE OF

DOCTOR OF PHILOSOPHY

©KHANH-TUOC LÊ, 1999

National Library of Canada
Acquisitions and Bibliographic Services
395 Wellington Street
Ottawa ON K1A 0N4
Canada

Bibliothèque nationale du Canada
Acquisitions et services bibliographiques
395, rue Wellington
Ottawa ON K1A 0N4
Canada

Your file Votre référence

Our file Notre référence

The author has granted a non-exclusive licence allowing the National Library of Canada to reproduce, loan, distribute or sell copies of this thesis in microform, paper or electronic formats.

The author retains ownership of the copyright in this thesis. Neither the thesis nor substantial extracts from it may be printed or otherwise reproduced without the author's permission.

L'auteur a accordé une licence non exclusive permettant à la Bibliothèque nationale du Canada de reproduire, prêter, distribuer ou vendre des copies de cette thèse sous la forme de microfiche/film, de reproduction sur papier ou sur format électronique.

L'auteur conserve la propriété du droit d'auteur qui protège cette thèse. Ni la thèse ni des extraits substantiels de celle-ci ne doivent être imprimés ou autrement reproduits sans son autorisation.

0-612-55353-1

Canada

ABSTRACT

Fast purinergic neurotransmission has recently been shown to be mediated through ionotropic P_{2X} receptors activated by extracellular adenosine 5'-triphosphate (ATP). ATP-sensitive P_{2X} proteins constitute a novel third gene superfamily of ligand-gated ion channels based upon unique structural motifs. Although mammalian ATP-gated recombinant P_{2X} proteins have been characterized extensively using various experimental methodologies such as functional studies in heterologous expression systems, yet, P_{2X} protein mapping within central nervous system (CNS), P_{2X} channel subunit composition pertaining to relevant native receptor phenotypes, and species-specific differences between mammalian P_{2X} orthologs remain to be investigated.

The **first manuscript** (Lê *et al.*, 1998a) reported the regional, cellular, and subcellular localization of $P2X_4$ gene product within adult rat brain and spinal cord structures. $P2X_4$ receptors were shown to be widely expressed on the postsynaptic side throughout the CNS. Further, this P_{2X} subunit was also observed in the present study to be expressed selectively on the presynaptic side within various central sensory pathways such as the olfactory bulb and the substantia gelatinosa within the dorsal horn of the spinal cord. Thus, these results were corroborated to ATP-elicited ionotropic P_{2X} responses involved in widespread central postsynaptic as well as presynaptic signaling.

The **second manuscript** (Lê *et al.*, 1998b) documented a novel P_{2X} receptor phenotype resulting from the heteropolymerization between major central $P2X_4$ and $P2X_6$ subunits. $P2X_{4+6}$ heteromultimeric channel phenotypes were characterized by distinct time-dependent protein expression levels and novel pharmacological profiles compared to $P2X_4$ homo-oligomers, while $P2X_6$ expressed alone from *Xenopus laevis* oocytes did not respond to ATP applications. Moreover, subunit-specific interaction between $P2X_4$ and

$P2X_6$ isoforms were directly demonstrated through chromatography-based co-purification assays thereby further strengthening observed *in vitro* $P2X_{4+6}$ pharmacological phenotypes.

The **third manuscript** (Lê *et al.*, 1999) was undertaken based upon similar reasoning as well as experimental strategies as the $P2X_{4+6}$ study (Lê *et al.*, 1998b). Namely, the existence of heteromultimeric $P2X_{1+5}$ receptors were screened with functional as well as biochemical assays demonstrating that this oligomeric complex gave rise to hybrid properties between homopolymeric $P2X_1$ and $P2X_5$ subunits. More specifically, $P2X_{1+5}$ channels displayed a $P2X_1$-subtype pharmacology by being highly sensitive to αβmATP applications. On the other hand, $P2X_{1+5}$ complexes gave rise to non-desensitizing channel kinetics, similar to homo-oligomeric $P2X_5$ subunits, in response to low micromolar ranges of αβmATP applications. Reciprocal co-purifications between interacting $P2X_1$ and $P2X_5$ subunits were also demonstrated in this study.

The **fourth manuscript** (Lê *et al.*, 1997) reported the molecular cloning of the human ortholog ($hP2X_{5R}$) of $rP2X_5$ subunit, which is being the most rare transcript among all reported rat P_{2X} cDNAs to date. $hP2X_{5R}$ subunit was found to be a 422 amino acid-long protein and having 62% homology to $rP2X_5$ receptors. Although most ATP-gated P_{2X} channel structural motifs were found in the $hP2X_{5R}$ primary sequence, yet, this protein was determined to have only one transmembrane domain. As opposed to $rP2X_5$ restricted spinal cord distribution patterns, $hP2X_{5R}$ mRNAs were found to be transcribed within various brain loci in addition to the immune system. $hP2X_{5R}$ was shown to display two splicing variants, but lacked a conserved domain in the pre-M2 region. Finally, $hP2X_{5R}$-injected *Xenopus laevis* oocytes did not respond to ATP applications.

These four manuscripts were selected, among other projects, to constitute the core of the present Ph.D. Thesis. Taken altogether, these studies used a multidisciplinary approach, namely, combinations of molecular biology, cell culture and protein chemistry techniques, as well as electrophysiological recordings. In an effort to contribute to a better assessment of the physiological roles of fast purinergic synaptic signaling (Lê *et al.*, 1998a) mediated likely by native receptors generated by heteromultimerization (Lê *et al.*, 1998b; Lê *et al.*, 1999) while keeping in mind that species-dependent differences between mammalian P_{2X} orthologs (Lê *et al.*, 1997) should be taken into account whenever rodent systems would be used for drug screening studies.

RÉSUMÉ

Il a été démontré récemment que la neurotransmission purinergique rapide est médiée par les récepteurs P_{2X} ionotropiques activés par l'adénosine 5'-triphosphate (ATP) extracellulaire. Basés sur des motifs structuraux uniques, les récepteurs P_{2X} constituent une troisième grande famille génétique de canaux ioniques activés par un ligand extracellulaire. Malgré le fait que la caractérisation des récepteurs P_{2X} recombinants a été menée de façon extensive en utilisant divers systèmes d'expressions hétérologues, la distribution *in situ* des protéines P_{2X} dans le système nerveux centrale (SNC); la composition en sous-unités des récepteurs P_{2X} correspondant aux différents phénotypes natifs; et la différence entre les orthologues P_{2X} des divers espèces mammifères restent à déterminer.

Le **premier manuscrit** (Lê *et al.*, 1998a) a rapporté la distribution de la protéine $P2X_4$ au niveau régional, cellulaire, et sub-cellulaire dans divers structures du cerveau et colonne vertébrale. Nous avons démontré que la sous-unité $P2X_4$ est présente dans la plupart des régions du SNC du côté post-synaptique chez le rat adulte. Les récepteurs qui contiennent $P2X_4$ sont exprimés de façon sélective du côté pré-synaptique dans divers systèmes sensoriels centraux, notamment, dans le bulbe olfactif ainsi que la corne dorsale de la moëlle épinière. Ces résultats corroborrent, donc, les réponses ionotropiques de type P_{2X} observées à la fois du côté post- et pré-synaptiques dans diverses préparations natives.

Le **deuxième manuscrit** (Lê *et al.*, 1998b) a documenté un nouveau phénotype P_{2X} hétéromultimérique composé des deux sous-unités centrales $P2X_4$ et $P2X_6$. Nous avons caractérisé le phénotype hétéropolymérique $P2X_{4+6}$ par son profil temporel d'expression et par ses propriétés pharmacologiques distinctes par rapport aux récepteurs

homo-oligomériques $P2X_4$. La sous-unité $P2X_6$ exprimée seule dans les ovocytes de *Xenopus laevis* ne répond pas aux applications d'ATP. De plus, les interactions spécifiques entre $P2X_4$ et $P2X_6$ ont été confirmées directement en utilisant une procédure de co-purification par l'entremise des principes de la chromatographie d'affinité.

Nous avons réalisé le **troisième projet** (Lê *et al.*, 1999) en nous basant sur les mêmes raisonnements ainsi que sur les mêmes procédures expérimentales que celui du projet portant sur le phénotype hétéromultimérique du $P2X_{4+6}$ (Lê *et al.*, 1998b). En occurence, l'existence du phénotype hétéro-oligomérique $P2X_{1+5}$ a été déterminée fonctionnellement par l'émergence de propriétés hybrides ainsi que biochimiquement par l'association réciproque entre les sous-unités $P2X_1$ et $P2X_5$. Nous montrons que la pharmacologie du $P2X_{1+5}$ est conferrée par la présence de la sous-unité $P2X_1$, tandis que la cinétique du complexe hétéro-oligomérique provient de la contribution de la sous-unité $P2X_5$.

Dans le **quatrième manuscrit** (Lê *et al.*, 1997) nous avons rapporté le clonage moléculaire de la sous-unité $P2X_5$ humaine ($hP2X_{5R}$). Nous prédisons que la sous-unité $hP2X_{5R}$ est une protéine membranaire de 422 résidus qui a 60% d'homologie avec la séquence de la sous-unité $P2X_5$ de rat ($rP2X_5$). Malgré le fait que la structure primaire de $hP2X_{5R}$ possède la plupart des motifs structuraux typiques des sous-unités de type P_{2X}, la topologie de $hP2X_{5R}$ révèle seulement un domaine transmembranaire. Cette singularité explique pourquoi cette sous-unité n'est pas fonctionelle sous forme homomultimérique. A l'opposé de $rP2X_5$ qui présente une distribution restreinte aux neurones sensoriels et spinaux, $hP2X_{5R}$ est transcrit à haut niveau dans plusieurs régions du cerveau ainsi que dans le système immunitaire.

Dans son ensemble, ces quatre manuscrits ont pour objectifs de contribuer à l'avancement des connaissances sur les rôles physiologiques que peuvent avoir les récepteurs P_{2X} dans les phénomènes de la transmission synaptique. En utilisant une approche multidisciplinaire, en occurrence, la biologie moléculaire, la culture cellulaire et la chimie des protéines, ainsi que l'électrophysiologie nous avons fait l'effort de documenter la distribution protéique dans le SNC (Lê *et al.*, 1998a), la composition des sous-unités à l'intérieur des phénotypes hétéromultimériques (Lê *et al.*, 1998b; Lê *et al.*, 1999), et ainsi que les variabilités entre espèces au niveau de la structure primaire et de la fonction (Lê *et al.*, 1997).

MANUSCRIPT LISTINGS

FIRST-AUTHORSHIP MANUSCRIPTS

Khanh-Tuoc Lê, Vincent Archambault, and Philippe Séguéla. Tetrameric structure of functional ATP-gated P_{2X} channels. ***Manuscript in Preparation***.

Khanh-Tuoc Lê, Éric Boué-Grabot, Vincent Archambault, and Philippe Séguéla. (1999) Functional and biochemical evidence for heteromeric ATP-gated channels composed of $P2X_1$ and $P2X_5$ subunits. *Journal of Biological Chemistry* **274**: 15415-15419.

Khanh-Tuoc Lê, Kazimierz Babinski, and Philippe Séguéla. (1998) Central $P2X_4$ and $P2X_6$ channel subunits co-assemble into a novel heteromeric ATP receptor. *Journal of Neuroscience* **18**: 7152-7159.

Khanh-Tuoc Lê, Pierre Villeneuve, Antoine R. Ramjaun, Peter S. McPherson, Alain Beaudet, and Philippe Séguéla. (1998) Sensory presynaptic and widespread somato-dendritic immunolocalization of central ionotropic P_{2X} ATP receptors. *Neuroscience* **83**: 177-190.

Khanh-Tuoc Lê, Michel Paquet, Dominique Nouel, Kazimierz Babinski, and Philippe Séguéla. (1997) Primary structure and expression of a naturally truncated human P_{2X} ATP receptor subunit from brain and immune system. *FEBS Letters* **418**: 195-199.

Khanh-Tuoc Lê, Hélène Maurice, and Patrick du Souich. (1996) First-pass metabolism of lidocaine in the anesthetized rabbit — Contribution of the small intestine. *Drug Metabolism and Disposition* **24**: 711-716.

SECOND-AUTHORSHIP MANUSCRIPT

Kazimierz Babinski, **Khanh-Tuoc Lê**, and Philippe Séguéla. (1999) Molecular cloning and regional distribution of a human proton sensor subunit with biphasic functional properties. *Journal of Neurochemistry* **72**: 51-57.

ABSTRACT LISTINGS

FIRST-AUTHORSHIP ABSTRACTS

Khanh-Tuoc Lê, Kazimierz Babinski, and Philippe Séguéla. (1998) Pharmacological and biochemical evidence for heteromeric ATP receptors containing central $P2X_4$ and $P2X_6$ subunits. *Society for Neuroscience Abstracts* **24**: 371.

Khanh-Tuoc Lê, Michel Paquet, Kazimierz Babinski, and Philippe Séguéla. (1997) Cloning and expression of a naturally truncated human P_{2X} receptor subunit from brain and immune system. *Society for Neuroscience Abstracts* **23**: 377.

Khanh-Tuoc Lê, Pierre Villeneuve, Antoine R. Ramjaun, Jishnu Mukerji, Peter S. McPherson, Alain Beaudet, and Philippe Séguéla. (1996) Cellular distribution of $P2X_4$ ATP-gated channels in rat brain and spinal cord. *Society for Neuroscience Abstracts* **22**: 335.

SECOND-AUTHORSHIP ABSTRACT

Kazimierz Babinski, **Khanh-Tuoc Lê**, Leonard Wolfe, and Philippe Séguéla. (1998) Functional properties and distribution of a human proton-gated channel with biphasic kinetics. *Society for Neuroscience Abstracts* **24**: 333.

ACKNOWLEDGMENTS

I am deeply indebted to my father, Mr. Thanh V. Lê; my mother, Mrs. Chi H. Phan; my only sister, Mrs. Dung C. Lê and her husband, Dr. Thang D. Vuong; and my two brothers, Mr. Mân K. Lê and Dr. Khánh N. Lê for having shared with me throughout my graduate school years including not so good as well as exhilarating times associated with tedious research training endeavors. Again, many heartfelt thanks to my family, especially to my mother for her moral support and without whom it would have been difficult to live this experience all by myself. Everything that I am today, I owe it to my loving mother.

I would like to take this opportunity to express my gratitude to my mentor, Dr. Philippe A. Séguéla. More specifically, my three-year stay in his laboratory was both exciting and rewarding in terms of scientific pursuits as well as interpersonal interactions. Stated otherwise, under the supervision of Dr. Séguéla, I have learned how to do good science, yet, still remain first and foremost a decent human being as well as a family man. Thank you, Philippe.

I would also like to thank my advisory committee members, Dr. Peter S. McPherson and Dr. Wayne S. Sossin, for their availability and helpful discussions throughout my training years. Thank you, Peter, for your scientific lessons and inspirations during our many daily cigarette sessions.

Although I have had many collaborators during my stay in Dr. Séguéla's laboratory, yet, I would like to express special thanks to Dr. Éric Boué-Grabot (current Post-Doctoral Fellow in Dr. Séguéla's laboratory), Mr. Pierre Villeneuve (former M.Sc. Candidate in Dr. Alain Beaudet's laboratory), and Mr. Vincent Archambault (former

summer student in Dr. Séguéla's laboratory). To a friend and colleague, Mr. Antoine R. Ramjaun (current Ph.D. Candidate in Dr. McPherson's laboratory), it was so inspiring to watch you work, Dude. To Mr. Ahmed Elhusseiny (current Ph.D. Candidate in Dr. Édith Hamel's laboratory), a simple thank you for your friendship.

My Ph.D. Candidacy, '95-'98, was supported in part by consecutive Ph.D. Studentships from the SAVOY Foundation for Epilepsy (Stipend only) as well as Dr. Séguéla's operating grants from the Medical Research Council (MRC) of Canada (Stipend and Tuition Fees).

Last but not least, I would like to thank my wife-to-be, Dr. Vy T. Hoang, especially for her unconditional love and support as well as generous understanding, especially, during the first few months during my Post-Doctoral Fellowships far from home (Cellular and Molecular Physiology, Yale University School of Medicine, New Haven, CT, USA).

THESIS FOREWORD

The present Thesis was structured to conform to the manuscript-based option permitted by McGill University. Thus, in accordance with the "Guidelines Concerning Thesis Preparation" of the Faculty of Graduate Studies and Research, the following excerpt was reproduced hereafter.

Candidates have the option of including, as part of the Thesis, the text of one or more papers submitted or to be submitted for publication, or the clearly-duplicated text of one or more published papers. These texts must be bound as an integral part of the Thesis.

If this option is chosen, **connecting texts that provide logical bridges between the different papers are mandatory**. The Thesis must be written in such a way that it is more than a mere collection of manuscripts; in other words, results of a series of papers must be integrated.

The Thesis must still conform to all other requirements of the "Guidelines for Thesis Preparation". **The Thesis must include** — A table of Contents, an Abstract both in English and French, an Introduction which clearly states the rationale and objectives of the study, a review of the literature, a final Conclusion and Summary, and a thorough bibliography or Reference list.

Additional material must be provided where appropriate (e.g., in appendices) and in sufficient detail to allow a clear and precise judgement to be made of the importance and originality of the research reported in the Thesis.

In the case of manuscripts co-authored by the Candidate and others, **the Candidate is**

required to make an explicit statement in the Thesis as to whom contributed to such work and to what extent. Supervisors must attest to the accuracy of such statements at the Doctoral Oral Defence. Since the task of Examiners is made more difficult in these cases, it is in the Candidate's interest to make perfectly clear responsibilities of all authors of co-authored papers.

ORIGINALITY & CO-AUTHORSHIP CONTRIBUTION CLAIMS

Results presented in the present Thesis constitute original contributions to the knowledge pertaining to potential roles of ATP-gated P_{2X} channels mediating synaptic transmission phenomena within the central nervous system. Data presented in this Thesis have been published in four papers, all of which I have signed either as first author or shared first co-authorship contributions. Part of these works have also been presented in poster format at the Society for Neuroscience Meetings in 1996, 1997, and 1998.

Chapter 3 The *first manuscript* entitled **Sensory Presynaptic and Widespread Somatodendritic Immunolocalization of Central Ionotropic P_{2X} ATP Receptors** has been published in *Neuroscience* (**83**: 177-190, 1998). This study was undertaken in collaboration with the laboratories of Dr. Alain Beaudet and Dr. Peter S. McPherson at the Montreal Neurological Institute. I have directly participated in the early stages of antigen production and immunization; I have prepared and affinity-purified the rabbit polyclonal anti-$P2X_4$ antibodies as well as validated specificities of these antibodies toward $P2X_4$ receptors transiently transfected in Human Embryonic Kidney cell lines (HEK-293A) by using *in situ* immunofluorescence and Western blotting techniques. Mr. Pierre Villeneuve (Second Author), from Dr. Beaudet's laboratory, have performed most of the immunocytochemistry aspects of this study by using anti-$P2X_4$ antibodies prepared by myself. Mr. Antoine R. Ramjaun (Third Author), from Dr. McPherson's laboratory, have contributed to the regional distribution of $P2X_4$ subunits within selected structures of the brain using Western blots.

Chapter 4 The *second manuscript* entitled **Central $P2X_4$ and $P2X_6$ Channel Subunits Co-Assemble into a Novel Heteromeric ATP Receptors** has been published in *Journal of Neuroscience* (**18**: 7152-7159, 1998). This study was

undertaken based upon my own initiatives. More specifically, I have proposed to Dr. Séguéla this interaction between $P2X_4$ and $P2X_6$ subunits as well as carried out every experiments presented in this paper. Further, Dr. Séguéla has taught me for the first time how to write a scientific paper during the preparation of this manuscript. Mr. Kazimierz Babinski (Second Author), from Dr. Séguéla's laboratory, has participated during the final stages of editing and revising the written text prior to submission.

Chapter 5 The *third manuscript* entitled **Functional and Biochemical Evidence for Heteromeric ATP-Gated Channels Composed of $P2X_1$ and $P2X_5$ Subunits** has been published in *Journal of Biological Chemistry* (**274**: 15415-15419, 1999). The electrophysiological experiments in this article were performed at equal contributions between myself and Dr. Éric Boué-Grabot (Co-First Author, Second Name), from Dr. Séguéla's laboratory. Further, I have shown and coached Mr. Vincent Archambault (Second Author, Third Name), from Dr. Séguéla's laboratory, for all biochemical aspects of this project. And finally, I have participated, in conjunction with Dr. Séguéla, to the writing stages of this paper.

Chapter 6 The *fourth manuscript* entitled **Primary Structure and Expression of a Naturally Truncated Human P_{2X} ATP Receptor Subunit from Brain and Immune System** has been published in *FEBS Letters* (**418**: 195-199, 1997). This study was undertaken with equal contributions between myself and Mr. Michel Paquet (First Co-Author, Second Name, Former Laboratory Technician), from Dr. Séguéla's laboratory, pertaining to both functional and biochemical aspects of this project. I have assisted Dr. Séguéla (main Contributor) during molecular cloning stages of the $hP2X_{5R}$ subunit. I have also collaborated with Dr. Dominique Nouel (Second Author,

Third Name), from Dr. Beaudet's laboratory, pertaining to the confocal microscopy aspects of the present study.

INDEX

ABSTRACT ii
RÉSUMÉ vi
MANUSCRIPT LISTINGS x
ABSTRACT LISTINGS xii
ACKNOWLEDGMENTS xiv
THESIS FOREWORD xvii
ORIGINALITY & CO-AUTHORSHIP CONTRIBUTION CLAIMS xx
INDEX xxiv
ABBREVIATION LISTINGS xxviii

CHAPTER 1 — GENERAL INTRODUCTION

1.1 INTRODUCTORY BACKGROUND 3
1.2 INTRODUCTION OVERVIEW 5
1.3 HISTORICAL PERSPECTIVES 5
1.3.1 PHARMACOLOGICAL CLASSIFICATION 6
1.3.2 NATIVE RESPONSE 7
1.3.3 AUTORADIOGRAPHIC BINDING DATA 9
1.3.4 ATP RELEASING SITE 10
1.3.5 ATP_{ASE}-MEDIATED ATP CATABOLISM 11
1.3.6 NOMENCLATURE LIMITATION 11
1.4 MOLECULAR BIOLOGY 12
1.4.1 MOLECULAR STRUCTURES 12
1.4.2 TRANSCRIPTION PATTERNS 14
1.4.3 PROTEIN MAPPING PROFILES 15
1.4.4 FUNCTIONAL CHARACTERISTICS 18
1.4.5 BIOPHYSICAL PROPERTIES 20
1.4.6 HUMAN ORTHOLOGS 22
1.5 PATHOPHYSIOLOGICAL CORRELATES 23
1.6 THERAPEUTICAL IMPLICATIONS 24
1.7 INTRODUCTION SUMMARY 24

CHAPTER 2 — RESEARCH OBJECTIVES

2.1 FIRST OBJECTIVE....28
2.2 SECOND OBJECTIVE....29
2.3 THIRD OBJECTIVE....30
2.4 FOURTH OBJECTIVE....31

CHAPTER 3

SENSORY PRESYNAPTIC AND WIDESPREAD SOMATODENDRITIC IMMUNOLOCALIZATION OF CENTRAL IONOTROPIC P_{2X} ATP RECEPTORS

3.1 RESEARCH RATIONALE....34
3.2 MANUSCRIPT REPRINT....36

CHAPTER 4

CENTRAL $P2X_4$ AND $P2X_6$ CHANNEL SUBUNITS CO-ASSEMBLE INTO A NOVEL HETEROMERIC ATP RECEPTORS

4.1 RESEARCH RATIONALE....79
4.2 MANUSCRIPT REPRINT....81

CHAPTER 5

FUNCTIONAL AND BIOCHEMICAL EVIDENCE FOR HETEROMERIC ATP-GATED CHANNELS COMPOSED OF $P2X_1$ AND $P2X_5$ SUBUNITS

5.1 RESEARCH RATIONALE....113
5.2 MANUSCRIPT REPRINT....115

CHAPTER 6

PRIMARY STRUCTURE AND EXPRESSION OF A NATURALLY TRUNCATED HUMAN P_{2X} ATP RECEPTOR SUBUNIT FROM BRAIN AND IMMUNE SYSTEM

6.1 RESEARCH RATIONALE 138
6.2 MANUSCRIPT REPRINT 140

CHAPTER 7 — GENERAL DISCUSSION 163

CHAPTER 8 — REFERENCES 179

CHAPTER 9 — MANUSCRIPT REPRINTS 204

ABBREVIATION LISTINGS

αβmATP	Alpha,beta-methylene ATP
ADP	Adenosine 5'-diphosphate
AMP	Adenosine 5'-monophosphate
ATP	Adenosine 5'-triphosphate
ATPases	Enzymes mediating ATP catabolism
BzATP	2',3'-(4-benzoyl)-benzoyl ATP
cDNA	Complementary deoxyribonucleic acid
CNS	Central nervous system
d	Day(s)
DRG	Dorsal root ganglion/ganglia
HEK-293A	Human embryonic kidney 293A cells
kDa	Kilodalton(s)
LTD	Long-term depression
LTP	Long-term potentiation
μg	Microgram(s)
μM	Micromolar
min	Minute(s)
ml	Milliliter(s)
mM	Millimolar
mRNA	Messenger ribonucleic acid
M2	Second transmembrane domain
ng	Nanogram(s)
PPADS	Pyridoxal 5-phosphate-6-azophenyl 2',4'-disulfonic acid
RB-2	Reactive blue 2
s	Second(s)

2MeSATP	2-Methylthio ATP
TNP-ATP	2',3'-*O*-trinitrophenyl-ATP
V_h	Holding membrane potential
WT	Wild-type

CHAPTER 1

GENERAL INTRODUCTION

1.1 INTRODUCTORY BACKGROUND

Cell to cell information transfers within the nervous system occur at relay stations known as neuro-neuronal and neuro-effector synapses and cell junctions. Intercellular transmission is mediated predominantly by chemical synapses, namely, 90% neurotransmitter-mediated versus 10% electrical. Pre- and/or postsynaptic ligand-activated integral membrane proteins/neurotransmitter receptors are either ionotropic (fast-acting) or metabotropic (slow-acting) receptors. Ionotropic receptors can be subdivided into excitatory cation-selective and inhibitory (anion-selective) neurotransmitter-gated ion channels.

Briefly, synaptic membrane depolarization and hyperpolarization are mediated by fast-acting ligand-gated cation and anion channels, respectively. Presynaptic membrane depolarization leads to calcium-dependent synaptic vesicle exocytosis and neurotransmitter release into synaptic clefts. Further, activation of postsynaptic ligand-gated cation channels by various released neurotransmitters leads to membrane depolarization, also known as excitatory postsynaptic potentials (EPSPs), and sequential action potential appearances within postsynaptic cells. On the other hand, neurotransmitter-gated anion channels lead generally to converse effects, namely, inhibitory postsynaptic potentials (IPSPs).

Formerly, fast-acting ligand-gated ion channels were thought to be comprised of two gene superfamilies based upon unique structural motifs. More specifically, the nicotinic acetylcholine (cation-selective) receptor superfamilies also encompasses serotonin- (cation-selective), GABA- (anion-selective), and glycine-gated (anion-selective). These

ion channels have been shown to be characterized by four transmembrane domains within each polypeptide which then co-assemble into five subunits or pentameric quaternary protein structures (Green and Millar, 1995; MacKinnon, 1995; references therein).

On the other hand, glutamate-gated ion channels comprise three subtypes known as NMDA, AMPA, and kainate receptors thought to display three transmembrane domains and a re-entrant loop within each isoform (MacKinnon, 1995; references therein) which interacts then with three or four other subunits forming, thus, tetrameric (Laube *et al.*, 1998; Rosenmund *et al.*, 1998) or pentameric quaternary complexes (Ferrer-Montiel and Montal, 1996), respectively. The latter issue remains a controversy (Laube *et al.*, 1998; references therein).

Recently, in nineteen ninety four, a third gene superfamily encoding ATP-gated channels or P_{2X} receptors mediating fast excitatory neurotransmission has emerged. That was the demonstration that excitatory neuronal networks do use another ionotropic neurotransmitter system in addition to major glutamatergic pathways. P_{2X} receptors mediate a fast excitatory synaptic signaling component, formely identified as a non-adrenergic and non-cholinergic (NANC) response by Burnstock (1972). These cation channels are characterized by a distinct transmembrane topology with respect to the other two gene superfamilies previously mentioned (nicotinic and excitatory amino acid receptor superfamilies) as well as being gated by extracellular nucleotides. Accordingly, the present chapter will introduce to the readership an overview pertaining to various aspects of the molecular biology of ATP-gated P_{2X} channels with a strong emphasis towards the central nervous system (CNS).

1.2 INTRODUCTION OVERVIEW

Briefly, the present overview of the literature within various research fields of ATP-gated P_{2X} ion channels has been subdivided into five main sections (1.3 to 1.7) including a section on classical pharmacological work [historical perspectives (1.3)]; a section on recent molecular characterization of ATP receptors [molecular biology (1.4)]; a section on possible pathophysiological scenarios involving P_{2X} receptors [pathophysiological correlates (1.5)] leading to future potential drug therapies targeting ATP-gated ion channels [therapeutical implications (1.6)] despite current limitation in terms of physiological importance of fast-acting purinergic neurotransmission phenomena [introduction summary (1.7)], especially within most supraspinal structures thought to have structure-function correlates.

1.3 HISTORICAL PERSPECTIVES

Potent purinergic responses in cardiovascular systems, mainly mediated by adenosine, including bradycardia and coronary vasodilatation as well as systemic blood pressure lowering effects have been reported for seven decades (Drury and Szent-Györgyi, 1929). Yet, experimental observations demonstrating that ATP was released from sensory nerves, thereby, suggesting for the first time the existence of purinergic neuro-transmission pathways have come much later (Holton and Holton, 1954). Hereafter, the present section has been further subdivided into pharmacological classification (1.3.1), native response (1.3.2), autoradiographic binding data (1.3.3), ATP releasing site (1.3.4), and ATPase-mediated ATP catabolism (1.3.5) as well as pharmacologically-based nomenclature limitation (1.3.6).

1.3.1 PHARMACOLOGICAL CLASSIFICATION

Although the possibility of ATP being a neurotransmitter has been met with resistance due to the paucity of specific antagonists, the existence of ATP-gated ionotropic components (purinoceptors) postulated by Burnstock (1972), were being gradually accepted. Adenosine effects and ATP responses were pharmacologically differentiated and their corresponding receptors designated as P1 and P2 receptors, respectively (Burnstock, 1978).

ATP or P2 receptors were then subsequently subclassified into P_{2Y} (G-protein-coupled) receptors and P_{2X} ion channels (Burnstock and Kennedy, 1985). These purinergic receptor categories were attributed based upon several pharmacological endpoints. P1 receptors were observed to be elicited by adenosine and its analogs as well as antagonized by methylxanthines such as caffeine and theophylline (Burnstock, 1978). On the other hand, due to the lack of specific P2 antagonists, P_{2Y} receptors and P_{2X} channels were differentiated based upon relative potency ratio between ATP and its analogs. In other words, 2MeSATP was reported to be more potent than ATP in activating P_{2Y} receptors (Burnstock and Kennedy, 1985). On the other hand, $\alpha\beta$mATP was found to be more potent than ATP in gating ionotropic P_{2X} channels (Burnstock and Kennedy, 1985). It should be noted, however, that this method of pharmacological identification for discriminating P_{2Y} from P_{2X} receptors will have to be reassessed with the advent of their molecular cloning studies coupled to *in vitro* pharmacological assays. The latter issue will be addressed in the upcoming section (1.4) pertaining to the molecular biology of P_{2X} receptors and their functional characterization from various heterologous expression systems.

1.3.2 NATIVE RESPONSE

Once ATP had been shown to be a *bona fide* neurotransmitter based upon compelling experimental observations (Dalziel and Westfall, 1994; Fredholm *et al.*, 1994; references therein), ATP-elicited ionotropic responses have been documented from various native electrophysiological recording preparations involving neuro-neuronal synapses including brain, spinal cord, and peripheral sensory ganglion neurons (Brake and Julius, 1996; references therein) by using the nomenclature scheme briefly elaborated above (Burnstock and Kennedy, 1985).

Ionotropic responses elicited by extracellular ATP and/or various ATP analogs have been reported from neuro-neuronal synapses within various brain structures (Edwards *et al.*, 1992; Mateo *et al.*, 1998; Ross *et al.*, 1998). For example, αβmATP-elicited ionotropic responses from a cholinergic pathway, namely, medial habenular neurons, constituted one of the first reports pertaining to a P_{2X} current phenotype observed within the brain (Edwards *et al.*, 1992). In this instance and contrary to αβmATP, ATP could not give rise to any responses under identical experimental conditions. This could be explained by the fact that extracellular ATP might be proned to degradation mediated by membrane-bound ecto-ATPases (North, 1996; references therein). Further, medial habenular neurons gave rise to moderately desensitizing currents in response to 300 μM αβmATP applications that were sensitive to suramin (10-30 μM) blockade (Edwards *et al.*, 1992). Other P_{2X} ionotropic responses have also been observed within various brain preparations, notably, cerebral cortex (Phillis *et al.*, 1975; Phillis *et al.*, 1979), hypothalamus (Chen *et al.*, 1994), locus coeruleus (Harms *et al.*, 1992; Tschöpl *et al.*, 1992; Shen and North, 1993; Fröhlich *et al.*, 1996), medial

vestibular (Chessel *et al.*, 1997) and mesencephalic nuclei (Khakh *et al.*, 1997). Although P_{2X} responses have been shown to be widespread throughout the brain, yet, pathophysiological implications and/or contexts pertaining to central ATP-gated ionotropic signaling remain unclear. Nevertheless, both hippocampus (Wierasko and Ehrlich, 1994; Balachandran and Bennett, 1996; Ross *et al.*, 1998) and cerebellum structures (Mateo *et al.*, 1998) where long-term potentiation (LTP) and long-term depression (LTD) forms of synaptic plasticity occur, display ATP-elicited fast-acting responses.

As opposed to aforementioned supraspinal sites, P_{2X} responses recorded from spinal cord preparations have been relatively less abundant. Nevertheless, available documentation has been concentrated upon studies pertaining to P_{2X} phenotypes observed mostly from the dorsal horn of the spinal cord (Jahr and Jessell, 1983; Fyffe and Perl, 1984; Salter and Henry, 1985; Salter and Hicks, 1994; Li and Perl, 1995; Bardoni *et al.*, 1997; Jo and Schlichter, 1999). Interestingly, within these anatomical loci of the spinal cord, notably, the substantia gelatinosa has been shown to be excited by multimodal sensory ganglion neuron central terminals (Fyffe and Perl, 1984). Indeed, ATP has been observed to elicit intracellular calcium increments (Salter and Hicks, 1994) and modulate (Li and Perl, 1995) or mediate (Jahr and Jessell, 1983; Bardoni *et al.*, 1997; Jo and Schlichter, 1999) synaptic transmission within the dorsal horn of the spinal cord.

Similarly, ATP is thought to produce different effects upon nociceptive *vis-à-vis* non-nociceptive pathways within the dorsal spinal cord (Salter and Henry, 1985); more specifically, non-nociceptive neurons responsive to ATP have been shown to correspond to mechanoreceptive units (Fyffe and Perl, 1984).

Various sensory ganglion cells have been shown to display fast-acting ATP-gated P_{2X} phenotypes (Krishtal *et al.*, 1983; Krishtal *et al.*, 1988; Bean, 1990; Bean *et al.*, 1990; Li *et al.*, 1993). More specifically, nodose ganglion neurons have been shown displaying ionotropic responses typical of P_{2X} receptors (Khakh *et al.*, 1995; Lewis *et al.*, 1995; Li *et al.*, 1996; Thomas *et al.*, 1998). Similarly, trigeminal ganglia have also been documented to express fast-acting ATP-elicited responses (Cook *et al.*, 1997; Khakh *et al.*, 1997). On the same token, dorsal root ganglia (DRG) have been demonstrated to give rise to synaptic transmission mediated, presumably, by P_{2X} ion channels (Krishtal *et al.*, 1983; Krishtal *et al.*, 1988; Bean, 1990; Robertson *et al.*, 1996; Gu and MacDermott, 1997). Peripheral sensory P_{2X} responses are thought to contribute to nociception (Burnstock,1996; Cook *et al.*, 1997) as well as proprioception signaling events (Fyffe and Perl, 1984; Khakh *et al.*, 1997). In retrospect, all P_{2X} ionotropic responses recorded from brain, spinal cord, and peripheral sensory ganglion neurons were either activated by αβmATP and/or blocked by suramin. In fact, suramin and/or PPADS insensitive ATP-activated P_{2X} phenotypes have not been documented so far in neurons (Barnard *et al.*, 1997).

1.3.3 AUTORADIOGRAPHIC BINDING DATA

Tritiated αβmATP ([^{3}H]αβmATP) had been shown to bind preferentially to P_{2X} receptors from various peripheral tissues such as rat bladder (Bo and Burnstock, 1990) and vas deferens (Bo *et al.*, 1992). Corroborating αβmATP-sensitive P_{2X} ionotropic responses recorded from various central neurons, autoradiographic binding studies using radiolabeled [^{3}H]αβmATP have documented widespread αβmATP binding site distribution patterns within both brain and spinal cord (Michel and Humphrey, 1993; Bo

and Burnstock, 1994; Balcar *et al.*, 1995) as well as various peripheral tissues (Michel and Humphrey, 1993). For instance, [^{3}H]αβmATP binding sites observed within various brain regions included striatum, cerebral cortex, cerebellum, and hippocampus (Michel and Humphrey, 1993). These results were subsequently further extended to include many more brain structures as well as spinal cord loci (Bo and Burnstock, 1994). In addition, high-affinity αβmATP binding sites were detected in peripheral tissues in the spleen, heart, and liver (Michel and Humphrey, 1993). Furthermore, [^{3}H]αβmATP has been observed to be displaced by suramin and RB-2 (Michel and Humphrey, 1993) as well as PPADS (Bo and Burnstock, 1994) thereby in agreement with most P2 antagonist-sensitive native electrophysiological recordings from central as well as peripheral preparations.

1.3.4 ATP RELEASING SITE

Extracellular ATP could potentially come from three modalities (Boarder and Hourani, 1998), depending upon the homeostasis state of living organisms or systems under investigation. First, cytosolic ATP can be transported to the extracellular milieu through specific transmembrane transporter proteins from various tissues such as smooth muscle and underlying cell wall within the vascular system (Boarder and Hourani, 1998). Since cytosolic ATP is an abundant source of energy, therefore, under stressful and/or traumatic conditions leading to cell membrane damage, lytic ATP constitutes the second source of extracellular nucleotides. Third and most importantly to neurotransmission phenomena, ATP has been demonstrated to be synaptically released alone or co-released with other neurotransmitters within cholinergic (Dowdall *et al.*, 1974; Unsworth and Johnson, 1990; Fu and Poo, 1991; Sperlagh and Vizi, 1991; Sun

and Stanley, 1996), noradrenergic (Sperlagh and Vizi, 1991), and glutamatergic (Gu and MacDermott, 1997) as well as GABAergic synapses (Jo and Schlichter, 1999).

1.3.5 ATP_{ASE}-MEDIATED ATP CATABOLISM

ATP released into synaptic clefts is dephosphorylated into ADP by membrane-bound ecto-ATPases (Stout and Kirley, 1996) and/or AMP via membrane-anchored ecto-ATP diphosphorylases (also known as ectoapyrases) (Kegel *et al.*, 1997) terminating ATP responses. AMP would then be hydrolyzed into adenosine as the final ATP metabolite by surface ecto-5'-nucleotidases (Zimmermann, 1992; references therein). Interestingly, these membrane-associated hydrolyzing enzymes have been shown to be as ubiquitously expressed as nucleotide receptors (Kegel *et al.*, 1997) such as P_{2X} ion channels. Similarly, these proteins display similar structural motifs to those of P_{2X} receptors. More specifically, these enzymes have two transmembrane domains connected by a large extracellular loop while having both N- and C-termini on the intracellular side (Kegel *et al.*, 1997). It is interesting to note that these ecto-ATPases also display ten cysteine residues in their extracellular domain (Kegel *et al.*, 1997). Based upon these observations, it is tempting to speculate that P_{2X} and ecto-ATPase subunits might associate into quaternary complexes integrating both signaling and termination components.

1.3.6 NOMENCLATURE LIMITATION

Taken altogether (sections 1.3.1 to 1.3.5 inclusively), a cautionary note should be raised. Several studies (before 1994) thought to characterize P_{2Y} receptors based upon

pharmacological criteria (Burnstock and Kennedy, 1985) have turned out, in hindsight, to correspond in fact to fast-acting P_{2X} responses within various brain structures (Ueno *et al.*, 1992; Shen and North, 1993). Similarly, recent evidence have strongly suggested that αβmATP might have a significant affinity for membrane-bound ecto-ATPases besides P_{2X} receptors, thus, making autoradiographic binding data difficult to interpret (see review by North, 1996).

1.4 MOLECULAR BIOLOGY

Expression and molecular cloning assays have unravelled a third family of ligand-gated ion channel having novel molecular structural motifs as well as distinctive trans-membrane protein topologies compared to nicotinic acetylcholine receptor and/or gluta-mate-gated channel gene families. Briefly, the present section has been subdivided into six sub-sections pertaining to molecular structures (1.4.1), transcription patterns (1.4.2), protein mapping profiles (1.4.3), functional characteristics (1.4.4), and biophysical properties (1.4.5) as well as human orthologs (1.4.6) of rodent ATP-gated P_{2X} ion channel subunits.

1.4.1 MOLECULAR STRUCTURES

ATP-gated $P2X_1$ (Valera *et al.*, 1994) and $P2X_2$ (Brake *et al.*, 1994) ionotropic channel subunits were the first two cloned P_{2X} receptors thanks to the use of expression cloning assays in *Xenopus laevis* oocytes starting from rat vas deferens poly(A)$^+$ RNAs (Valera *et al.*, 1994) and from PC12 cell poly(A$^+$) RNAs (Brake *et al.*, 1994). The primary structures of $P2X_1$ and $P2X_2$ receptors were predicted to code for 399 (Valera *et al.*,

1994) and 472 amino acids (Brake *et al.*, 1994), respectively. Ten extracellular cysteine residues are conserved between these two proteins (Brake *et al.*, 1994; Valera *et al.*, 1994); $P2X_1$ as well as $P2X_2$ possess several potential *N*-linked glycosylation sites within their respective hydrophilic extracellular loop, which is connected by two membrane-spanning domains. In the absence of a signal peptide, both N- and C-termini are located on the intracellular side (Brake *et al.*, 1994; Valera *et al.*, 1994; Torres *et al.*, 1998a). These P_{2X} isoforms were found to have a short extracellular sequence similar to a motif conferring ATP-binding capacity (Walker *et al.*, 1982; Brake *et al.*, 1994; Valera *et al.*, 1994) and also a sequence, preceding the second transmembrane domain, similar to H5 or P-loops found in voltage-activated or inward-rectifier potassium channels (MacKinnon, 1995); the intracellular N-terminal domain of respective $P2X_1$ and $P2X_2$ channels contains conserved consensus PKC phosphorylation sites (Brake *et al.*, 1994; Valera *et al.*, 1994), while the longer intracellular C-terminus of $P2X_2$ receptors also contained potential PKC and PKA phosphorylation sites as well as SH3 binding domains (Brake *et al.*, 1994).

Other members of the P_{2X} gene family were identified by homology cloning methodologies based upon $P2X_1$ and $P2X_2$ sequences. Namely, $P2X_3$ from sensory neurons with 397 amino acids (Chen *et al.*, 1995; Lewis *et al.*, 1995); $P2X_4$ from brain at 388 residues (Bo *et al.*, 1995; Buell *et al.*, 1996a; Séguéla *et al.*, 1996; Soto *et al.*, 1996a; Wang *et al.*, 1996); $P2X_5$ from the heart consisting of 455 amino acids (Collo *et al.*, 1996; Garcia-Guzman *et al.*, 1996); and $P2X_6$ from brain being the shortest protein of the family at 379 residues (Collo *et al.*, 1996; Soto *et al.*, 1996b); on the other hand $P2X_7$ cDNA isolated from brain encodes the longest subunit with 595 amino acids (Surprenant *et al.*, 1996). All these P_{2X} isoforms contained the specific sequence motifs found

in $P2X_1$ and $P2X_2$ channels, notably, ten conserved cysteine, twelve glycine, and six lysine residues believed to be involved in protein structure stabilization as well as presumably forming folding motif for ATP binding in the extracellular domain (Buell *et al.*, 1996b).

1.4.2 TRANSCRIPTION PATTERNS

Based upon *in situ* hybridization results, Northern blot data, and/or RT-PCR analyses pertaining to both central and peripheral nervous systems, mRNA transcripts encoding neuronal P_{2X} proteins range from restricted and discrete to ubiquituous throughout the nervous system. For instance, RNA messages coding for $P2X_4$ (Bo *et al.*, 1995; Buell *et al.*, 1996a; Collo *et al.*, 1996; Séguéla *et al.*, 1996; Soto *et al.*, 1996a; Wang *et al.*, 1996) and $P2X_6$ (Collo *et al.*, 1996; Soto *et al.*, 1996b) receptors were found to be widely transcribed throughout the brain and distributed in an overlapping fashion in most central regions (Collo *et al.*, 1996). Similarly, $P2X_2$ mRNA (Brake *et al.*, 1994) was also observed to be expressed in the brain (Brake *et al.*, 1994; Collo *et al.*, 1996), although to a much lesser extent than major brain $P2X_4$ and $P2X_6$ transcripts. On the other hand, $P2X_1$ (Valera *et al.*, 1994), $P2X_3$ (Chen *et al.*, 1995; Lewis *et al.*, 1995), and $P2X_5$ (Collo *et al.*, 1996; Garcia-Guzman *et al.*, 1996) as well as non-neuronal $P2X_7$ (Surprenant *et al.*, 1996; Collo *et al.*, 1997) mRNAs were found to be minor transcripts or absent from adult brain neurons (Collo *et al.*, 1996; Collo *et al.*, 1997), although $P2X_1$ mRNA has been observed to be transcribed in neonatal brain neurons (Kidd *et al.*, 1995).

The lamina III of the cervical spinal cord constituted the only spinal cord locus devoid of P_{2X} mRNAs (Collo *et al.*, 1996) while both $P2X_3$ and $P2X_7$ transcripts were found to be

absent altogether from the spinal cord (Collo *et al.*, 1996; Collo *et al.*, 1997). On the other hand, all other laminae expressed both $P2X_4$ and $P2X_6$ mRNAs. Further, excluding laminae I/III/IV, the $P2X_2$ isoform was positively identified within adult spinal cord (Collo *et al.*; 1996). $P2X_1$ and $P2X_5$ transcripts were observed only in the ventral horn of the spinal cord including laminae V to IX (Collo *et al.*, 1996).

Interestingly, all six neuronal P_{2X} mRNAs ($P2X_1$ to $P2X_6$ inclusively) have been shown to be transcribed within all peripheral sensory ganglion neurons studied (Collo *et al.*, 1996). Taken altogether, these studies have highlighted several interesting observations. For example, the mutually overlapping regional pattern pertaining to $P2X_4$ and $P2X_6$ messages (Collo *et al.*, 1996) seems to occur only within brain. On the same line of thought, similar co-transcription patterns have also been reported for $P2X_1$ and $P2X_5$ mRNAs within the ventral horn of the spinal cord (Collo *et al.*, 1996). On the other hand, $P2X_5$ transcripts turned out to be the most rare message among all known P_{2X} subunits (Collo *et al.*, 1996). Similarly, $P2X_3$ mRNAs have been shown to display the most restricted transcription pattern within the P_{2X} gene family (Collo *et al.*, 1996). More specifically, only primary sensory neurons have been shown to transcribe $P2X_3$ messages (Chen *et al.*, 1995; Lewis *et al.*, 1995), a unique feature among transmitter-gated channels.

1.4.3 PROTEIN MAPPING PROFILES

There have been several immunocytochemical studies regarding $P2X_1$ (Vulchanova *et al.*, 1996), $P2X_2$ (Vulchanova *et al.*, 1996; Kanjhan *et al.*, 1996; Vulchanova *et al.*, 1997), $P2X_3$ (Cook *et al.*, 1997; Vulchanova *et al.*, 1997), and $P2X_7$ (Collo *et al.*, 1997) proteins.

Although most of these protein mapping reports have corroborated and further extended previous *in situ* hybridization results pertaining to P_{2X} receptor distribution at cellular levels (Barnard *et al.*, 1997; North and Barnard, 1997).

Confirming $P2X_1$ mRNA distribution patterns from *in situ* hybridization data (Collo *et al.*, 1996), $P2X_1$ immunostainings were observed to be negative from the adult brain (Vulchanova *et al.*, 1996). On the other hand, positive $P2X_1$ immunoreactivities were found within spinal cord superficial dorsal horn layers, the sites of multiple sensory pathways, at both post- and presynaptic levels (Vulchanova *et al.*, 1996). However, based upon *in situ* hybridization results, $P2X_1$ mRNA transcripts were found to be transcribed only from motor neurons in laminae V to IX (Collo *et al.*, 1996). Reason(s) for these apparent discrepancies, between *in situ* hybridization results and immunohistochemical studies regarding $P2X_1$ channels, are currently neither raised nor addressed.

Contrary to $P2X_1$ negative protein expression within brain structures, $P2X_2$ subunits were positively immunostained within discrete central structures (Vulchanova *et al.*, 1996). For instance, $P2X_2$ proteins were found to be expressed in the hypothalamus and various catecholaminergic nuclei, notably, the olfactory bulb (Vulchanova *et al.*, 1996). Reminiscent of $P2X_1$ distribution observations, the hindbrain solitary tract nucleus has been previously shown to lack $P2X_2$ mRNA transcripts (Collo *et al.*, 1996) but $P2X_2$ positive immunolabeling was subsequently demonstrated within the same locus (Vulchanova *et al.*, 1996). Another inconsistent observation can be made concerning $P2X_2$ immunoreactivities within spinal cord dorsal horn lamina I and II. For example, $P2X_2$ positive stainings were observed within the most superficial aspect of

the dorsal horn, namely, the Lissauer's tract (Vulchanova *et al.*, 1996). However, the same group subsequently reported that $P2X_2$ subunits were not expressed within this same locus (Vulchanova *et al.*, 1997). Similarly, $P2X_2$ immunostainings were not observed within the cerebellum (Vulchanova *et al.*, 1996) thereby apparently confirming $P2X_2$ *in situ* hybridization data (Collo *et al.*, 1996), yet, $P2X_2$ was also found to be expressed within various cerebellar loci by another group (Kanjhan *et al.*, 1996).

Corroborating $P2X_3$ mRNA distribution data (Collo *et al.*, 1996), $P2X_3$ proteins was determined to be absent from the brain (Cook *et al.*, 1997; Vulchanova *et al.*, 1997). Mismatches arised between $P2X_3$ mRNA transcript distribution (Collo *et al.*, 1996) and protein expression (Vulchanova *et al.*, 1997) involving the spinal cord dorsal horn. For instance, it has been documented through *in situ* hybridization data that $P2X_3$ was not present within the spinal cord (Collo *et al.*, 1996). On the other hand, $P2X_3$ proteins were subsequently found to be expressed from the inner part of the spinal cord dorsal horn lamina II (Vulchanova *et al.*, 1997). This could be explained by the fact that $P2X_3$ subunits are expressed by central terminals of peripheral sensory ganglion neurons.

Further, $P2X_7$ immunocytochemical results have demonstrated that this subunit was in fact the only known non-neuronal P_{2X} isoform, namely, being expressed by microglial and ependymal cells from brain and also by lymphocytes and macrophages (Collo *et al.*, 1997). In hindsight, all these immunocytochemistry data pertaining to $P2X_1$, $P2X_2$, $P2X_3$, and $P2X_7$ subunits turned out to be either excluded from or expressed in a discrete fashion within supraspinal structures. Therefore, it would be relevant to pursue protein mapping studies regarding major central P_{2X} subunits such as $P2X_4$ and/or $P2X_6$ receptors. Similarly, $P2X_5$ protein distribution patterns remain to be investigated.

1.4.4 FUNCTIONAL CHARATERISTICS

Recombinant P_{2X} receptors have been functionally characterized in various heterologous protein expression systems, especially from HEK-293 cells and *Xenopus laevis* oocytes. Purinergic agonist profiles and P2 antagonist sensitivities as well as pharmacological co-factor effects have been documented. More specifically, heterologously expressed recombinant homomultimeric P_{2X} subunits have been classified into three subtypes based upon their sensitivities to the agonist αβmATP, and upon their sensitivities to P2 antagonists suramin and PPADS, as well as upon their channel desensitization kinetics. P_{2X} receptors that are rapidly desensitized, αβmATP-sensitive, and blocked by both suramin and PPADS, $P2X_1$ (Valera *et al.*, 1994) and $P2X_3$ (Chen *et al.*, 1995; Lewis *et al.*, 1995) are thus grouped together. Non-desensitizing $P2X_2$ (Brake *et al.*, 1994) and $P2X_5$ (Collo *et al.*, 1996; Garcia-Guzman *et al.*, 1996) are both insensitive to αβmATP applications, yet, they are blocked by suramin and PPADS thereby constituting another P_{2X} subgroup. On the other hand, moderately-desensitizing $P2X_4$ (Bo *et al.*, 1995; Buell *et al.*, 1996a; Wang *et al.*, 1996) and $P2X_6$ (Collo *et al.*, 1996) are neither sensitive to αβmATP nor blocked by P2 antagonists representing, still, a distinct subgroup. It should be noted, however, that $P2X_4$ was also reported to be slightly sensitive to both suramin and PPADS (Soto *et al.*, 1996a). On the same token, pre-incubated suramin (100 μM and 100 μM ATP) as well as PPADS (100 μM and 1 μM ATP) were found to be efficient $P2X_4$ blockers (Séguéla *et al.*, 1996). Further, $P2X_6$ channels expressed from *Xenopus laevis* oocytes were determined to be non-responsive to applications of ATP and various purinergic ligands (Soto *et al.*, 1996b). It is not clear why rat $P2X_6$ subunits possessing a $P2X_4$-like phenotype, as mentioned formerly, were described in transfected mammalian HEK-293 cells (Collo *et al.*, 1996).

Homomultimeric $P2X_7$ receptors (Surprenant *et al.*, 1996) constitute a special group by itself compared to the other six P_{2X} subunits. First, non-desensitizing $P2X_7$ channels are activated by ATP only at 100 μM or more (EC_{50} = 115 μM); on the other hand, they are sensitive to BzATP (EC_{50} = 7 μM) (Surprenant *et al.*, 1996). Second, $P2X_7$-mediated BzATP responses were found to be relatively insensitive and moderately sensitive to suramin and PPADS, respectively (Surprenant *et al.*, 1996). Third and most importantly, $P2X_7$ proteins are bifunctional molecules. In other words, they function as non-selective small cation channels similar to other P_{2X} isoforms under brief and well spaced-out agonist applications; conversely, under short frequent ligand applications, $P2X_7$ receptors gave rise to lytic pores permeant to large hydrophilic molecules in the hundreds of dalton range (Surprenant *et al.*, 1996).

Another P_{2X} phenotype worth separating from homomultimeric $P2X_1$ to $P2X_7$ receptors, inclusively, constitute the heteropolymers composed of $P2X_2$ and $P2X_3$ ($P2X_{2+3}$) subunits with hybrid functional properties (Lewis *et al.*, 1995). $P2X_{2+3}$ high αβmATP sensitivity is conferred by $P2X_3$ subunits but $P2X_{2+3}$ non-desensitizing channel kinetics come from the contributions of $P2X_2$ subunits. Further, this phenotype has been observed natively in sensory neurons (Lewis *et al.*, 1995) where $P2X_2$ and $P2X_3$ mRNA and proteins have been localized (Collo *et al.*, 1996). Direct physical interactions between $P2X_2$ and $P2X_3$ subunits has been recently demonstrated through co-immunoprecipitation assays via a bacculovirus-infected Sf9 cell expression system (Radford *et al.*, 1997). Until recently, the $P2X_{2+3}$ hetero-oligomeric channel phenotype constituted the only known example whereby two different P_{2X} subunits assemble together to give rise to a novel receptor phenotype unaccounted for by either homomultimeric components.

1.4.5 BIOPHYSICAL PROPERTIES

Various aspects pertaining to biophysical properties of recombinant P_{2X} subunits have been investigated. More specifically, ionic selectivity and channel rectification behavior as well as calcium permeability have been studied. Results on receptor domains thought to be involved in channel desensitization kinetics as well as membrane topologies have been reported. Single channel conductance values as well as determinants of the ion conduction vestibule have also been analyzed. Most recently, the formation of large pores by neuronal P_{2X} subunits have been demonstrated.

Reminiscent of nicotinic acetylcholine and glutamate-activated receptor gene superfamilies, ATP-gated P_{2X} ion channels have been shown to be equally permeable to monovalent cations, namely, potassium and sodium ions (Buell *et al.*, 1996b). On the same token, channel rectification properties have been observed to be subunit-dependent. More specifically, only $P2X_2$ and $P2X_3$ subunits have been reported to display marked inwardly rectifying properties (Brake *et al.*, 1994; Chen *et al.*, 1995). Similar to NMDA (Rogers and Dani, 1995) and α7 nicotinic receptors (Séguéla *et al.*, 1993), although to a lesser extent, P_{2X} receptors also display a high permeability to calcium (pCa/pNa = 4) (Lewis *et al.*, 1995; Buell *et al.*, 1996a; Soto *et al.*, 1996a), a property with important physiological consequences.

Structural elements thought to modulate channel kinetic properties have been studied for $P2X_1$ and $P2X_2$ subunits (Werner *et al.*, 1996). Briefly, it was shown that neither the extracellular domain nor both N- as well as C-termini were required to confer channel kinetic properties. $P2X_2$-like non-desensitizing kinetics were found to be dominant over

$P2X_1$-like strong desensitizing properties. Further, it was concluded that these specific kinetic properties were presumably due to intrinsic conformational changes at the level of the quaternary structure of the channel complex (Werner *et al.*, 1996). Interestingly, in a recent topological determination report confirming that P2X receptors are characterized by a large extracellular domain connected by two transmembrane segments of which both N- and C-termini are on the intracellular side (Torres *et al.*, 1998a), $P2X_2$ and $P2X_3$ monomeric subunits in tandem ($P2X_2$-$P2X_3$) have been shown to behave similarly to $P2X_{2+3}$ channels (Torres *et al.*, 1998a). Therefore, these two studies (Werner *et al.*, 1996; Torres *et al.*, 1998a) strongly suggest that either $P2X_{2+2+3+3}$ (identical subunits in adjacent positions) or $P2X_{2+3+2+3}$ (similar isoforms in opposite configurations) would give rise to non-desensitizing kinetic properties.

Reported native P_{2X} receptor phenotype single channel conductance values ranged approximately from 10 to 20 pS (Nakazawa *et al.*, 1990; Fieber and Adams, 1991;Vincent, 1992; Silinski and Gerzanich, 1993; Sun and Stanley, 1996; Khakh *et al.*, 1997). This is in agreement with single channel conductance estimates reported for recombinant $P2X_1$, $P2X_2$, and $P2X_4$ subunits being 18, 21, and 9 pS, respectively (Evans, 1996). On the other hand, $P2X_3$ receptor currents were too flickery to warrant reliable estimates (Evans, 1996). Unitary conductance values for $P2X_5$, $P2X_6$, and $P2X_7$ subunits remain to be determined. However, $P2X_6$ receptors have been shown to be silent under similar experimental conditions studied for other P_{2X} isoforms heterologously expressed from *Xenopus laevis* oocytes (Soto *et al.*, 1996b). It would be interesting to pursue single channel conductance studies pertaining to $P2X_7$ subunits, notably, under conditions whereby these receptors would give rise to lytic pore formation (Surprenant *et al.*, 1996). In addition to unitary conductance estimates, the localization of the conduction

vestibule of P_{2X} channels has been analyzed. More specifically, it was found, using substituted cysteine accessibility method (SCAM), that the M2 domain of each interacting subunit formed the conduction vestibule within P_{2X} complexes (Rassendren *et al.*, 1997a; Egan *et al.*, 1998).

Last but not least, it has been shown recently that, besides non-neuronal $P2X_7$ subunits, neuronal $P2X_2$ and $P2X_4$ as well as heteromultimeric $P2X_{2+3}$ receptors (Khakh *et al.*, 1999; Virginio *et al.*, 1999) were capable of giving rise to quaternary complexes permeable to large cations in a similar manner to $P2X_7$ channels (Surprenant *et al.*, 1996). However, neuronal P_{2X} subunits (Khakh *et al.*, 1999; Virginio *et al.*, 1999) could not give rise to lytic pores leading to cell death as it was observed for $P2X_7$ (Surprenant *et al.*, 1996). Homomultimeric $P2X_1$ or $P2X_3$ (Nicke *et al.*, 1998), and $P2X_2$ subunits (Kim *et al.*, 1997) have been shown to give rise to trimeric and tetrameric quaternary structures, respectively; thus, native P_{2X} subunit composition and stoichiometry remain to be established (Virginio *et al.*, 1999) not only pertaining to P_{2X} channels *per se* but also under conditions whereby large pore complexes are formed.

1.4.6 HUMAN ORTHOLOGS

Although most reported studies pertaining to recombinant P_{2X} receptors have come from rodent systems; nevertheless, the mammalian P_{2X} gene family has also been expanded to include human P_{2X} orthologs (hP_{2X}). More specifically, excluding $hP2X_2$ and $hP2X_5$ of which both primary sequences remain unknown, $hP2X_1$ (Valera *et al.*, 1995), $hP2X_3$ (Garcia-Guzman *et al.*, 1997a), $hP2X_4$ (Garcia-Guzman *et al.*, 1997b), $hP2X_6$ (Urano *et al.*, 1997), and $hP2X_7$ (Rassendren *et al.*, 1997b) subunits have been cloned

and characterized. Briefly, the homology between human and rat counterparts is 89%, 93%, 87%, and 80% for $P2X_1$, $P2X_3$, $P2X_4$, and $P2X_7$, respectively (Soto *et al.*, 1997). Human $P2X_1$, $P2X_3$, $P2X_4$, and $P2X_7$ subunits have been reported to have similar biophysical properties with their rodent orthologs. Although the primary sequence for $hP2X_6$ has been reported (Urano *et al.*, 1997), yet, its functional properties remain to be investigated.

1.5 PATHOPHYSIOLOGICAL CORRELATES

ATP released into the extracellular milieu is believed to be implicated either directly or indirectly in various pathophysiological conditions based upon mostly circumstantial experimental observations. For instance, ATP has been observed to elicit pain sensations both in animal models and human blister preparations. In agreement with these observations, most P_{2X} genes have been found in sensory neurons notably in nociceptive pathways based upon *in situ* hybridization and immunocytochemical studies as previously mentioned. Therefore, we hypothesize that there is a link between the nociceptive responses elicited by extracellular ATP and painful sensations. However, ATP activates P_{2X} channels as well as P_{2Y} receptors and many other less well characterized P2 transmembrane proteins in addition to P1 receptors following its degradation to ADP and adenosine by various membrane-bound ATPases.

Another example where P_{2X} receptors could play a role is during global forebrain ischemia attacks (Braun *et al.*, 1998). Hypoxia-induced ATP release may be damaging to neurons as well as microglia through P_{2X}-mediated calcium influxes (Edwards, 1996). Further, transient forebrain ischemic attacks are known to affect selectively hippo-

campal CA3 neurons (Kraig *et al.*, 1995; Braun *et al.*, 1998) where P_{2X} currents have been recorded (Ross *et al.*, 1998). Moreover, the mossy fibers contacting CA3 neurons contain the densest pools of releasable zinc in the brain (Crawford and Connor, 1972) and this divalent cation can potentiate excitatory P_{2X} receptors (Li *et al.*, 1993). Another non-exclusive possibility arises when ATP, known to be co-released with glutamate (Inoue *et al.*, 1995), potentiates glutamate cytotoxicity (Braun *et al.*, 1998). Despite these potential effects, direct P_{2X} receptor involvement under hypoxia conditions within hippocampal neurons and microglia remains to be demonstrated.

1.6 THERAPEUTICAL IMPLICATIONS

To what extent and under which conditions ATP-gated P_{2X} ion channels are involved in various peripheral sensory modalities, notably pain perceptions, will be the field of intense research. More specifically, future studies employing molecular genetic techniques such as gene knockout animal models would be helpful in assessing, for instance, the role of exclusively sensory neuron-expressed $P2X_3$ subunits. Moreover, blockers used so far in P_{2X} research are in fact non-specific P2 antagonists. Thus, it would be helpful to design P_{2X}-specific blockers in order to validate ATP-gated channels as potential therapeutical targets.

1.7 INTRODUCTION SUMMARY

In conclusion, although classical pharmacological studies coupled to modern molecular biological techniques has provided significant advancements in the field of fast-acting purinergic neurotransmission, there still remains a number of unresolved issues awai-

ting to be addressed. For instance, subcellular protein localization of major central P_{2X} subunits are currently unavailable, thus, rendering it difficult to assess the physiological contribution of P_{2X} ion channels within various brain structures. Similarly, relevant central P_{2X} subunit composition as well as species-dependent properties remain to be investigated. Accordingly, our significant contributions to these aforementioned issues will be described more elaborately in the upcoming chapters.

CHAPTER 2

RESEARCH OBJECTIVES

As can be assessed from the previous chapter, despite extensive ATP-gated P_{2X} ion channel functional characterization, there are still several unaddressed issues pertaining to P_{2X} protein localization within the CNS (Lê *et al.*, 1998a); relevant P_{2X} isoform composition within heteropolymeric receptors (Lê *et al.*, 1998b; Lê *et al.*, 1999); and species-dependent P_{2X} ortholog properties (Lê *et al.*, 1997). Accordingly, all four selected research objectives are centered around these themes. Therefore, the present chapter will present, more elaborately, the research rationale behind each of these selected published manuscripts as well as the different methodologies used.

2.1 FIRST OBJECTIVE

SENSORY PRESYNAPTIC AND WIDESPREAD SOMATODENDRITIC IMMUNOLOCALIZATION OF CENTRAL IONOTROPIC P_{2X} ATP RECEPTORS (Lê *et al.*, 1998a) — ***Research Rationale.*** Although *in situ* hybridization and Northern blot data were available from ATP-gated P_{2X} receptor molecular cloning studies (Buell *et al.*, 1996b), regional and cellular as well as subcellular P_{2X} protein expression profiles within CNS structures are currently limited thereby rendering difficult the task to assess the potential physiological contributions of central ATP-gated channels and fast purinergic transmission. Therefore, we document in the **first manuscript** (Lê *et al.*, 1998a) the protein localization of a predominant central P_{2X} subunit, $P2X_4$, at the regional, cellular, and ultrastructural level using affinity-purified rabbit polyclonal antibodies raised against the predicted C-terminal domain of the protein reported by Séguéla *et al.* (1996) and elsewhere (Bo *et al.*, 1995; Buell *et al.*, 1996a; Soto *et al.*, 1996a; Wang *et al.*, 1996).

Methodologies. First, both *in situ* immunofluorescence and immunoblotting strategies

were used to validate the specificity of our anti-$P2X_4$ polyclonal antibodies from various P_{2X} cDNAs transiently transfected into HEK-293A cells. Second, $P2X_4$ protein regional distribution patterns were determined from standard western blotting techniques from various homogenates of rat brain structures. Third, $P2X_4$ cellular protein localization were analyzed through standard immunocytochemical stainings, within brain and spinal cord. Fourth, the study demonstrated sensory pre- and postsynaptic $P2X_4$ localization.

2.2 SECOND OBJECTIVE

CENTRAL $P2X_4$ AND $P2X_6$ CHANNEL SUBUNITS CO-ASSEMBLE INTO A NOVEL HETEROMERIC ATP RECEPTOR (Lê *et al.*, 1998b) — ***Research Rationale.*** Based upon electrophysiological recordings involving various preparations from brain (Edwards *et al.*, 1992; Mateo *et al.*, 1998; Ross *et al.*, 1998), spinal cord (Bardoni *et al.*, 1997), and peripheral nervous system (Sun and Stanley, 1996; Gu and MacDermott, 1997), native P_{2X} pharmacological phenotypes have been shown to be activated by αβmATP and/or blocked by suramin. Similarly, previously reported autoradiographic binding data using [^{3}H]αβmATP ligand have revealed widespread binding sites for this radioactive ATP analog within various CNS structures (Michel and Humphrey, 1993; Bo and Burnstock, 1994; Balcar *et al.*, 1995). However, according to *in situ* hybridization data obtained with P_{2X} probes (Collo et al., 1996) only $P2X_4$ and $P2X_6$ mRNAs were both predominantly and widely transcribed in an overlapping pattern within rat brain (Collo *et al.*, 1996). These two central P_{2X} isoforms have been characterized by their lack of sensitivity to both αβmATP and suramin block (Bo *et al.*, 1995; Buell *et al.*, 1996a; Collo *et al.*, 1996; Wang *et al.*, 1996). We report in the **second manuscript** (Lê

et al., 1998b) the demonstration of the association between $P2X_4$ and $P2X_6$ subunits that gave rise to a novel P_{2X} phenotype more sensitive to αβmATP and suramin than $P2X_4$ homomers. This subunit-specific heteromultimeric interaction generating $P2X_{4+6}$ channels was also confirmed biochemically.

Methodologies. First, *Xenopus laevis* oocytes co-expressing $P2X_4$ and $P2X_6$ subunits responding to ATP, αβmATP, and 2MeSATP as well as to P2 antagonists such as suramin, PPADS, and RB-2 were assessed and compared to responses in oocytes expressing $P2X_4$ or $P2X_6$ alone under identical experimental conditions. Novel pharmacological profiles from heteropolymeric $P2X_{4+6}$ receptors were corroborated and strengthened by an established co-purification assay (Tinker *et al.*, 1996).

2.3 THIRD OBJECTIVE

FUNCTIONAL AND BIOCHEMICAL EVIDENCE FOR HETEROMERIC ATP-GATED CHANNELS COMPOSED OF $P2X_1$ AND $P2X_5$ SUBUNITS (Lê *et al.*, 1999) — ***Research Rationale.*** Besides $P2X_4$ and $P2X_6$ being major subunits within various brain structures, *in situ* hybridization data have also indicated that $P2X_1$ and $P2X_5$ were major transcripts within various laminae of the ventral horn of the spinal cord (Collo *et al.*, 1996). All neuronal P_{2X} mRNAs, including $P2X_1$ and $P2X_5$, have been reported to be transcribed in primary sensory neurons (Collo *et al.*, 1996). Native sensory P_{2X} responses recorded have been accounted for by the expression of heteromultimeric $P2X_{2+3}$ receptors (Lewis *et al.*, 1995). However, recent immunocytochemical results have indicated that certain populations of sensory neurons did not co-localize their expressed $P2X_2$ and $P2X_3$ subunits (Vulchanova *et al.*, 1997). These observations point toward

the intringuing possibility that previously thought $P2X_{2+3}$-mediated responses from some sensory neurons might, in fact, have been mediated by other receptors. Accordingly, the **third manuscript** (Lê *et al.*, 1999) was undertaken assuming that $P2X_{1+5}$ receptor would display hybrid functional properties between $P2X_1$ pharmacology and $P2X_5$ channel kinetics. In response to low αβmATP concentrations (1-10 μM), *Xenopus* oocytes expressing $P2X_5$ receptor alone should not give rise to any significant responses (Collo *et al.*, 1996); whereas homomultimeric $P2X_1$ channels should give rise to rapidly desensitizing currents (Valera *et al.*, 1994); on the other hand, oocytes co-expressing $P2X_1$ and $P2X_5$ subunits should give rise to non-desensitizing responses similar to those observed for $P2X_{2+3}$ heteromultimeric receptors (Lewis *et al.*, 1995).

Methodologies. Strategies adopted here will be similar but more complete than those used for the $P2X_{4+6}$ project (Lê *et al.*, 1998b). First, TNP-ATP IC_{50} values were measured to assess any differences between $P2X_1$, $P2X_5$, and $P2X_{1+5}$ receptor phenotypes; in addition to respective ATP, αβmATP, and ADP EC_{50} values. Second, reciprocal co-purification were performed between $P2X_1(His)_6$ and $P2X_5$-Flag as well as between $P2X_5(His)_6$ and $P2X_1$-Flag.

2.4 FOURTH OBJECTIVE

PRIMARY STRUCTURE AND EXPRESSION OF A NATURALLY TRUNCATED HUMAN P_{2X} ATP RECEPTOR SUBUNIT FROM BRAIN AND IMMUNE SYSTEM (Lê *et al.*, 1997) ***— Research Rationale.*** ATP-gated P_{2X} ion channels are thought to play a significant role in various nociceptive signaling pathways (Cook *et al.*, 1997). Species-dependent properties of P_{2X} receptors should be taken into account in the development of P_{2X}-

specific antagonists with therapeutical values such as novel analgesic agents. Therefore, this cloning project corresponding to the **fourth manuscript** (Lê *et al.*, 1997) was undertaken to characterize the human ortholog to rat $P2X_5$, which has been shown to display the most restricted distribution among all rat P_{2X} subtypes (Buell *et al.*, 1996b).

Methodologies. Taking advantage of the molecular cloning of a predominant central $P2X_4$ isoform previously reported by Séguéla *et al.* (1996) and elsewhere (Bo *et al.*, 1995; Buell *et al.*, 1996a; Soto *et al.*, 1996a; Wang *et al.*, 1996), the $P2X_4$ sequence was used for virtual screening of the dbEST database (Lennon *et al.*, 1996) with the TBLASTN algorithm. $hP2X_{5R}$ cDNA was nuclear-injected into *Xenopus laevis* oocytes for functional as well as pharmacological studies. $hP2X_{5R}$ cDNA was transiently transfected in human embryonic kidney cells (HEK-293A) for biochemical characterization of the encoded protein using, namely, Western blots and *in situ* immunofluorescence.

CHAPTER 3

3.1 RESEARCH RATIONALE

ATP is now recognized as a *bona fide* neurotransmitter (Brake and Julius, 1996). Extracellular ATP-mediated P_{2X} responses have been documented in various CNS structures by electrophysiological recordings (Buell *et al.*, 1996b). Further, indirect evidence regarding the anatomical distribution of the receptors mediating these purinergic ionotropic responses have also been described through autoradiographic binding studies (Michel and Humphrey, 1993; Bo and Burnstock, 1994; Balcar *et al.*, 1995). On the same token, mRNA distribution patterns were available recently from ATP-gated P_{2X} channel cloning works (Collo *et al.*, 1996). However, contributions of P_{2X} ion channels to fast acting purinergic synaptic signaling can only be assessed with precise anatomical distribution patterns based upon immunocytochemistry data. Indeed, there have been several protein mapping studies pertaining to P_{2X} subunits (Kanjhan *et al.*, 1996; Vulchanova *et al.*, 1996; Collo *et al.*, 1997; Cook *et al.*, 1997; Vulchanova *et al.*, 1997; Bradbury *et al.*, 1998; Vulchanova *et al.*, 1998); yet, P_{2X} protein localization of predominant central subunits, notably $P2X_4$, within both brain and spinal cord was still unaddressed thereby rendering difficult the task of assessing the physiological role of neuronal ATP-activated receptors. Taking advantage of the molecular cloning of the major central $P2X_4$ isoform reported by our laboratory (Séguéla *et al.*, 1996) and elsewhere (Bo *et al.*, 1995; Buell *et al.*, 1996a; Soto *et al.*, 1996a; Wang *et al.*, 1996), this project was pursued to document its protein localization within both brain and spinal cord. Subunit-specific anti-$P2X_4$ antibodies raised against the C-terminal domain of $P2X_4$ receptors will be used. The present immunocytochemistry study allowed the localization of $P2X_4$ subunits at regional, cellular, and ultrastructural levels. Main issues addressed were, firstly, are $P2X_4$-containing receptors expressed on postsynaptic, presynaptic elements, or both? And secondly, to what extent could $P2X_4$-mediated responses be significant in known pathways within the CNS?

3.2 MANUSCRIPT REPRINT

SENSORY PRESYNAPTIC AND WIDESPREAD SOMATODENDRITIC IMMUNOLOCALIZATION OF CENTRAL IONOTROPIC P_{2X} ATP RECEPTORS

KHANH-TUOC LÊ, PIERRE VILLENEUVE, ANTOINE R. RAMJAUN,
PETER S. MCPHERSON, ALAIN BEAUDET, AND PHILIPPE SÉGUÉLA. (1998)

NEUROSCIENCE **83**: 177-190

ABSTRACT

Recent evidence suggests that extracellular ATP plays a neurotransmitter role in the central nervous system. Its fast ionotropic effects are exerted through a family of P_{2X} ATP-gated channels expressed in brain and spinal cord. To determine the physiological significance of central ATP receptors, we have investigated the localization of a major neuronal P_{2X} receptor at the cellular and subcellular levels using affinity-purified antibodies directed against the C-terminal domain of $P2X_4$ subunit. Subunit-specific anti-$P2X_4$ antibodies detected a single band of 57 000 ± 3000 MW in transfected HEK-293A cells and in homogenates from adult rat brain. The strongest expression of central P_{2X} receptors was observed in the olfactory bulb, lateral septum, cerebellum and spinal cord. $P2X_4$ immunoreactivity was also evident in widespread areas including the cerebral cortex, hippocampus, thalamus and brainstem. In all regions examined, P_{2X} receptors were associated with perikarya and dendrites where they were concentrated at the level of afferent synaptic junctions, confirming a direct involvement of post-synaptic ATP-gated channels in fast excitatory purinergic transmission. Moreover, $P2X_4$-containing purinoceptors were localized in axon terminals in the olfactory bulb and in the substantia gelatinosa of nucleus caudalis of the medulla and dorsal horn of the spinal cord, demonstrating an important selective presynaptic role of ATP in the modulation of neurotransmitter release in central sensory systems.

INTRODUCTION

The role of extracellular ATP as a neurotransmitter at neuro-effector and neuro-neuronal synapses in the peripheral nervous system has been convincingly demonstrated

(see review in Zimmermann, 1994). Furthermore, a growing body of neurophysiological evidence suggests that ATP is involved in widespread excitatory transmission in the CNS (Jahr and Jessel, 1983; Fyffe and Perl, 1984; Edwards *et al.*, 1992; Ueno *et al.*, 1992; Day *et al.*, 1993; Furukawa *et al.*, 1994; Hiruma and Bourque, 1995). Ionotropic peripheral and central effects of extracellular ATP are exerted through a family of P_{2X} purinoceptors.

Seven different genes coding for mammalian central and peripheral P_{2X} ATP receptor subunits have been cloned so far. These genes have distinct but partially overlapping anatomical patterns of transcription that suggest tissue-specific heteromeric assembly of P_{2X} subunits (Lewis *et al.*, 1995). $P2X_1$ subunits are expressed predominantly in smooth muscle cells (Valera *et al.*, 1994). $P2X_2$ mRNA is found in sympathetic and sensory neurones as well as in the pituitary gland (Brake *et al.*, 1994). $P2X_3$ is expressed exclusively in sensory neurones (Chen *et al.*, 1995; Lewis *et al.*, 1995), while $P2X_5$ is also present in sensory neurones and in a subset of spinal motorneurones (Collo *et al.*, 1996; Garcia-Guzman *et al.*, 1996). The cytolytic $P2X_7$ receptor was found to be expressed in immune cells and glial cells of central and peripheral nervous system (Surprenant *et al.*, 1996).

In situ hybridization studies have shown that $P2X_4$ (Bo *et al.*, 1995; Buell *et al.*, 1996; Séguéla *et al.*, 1996) and $P2X_6$ (Collo *et al.*, 1996) are the only two members of the P_{2X} gene family to be widely transcribed in the adult CNS and in periphery. Whether recorded in recombinant form in *Xenopus* oocytes (Séguéla *et al.*, 1996; Soto *et al.*, 1996) and transfected HEK-293A cells (Buell *et al.*, 1996; Collo *et al.*, 1996), or natively in cultured epithelial cells from rat maxillary salivary gland (Buell *et al.*, 1996), the homo-

meric forms of these two receptors display a characteristic low sensitivity to the classical purinergic antagonists suramin and pyridoxal-phosphate-6-azophenyl-2',4'-disulphonic acid as well as slow desensitization kinetics. There is still no information available, however, on the cellular and subcellular distribution of these proteins in mammalian CNS. Yet, this information is critical to our understanding of the physiological role of central ATP-gated channels.

Taking advantage of the cloning of neuronal P_{2X} receptors, we have developed subunit-specific polyclonal antibodies directed against $P2X_4$, one major and widespread component of central P_{2X} receptors. We report here the localization of this receptor-channel subunit at the regional, cellular and ultrastructural levels in the adult rat brain and spinal cord. A summary of this work has been presented at the XXVIth Annual Meeting of Society for Neuroscience (Lê *et al.*, 1996).

MATERIALS AND METHODS

Development and Purification of Subunit-Specific Anti-$P2X_4$ Antibodies

The cDNA coding for the C-terminal domain of rat $P2X_4$, corresponding to the last 31 amino acids, the stop codon plus the 3' untranslated region, was amplified in polymerase chain reaction (PCR) from a full-length clone (Séguéla *et al.*, 1996) using a sense primer (TC*GGATCC*CTCTACTGCATGAAGAAG) containing an artificial *Bam*HI restriction site and a reverse pcDNAI vector primer. The 672 base pair PCR product was double digested with *Bam*HI and *Eco*RI for subcloning in frame with glutathione-S-transferase (GST) protein in the prokaryotic expression vector pGEX-2T (Pharmacia). The same

PCR product was double digested with *Bam*HI and *Xba*I (a natural site present in $P2X_4$) for subcloning in frame with maltose-binding protein (MBP) in the prokaryotic expression vector pMAL-c2 (New England Biolabs) for affinity purification purpose. The production of GST-$P2X_4$ fusion protein was induced by 0.1 mM isopropyl-β-thiogalactopyranoside in culture and milligrams of the bacterial protein of 32 000 MW were purified directly on preparative sodium dodecyl sulphate-polyacrylamide gel electrophoresis (SDS-PAGE). Excised bands containing 0.2-0.5 mg of GST-$P2X_4$ were mixed with Freund's complete adjuvant to initiate a standard immunization procedure in rabbits (Harlow and Lane, 1988). A similar protocol of induction was used to produce a 46 000 MW MBP-$P2X_4$ fusion protein that was separated on 12% SDS-PAGE, blotted and dried on polyvinylidene difluoride (PVDF) membrane. Protein concentrations were estimated by comparision with bovine serum albumin standards in Coomassie Blue staining. IgGs from positive sera previously selected in western blots were affinity-purified by solid-phase adsorption using MBP-$P2X_4$ on PVDF strips, eluted under acidic conditions (50 mM glycine buffer pH 2.5) prior to rapid neutralization in 2 M Tris buffer pH 8.0 and followed by 16 h dialysis in 0.01 M phosphate buffer pH 7.4 containing 2% sucrose and 1 mM EDTA.

Construction of Epitope-Tagged P_{2X} Receptor Subunits

$P2X_1$ and $P2X_4$ receptor subunits were epitope-tagged both to facilitate the localization of the two subunits in heterologous expression systems and to validate the subunit specificity of the immunoreactivity observed with anti-$P2X_4$ polyclonal antibodies. The C-terminal Flag octapeptide DYKDDDDK (IBI) was inserted in mutagenic PCR using oligonucleotide primers designed for the replacement of the natural stop codon of $P2X_1$

(anti-sense TCA*CTCGAG*GGAGGTCCTCATGTTCTCC) and $P2X_4$ subunits (anti-sense TGA*CTCGAG*GCGACACTGGTTCATCTC) by an artificial *Xho*I site. Full-length mutant P_{2X} subunits cDNAs were amplified in PCR using *Pfu* polymerase (Stratagene) then ligated in-frame to an *Xho*I-*Xba*I cassette containing the Flag peptide followed by a stop codon (Mukerji *et al.*, 1996), before subcloning in the pcDNAI eukaryotic expression vector (Invitrogen).

Heterologous Expression of Homomeric P_{2X} Receptors in HEK-293A Cells

For transfection of epitope-tagged and wild-type P_{2X} subunits in mammalian cells, HEK-293A (ATCC #CRL-1573) were grown in Dulbecco's modified Eagle's medium-10% heat-inactivated fetal bovine serum (Wisent, St-Bruno, Québec) containing penicillin and streptomycin. Freshly plated cells reaching 30-50% confluency were used for transient transfection using the calcium phosphate method on 90 mm dishes with 10 μg supercoiled plasmid DNA/10^6 cells. Heterologous expression of P_{2X} receptor subunits was assayed by immunofluorescence and western blot at 36-48 h of post-transfection time.

Immunolocalization of P_{2X} Receptors in Transfected HEK-293A Cells

After 24-36 h of post-transfection time, HEK-293A cells were plated at 50-70% confluency in poly-L-lysine coated chambers. Four hours later, adherent cells were washed in phosphate-buffered saline and fixed for 20 min at room temperature with 4% paraformaldehyde in 0.1 M phosphate buffer, pH 8.0. After blocking non-specific sites with 2% normal goat serum (NGS), fixed cells were incubated with affinity-purified and pre-

adsorbed primary antibodies $P2X_4$ (1 μg/ml) or M2 (10 μg/ml) anti-Flag peptide antibodies overnight at 4 °C in 0.05 M Tris-saline buffer pH 7.2 containing 0.5% Triton X-100, 5% NGS and 5% dry milk powder. Bound antibodies were detected by immunofluorescence after 1 h incubation with fluorescein isothiocyanate-labelled goat anti-rabbit (1 μg/ml) or Texas Red-Labelled goat anti-mouse (2 μg/ml) secondary antibodies (ImmunoResearch Labs).

Western Blot of Homogenates from Transfected Cells and Rat Brain Regions

Transfected HEK-293A cells were lifted in Hank's modified calcium-free medium with 20 mM EDTA, pelleted at low speed and homogenized in 10 volumes of 10 mM HEPES buffer pH 7.4 containing the protease inhibitors phenylmethylsulfonylfluoride (0.2 mM) and benzamidine (1 mM). Lysates were pelleted at 14 000 *g* for 5 min to remove cell debris before protein assay. Various brain regions (see Fig. 3.4) were dissected from an adult rat and homogenized at 1:10 (w:v) in 20 mM HEPES buffer pH 7.4 containing 0.32 M sucrose, 0.83 mM benzamidine, and 0.23 mM phenylmethylsulphonylfluoride using a polytron, then pelleted at 14 000 *g* for 5 min. Protein concentrations in homogenates were determined using the method of Lowry *et al.* (1951) as modified by Peterson (1977) and equal amounts of protein (150 μg/lane) were run on 10-12% SDS-PAGE, then transferred to nitrocellulose. Depending on the sample, probing was performed with the following primary antibodies: affinity-purified rabbit anti-$P2X_4$ anti-bodies (2 μg/ml) pre-adsorbed with MBP alone, affinity-purified anti-$P2X_4$ (2 μg/ml) pre-adsorbed with MBP-$P2X_4$ (negative controls) or mouse mAb M2 (10 μg/ml, IBI). Appropriate secondary species-specific peroxidase-labelled antibodies were used for visualization by enhanced chemiluminescence (ECL; Amersham).

Immunocytochemistry in Rat Brain and Spinal Cord

Adult male Sprague-Dawley rats (140-180 g; Charles River, Canada) were deeply anaesthetized with sodium pentobarbital (80 mg/kg, i.p.) and perfused transaortically with 375 ml of 2% paraformaldehyde (light microscopy) or with 75 ml of a mixture of 3.75% acrolein and 2% paraformaldehyde followed by 300 ml of 2% paraformaldehyde (for electron microscopy) in 0.1 M phosphate buffer, pH 7.4. Brains and spinal cords were dissected out and postfixed for 1 h by immersion in the same fixative. For light microscopic immunohistochemistry, they were then cryoprotected for 48 h by immersion in a 30% sucrose solution in 0.2 M phosphate buffer pH 7.4 at 4 °C, frozen in isopentane at -45 °C, and sectioned at a thickness of 30 μm on a freezing microtome. Sections were rinced in phosphate buffer pH 7.4, and incubated for 30 min in 0.1 M Tris buffer saline, pH 7.4 (TBS) containing 0.03% H_2O_2. For electron microscopic immunocytochemistry, the olfactory bulb, cerebellum and cervical spinal cord were blocked off with a razor blade and serially sectioned at 40 mm thickness on a vibrating microtome (Vibratome). Both frozen and Vibratome sections were then incubated overnight at 4 °C in Triton X-100 and 20 μg/ml affinity-purified $P2X_4$ antibodies pre-adsorbed with MBP. Negative control samples were incubated with $P2X_4$ antibodies pre-adsorbed with MBP-$P2X_4$ or with GST-$P2X_4$, with pre-immune serum (1:1000), or in the absence of primary antibodies. All sections were then rinsed in TBS and processed using the avidin-peroxidase-biotin staining method (ABC Elite, Vector Labs). Briefly, they were incubated with 1:100 biotinylated goat anti-rabbit and 1% NGS for 1 h followed by 1:100 avidin-peroxidase complex for an additional hour. Bound peroxidase was visualized by immersion of the sections in 0.01 M Tris buffer, pH 7.6, containing 0.05% 3,3'diaminobenzidine (DAB), 0.04% nickel chloride and 0.01% H_2O_2. Frozen sections

were then mounted on gelatin-coated slides, dehydrated in graded ethanols, defatted in xylene and coverslipped for light microscopic observation (Paxinos and Watson, 1986). Vibratome-cut sections were postfixed in 2% OsO_4 in 0.1 M phosphate buffer containing 7% dextrose, dehydrated in graded ethanols and embedded in Epon between two acetate sheets. They were then mounted at the tip of Epon blocks and cut at 80 nm thickness on a Reichert ultra-microtome, collected on Formvar-coated copper grids and examined with a JEOL 100CX electron microscope.

RESULTS

Subunit Specificity of Antibodies Directed Against Rat $P2X_4$

The subunit specificity of affinity-purified $P2X_4$ antibodies was tested on HEK-293A cells transfected with various members of the P_{2X} gene family. Members of this gene family display low intersubunit homology in the C-terminal domain chosen for the production of $P2X_4$ antibodies (Fig. 3.1). Since the primary structure of the $P2X_1$ subunit is the closest to that of $P2X_4$ in this region, we expressed epitope-tagged $P2X_1$ subunits in HEK-293A cells to challenge the specificity of our $P2X_4$ antibodies. No immunofluorescence was visible above background level in permeabilized HEK-293A cells expressing Flag-tagged $P2X_1$ (Fig. 3.2), Flag-tagged $P2X_2$ or the wild-type subunits (data not shown). In western blots of crude homogenates from transfected cells, $P2X_4$ antibodies and anti-Flag mAb M2 recognized the same major protein band of 57 000 ± 3000 MW (n = 4) corresponding to Flag-tagged $P2X_4$ monomers (Fig. 3.3). $P2X_4$ antibodies detected a major protein band of 56 000 ± 3000 MW (n = 4) corresponding to wild-type $P2X_4$ monomers. In keeping with our immunofluorescence results on whole cells, $P2X_4$

antibodies did not bind to homologous $P2X_1$ subunits in homogenates (Fig. 3.3). An immunoreactive band of 100 000 MW was detectable in homogenates of HEK-293A cells transfected with epitope-tagged $P2X_4$ receptors (Fig. 3.3). This labelling, observed both with M2 and $P2X_4$ antibodies, likely corresponds to multimers of overexpressed P_{2X} subunits. In western blots of crude homogenates from multiple regions of the adult rat brain, affinity-purified $P2X_4$ antibodies labelled a single major band of 57 000 ± 3000 MW (n = 7) (Fig. 3.4) in concordance with the size of $P2X_4$ subunits heterogously expressed in HEK-293A cells. The labelling of a single major band demonstrated the monospecificity of our affinity-purified antibodies. $P2X_4$ immunoreactivity was detectable in all brain regions examined. However, relative $P2X_4$ protein levels varied considerably between areas, i.e., from very low expression in the striatum to very high expression in the olfactory bulb (Fig. 3.4).

Light Microscopic Localization of $P2X_4$ Subunits in Rat Brain and Spinal Cord

In rat brain sections, $P2X_4$ immunoreactivity was detected with variable intensity throughout the neuraxis. Incubation of control sections with either preimmune serum or with purified serum pre-adsorbed with the C-terminal fragment of $P2X_4$ in MBP-$P2X_4$ markedly decreased or completely abolished the immunoreactivity in most regions examined (Fig. 3.5). Only those regions in which adsorption controls showed a marked decrease in $P2X_4$ signals are considered below.

The most intense $P2X_4$ immunoreactivity in rat brain was detected in the glomerular layer of the olfactory bulb (Figs. 3.5-A, 3.6-A) and in the outer layers of the nucleus of the spinal trigeminal tract and dorsal horn of the spinal cord (Fig. 3.6-B). In both of

these regions, the labelling was diffusely distributed throughout the neuropil (Fig. 3.6-A, B). In all other brain areas, $P2X_4$ immunostaining was confined to neuronal perikarya and proximal dendrites.

Rostrally, intensely immunoreactive neurones were observed in the mitral cell layer of the olfactory bulb (Fig. 3.6-A). Perikarya and proximal dendrites of tufted cells in the external plexiform layer were much less frequently and only weakly stained.

Moderately immunoreactive pyramidal cells were detected throughout the cerebral cortex. These were particularly numerous in layers II and III (Fig. 3.7-A), but were also scattered throughout layer V. There were no consistent patterns between differences in labelling patterns between different cytoarchitectonic areas.

Intensely $P2X_4$-immunopositive neurones were observed in the lateral septal nucleus (Fig. 3.7-B, C). These neurons showed granular staining of the perikaryon extending into proximal dendrites (Fig. 3.7-B). More medially, small, less intensely labelled cells were visible on the midline, within the medial septal nucleus (Fig. 3.7-C). These labelled cells were co-extensive ventrally with equally moderately labelled neurons in the vertical limb of the diagonal band of broca (Fig. 3.7-C). In the caudate-putamen, sparse, lightly immunoreactive spiny type II neurons were visible, most prominently in the ventrolateral segment. No immunoreactive cells were apparent in the nucleus accumbens.

In the hippocampus, a subset of moderately to densely stained neurons were detected throughout the pyramidal layer of the CA1, CA2 and CA3 subfields. As can be seen in

Fig. 3.8, these labelled cells were most numerous in CA2 and at the CA2/CA3 border, as well as at the hilar extremity of CA3. Multiple $P2X_4$-immunoreactive cells were also visible within the granule cell layer of the dentate gyrus. In addition, small, intensely labelled cells were dispersed throughout the hilus as well as in striata oriens and radiatum of the hippocampus.

The reticular, anterodorsal and ventrolateral nuclei of the thalamus exhibited large numbers of moderately immunoreactive nerve cell bodies over relatively high non-specific background labeling.

In the hypothalamus, weakly immunoreactive nerve cell bodies were apparent within the anterior hypothalamic and suprachiasmatic nuclei. In the former, $P2X_4$-immunoreactive cells were sparse and mainly distributed in the lateral segment of the nucleus. In the latter, $P2X_4$-immunoreactive perikarya were more numerous, more intensely immunoreactive, and uniformly distributed throughout the nucleus.

Within the brainstem, only a few nuclei showed significant immuno-adsorbable cellular staining. These include the dorsal tegmental and dorsal raphe nuclei of the midbrain and the main sensory nucleus of the trigeminal nerve. Moderate, highly punctate perikaryal staining was also observed in the substantia gelatinosa of the nucleus of the spinal trigeminal tract (nucleus caudalis) and dorsal horn of the spinal cord. These immunolabeled cells often poorly stood out against the intense neuropil staining in their surround (Fig. 3.6-B).

In the cerebellar cortex, Purkinje cells were consistently heavily labelled (Fig. 3.9-A).

The immunostaining was most pronounced at the level of their perikarya, where at high magnification it took the form of small intracytoplasmic puncta, but was also observed, albeit more weakly, throughout their dendritic tree (Fig. 3.9-A). Only sparse, weakly immunoreactive neurons, presumably Golgi cells from their size and localization, were detected in the granule cell layer. Finally, central non-neuronal cells including leptomeningeal cells of the pia mater (Fig. 3.9-B), perivascular cells and some endothelial cells of intraparenchymal blood vessels showed intense $P2X_4$ immunoreactivity.

Electron Microscopic Localization of $P2X_4$ Subunits in the Olfactory Bulb, Cervical Spinal Cord and Cerebelum

In olfactory bulb glomeruli, $P2X_4$ immunoreactivity was evident within both dendrites (not shown) and axon terminals (Fig. 3.10-A). In both structures, the labelling was diffusely distributed throughout the cytoplasm and heavily deposited over synaptic specializations (Fig. 3.10-B). In layers I and II of the dorsal horn of the spinal cord, $P2X_4$ immunoreactivity was detected within neuronal perikarya, dendrites and axon terminals. In perikarya and dendrites, the reaction product was mainly absorbed on the outer surface of mitochondria, microtubules and various vesicular elements (Fig. 3.10-C, D). Heavy DAB deposits were also visible along the plasma membrane, predominently at the level of synaptic junctions (Fig. 3.10-C). In axon terminals, the reaction product was present throughout the cytoplasm and heavily concentrated on the membrane of synaptic vesicles and over synaptic densities (Fig. 3.10-E, F).

In cerebellar cortex, $P2X_4$ immunolabelling was mainly evident over the perikarya and dendrites of Purkinje cells (Fig. 3.11). In both of these structures, heavy chromogen

deposits were apparent along the plasma membrane (Fig. 3.11-B, C) as well as over the membranes of a variety of intracellular organelles including cisterns of rough endoplasmic reticulum (Fig. 3.11-A, C), Golgi saccules and vesicles (Fig. 3.11-A) and mitochondria (Fig. 3.11-A, B). In some instances, plaques of heavy DAB deposits were visible over clusters of endoplasmic reticulum cisternae and Golgi saccules (Fig. 3.11-A) which likely accounted for the intracytoplasmic granularity observed in the light microscope.

DISCUSSION

Affinity-purified $P2X_4$ antibodies detect wild-type $P2X_4$ channel subunits migrating at a MW of 56-57 000 both in heterologous systems and in adult rat brain. The significant difference between the predicted MW of non-glycosylated $P2X_4$ subunit (44 000) and the observed MW strongly suggests that the protein is N-glycosylated on several of the six potential glycosylation sites found in the presumed extracellular domain of rat $P2X_4$. A post-translational modification of similar magnitude has been previously reported for the rat $P2X_1$ subunit (Collo *et al.*, 1996).

The assessment of the subunit-specificity of our polyclonal $P2X_4$ antibodies rests on convergent structural, biochemical and anatomical data. From a structural point of view, each member of the P_{2X} receptor family has a unique C-terminal domain. A high degree of divergence is observed in this domain even between subunits that have similar functional properties in the homomeric form. As neither $P2X_1$ transcripts (Collo *et al.*, 1996) nor $P2X_1$ subunits (Vulchanova *et al.*, 1996) are detected in the adult rat brain, the most likely candidate for cross-reactivity would have been the $P2X_6$ subunit which, like $P2X_4$, is widely expressed in the CNS (Collo *et al.*, 1996). However, $P2X_6$ displays a

short C-terminal domain that does not share any related sequence with $P2X_4$, making it unlikely to account for the observed immunoreactivity. The immunolabeling of a single major band of the expected size in homogenates from brain regions demonstrates that the set of epitopes recognized by anti-$P2X_4$ antibodies in the C-terminal domain of these ATP-gated channels is unique in the mammalian CNS. Furthermore, the regional distribution of $P2X_4$ immunoreactivity in rat brain conforms to the results of earlier *in situ* hybridization studies (Bo *et al.*, 1995; Buell *et al.*, 1996; Collo *et al.*, 1996; Séguéla *et al.*, 1996), confirming the specificity of the signal.

The selective distribution of $P2X_4$ immunoreactivity observed here in the rat CNS is also in good qualitative and quantitative agreement with the results of autoradiography using radiolabelled [^{3}H]α,β-methylene ATP (Michel and Humphrey, 1993; Bo and Burnstock, 1994; Balcar *et al.*, 1995). However, $P2X_4$ and $P2X_6$ subunits generate homomeric receptors insensitive to α,β-methylene ATP. Therefore, the correlation between the $P2X_4$ immunostaining reported here and previous radioligand binding results implies two non-exclusive possibilities: (a) α,β-methylene ATP binds with high-affinity to $P2X_4$ and $P2X_6$ homomeric receptors but is not an agonist because its binding site is not coupled to channel gating; (b) an unidentified central subunit with a similar widespread regional distribution confers α,β-methylene ATP binding and sensitivity to heteromeric channels containing $P2X_4$ and/or $P2X_6$ subunits.

The most intense $P2X_4$ expression in the rat brain was detected in the glomeruli of the olfactory bulb and in the dorsal horn of the spinal cord, two regions in which the immunostaining pervaded the entire neuropil. In olfactory bulb glomeruli, the labeling was found by electron microscopy to be associated with both axonal and dendritic pro-

cesses. In view of the strong labeling of primary afferent axons observed in the olfactory nerve layer by light microscopy, axonal $P2X_4$ immunoreactivity is likely to be mainly associated with primary afferents in the glomeruli. Labelled dendrites presumably belong to either tufted cells, as both of these have been shown to extend their dendrites within glomeruli (Pinching and Powell, 1971; DeVries and Baylor, 1993). This interpretation conforms to the recent demonstration of $P2X_4$ mRNA within these two cell types by *in situ* hybridization (Buell *et al.*, 1996).

In the spinal cord, intense $P2X_4$ immunoreactivity was observed by electron and/or light microscopy over neuronal perikarya and axon terminals in the marginal layer and in the substantia gelatinosa of the spinal cord and nucleus caudalis, two areas involved in pain information processing where ATP has been previously shown to modulate synaptic transmission (Li and Perl, 1995). Whether the axonal $P2X_4$ subunits visualized here by immunohistochemistry are located on primary sensory afferent fibers or are part of local circuits remains to be established. The detection of $P2X_4$ mRNA in sensory neurons of dorsal root ganglia (Lewis *et al.*, 1995) supports the former possibility.

In all other regions of the rat brain, $P2X_4$ immunoreactivity was associated with neuronal perikarya and proximal dendrites, thereby accounting for the good correlation with *in situ* hybridization data. Within $P2X_4$-immunoreactive cells, the bulk of the immunostaining was consistently intracellular, in the form of small intracytoplasmic "hot spots". Such a high proportion of intracellular receptors has been reported for other types of neuronal transmitter-gated channels, including nicotinic acetylcholine receptors (Hill *et al.*, 1993) and glutamate-gated channels (Rogers *et al.*, 1991). Electron microscopic observations confirmed the heterogeneity of $P2X_4$ intracytoplasmic labeling

and showed that these "hot spots" correspond to stacks of rough endoplasmic reticulum cisterns and to congregated Golgi saccules and vesicles, i.e., to putative sites of synthesis, storage and transport of the ATP receptors.

Dense chromogen deposits were also observed along the outer mitochondria membrane and microtubules of labeled perikarya and dendrites, as well as over membranes of synaptic vesicles within labelled axon terminals. The interpretation of these labeling patterns should be subject to caution, however, given the reported limitations in the subcellular resolution of DAB cytochemistry (Novikoff *et al.*, 1972).

A major finding of the present ultrastructural investigation is that $P2X_4$ is associated both with intraneuronal perikarya/dendrites and with axon terminals, indicating that they mediate both post- and pre-synaptic ATP signalling. In the olfactory bulb, this double localization suggests that fast purinergic transmission is involved in both pre- and postsynaptic regulation of olfactory and nociceptive sensory pathways, an interpretation strengthened by the presynaptic localization of $P2X_1$ and $P2X_2$ subtypes in the same areas (Vulchanova *et al.*, 1996). This argues strongly in favor of ATP playing a specific modulatory role in sensory information processing through heteromeric $P2X_4$-containing ionotropic receptors.

In other brain areas studied, such as the hippocampus and cerebellar cortex, it appears that ATP mainly plays a postsynaptic neurotransmitter role through $P2X_4$-containing receptors. In the hippocampus, the highest levels of $P2X_4$ immunoreactivity were detected in the pyramidal layer of all CA subfields as well as in granule cells of the dentate gyrus. ATP-induced currents mediated by homomeric $P2X_4$ receptors are potentiated

by extracellular zinc (Séguéla *et al.*, 1996; Soto *et al.*, 1996). This potentiation of fast purinergic responses by zinc, recorded in various preparations (Cloues *et al.*, 1993; Li *et al.*, 1993; Koizumi *et al.*, 1995), is a general property of neuronal ATP-gated channels. The hippocampal mossy fibers that synapse on CA3 pyramidal cells contain the highest concentration of releasable zinc in the brain (Crawford and Connor, 1972). Therefore, in contrast to the receptors expressed in CA2 where pyramidal cells are not contacted by mossy fibers, the activity of $P2X_4$-containing ATP-gated channels localized on the dendrites of CA3 pyramidal cells and/or interneurons could be regulated by synaptic zinc, the dysfunction of which may have pathological consequences (Reece *et al.*, 1994; Buhl *et al.*, 1996). The cerebellar cortex is the central structure which shows the highest level of $P2X_4$ subunit expression by *in situ* hybridization (Buell *et al.*, 1996; Séguéla *et al.*, 1996; Soto *et al.*, 1996). We demonstrate here that $P2X_4$ receptors are associated with both the perikaryal and dendritic membranes of Purkinje cells. The main sources of direct excitatory input to the Purkinje cells are the parallel fibers from granule cells and the climbing fibers from the inferior olivary complex (Palay and Chan-Palay, 1974). Thus, our results suggest that ATP may be co-released with excitatory amino acids to control the firing activity of Purkinje cells. And finally, the significant levels of $P2X_4$ receptor expression observed in subpopulations of leptomeningeal cells of the pia mater and perivascular cells suggest an unexpected role for extracellular ATP as a signalling molecule in various vascular-related non-excitable cells through the activation of ionotropic receptors.

CONCLUSION

Fast purinergic currents recorded in response to the activation of P_{2X} channels display

a significant primary calcium component due to their high permeability to divalent cations (Buell *et al.*, 1996b; Soto *et al.*, 1996). Our ultrastructural data on the pre-synaptic expression of $P2X_4$ channel subunit indicate that, by increasing intracellular calcium, $P2X_4$-containing ATP receptors may selectively control excitatory synaptic transmission in central sensory systems like the olfactory bulb and the substantia gelatinosa of spinal cord.

FIGURE 3.1 Alignment of the C-terminal domains of rat P_{2X} ATP-gated channel subunits. The $P2X_4$ domain (amino acids 358-388) targeted for polyclonal anti-fusion protein antibodies production is compared with the corresponding sequences in known members of the P_{2X} gene family. $P2X_1$ channel subunit displays the closest primary structure to $P2X_4$ in this region with 35% homology. Conserved residues in the same relative position in all P_{2X} channel subunits are indicated in bold.

P2x4 LYCMKKKYYYRDKKYKYVEDYEQGLSGEMNQ*

P2x1 LHILPKRHYYKQKKFKYAEDMGPGEGEHDPVATSSTLGLQENMRTS*

P2x2 LTFMNKNKLYSHKKFDKVRTPKHPSSRWPVTLALVLGQIPPPPSH(68 aa)PKGLAQL*

P2x3 LNFLKGADHYKARKFEEVTETTLKGTASTNPVFASDQATVEKQSTDSGAYS*

P2x5 IYLIRKSEFYRDKKFEKVRGQKEDANVEVEANEMEQERP(51 aa)ILHPVKT*

P2x6 LYVDREAGFYWRTKYEEARAPKATTNSA*

P2x7 CEPCAVNEYYYRKKCEPIVEPKPTLKYVSFVDEPHIWMVDQQLLGKSL(167 aa)SGFKYPY*

FIGURE 3.2 Subunit-specificity of anti-$P2X_4$ antibodies in transfected HEK-293 cells. By immunofluorescence, affinity-purified anti-$P2X_4$ antibodies detect the expression of Flag-tagged $P2X_4$ subunits ($P2X_4$-Flag) but not that of homologous Flag-tagged $P2X_1$ subunits ($P2X_1$-Flag). As positive controls, both epitope-tagged $P2X_1$ and $P2X_4$ channel subtypes are visualized with anti-Flag mAb M2.

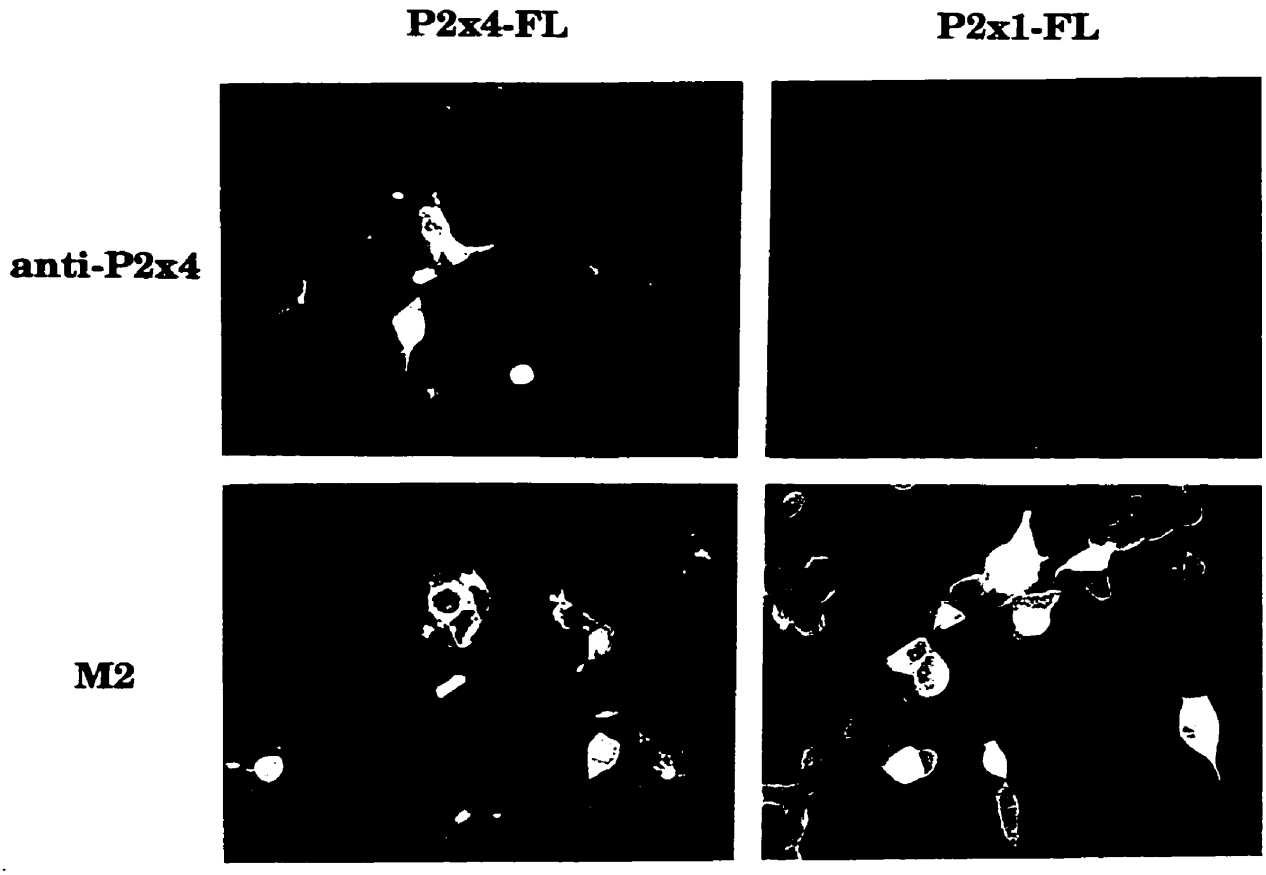
P2x4-FL
P2x1-FL
anti-P2x4
M2

FIGURE 3.3 Western blots of epitope-tagged and wild-type $P2X_4$ channels from homogenates of transiently transfected HEK-293A cells. Both mAb M2 and anti-$P2X_4$ antibodies detect Flag-tagged $P2X_4$ and anti-$P2X_4$ antibodies recognize wild-type $P2X_4$ channel subunit (56 000 ± 3000 MW). The same amount of total proteins (150 μg) has been loaded in each lane. Each sample has been assayed by immunofluorescence after expression with appropriate antibodies for checking the efficiency of the transfection.

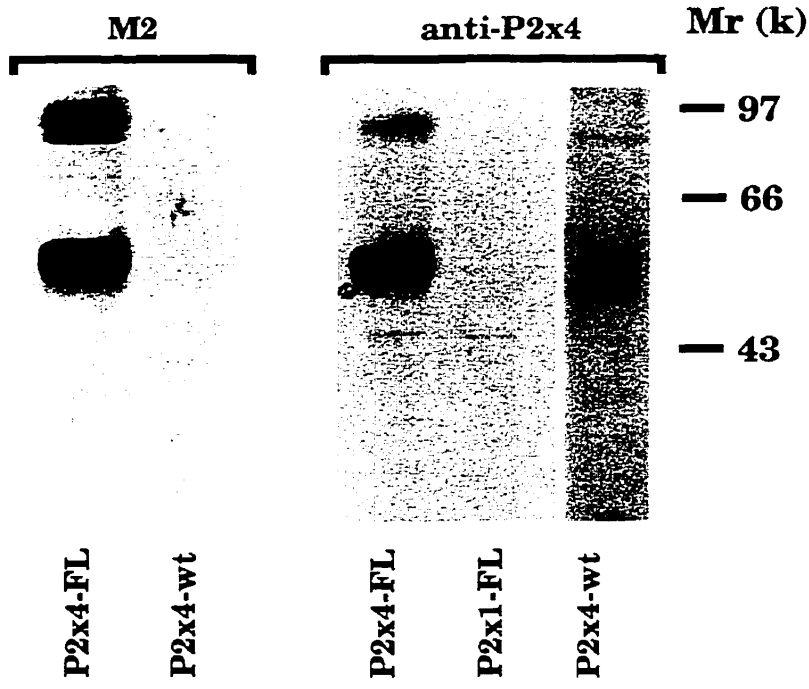
M2
anti-P2x4
Mr (k)
97
66
43
P2x4-FL
P2x4-wt
P2x4-FL
P2x1-FL
P2x4-wt

FIGURE 3.4 Western blot of rat brain homogenates from microdissected regions using affinity-purified anti-$P2X_4$ antibodies. The single major band detected displays a MW of 57 000 ± 3000 corresponding to $P2X_4$ monomers in all regions examined. The same amount of total proteins (150 μg) has been loaded in each lane. WB, whole brain; BS, brainstem; CB, cerebellum; ST, striatum; HP, hippocampus; OB, olfactory bulb; CX, cerebral cotex.

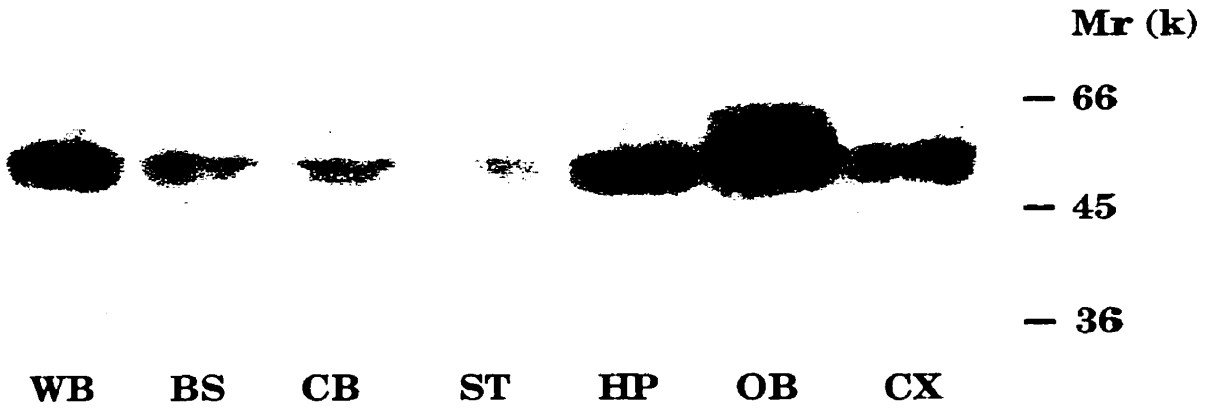
Mr (k)
66
45
36
WB
BS
CB
ST
HP
OB
CX

FIGURE 3.5 $P2X_4$ immunoreactivity in rat olfactory bulb before (**A**) and after (**B**) pre-adsorption of affinity-purified primary antibodies with an excess of antigen. Immunolabeling in the olfactory nerve layer (ON), glomerular layer (GI), and mitral cell layer (Mtr) in (**A**) is abolished in sections incubated with pre-adsorbed antibodies (**B**). Scale bar: 500 μm.


ON
GL
ML
A
B

FIGURE 3.6 Distribution of $P2X_4$ immunoreactivity in the olfactory bulb (**A**) and dorsal horn of the spinal cord (**B**). (**A**) Labeling in the olfactory bulb is concentrated over the olfactory nerve layer (ON), glomerular layer (GI), and individual mitral cells (Mtr). Note that individual glomeruli are not equally densely immunoreactive, and that weakly labeled cells are apparent in the external plexiform layer (EPI). Scale bar: 60 μm. (**B**) $P2X_4$ immunoreactivity in the dorsal horn is concentrated over the outer marginal layer (I) and substantia gelatinosa (II). Only weak labeling is detected over layer III. Scale bar: 120 μm.

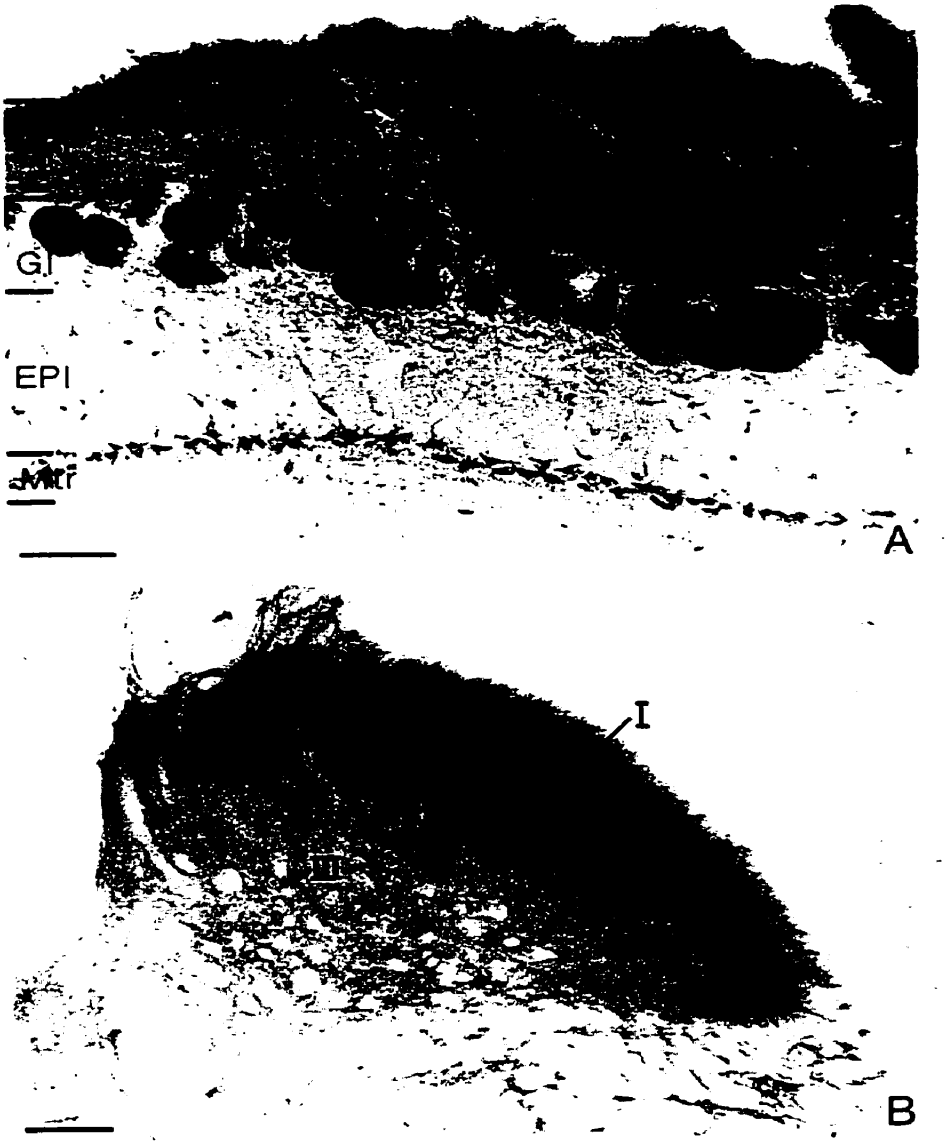
GI
EPI
Mtf
A
I
III
B

FIGURE 3.7 Distribution of $P2X_4$ receptor subunits in the piriform cortex (**A**), lateral septum (**B**), and basal forebrain (**C**). (**A**) Moderately to densely labeled pyramidal cells are apparent throughout layers II-III. Scale bar: 200 μm. (**B**) Higher magnification of the framed area in (**C**). Note the heterogeneity of the perikaryal labeling. LV, lateral ventricle. Scale bar: 75 μm. (**C**) $P2X_4$-immunoreactive cells are visible throughout the lateral septum (LS), medium septum (MS), and diagonal band of Broca (DBB). CPu, caudate putamen; ac, anterior commissure. Scale bar: 500 μm.

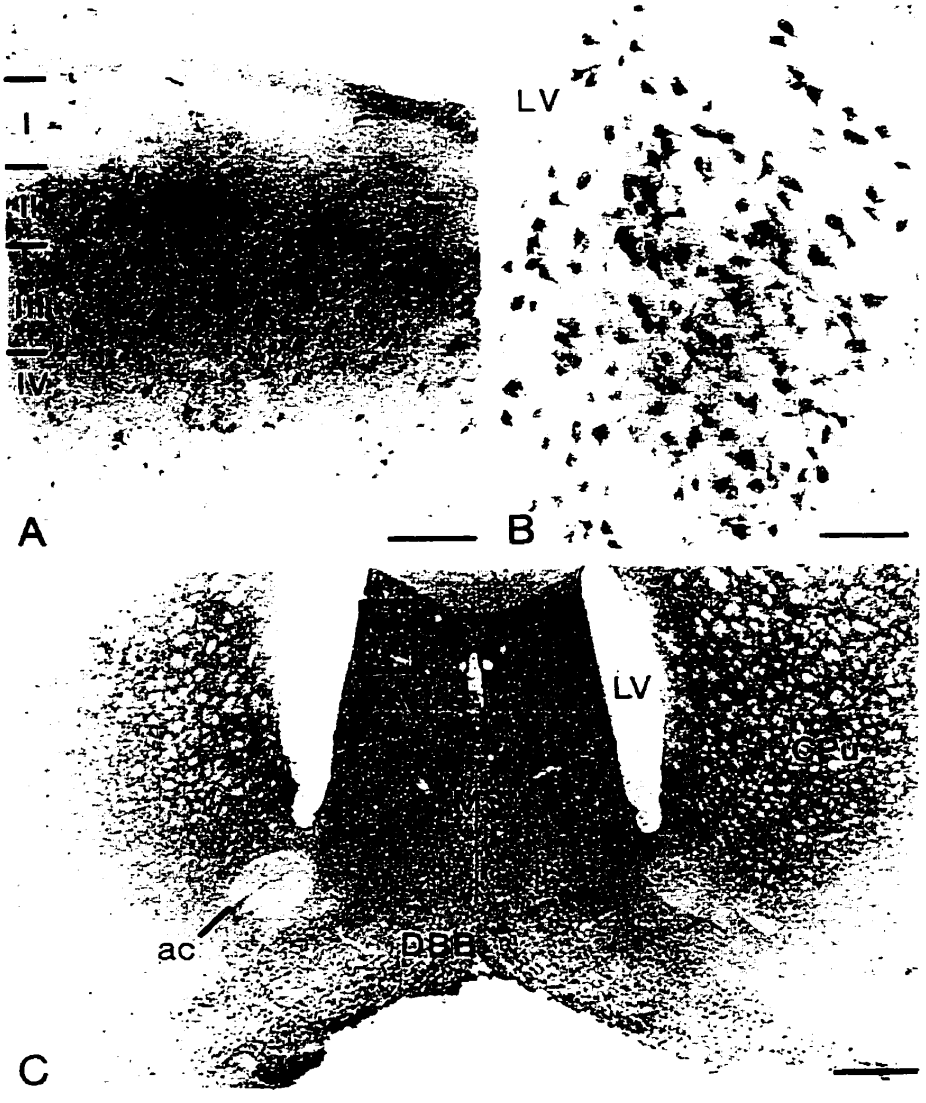
I
III
IV
A
LV
B
LV
ac
DBB
C

FIGURE 3.8 Immunolocalization of $P2X_4$ receptor subunits in hippocampus. Immunolabelled cells are scattered throughout CA1, CA2, and CA3 subfields of the hippocampus as well as within the granule cell layer (gc) and hilus (hi) of the dentate gyrus. In the hippocampus, $P2X_4$-immunoreactive cells are mainly found in the pyramidal cell layer (py), of which they nonetheless constitute a subpopulation of interneurons and small pyramidal cells (arrows within inserts). Only sparse immunolabeled cells are evident in strata oriens (or) and radiatum (ra). Scale bar: 300 μm. Insert scale bar: 50 μm.


CA1
or
py
ra
CA2
CA3

FIGURE 3.9 Distribution of $P2X_4$ immunoreactivity in cerebellar cortex (**A**) and pia mater (**B**). (**A**) In cerebellar cortex, Purkinje cells (PL) are intensely immunoreactive. Partial filling of their dendritic tree is also evident in the molecular layer (ML: arrows). Only sparse, weakly labeled cells are apparent in the granule cell layer (GL). Scale bar: 120 μm. (**B**) In the pia mater, leptomeningeal cells are intensely positive for $P2X_4$ immunoreactivity. Scale bar: 40 μm.

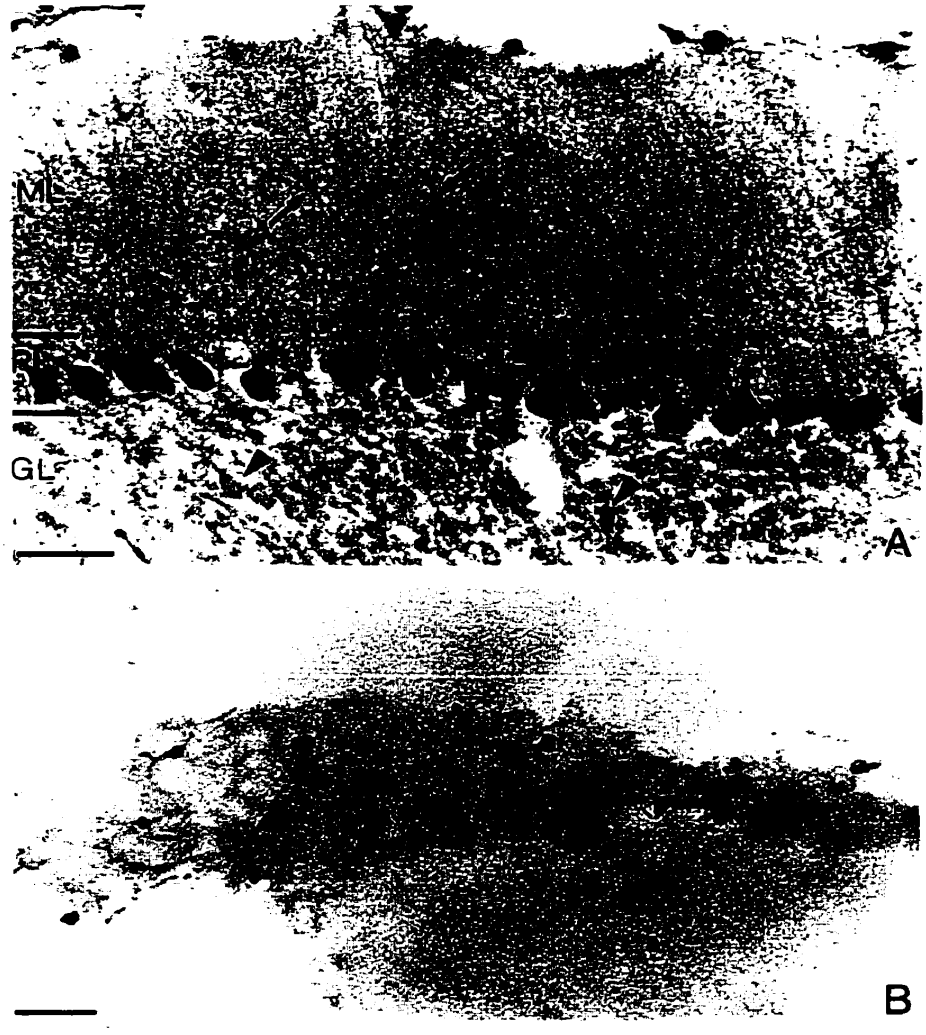
ML
GL
A
B

FIGURE 3.10 Fine structural distribution of $P2X_4$ immunoreactivity in olfactory bulb glomeruli (**A, B**) and substantia gelatinosa (**C-E**). (**A**) Numerous $P2X_4$-immunoreactive axon terminals (arrows) are seen to synapse on immunonegative dendritic trunks (Den). (**B**) $P2X_4$-immunoreactive axon terminals in synaptic contact with a dendritic branch (Den). Note the heavy chromogen deposits on the membrane of synaptic vesicles as well as at the level of the synaptic specialization (arrowheads). (**C, D**) $P2X_4$-iimunoreactive dendrites (Den) in the substantia gelatinosa of the spinal cord. Dense DAB deposits are apparent at the level of synaptic junctions (arrowheads) as well as over microtubules and the outer membrane of mitochondria. (**E, F**) $P2X_4$-immunoreactive axon terminals in the substantia gelatinosa. Both terminals show diffuse labeling of their cytoplasm and are seen in asymmetrical synaptic contact (arrows) with unlabeled dendrites (Den). Scale bars: 0.5 μm.

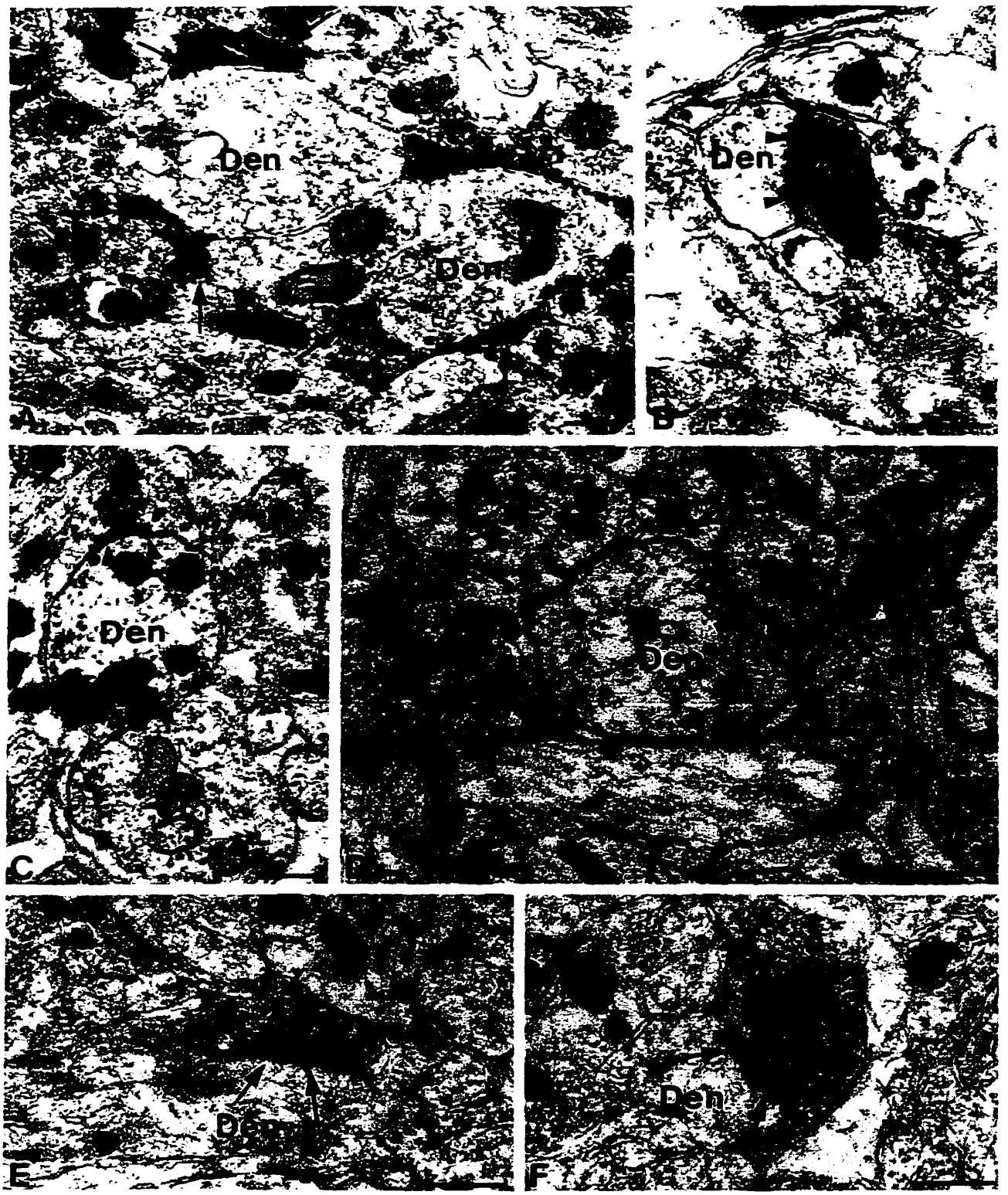
Den
Den
A
Den
B
Den
C
Den
D
Den
E
Den
F

FIGURE 3.11 Electron microscopic localization of $P2X_4$ immunoreactivity in cerebellar cortex. (**A-C**) $P2X_4$-immunoreactive Purkinje cell perikarya. (**A**) Plaques of dense chromogen deposits are apparent over cisterns of smooth endoplasmic reticulum (thin arrows) and stacks of Golgi saccules (thick arrows). (**B**) $P2X_4$ immunoreactivity is evident (arrowheads) as well as on the outer membrane of mitochondria (arrows). (**C**) $P2X_4$-immunoreactive deposits on cisterns of rough endoplasmic reticulum. Scale bar: 0.5 μm.

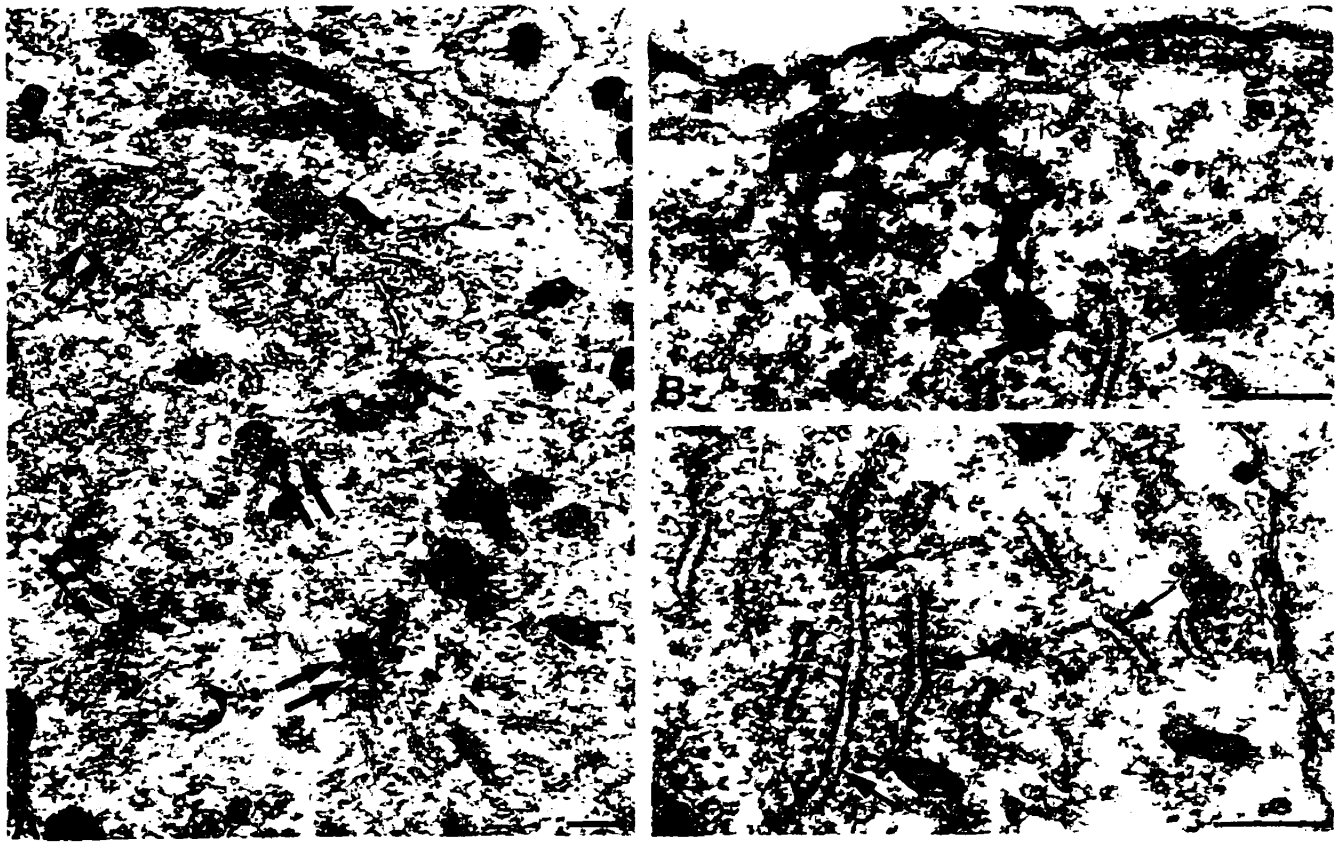
B

CHAPTER 4

4.1 RESEARCH RATIONALE

Native electrophysiological recordings of central P_{2X} responses, notably in brain (Edwards *et al.*, 1992; Mateo *et al.*, 1998; Ross *et al.*, 1998) as well as in spinal cord (Bardoni *et al.*, 1997) have consistently been shown to be sensitive to αβmATP and/or blocked by suramin. Further, autoradiographic binding data involving [^{3}H]αβmATP have revealed widespread binding site profiles of this agonist within both brain and spinal cord (Michel and Humphrey, 1993; Bo and Burnstock, 1994; Balcar *et al.*, 1995), in agreement with aforementioned native αβmATP-sensitive electrophysiological responses.

However, according to *in situ* hybridization results using $P2X_1$- (Valera *et al.*, 1994) to $P2X_7$-specific probes (Surprenant *et al.*, 1996), only $P2X_4$ and $P2X_6$ mRNAs are both predominantly and widely transcribed in an overlapping pattern within rat brain (Collo *et al.*, 1996). Finally, our own $P2X_4$ protein mapping data (Lê *et al.*, 1998a) have shown a good correlation between $P2X_4$ mRNA distribution patterns (Collo *et al.*, 1996) and $P2X_4$ immunoreactivity (Lê *et al.*, 1998a).

Thus, functional characterization of heterologously expressed central P_{2X} homo-oligomers did not fit with native P_{2X} current phenotypes or αβmATP autoradiographic binding data from various central preparations. Indeed, recombinant $P2X_4$ or $P2X_6$ subunits have been known to be unresponsive to αβmATP applications as well as insensitive to suramin block (Bo *et al.*, 1995; Buell *et al.*, 1996a; Collo *et al.*, 1996; Wang *et al.*, 1996). Therefore, to address these discrepancies, this project was undertaken in order to assess whether $P2X_4$ and $P2X_6$ subunits could interact together thereby giving rise to a novel heteromultimeric $P2X_{4+6}$ channel phenotype displaying higher sensitivities to αβmATP as well as suramin block.

4.2 MANUSCRIPT REPRINT

CENTRAL $P2X_4$ AND $P2X_6$ CHANNEL SUBUNITS CO-ASSEMBLE INTO A NOVEL HETEROMERIC ATP RECEPTOR

KHANH-TUOC LÊ, KAZIMIERZ BABINSKI, AND PHILIPPE SÉGUÉLA. (1998)

JOURNAL OF NEUROSCIENCE **18**: 7152-7159

ABSTRACT

Ionotropic ATP receptors are widely expressed in mammalian central nervous system. Despite extensive functional characterization of neuronal homomeric P_{2X} receptors in heterologous expression systems, the subunit composition of native central P_{2X} ATP-gated channels remains to be elucidated.

$P2X_4$ and $P2X_6$ are major central subunits with highly overlapping mRNA distribution at both regional and cellular level. When expressed in *Xenopus* oocytes, $P2X_6$ subunits assemble into silent channels unresponsive to ATP applications. On the other hand, $P2X_4$ subunits assemble into slowly desensitizing ATP-gated channels insensitive to the partial agonist α,β-methylene ATP and to non-competitive antagonists suramin and pyridoxal-5-phosphate-6-azophenyl-2',4'-disulphonic acid.

We demonstrate here that the co-injection of $P2X_4$ and $P2X_6$ subunits in *Xenopus* oocytes leads to the generation of a novel pharmacological phenotype of ionotropic ATP receptors. These heteromeric $P2X_{4+6}$ receptors are activated by low micromolar α,β-methylene ATP (EC_{50} = 12 μM) and are blocked by suramin and by Reactive Blue 2 which has the property, at low concentrations, to potentiate homo-meric $P2X_4$ receptors. The assembly of $P2X_4$ with $P2X_6$ subunits results from subunit-dependent interactions, as shown by their specific co-purification from HEK-293A cells transiently transfected with various epitope-tagged P_{2X} channel subunits. Our data strongly suggest that the numerous cases of neuronal co-localizations of $P2X_4$ and $P2X_6$ subunits observed in mammalian central nervous system reflect the native expression of heteromeric $P2X_{4+6}$ channels with unique functional properties.

INTRODUCTION

Fast purinergic neurotransmission is mediated by non-selective cation channels gated by extracellular ATP. These transduction proteins, designated as P_{2X} receptors, constitute a distinct class of neurotransmitter-gated channels on the basis of their primary cDNA sequences and their predicted transmembrane protein topology. Currently, seven mammalian P_{2X} genes have been identified with either expression or homology cloning assays (Buell *et al.*, 1996). Among the neuronal P_{2X} receptors, only $P2X_4$ and $P2X_6$ isoforms are predominantly expressed in the adult rat brain where they show an overlapping pattern of regional and cellular distribution at the mRNA level (Collo *et al.*, 1996). Both rat $P2X_4$ and $P2X_6$ homomeric subunits are considered as weakly responsive to α,β-methylene ATP (αβmATP) and insensitive to P2 antagonists suramin and pyridoxal-5-phosphate-6-azophenyl-2',4'-disulphonic acid (PPADS) when expressed in HEK-293A cells or *Xenopus laevis* oocytes heterologous systems (North and Barnard, 1997). Yet, native ionotropic purinergic responses from rat medial habenula, cerebellum and hippocampus were blocked by P2 antagonists and most native ATP receptors are activated by αβmATP (Edwards *et al.*, 1992; Mateo *et al.*, 1998; Ross *et al.*, 1998). Moreover, high affinity [^{3}H]-αβmATP autoradiographic binding sites have been localized in specific but widespread regions within the brain and spinal cord (Michel and Humphrey, 1993; Bo and Burstock, 1994; Balcar *et al.*, 1995). Discrepancies between pharmacological profiles of heterologously expressed homo-oligomeric P_{2X} subunits and electrophysiological recordings from neuronal preparations likely reflect the existence of native heteromeric phenotypes of P_{2X} receptors in central nervous system. Indeed, one such hybrid P_{2X} phenotype was recorded in sensory neurons (Khakh *et al.*, 1995; Lewis *et al.*, 1995) and has been proposed to result from the association between $P2X_2$ and

$P2X_3$ subunits (Lewis *et al.*, 1995; Radford *et al.*, 1997). We describe in this report a novel P_{2X} heteromeric receptor containing central $P2X_4$ and $P2X_6$ subunits. This phenotype of ATP-gated channel is endowed with a unique pharmacology characterized by increased sensitivities to αβmATP, 2-methylthio ATP (2MeSATP), suramin, and Reactive Blue 2 (RB-2) in the *Xenopus* oocyte expression system.

MATERIALS AND METHODS

Molecular Biology

Wild-type full-length $P2X_6$ subunit cDNA was obtained by RT-PCR using adult rat spinal cord RT-cDNA template, *Expand* DNA polymerase (Boehringer-Mannheim) and exact match primers based upon published primary sequences (Collo *et al.*, 1996; Soto *et al.*, 1996).

Construction of $P2X_1$-Flag and $P2X_4$-Flag were reported previously (Lê *et al.*, 1998). To generate epitope-tagged $P2X_6$-Flag and $P2X_4$-$(His)_6$ subunits, a *Xho*I-*Xba*I cassette containing an inframe His_6 epitope followed by an artificial stop codon was grafted to the full-length *Hind*III-*Xho*I $P2X_4$ construct.

The $P2X_4$-$(His)_6$ mutant was then subcloned directionally into the *Hind*III and *Xba*I sites of pcDNAI vector (Invitrogen) for CMV-driven heterologous expression in mammalian cells and *Xenopus laevis* oocytes. Epitope-tagged and RT-PCR constructs were subjected to dideoxy sequencing either manually with Sequenase (UBI) or with an ALF DNA sequencer (Pharmacia-LKB).

Cell Culture and Protein Chemistry

For cDNA transfections of epitope-tagged and wild-type P_{2X} subunits into mammalian cells, HEK-293A cells (ATCC #CRL-1573) were cultured in Dulbecco's modified Eagle's medium (D-MEM)-10% heat-inactivated fetal bovine serum (FBS) (Wisent, St. Bruno, Quebec) containing penicillin and streptomycin. Freshly plated cells reaching 30-50% confluency were used for transient cDNA transfections with the calcium phosphate method on 90 mm cell culture dishes (Falcon) with 10 μg of supercoiled plasmid cDNA/10^6 cells (Lê *et al.*, 1998). For Western blots, transfected HEK-293A cells were lifted in Hank's modified calcium-free medium with 20 mM EDTA, pelleted at low centrifugation and homogenized in 10 volumes of 10 mM HEPES buffer, pH 7.4, containing protease inhibitors phenylmethylsulfonyl fluoride (0.2 mM) and benzamidine (1 mM). Cell lysates were pelleted at 14 000 x *g* for 5 min and membrane proteins in supernatants were solubilized with SDS-containing loading buffer. Approximately 150 μg of protein per lane were run on 12% SDS-PAGE, then transferred to nitrocellulose. Immunoprobing was performed with mouse mAb M2 (10 μg/ml, IBI) followed by peroxidase-labelled anti-mouse secondary antibodies for visualization by enhanced chemiluminescence (Amersham). Co-purification of associated P_{2X} subunits were performed as previously described for IRK channels (Tinker *et al.*, 1996) with minor modifications. Cell lysates were solubilized with 1% Triton X-100 for 2 h at 4 °C. Unsolubilized materials were pelleted at 10 000 x *g* and supernatants were incubated with 50 ml of 50% slurry of equilibrated Ni-NTA-Resin (Qiagen) for 2 h at 4 °C. Nickel beads were then washed six times in TBS containing 25 mM imidazole and 1% Triton X-100. Bound proteins were eluted from Ni-NTA-Resin with 500 mM imidazole, diluted 1:1 (v/v) with SDS-containing loading buffer and warmed for 10 min at 37 °C. Samples were then loaded

onto a 12% SDS-PAGE, transferred to nitrocellulose, and analysed in Western blots using chemiluminescence as above.

Electrophysiology

For electrophysiological recordings in oocytes, ovary lobes were surgically removed from *Xenopus laevis* frogs anesthetized with Tricaine (Sigma), and treated for 3 h at room temperature with type II collagenase (Gibco-BRL) in calcium-free Barth's solution under vigorous agitations. Stages V-VI oocytes were then defolliculated chemically before nuclear microinjections of 5-10 ng cDNA coding for each P_{2X} channel subunit.

Following 2-5 days of incubation at 19 °C in Barth's solution containing 1.8 mM calcium chloride ($CaCl_2$) and 10 μg/ml gentamicin, P_{2X} currents were recorded in a two-electrode voltage-clamp configuration using an OC-725B amplifier (Warner Instruments). Signals were low-pass filtered at 1 kHz, acquired at 500 Hz using a Macintosh IIci equipped with an A/D card NB-MIO-16XL (National Instruments). Traces were post-filtered at 100 Hz in Axograph (Axon Instruments). Agonists, antagonists, and co-factors (zinc chloride, pH 6.5, and pH 8.0) were dissolved in Ringer's solution containing 115 mM NaCl, 2.5 mM KCl, 1.8 mM $CaCl_2$ in 10 mM HEPES (pH 7.4) at room temperature, and applied on oocytes at a constant flow rate of 12 ml/min.

Statistical Analysis

All comparisons involving two variances were performed with Fisher's F values (variance homogeneity requirements) and with Student's t tests for two unpaired groups. Two-

tailed statistical thresholds, for both Fisher's F and Student's t critical values, were set at $p < 0.05$.

RESULTS

Functional Impact of $P2X_6$ Subunit Expression on ATP-Induced Currents

In response to 100 μM ATP, *Xenopus* oocytes microinjected with a mix of $P2X_4$ and $P2X_6$ cDNAs (molar ratio of 1:1) gave rise to currents with kinetic profiles similar to those observed with oocytes expressing $P2X_4$ alone (Fig. 4.1-A). $P2X_6$ by itself appeared to be silent in *Xenopus* oocytes since no current was detected during ATP applications (Fig. 4.1-A), in agreement with what has been previously reported (Soto *et al.*, 1996). Comparison of peak current amplitudes after 3 days of expression revealed however that currents from cells co-expressing $P2X_4$ + $P2X_6$ subunits were reproducibly and significantly smaller than currents from cells expressing only $P2X_4$ receptors (Fig. 4.1-A, B) suggesting the possibility that the $P2X_6$ channel subunit can heteropolymerize with other members of the P_{2X} family. We co-expressed $P2X_6$ together with $P2X_1$ (Valera *et al.*, 1994) or with $P2X_2$ (Brake *et al.*, 1994). In response to 100 μM ATP, there were no differences between peak currents recorded from oocytes co-expressing $P2X_1$ + $P2X_6$ and those expressing $P2X_1$ alone (Fig. 4.1-C) after three days of expression. Similarly, we did not observe any functional impact of $P2X_6$ on the expression of $P2X_2$, under the same experimental conditions (Fig. 4.1-D), eliminating the possibility of a general inhibitory effect of $P2X_6$ on protein synthesis or on translocation. Thus these data indicate either that the subunit-specific interaction between $P2X_4$ and $P2X_6$ isoforms generates an heteromeric $P2X_{4+6}$ receptor, or that $P2X_6$ subunits exert a specific

inhibitory function on $P2X_4$ receptor expression. If $P2X_{4+6}$ heteromers are expressed, smaller peak currents could result from a lower affinity for ATP or a smaller single conductance in comparison with homomeric $P2X_4$ channels. Alternatively, smaller ATP responses at day 3 could simply reflect a slower kinetics of receptor expression.

To further characterize a time-dependent effect, we studied the time-course of expression, daily recording peak currents in response to 100 μM ATP from oocytes expressing either $P2X_4$ + $P2X_6$ cDNAs or $P2X_4$ cDNA alone. Figure 4.2 demonstrates that ATP receptors in oocytes co-expressing $P2X_4$ + $P2X_6$ subunits, compared to $P2X_4$ alone, needed a longer time to reach the same levels of ATP-induced currents. However, between day 2 and day 5 after injection, there was a dramatic 7-fold increase in peak current amplitudes in oocytes co-expressing $P2X_4$ + $P2X_6$ subunits. This profile is in striking contrast with the time-course of $P2X_4$ expression which slowly decayed over the same period.

Agonist Sensitivity Profile of $P2X_{4+6}$ Heteromeric Receptors

No significant difference was detected between the EC_{50} values derived from ATP dose-response profiles of $P2X_{4+6}$ (6.3 ± 0.9 μM) channel phenotype vs. homomeric $P2X_4$ (4.2 ± 1.1 μM) receptors (Fig. 4.3-A) expressed in oocytes. However, the partial agonist 2MeSATP had EC_{50} values of 7.67 ± 1.01 μM and 26 ± 1.8 μM for $P2X_{4+6}$ and $P2X_4$ receptors, respectively, a statistically significant difference (Fig. 4.3-B). Even more striking, in response to 100 μM αβmATP on day 3 after injection, oocytes expressing $P2X_{4+6}$ heteromeric channels gave rise to peak current amplitudes of 0.7 ± 0.13 μA compared to 0.12 ± 0.02 μA only from oocytes expressing $P2X_4$ homomeric receptors, in marked contrast with the situation observed in response to ATP (compare Fig. 4.4-A

with Fig. 4.1-B). The αβmATP EC_{50} values were found to be 12 ± 2 μM for $P2X_{4+6}$ and 55 ± 2 μM for $P2X_4$ channel phenotypes (Fig. 4.4-B). Therefore, αβmATP shows more potency and has a higher affinity on $P2X_{4+6}$ receptors than on $P2X_4$ receptors. These different sensitivities to 2MeSATP and αβmATP constitute more experimental evidence for a functional association between $P2X_4$ and $P2X_6$ subunits co-expressed in *Xenopus* oocytes.

Sensitivity of $P2X_{4+6}$ Receptors to Suramin, PPADS and RB-2

It is widely recognized that neither $P2X_4$ nor $P2X_6$ homomeric receptors are completely blocked by suramin or PPADS up to 100 μM without pre-incubation (Buell *et al.*, 1996). In response to 100 μM ATP + 10 μM suramin co-applications without pre-incubation, oocytes expressing $P2X_{4+6}$ gave rise to residual currents of 61 ± 3% (Fig. 4.5) of the response to 100 μM ATP (100%). Under the same experimental conditions, oocytes expressing $P2X_4$ receptors alone were almost unaffected (93 ± 3%, Fig. 4.5).

We have also found that 10 μM PPADS co-applied with 100 μM ATP gave rise to peak current amplitudes of 83 ± 7% and 103 ± 6% for $P2X_{4+6}$ and $P2X_4$ receptor phenotypes, respectively (Fig. 4.5-B), but we did not find any significant difference between this 17% inhibition on $P2X_{4+6}$ and no effect on $P2X_4$. We have also investigated the effects of RB-2 by co-applying 10 μM of the antagonist with 100 μM ATP: oocytes expressing $P2X_{4+6}$ receptor phenotypes were characterized by residual peak currents of 60 ± 9% compared to potentiated peak currents of 123 ± 18% from oocytes expressing $P2X_4$ receptors alone (Fig. 4.5). In other words, 10 μM RB-2 blocked $P2X_{4+6}$ heteromeric channels by up to 40% but increased $P2X_4$ response by more than 20%. A potentiating effect of RB-

2 on $P2X_4$ homomeric receptors has been reported in oocytes, albeit to a smaller extent (Bo *et al.*, 1995).

Sensitivity of $P2X_{4+6}$ Receptors to Co-Agonists Zinc Ions and Protons

We have reported previously that 10 μM extracellular zinc ions co-applied with 10 μM ATP potentiated $P2X_4$ peak currents by almost two-fold (Séguéla *et al.*, 1996). In addition, it has also been shown that the sensitivity to ATP of homomeric $P2X_4$ channels is modulated by external pH: pH < 7 inhibits ATP responses while pH > 8 has no significant effects (Stoop *et al.*, 1997). Therefore, we checked if these co-agonists applied with ATP could discriminate between $P2X_{4+6}$ and $P2X_4$ receptor phenotypes. In response to 10 μM zinc ions + 10 μM ATP co-applications, there were no significant differences between potentiating factors of 1.8 ± 0.19 and 1.8 ± 0.21 for $P2X_{4+6}$ heteromeric channels and $P2X_4$ homomeric receptors, respectively (Fig. 4.6-A). There was also no significant difference between these two receptor phenotypes with respect to ATP (20 μM) applied at pH 6.5. In both cases, residual peak current amplitudes were 46 ± 4% of control values measured at pH 7.4 (Fig. 4.6-B). When 20 μM ATP was applied at pH 8.0, it elicited peak currents of 121 ± 4% and 106 ± 4% for $P2X_{4+6}$ heteromers and $P2X_4$ homomers, respectively (Fig. 4.6-C). Thus, contrary to αβmATP, 2MeSATP and to antagonists suramin and RB-2, co-factors zinc and protons did not discriminate between $P2X_{4+6}$ and $P2X_4$ receptors on a pharmacological basis.

Subunit-Specific Association of $P2X_4$ with $P2X_6$ Subunits

Before testing their biochemical interactions, the expression of Flag-tagged $P2X_1$, $P2X_4$,

and $P2X_6$ subunit proteins in transiently transfected HEK-293A cells was confirmed by immunoblots of total membrane proteins (Fig. 4.7-A, lanes 1-6). Homogenates from HEK-293A cells transiently co-transfected with cDNA templates encoding $P2X_4$-$(His)_6$ and either $P2X_1$-Flag, $P2X_4$-Flag, or $P2X_6$-Flag constructs were analysed for co-purifications. Following solid-phase binding of $P2X_4$-$(His)_6$ proteins on poly-His-binding resin, we detected the co-precipitation of $P2X_4$-Flag subunits, confirming that $P2X_4$ subunits interacted between themselves to generate a homomultimeric complex (positive controls, in Fig. 4.7-B, lane 1). Co-expression of $P2X_4$-$(His)_6$ with $P2X_6$-Flag subunits gave a positive band corresponding to the expected size of $P2X_6$ (51 kDa, Fig. 4.7-B, lane 3), demonstrating directly for the first time that $P2X_4$ and $P2X_6$ subunits do physically interact in a multimeric complex. Co-expression of $P2X_4$-$(His)_6$ with $P2X_1$-Flag subunits did not give any signal when probed with anti-Flag M2 antibodies after purification, confirming that $P2X_4$ and $P2X_1$ subunits do not heteropolymerize (Fig. 4.7-B, lane 5). All control co-expressions including $P2X_4$-WT (lacking the poly-His motif) co-transfected with Flag-tagged $P2X_4$, $P2X_6$ or $P2X_1$ subunits were negative after purification on poly-His-binding resin (Fig. 4.7-B, lanes 2, 4, and 6).

DISCUSSION

Functional Identification of $P2X_{4+6}$ Heteromeric Receptors

In the present study, we first observed an apparent inhibition of $P2X_6$ subunits on ATP-induced currents in oocytes expressing $P2X_4$ subunits (Fig. 4.1-B). However, neither ATP-induced currents mediated by $P2X_1$ subunits (Fig. 4.1-C) nor currents mediated by $P2X_2$ subunits (Fig. 4.1-D) were affected, strongly suggesting that $P2X_4$ and $P2X_6$ iso-

forms associate together, in a subunit-specific fashion, into a novel heteromeric P_{2X} channel. Functional $P2X_{4+6}$ protein assembly and/or plasma membrane channel targeting appeared to be on a different time scale compared to $P2X_4$ receptors. Indeed, in response to 100 μM ATP, $P2X_{4+6}$ heteromultimers gave rise to increasing peak currents even after five days of expression, while $P2X_4$ homopolymers yielded decreasing peak current amplitudes under identical conditions (Fig. 4.2). We did not find any difference between the EC_{50} of ATP for both homomeric and heteromeric receptor isoforms (Fig. 4.4-A), so we concluded that the apparent inhibitory effect of $P2X_6$ on $P2X_4$ recorded three days after injection was mainly due to a slower expression of $P2X_{4+6}$ receptors on the cell surface, assuming similar channel conductance. These findings constituted our first set of experimental evidence demonstrating an heteropolymerization between $P2X_4$ and $P2X_6$ subunits. It has been previously noticed that $P2X_6$ subunits/channels express poorly in HEK-293A cells (Collo *et al.*, 1996), and are silent to ATP in the *Xenopus* oocyte expression system (Soto *et al.*, 1996), as observed here. However, maximal ATP-induced peak currents were significantly larger at day 5 in the case of $P2X_{4+6}$ channels than in the case of $P2X_4$ alone (Fig. 4.2). This situation is reminiscent of epithelial sodium-selective channels, belonging to another family of two-transmembrane-domain cation channels, whereby a fully functional channel requires the heteropolymerization of α subunits with β and γ subunits, both inactive when expressed alone (Canessa *et al.*, 1994).

Unique Pharmacological Profiles of $P2X_{4+6}$ Heteromeric Receptors

We made the assumption that the association between $P2X_4$ and $P2X_6$ subunits should be reflected in some unique aspects of the pharmacological profile of the resulting hete-

romeric receptor. Although $P2X_4$ seemed the dominant subunit for the sensitivity to ATP in the heteromers, we observed a statistical difference between EC_{50} values of 2MeSATP for $P2X_{4+6}$ heteromeric channels and $P2X_4$ receptors (Fig. 4.4-B). Furthermore, in response to 100 μM αβmATP applications, oocytes co-expressing $P2X_4$ and $P2X_6$ subunits gave rise to larger maximal peak currents than oocytes expressing $P2X_4$ isoforms alone (Fig. 4.3-A), despite slower kinetics of expression. Indeed, we measured a lower EC_{50} of αβmATP for $P2X_{4+6}$ than for $P2X_4$ channel species (Fig. 4.3-B). Therefore, in addition to opposite protein expression profiles between $P2X_{4+6}$ and $P2X_4$ channels, these observations strongly indicate that $P2X_4$ and $P2X_6$ subunits generate a novel receptor phenotype characterized by an unique agonist profile, namely increased 2MeSATP and αβmATP sensitivity. Moreover, these data provide for the first time experimental evidence for moderately-desensitizing αβmATP-activated ionotropic responses.

Further, we probed the sensitivity of $P2X_{4+6}$ heteromers to P2 antagonists suramin, PPADS, and RB-2 co-applied with ATP. We found that suramin significantly blocked $P2X_{4+6}$ activity without inhibiting significantly $P2X_4$ homomeric receptors (Fig. 4.5-A): 10 μM suramin co-applied with 100 μM ATP decreased $P2X_{4+6}$ heteromeric receptor peak current amplitudes by up to 40% compared to 7% for $P2X_4$ homomeric channels. PPADS inhibited weakly $P2X_{4+6}$ while it had no measurable effects upon oocytes expressing $P2X_4$ subunits alone (Fig. 4.5-B). Low concentrations of RB-2 provided the most dramatic differential effect by inhibiting $P2X_{4+6}$ heteromers while potentiating $P2X_4$ channel activity. Suramin and RB-2 would thus be useful pharmacological tools to investigate the expression of native $P2X_{4+6}$ heteromers in αβmATP-sensitive neuronal preparations.

Biochemical Evidence of $P2X_{4+6}$ Heteropolymers

We demonstrated direct interactions between the two predominant brain $P2X_4$ and $P2X_6$ isoforms through the use of an established co-purification assay (Tinker *et al.*, 1996). Based upon our co-precipitation results with epitope-tagged subunits in non-denaturing conditions, $P2X_4$ associate with $P2X_6$ subunits (Fig. 4.6-B). In *Xenopus* oocytes, this heteropolymerization underlies the specific pharmacological and electrophysiological phenotype of a novel heteromeric channel distinct from either $P2X_4$ or $P2X_6$ homomeric receptors. On the other hand, $P2X_4$ and $P2X_1$ subunits did not seem to interact significantly with each other (Fig. 4.6-B). Furthermore, the absence of obvious phenotypical differences between oocytes co-expressing $P2X_6$ + $P2X_1$ and $P2X_1$ subunits alone (Fig. 4.1-C), or between $P2X_6$ + $P2X_2$ and $P2X_2$ homomers (Fig. 4.1-D), indicate that structural determinants of association between $P2X_4$ and $P2X_6$ isoforms are subunit-dependent. A similar biochemical approach using co-purification of $P2X_4$ with chimeric subunits based on $P2X_6$ and $P2X_1$ structures could lead to the identification of the domain(s) involved in this specific heteropolymerization.

Functional Correlates of Native $P2X_{4+6}$ Heteromers

Purinergic responses from CA3 neurons in rat hippocampal slices have been recently shown to be activated by αβmATP and inhibited by suramin but not by PPADS (Ross *et al.*, 1998). Based upon *in situ* hybridization results (Collo *et al.*, 1996), $P2X_4$ and $P2X_6$ are the only P_{2X} subunits expressed at significant levels in adult rat hippocampus, namely in CA1-CA4 hippocampal subfields and in the dentate gyrus. Thus, our functional data obtained from recombinant receptors are in close agreement with this

native phenotype and suggest that the sensitivities to αβmATP and to suramin of rat CA3 neurons might be mediated through native $P2X_{4+6}$ heteromeric channels.

Neonatal rat cerebellar Purkinje cells have been characterized as having purinergic receptors with $P2X_2$-like pharmacological profile in eliciting extracellular calcium influxes (Mateo *et al.*, 1998). This conclusion rested upon αβmATP insensitivity, potency ratio ATP/2MeSATP, as well as suramin and PPADS blockade after pre-incubation. However, on recombinant $P2X_{4+6}$ receptors, the concentration of αβmATP used in Mateo *et al.* (50 μM; 1998) was roughly 10% as efficacious as 50 μM ATP in eliciting ionotropic responses so αβmATP-mediated intracellular calcium increases could have remained undetected, and consequently interpretated as αβmATP unresponsiveness. The developmental regulation of expression levels of neuronal P_{2X} genes in cerebellum is not established so far. Adult rat Purkinje neurons are known to transcribe $P2X_4$ and $P2X_6$ mRNA (Collo *et al.*, 1996) and have been shown to translate high levels of $P2X_4$ subunits (Lê *et al.*, 1998), whereby $P2X_2$ mRNAs (Collo *et al.*, 1996) or subunits (Vulchanova *et al.*, 1996) were previously reported to be absent (but see Kanijhan *et al.*, 1996). It is also possible that native P_{2X} receptors in neonatal Purkinje cells are composed of three subunits, namely $P2X_2$, $P2X_4$ and $P2X_6$, assembled in a heteromeric complex where $P2X_2$ is pharmacologically dominant.

We have recorded in oocytes purinergic currents mediated by $P2X_{4+6}$ heteromeric channels that were significantly more sensitive to the agonists αβmATP and 2MeSATP, as well as to the antagonist suramin compared to $P2X_4$ homomeric receptors. So, it is likely that the moderately desensitizing αβmATP-activated and suramin-sensitive postsynaptic purinergic responses recorded from medial habenula (Edwards *et al.*,

1992) could be accounted for by the expression of postsynaptic $P2X_{4+6}$ receptors, as *in situ* hybridization results demonstrate the exclusive presence of $P2X_4$ and $P2X_6$ transcripts in this region (Collo *et al.*, 1996).

The widespread distribution of high affinity [^{3}H]-αβmATP binding sites within the rat CNS (Michel and Humphrey, 1993; Bo and Burnstock, 1994; Balcar *et al.*, 1995), appears to correlate with *in situ* hybridization data on $P2X_4$ and $P2X_6$ mRNA distributions (Séguéla *et al.*, 1996; Collo *et al.*, 1996) as well as with the immunocytochemical localization of $P2X_4$ protein (Lê *et al.*, 1998). These neuroanatomical evidence strongly suggest that the $P2X_{4+6}$ channel phenotype might be present in most rat brain and spinal cord regions. Moreover, we have shown that $P2X_4$ subunit is a major presynaptic purinoceptor component in laminae I-II of spinal cord and in olfactory glomeruli (Lê *et al.*, 1998), two regions where $P2X_6$ is also expressed (Collo *et al.*, 1996), therefore the heteromeric $P2X_{4+6}$ ATP-gated cation channels could play a significant role in the regulation of excitatory transmitter releases in central sensory synapses.

FIGURE 4.1 Representative heteromultimeric $P2X_{4+6}$ channel current phenotype. (**A**) ATP-induced currents following heterologous expression of $P2X_4$, $P2X_6$, and $P2X_4$ + $P2X_6$ (1:1 molar ratio) subunits recorded 3 days after corresponding cDNA nuclear micro-injections in *Xenopus* oocytes. (**B**) $P2X_4$-dependent functional impact of $P2X_6$ on ATP-induced response ($P2X_4$ expressed alone 1x: 5 ng of cDNA, 2x: 10 ng). (**C**) $P2X_1$ receptor ($P2X_1$ 1x: 5 ng, 2x: 10 ng) functional expression is unaffected by co-expressed $P2X_6$ subunits. (**D**) $P2X_2$-mediated ($P2X_2$ 1x: 5 ng, 2x: 10 ng) ATP-induced peak current amplitudes are unchanged in the presence of $P2X_6$ subunits (average ± SEM values from 3-15 oocytes in 2-4 independant experiments, double asterisks denote significant difference with $p < 0.01$).

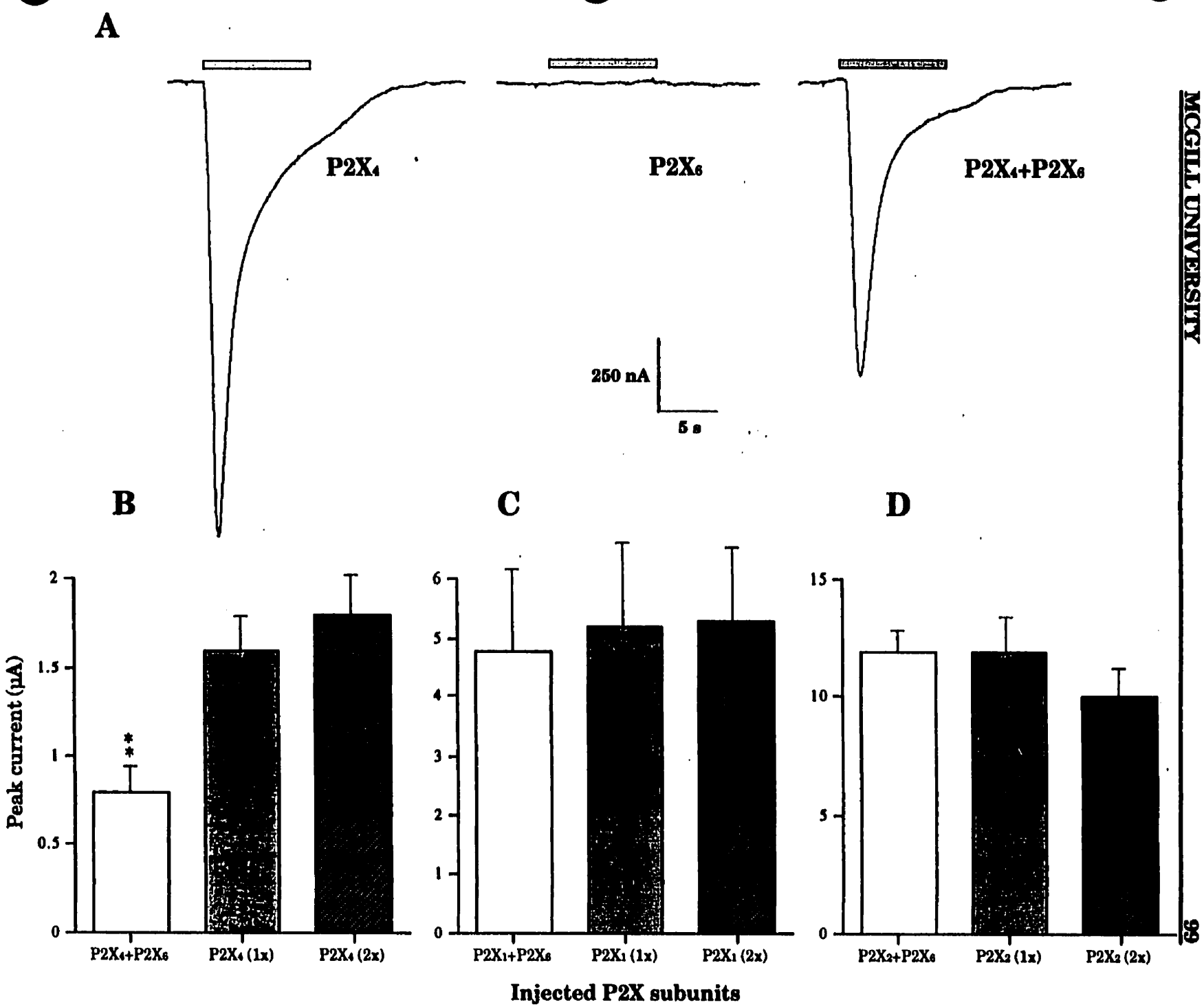

MCGILL UNIVERSITY

FIGURE 4.2 Time-course of heteromultimeric $P2X_{4+6}$ expression. Kinetics of appearance of functional ATP receptors on plasma membranes is strikingly different in oocytes co-injected with $P2X_4$ + $P2X_6$ subunits compared to those injected with $P2X_4$ subunits (average ± SEM values from 3-15 oocytes in 2-8 independent experiments).

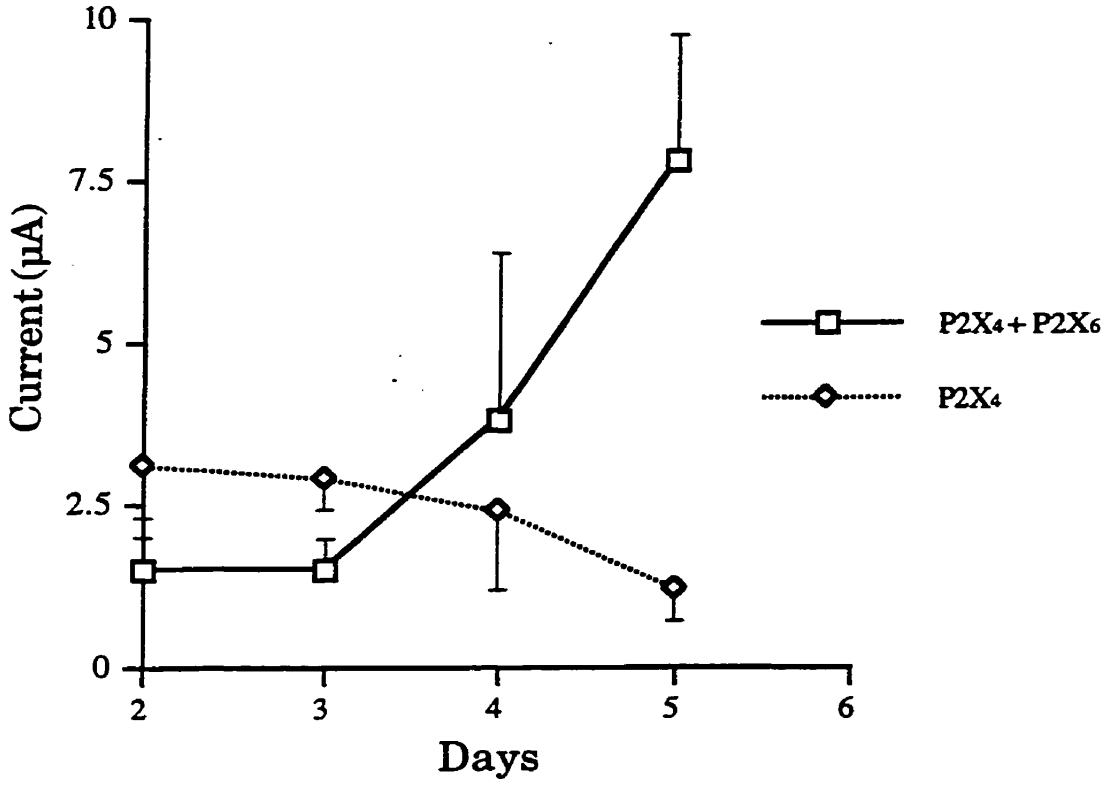
10
7.5
5
2.5
0
Current (μA)
2
3
4
5
6
Days
P2X4 + P2X6
P2X4

FIGURE 4.3 Sensitivity of $P2X_{4+6}$ receptors to ATP and 2MeSATP agonists. (**A**) Similar ATP dose-response profile between heteromeric $P2X_{4+6}$ channels and homomeric $P2X_4$ receptors in *Xenopus* oocytes. (**B**) Heteromultimeric $P2X_{4+6}$ receptors showed increased sensitivity to 2MeSATP compared to $P2X_4$ receptors. Values are normalized to the response to 300 μM ATP (averages ± SEM from 3-7 oocytes/point in two independent experiments).

A

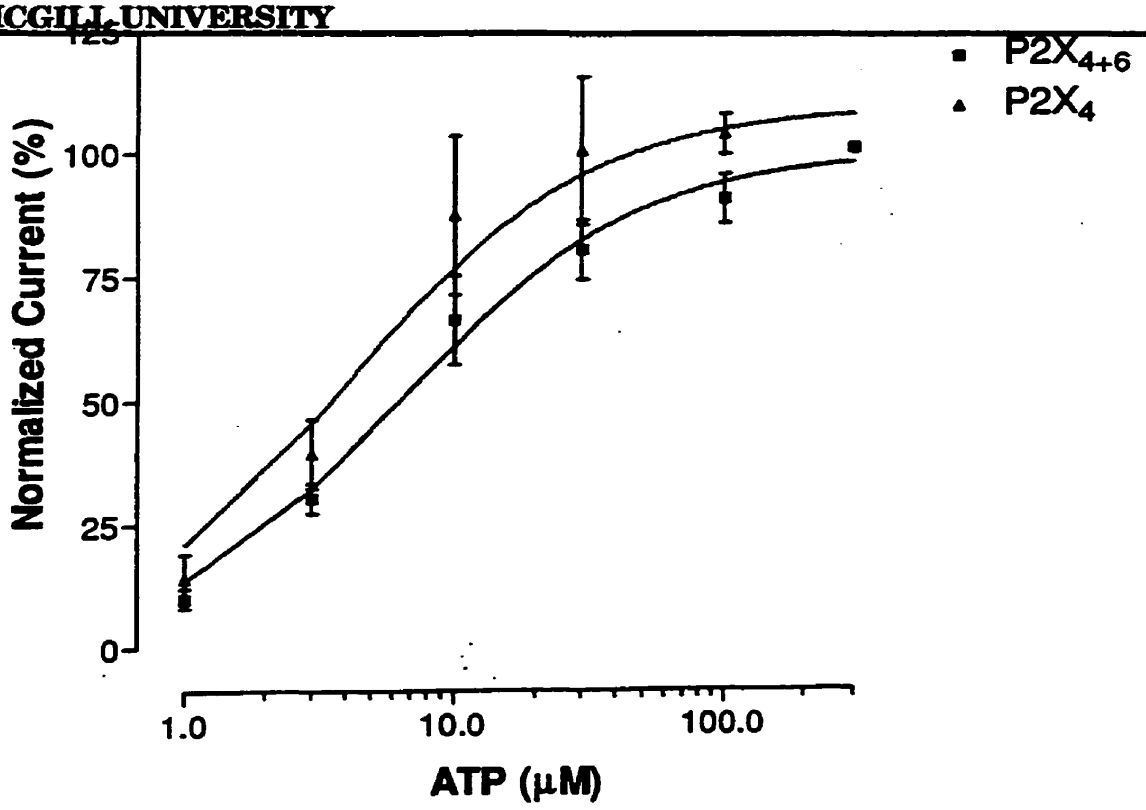
Normalized Current (%)
125
100
75
50
25
0
1.0
10.0
100.0
ATP (μM)
P2X4+6
P2X4

B

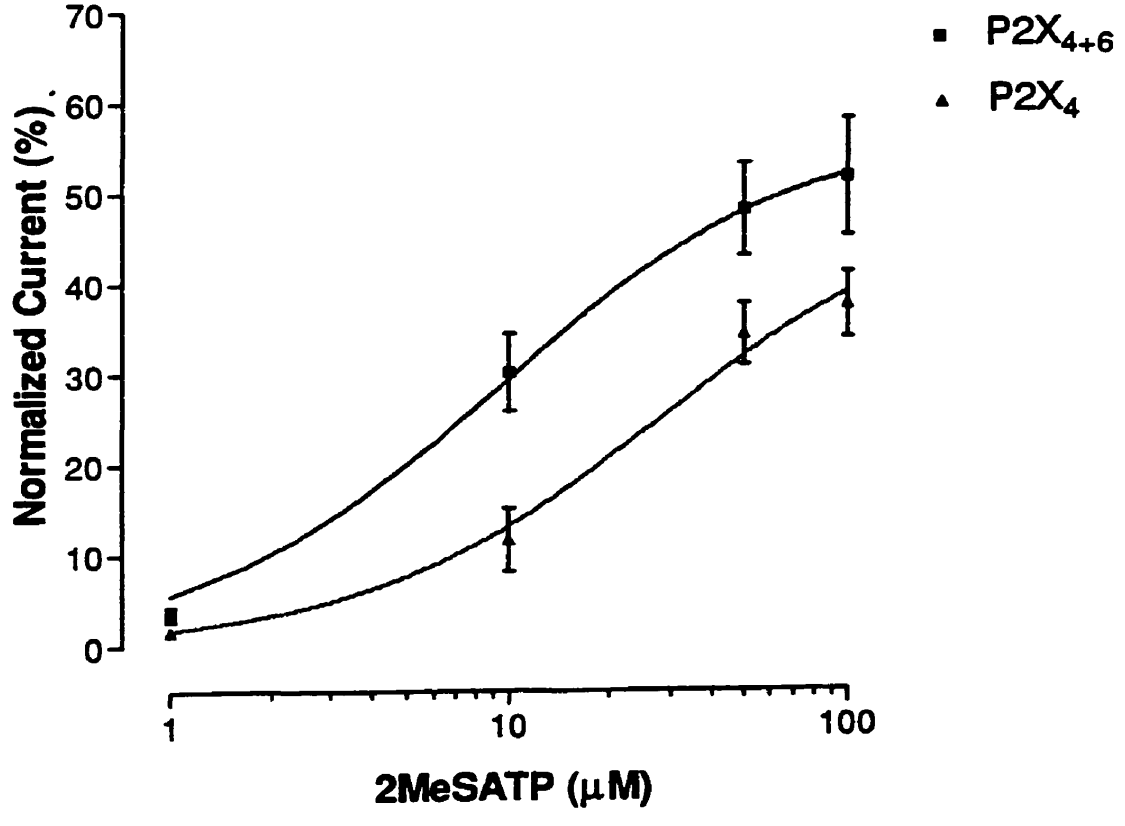
Normalized Current (%)
70
60
50
40
30
20
10
0
1
10
100
2MeSATP (μM)
P2X4+6
P2X4

FIGURE 4.4 Sensitivity of $P2X_{4+6}$ receptors to the agonist αβmATP. (**A**) Differential αβmATP responsiveness measured in peak current amplitudes between *Xenopus* oocytes expressing either $P2X_{4+6}$ channels or $P2X_4$ at day 3 after injection, see Fig. 4.1-B for comparison of ATP-induced peak currents. (**B**) Normalized dose-response curves of $P2X_{4+6}$ and $P2X_4$ receptor species for αβmATP. Values are normalized to the response to 100 μM ATP, double asterisks denote significant difference with $p < 0.01$ (averages ± SEM from 5-8 oocytes/point in two independent experiments).

A

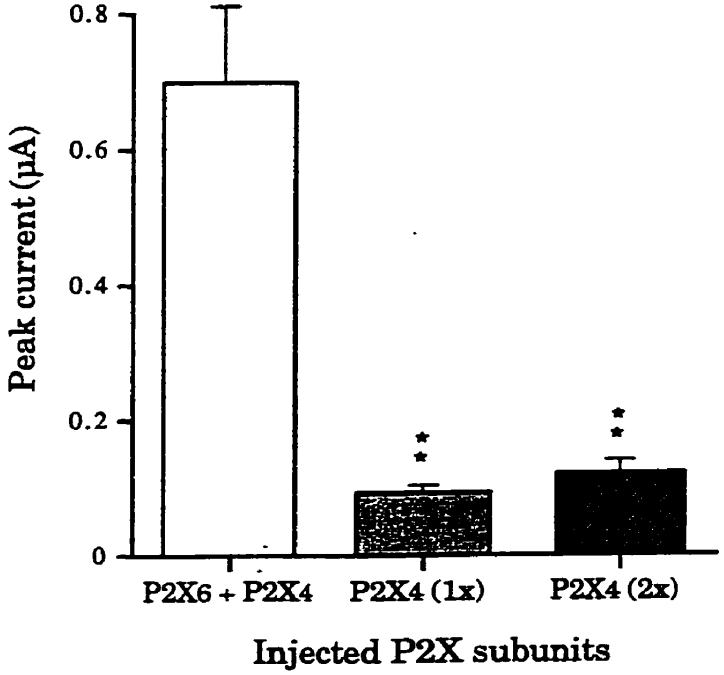
0.8
0.6
0.4
0.2
0
Peak current (μA)
P2X6 + P2X4
P2X4 (1x)
P2X4 (2x)
Injected P2X subunits

B

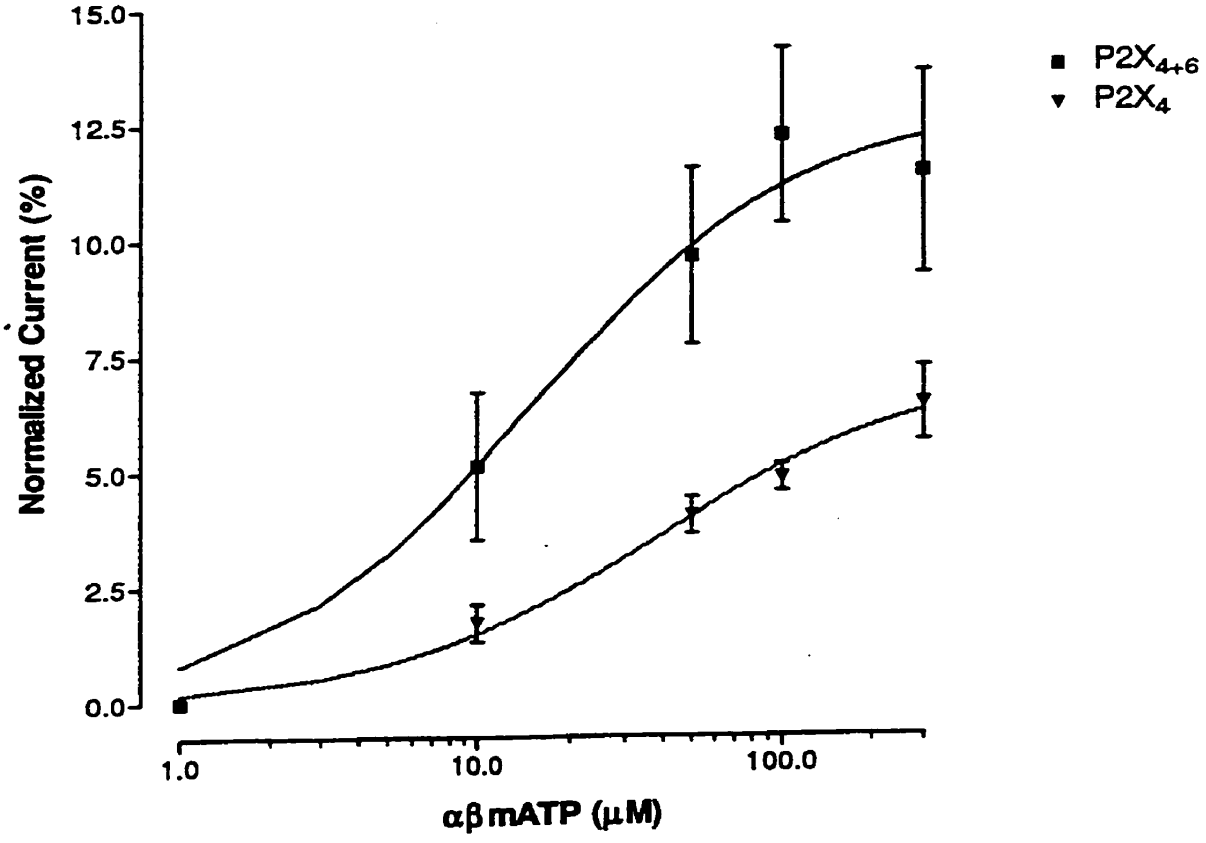
15.0
12.5
10.0
7.5
5.0
2.5
0.0
Normalized Current (%)
1.0
10.0
100.0
αβmATP (μM)
P2X4+6
P2X4

FIGURE 4.5 Sensitivity of $P2X_{4+6}$ to P_{2X} antagonists. Suramin, PPADS, and RB-2 were tested for their blocking properties on heteromeric $P2X_{4+6}$ channels and on homomeric $P2X_4$ receptors. Note that $P2X_{4+6}$ receptors are inhibited while $P2X_4$ receptors are potentiated by 10 μM RB-2. Values are normalized to the response to ATP only (averages ± SEM from 5 oocytes/experiment, one and two asterisks denote significant difference with $p < 0.05$ and 0.01, respectively).

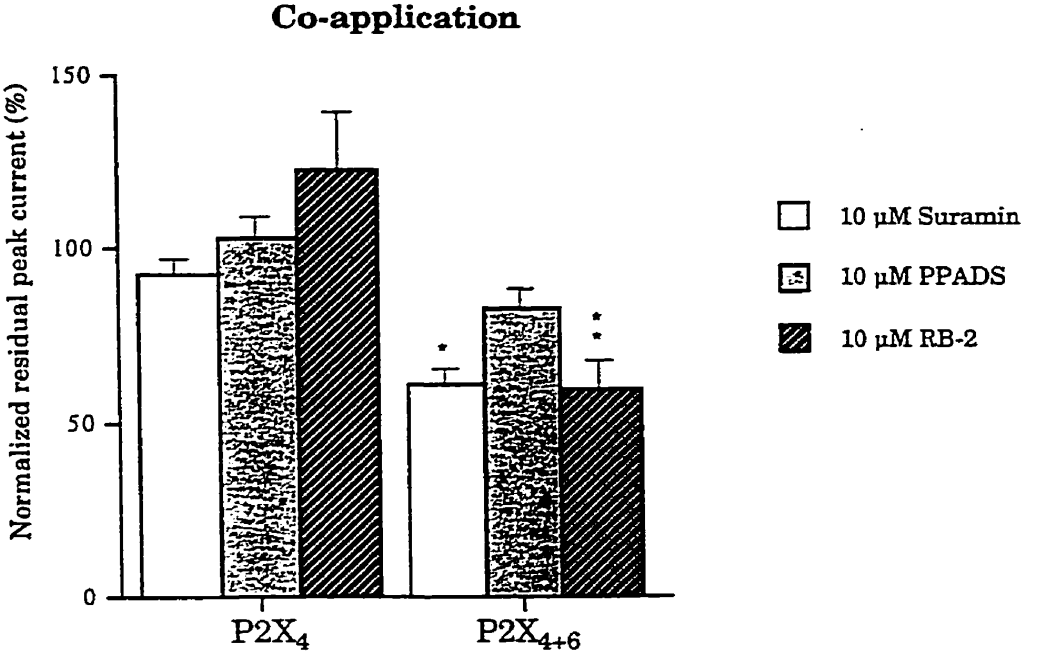
Co-application
Normalized residual peak current (%)
150
100
50
0
P2X4
P2X4+6
10 µM Suramin
10 µM PPADS
10 µM RB-2

B

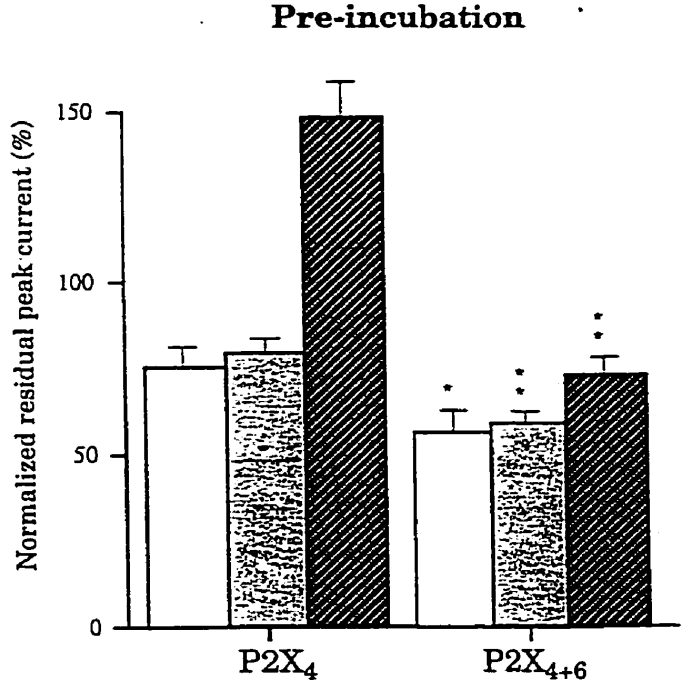
Pre-incubation
Normalized residual peak current (%)
150
100
50
0
P2X4
P2X4+6

FIGURE 4.6 Sensitivity of $P2X_{4+6}$ to the extracellular co-factors zinc ions and pH. Extracellular Zn^{++}, pH 6.5 and pH 8.0, co-applied with ATP, did not allow to differentiate between $P2X_{4+6}$ or $P2X_4$ receptors. Values are normalized to the response to ATP only (averages ± SEM from 4 oocytes/experiment).

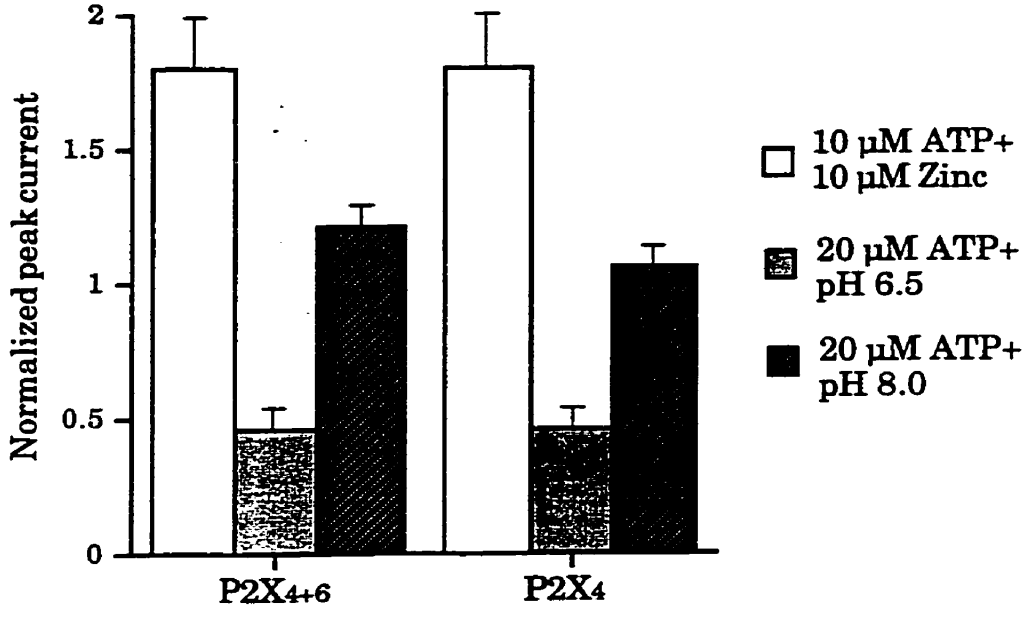
Normalized peak current
2
1.5
1
0.5
0
P2X4+6
P2X4
10 µM ATP+
10 µM Zinc
20 µM ATP+
pH 6.5
20 µM ATP+
pH 8.0

FIGURE 4.7 Subunit-specificity of $P2X_4$ + $P2X_6$ heteropolymerization. (**A**) Immunoblot of Flag-tagged $P2X_1$, $P2X_4$ and $P2X_6$ subunits probed with anti-Flag M2 monoclonal antibodies in total membrane proteins from transiently transfected HEK-293A cells. (**B**) From the same samples, immunoblot of Flag-tagged $P2X_1$, $P2X_4$ and $P2X_6$ subunits probed with M2 antibodies after co-purification through $P2X_4$-$(His)_6$ subunits. Co-transfections in lane 1: $P2X_4$-$(His)_6$ + $P2X_4$-Flag; lane 2: $P2X_4$-WT + $P2X_4$-Flag; lane 3: $P2X_4$-$(His)_6$ + $P2X_6$-Flag; lane 4: $P2X_4$-WT + $P2X_6$-Flag; lane 5: $P2X_4$-$(His)_6$ + $P2X_1$-Flag; lane 6: $P2X_4$-WT + $P2X_1$-Flag.

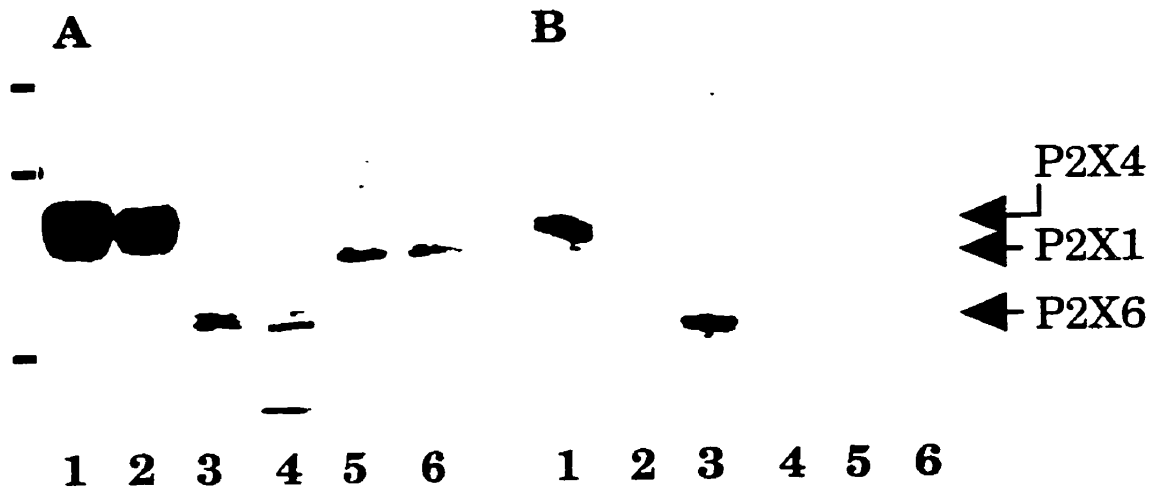
A
B
P2X4
P2X1
P2X6
1 2 3 4 5 6 1 2 3 4 5 6

CHAPTER 5

5.1 RESEARCH RATIONALE

αβmATP autoradiography binding sites have been reported for various spinal cord laminae (Michel and Humphrey, 1993; Bo and Burnstock, 1994; Balcar *et al.*, 1995). Moreover, $P2X_1$ and $P2X_5$ (Collo *et al.*, 1996; Garcia-Guzman *et al.*, 1996) mRNAs have been shown to be predominantly transcribed in an overlapping fashion within the ventral horn of the spinal cord (Collo *et al.*, 1996). Further, both $P2X_1$ and $P2X_5$ have also been reported to be present within sensory neurons (Collo *et al.*, 1996). Moreover, heteropolymeric $P2X_{2+3}$ receptor phenotype composed of co-assembled $P2X_2$ (Brake *et al.*, 1994) and $P2X_3$ subunits seemed to account for native P_{2X} responses recorded from various sensory ganglia (Lewis *et al.*, 1995).

However, it has recently been shown using immunocytochemistry that $P2X_2$ and $P2X_3$ subunits did not co-localize extensively in sensory neurons (Vulchanova *et al.*, 1997). At this point, it was known that hetero-multimeric $P2X_{2+3}$ (Lewis *et al.*, 1995; Radford *et al.*, 1997) and $P2X_{4+6}$ (Lê *et al.*, 1998b) receptor phenotypes were present in the peripheral nervous system and brain, respectively. Similarly, heteropolymeric $P2X_{1+5}$ channels might be expressed by motoneurons within the ventral horn of the spinal cord as well as primary sensory neurons.

Therefore, looking for channels generated from the assembly of P_{2X} subunits from two distinct functional groups, this study was undertaken based upon similar methodology as the $P2X_{4+6}$ heteromultimerization project (Lê *et al.*, 1998b). The existence of $P2X_{1+5}$ receptors, co-assembled from $P2X_1$ and $P2X_5$ subunits, was assayed functionally and biochemically, demonstrating that this hybrid complex is similar to $P2X_{2+3}$ receptors in terms of pharmacology as well as channel kinetics, likely accounting for native responses recorded from sensory neurons lacking co-localized $P2X_2$ and $P2X_3$ proteins.

5.2 MANUSCRIPT REPRINT

FUNCTIONAL AND BIOCHEMICAL EVIDENCE FOR HETEROMERIC ATP-GATED CHANNELS COMPOSED OF $P2X_1$ AND $P2X_5$ SUBUNITS

KHANH-TUOC LÊ, ÉRIC BOUÉ-GRABOT, VINCENT ARCHAMBAULT,

AND PHILIPPE SÉGUÉLA. (1999)

JOURNAL OF BIOLOGICAL CHEMISTRY **274**: 15415-15419

ABSTRACT

The mammalian P_{2X} receptor gene family encodes two-transmembrane domain non-selective cation channels gated by extracellular ATP. Anatomical localization data obtained by *in situ* hybridization and immunocytochemistry have shown that neuronal P_{2X} subunits are expressed in specific but overlapping distribution patterns. Therefore, the native ionotropic ATP receptor diversity most likely arises from interactions between different P_{2X} subunits that generate heteromultimers phenotypically distinct from homomeric channels. Rat $P2X_1$ and $P2X_5$ mRNAs are localized within common subsets of peripheral and central sensory neurons as well as spinal motoneurons. The present study demonstrates a functional association between $P2X_1$ and $P2X_5$ subunits giving rise to hybrid ATP-gated channels endowed with the pharmacology of $P2X_1$ and the kinetics of $P2X_5$. When expressed in *Xenopus* oocytes, hetero-oligomeric $P2X_{1+5}$ receptors were characterized by slowly desensitizing currents highly sensitive to the agonist α,β-methylene ATP (EC_{50} = 1.1 μM) and to the antagonist trinitrophenyl-ATP (IC_{50} = 64 nM), observed with neither $P2X_1$ nor $P2X_5$ alone. Direct physical evidence for $P2X_{1+5}$ co-assembly was provided by reciprocal subunit-specific co-purifications between epitope-tagged $P2X_1$ and $P2X_5$ subunits transfected in HEK-293A cells.

INTRODUCTION

Ionotropic ATP receptors constitute a unique class of neurotransmitter-gated ion channels generated from the assembly of P_{2X} subunits having two transmembrane-spanning domains and a protein architecture similar to amiloride-sensitive sodium channels (Buell *et al.*, 1996; North and Barnard, 1997). Functional characterization studies of

the seven cloned P_{2X} subunits heterologously expressed as homomeric channels allowed to classify them in three groups according to their properties of desensitization and to their sensitivity to the agonist α,β-methylene ATP (αβmATP), namely, rapidly desensitizing and αβmATP-sensitive receptors including $P2X_1$ and $P2X_3$ (Valera *et al.*, 1994; Chen *et al.*, 1995; Lewis *et al.*, 1995); moderately desensitizing and αβmATP-insensitive receptors including $P2X_4$ and $P2X_6$ (Bo *et al.*, 1995; Buell *et al.*, 1996; Collo *et al.*, 1996; Garcia-Guzman *et al.*, 1996; Séguéla *et al.*, 1996; Soto *et al.*, 1996; Wang *et al.*, 1996); and non-desensitizing as well as αβmATP-insensitive receptors including $P2X_2$, $P2X_5$, and $P2X_7$ (Brake *et al.*, 1994; Collo *et al.*, 1996; Garcia-Guzman *et al.*, 1996; Surprenant *et al.*, 1996). Results from Northern blots and *in situ* hybridization data (Collo *et al.*, 1996) have indicated that the six neuronal P_{2X} subunit-encoding genes are transcribed in specific but overlapping populations in both central and peripheral nervous systems (Buell *et al.*, 1996; Collo *et al.*, 1996). This strongly suggests that neuronal P_{2X} subunits belonging to different functional groups might co-assemble into heteromultimeric channels.

All P_{2X} subunits have been detected in peripheral sensory ganglia, reinforcing the view that synaptically or lytically released ATP could play an important signaling role in sensory pathways (Buell *et al.*, 1996; Collo *et al.*, 1996; Cook *et al.*, 1997). Rat $P2X_3$ subunits have been reported to be exclusively expressed in small to medium-sized isolectin B4-positive nociceptive neurons in nodose, trigeminal, and dorsal root ganglia (Chen *et al.*, 1995; Lewis *et al.*, 1995; Cook *et al.*, 1997). A significant proportion of sensory neurons are thought to express hetero-oligomeric $P2X_{2+3}$ receptors based on their sustained response to αβmATP applications (Lewis *et al.*, 1995). However, recent immunocytochemistry results have demonstrated that $P2X_2$ and $P2X_3$ subunits in rat dorsal root

ganglia are rarely co-localized at the level of central primary afferents in the dorsal horn of the spinal cord, despite their high degree of co-localization in somata, indicating different subunit-specific subcellular targetings (Vulchanova *et al.*, 1997). Altogether, these data suggest that physiologically-relevant associations of neuronal P_{2X} subunits, giving rise to phenotypes that are not mediated by the previously described $P2X_{2+3}$ (Lewis *et al.*, 1995; Radford *et al.*, 1997) or $P2X_{4+6}$ (Lê *et al.*, 1998) receptors, remain to be discovered.

Rat $P2X_5$ subunit-encoding mRNAs have the most restricted distribution in the P_{2X} family, yet, *in situ* hybridization studies have indicated that $P2X_1$ and $P2X_5$ mRNAs are co-localized in primary sensory neurons as well as within subsets of large motoneurons in the ventral horn of the spinal cord (Buell *et al.*, 1996; Collo *et al.*, 1996). We report here the characterization of a novel heteromeric P_{2X} receptor with hybrid properties generated by co-expression and co-assembly of $P2X_1$ with $P2X_5$ subunits in *Xenopus laevis* oocytes and transfected HEK-293A cells, further strengthening arguments for a diversity of native ATP-gated channels and purinergic phenotypes in mammalian neurons.

MATERIALS AND METHODS

Molecular Biology

Full-length wild-type rat $P2X_1$ and $P2X_5$ cDNAs were obtained through PCR amplifications using A10 smooth muscle cells (ATCC #CRL-1476) and adult rat spinal cord RT-cDNA templates, respectively. Reactions were performed with exact-match oligonu-

cleotide primers based upon published primary sequences (Valera *et al.*, 1994; Collo *et al.*, 1996; Garcia-Guzman *et al.*, 1996) using *Pfu* DNA polymerase (Stratagene) to minimize artifactual mutations. Epitope-tagged P_{2X} subunits with C-terminal hexahistidine motif $(His)_6$ or Flag peptide were constructed as reported previously (Lê *et al.*, 1998). Briefly, an *Xho*I-*Xba*I stuffer cassette containing in-frame Flag or His_6 epitopes followed by an artificial stop codon was ligated to $P2X_1$ and $P2X_5$ cDNAs previously mutated in order to replace their natural stop codon with an *Xho*I restriction site. $P2X_1$-Flag, $P2X_1$-His_6, $P2X_5$-Flag, and $P2X_5$-His_6 were then subcloned directionally into *Hind*III-*Xba*I sites of pcDNAI vector (Invitrogen, San Diego, CA) compatible with CMV-driven heterologous expression in HEK-293A cells and *Xenopus laevis* oocytes. RT-PCR products as well as mutant epitope-tagged subunits were subjected to automatic dideoxy sequencing (Sheldon Biotechnology Center, Montreal, QC).

Cell Culture and Protein Chemistry

cDNA transfections of epitope-tagged P_{2X} subunits were performed in mammalian cells. HEK-293A cells (ATCC #CRL-1573) were cultured in Dulbecco's modified Eagle medium and 10% heat-inactivated fetal bovine serum (Wisent, St. Bruno, QC) containing penicillin and streptomycin. Cells reaching 30-50% confluency were used for transient cDNA transfections with the calcium phosphate method with 10 μg of supercoiled plasmid cDNA per 10^6 cells. Transfected HEK-293A cells used for Western blots were then lifted in Hank's modified calcium-free medium with 20 mM EDTA, pelleted at low centrifugation, and homogenized in 10 volumes of 10 mM HEPES buffered at pH 7.4 with 0.3 M sucrose including protease inhibitors phenylmethylsulfonyl fluoride (0.2 mM) and benzamidine (1 mM). Membranes from cell lysates were solubilized with 1% Triton X-

100 (Sigma) for 2 h at 4 °C, pelleted at 14 000 x *g* for 5 min, and remaining membrane proteins within supernatants were used for Western blots. Solubilized proteins were incubated with 25 µl of equilibrated Ni-NTA resin (Qiagen, Hilden, Germany) for 2 h at 4 °C under agitation. Then Ni-NTA beads were washed six times in Tris-buffered saline containing 25 mM imidazole and 1% Triton X-100. Bound proteins were eluted from His_6-binding resin with 500 mM imidazole, diluted 1:1 (v/v) with SDS-containing loading buffer. Samples were then loaded onto 10-12% SDS-PAGE and transferred to nitrocellulose. Immunostainings were performed with M2 murine monoclonal antibodies (10 µg/ml) (Sigma) or chicken anti-Flag polyclonal antibodies (1:200) (Aves) followed by incubations with corresponding species-specific peroxidase-labeled secondary antibodies (1:5 000-1:20 000) for visualization by ECL (Amersham).

Electrophysiology

Electrophysiological recordings were performed in *Xenopus* oocytes. Ovary lobes were surgically retrieved from *Xenopus laevis* frogs under deep tricaine (Sigma) anesthesia. Oocyte-containing lobes were then treated for 3 h at room temperature with type II collagenase (Life Technologies, Gaithersburg, MD) in calcium-free Barth's solution under vigorous agitations. Stages V-VI oocytes were then chemically defolliculated before nuclear micro-injections of 5-10 ng of cDNA coding for each P_{2X} channel subunits. Following 2-5 days of incubation at 19 °C in Barth's solution containing 1.8 mM calcium chloride and 10 µg/ml gentamicin (Sigma), elicited P_{2X} currents were recorded in a two-electrode voltage-clamp configuration using an OC-725B amplifier (Warner Instruments). Responsive signals were low-pass filtered at 1 kHz, acquired at 500 Hz using a Macintosh IIci computer equipped with a NB-MIO-16XL analog-to-digital card (Natio-

nal Instruments). Recorded traces were post-filtered at 100 Hz in Axograph (Axon Instruments). Agonists, antagonists, and P_{2X} co-factors (10 μM zinc chloride, pH 6.4, and pH 8.4) were prepared at room temperature in Ringer's perfusion solution containing 115 mM NaCl, 2.5 mM KCl, 1.8 mM $CaCl_2$, and 10 mM HEPES buffered at pH 7.4. Solutions were perfused onto oocytes at a constant flow rate of 10-12 ml/min. Dose-response curves were fitted to the Hill sigmoidal equation, and EC_{50} as well as IC_{50} values were determined using the software Prism 2.0 (Graphpad, San Diego, CA).

RESULTS AND DISCUSSION

To assess the presence of $P2X_{1+5}$ heteromers in *Xenopus* oocytes co-injected with both subunits, we tested the expression of inward currents during prolonged applications (5-10 s) of 50 μM αβmATP, exploiting the fact that homomeric $P2X_5$ channels are almost insensitive to this agonist when applied at concentrations below 100 μM (Fig. 5.1) (Collo *et al.*, 1996; Garcia-Guzman *et al.*, 1996); homomeric $P2X_1$ receptors desensitize strongly in the first seconds of agonist applications; whereas a slowly-desensitizing response induced by 50 μM αβmATP was observed in oocytes co-injected with $P2X_1$ and $P2X_5$ subunits in a 1:1 cDNA molar ratio (Fig. 5.1). This hybrid phenotype was the unambigous trademark of the expression of heteromeric $P2X_{1+5}$ receptors. Oocytes expressing $P2X_{1+5}$ receptors showed robust 50 μM αβmATP-induced whole-cell currents with amplitudes in the range of 3-15 μA at V_h = -50 mV after 2-5 days of post-injection time, similar to currents recorded from oocytes expressing $P2X_1$ alone (Fig. 5.1).

$P2X_{1+5}$ receptors slowly desensitized during agonist applications but showed complete recovery within 2 min (Fig. 5.2), a noticeable difference with homomeric $P2X_5$ receptors

that do not desensitize in heterologous systems (Fig. 5.1) (Collo *et al.*, 1996; Garcia-Guzman *et al.*, 1996). However, $P2X_{1+5}$ receptors (Fig. 5.2-B, D) recovered significantly faster than $P2X_1$ receptors, the latter recovering less than 50% of their initial response after 5 min of washout (Fig. 5.2-A, C). We noticed slight differences in the rate of desensitization of $P2X_{1+5}$ receptors between oocytes (Fig. 5.2). These phenotypic variations could be due to the expression of populations of heteromeric channels with different subunit stoichiometries, a cell-dependent variable that is not controlled in these experiments of co-injections. The kinetic properties of $P2X_2$ receptors have been shown to be modulated by protein kinase A activity (Chow *et al.*, 1998). Thus, it is possible that inter-individual differences in the levels of endogenous kinase activity present in oocytes could have some impact on the properties of desensitization of $P2X_{1+5}$ receptors. Furthermore, the correlation between the number of $P2X_5$ subunits and the kinetic properties of the oligomeric complex, that has been reported to be a trimer for homomeric $P2X_1$ channels (Nicke *et al.*, 1998), is not yet known.

$P2X_{1+5}$ receptors were challenged with ATP, $\alpha\beta$mATP, and ADP at various concentrations for comparision with the pharmacology of homomeric $P2X_1$ and $P2X_5$ receptors. We measured EC_{50} values for $P2X_{1+5}$ heteromers of 0.4 ± 0.2 μM for ATP, 1.1 ± 0.6 μM for $\alpha\beta$mATP, and 13 ± 4 μM for ADP (Fig. 5.3). These EC_{50} values were not significantly different from those obtained with homomeric $P2X_1$ receptors in the same experimental conditions, namely, 0.7 ± 0.1 μM for ATP, 2.4 ± 1 μM for $\alpha\beta$mATP, and 47 ± 9 μM for ADP (Fig. 5.3), in good agreement with previously published data (Valera *et al.*, 1994). Differences in the apparent Hill coefficient n_H (cooperativity index) of ADP activation between $P2X_1$ ($n_H = 4.9 \pm 2.3$) and $P2X_{1+5}$ ($n_H = 1.6 \pm 0.8$) (Fig. 5.3-C) could be due to the fact that we record from a heterogeneous population of $P2X_1$-containing

receptors with varying stoichiometries. Amplitudes of peak currents from $P2X_5$-expressing oocytes were too small to carry out complete dose-response curve experiments with these agonists (Fig. 5.1). No significant differences were observed between $P2X_{1+5}$ and $P2X_1$ receptors during co-applications of extracellular zinc ions (10 μM), protons (pH 6.4), or alkaline solutions (pH 8.4) with sub-saturating ATP concentrations (0.1 μM; data not shown).

Our results suggest that $P2X_1$ subunits confer their high αβmATP sensitivity to the $P2X_{1+5}$ heteromers. Another specific pharmacological property of $P2X_1$ subunits, potent inhibitory effects of trinitrophenyl-ATP (TNP-ATP) (Thomas *et al.*, 1998; Virginio *et al.*, 1998), is observed in the heteromeric receptors (Fig. 5.4-A). In conditions of co-applications of TNP-ATP and αβmATP without pre-incubations, we measured IC_{50} values of 64 ± 14 nM on $P2X_{1+5}$ and 200 ± 120 nM on $P2X_1$ receptors (Fig. 5.4-B). This subunit association is therefore reminiscent of the association between $P2X_2$ and $P2X_3$ in which $P2X_3$ is the pharmacologically dominant component both for αβmATP sensitivity (Chen *et al.*, 1995; Lewis *et al.*, 1995) and TNP-ATP block (Thomas *et al.*, 1998; Virginio *et al.*, 1998).

To demonstrate direct associations between $P2X_1$ and $P2X_5$ subunits that underlie their assembly in hybrid heteromers, we assayed their physical interactions by co-purifying epitope-tagged subunits in transfected HEK-293A cells. Purifying $P2X_5$-His_6 on nickel-binding resin in non-denaturing conditions (see Materials and Methods for details) allowed the detection of co-transfected $P2X_1$-Flag in Western blots (Fig. 5.4, lane C). Reciprocally, $P2X_1$-His_6 was shown to co-assemble with $P2X_5$-Flag (Fig. 5.4, lane D). Positive controls included pseudo-homomeric receptors composed of $P2X_1$-His_6 + $P2X_1$-Flag or

$P2X_5$-His_6 + $P2X_5$-Flag (Fig. 5.4, lanes A and B). Technical controls of transfections with one P_{2X} subunit only or with sham-transfected HEK-293A cells were negative (data not shown).

Peripheral sensory neurons have been reported to express ATP-gated channels with a slow rate of desensitization and a high sensitivity to αβmATP characterized by EC_{50} values in the low micromolar range (Lewis *et al.*, 1995; and references therein). This sensory phenotype was thought to be exclusively accounted for by the co-assembly of $P2X_2$ and $P2X_3$ subunits into heteromeric $P2X_{2+3}$ receptors (Lewis *et al.*, 1995; Radford *et al.*, 1997). Alternatively, we propose from our results that slowly-desensitizing and αβmATP-elicited responses could be mediated by hybrid $P2X_{1+5}$ heteromeric receptors endowed with the pharmacology of $P2X_1$ and the kinetics of $P2X_5$. Our data suggest to use TNP-ATP as a specific antagonist of $P2X_1$-containing ATP-gated channels. In spinal motoneurons whereby $P2X_3$ is absent, complete blockade of slowly-desensitizing P_{2X} responses by 1 μM TNP-ATP would indicate the expression of $P2X_{1+5}$ heteromeric channels.

Using subunit-specific polyclonal antibodies, Vulchanova *et al.* (1996) described a strong $P2X_1$ immunoreactivity in laminae I-II of the spinal cord, corresponding to presynaptic labeling of central axon terminals from dorsal root ganglia sensory neurons. As $P2X_2$ and $P2X_3$ subunits do not appear to co-assemble in heteromeric channels in these primary afferents (Vulchanova *et al.*, 1997), a presynaptic localization of $P2X_{1+5}$ receptors would provide sensory axon terminals with high sensitivity to ATP and slowly-desensitizing voltage-independent calcium entry that could play a modulatory role in the release of central neurotransmitters such as glutamate and substance P (Gu and Mac-

Dermott, 1997). Effects of presynaptic $P2X_{1+5}$ receptors on the release of sensory transmitters can now be experimentally challenged with applications of the blocker TNP-ATP at low concentrations.

In the central nervous system, an important role for purines in motor systems is deduced both from the distribution of several P_{2X} subunit-encoding mRNAs within cranial and spinal motor nuclei (Collo *et al.*, 1996) and from the powerful cellular effects of extracellular ATP on motor outflow (Funk *et al.*, 1997). More specifically, a subset of large projection motoneurons in lamina IX of the rat spinal cord has been characterized by the co-expression of $P2X_1$ and $P2X_5$ subunits (Collo *et al.*, 1996). We propose from their functional properties that highly agonist-sensitive $P2X_{1+5}$ receptors might provide a specific excitatory function to the control of motricity, by allowing a sustained entry of extracellular calcium into motoneurons in responses to minute amounts of released ATP.

FIGURE 5.1 Co-expressions of $P2X_1$ and $P2X_5$ ($P2X_{1+5}$) yielded slowly-desensitizing currents which were activated by αβmATP. Whole-cell currents were recorded from oocytes after nuclear injections with $P2X_1$ cDNA alone, $P2X_5$ cDNA alone, and co-injected $P2X_1$ and $P2X_5$ cDNAs ($P2X_{1+5}$) on prolonged 50 μM αβmATP applications. Fast desensitizations of αβmATP-induced currents occurred from oocytes expressing $P2X_1$ receptors alone but not from those co-expressing $P2X_1$ and $P2X_5$ subunits. On the other hand, $P2X_5$-expressing oocytes showed weak currents toward 50 μM ATP and no detectable responses to 50 μM αβmATP applications. Oocytes were voltage-clamped at V_h=-100 mV. Bars represent durations of agonist applications.

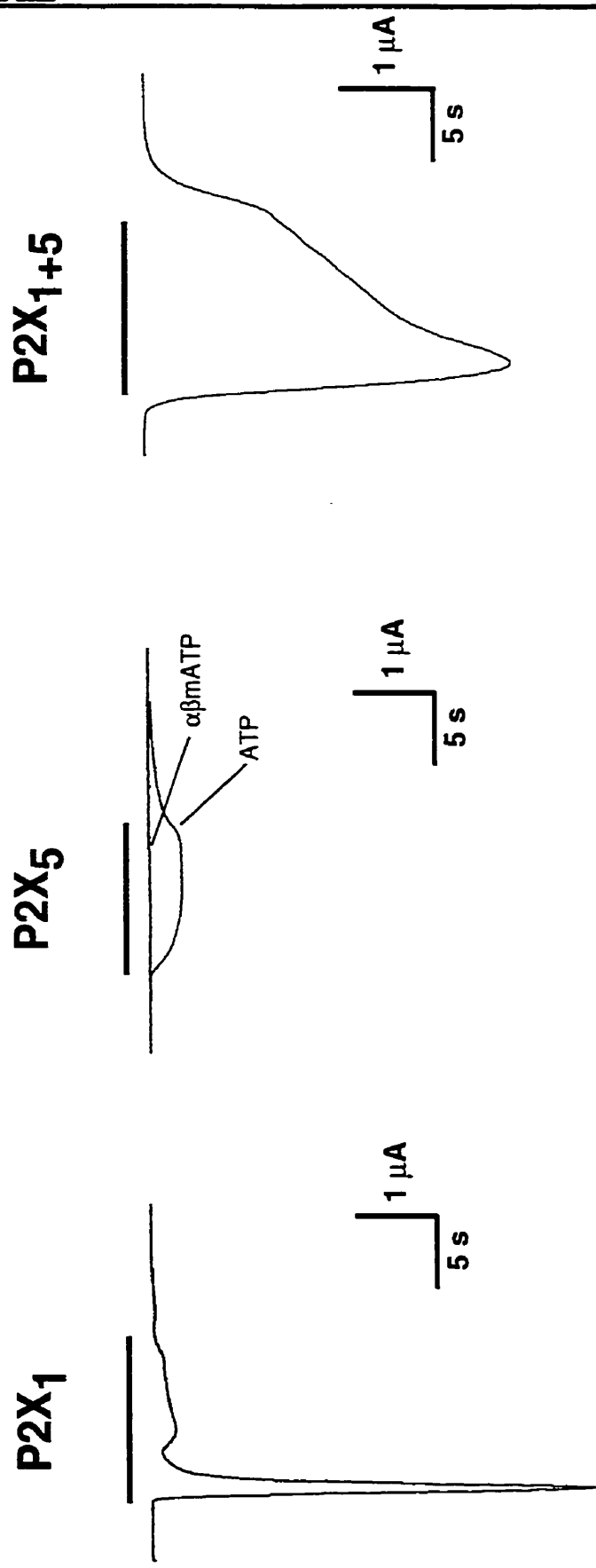
P2X1+5
1 μA
5 s
P2X5
αβmATP
ATP
1 μA
5 s
P2X1
1 μA
5 s

FIGURE 5.2 Desensitization recovery rate comparisions between homomeric $P2X_1$ and hetero-oligomeric $P2X_{1+5}$ receptors. (**A**) and (**B**) represent superimposed whole-cell currents recorded from individual oocytes expressing $P2X_1$ (**A**) or $P2X_{1+5}$ channels (**B**) during 2 applications of αβmATP separeated by different time intervals as indicated. 5-second applications of αβmATP at 1 μM for $P2X_1$ and 10 μM for $P2X_{1+5}$ were recorded at holding potentials of -100 mV. (**C**) and (**D**) represent mean peak currents evoked by repeated applications of αβmATP for $P2X_1$ (**C**) and $P2X_{1+5}$ receptors (**D**). Currents were normalized to the first-response value (t = 0) in the same oocyte (n = 5).

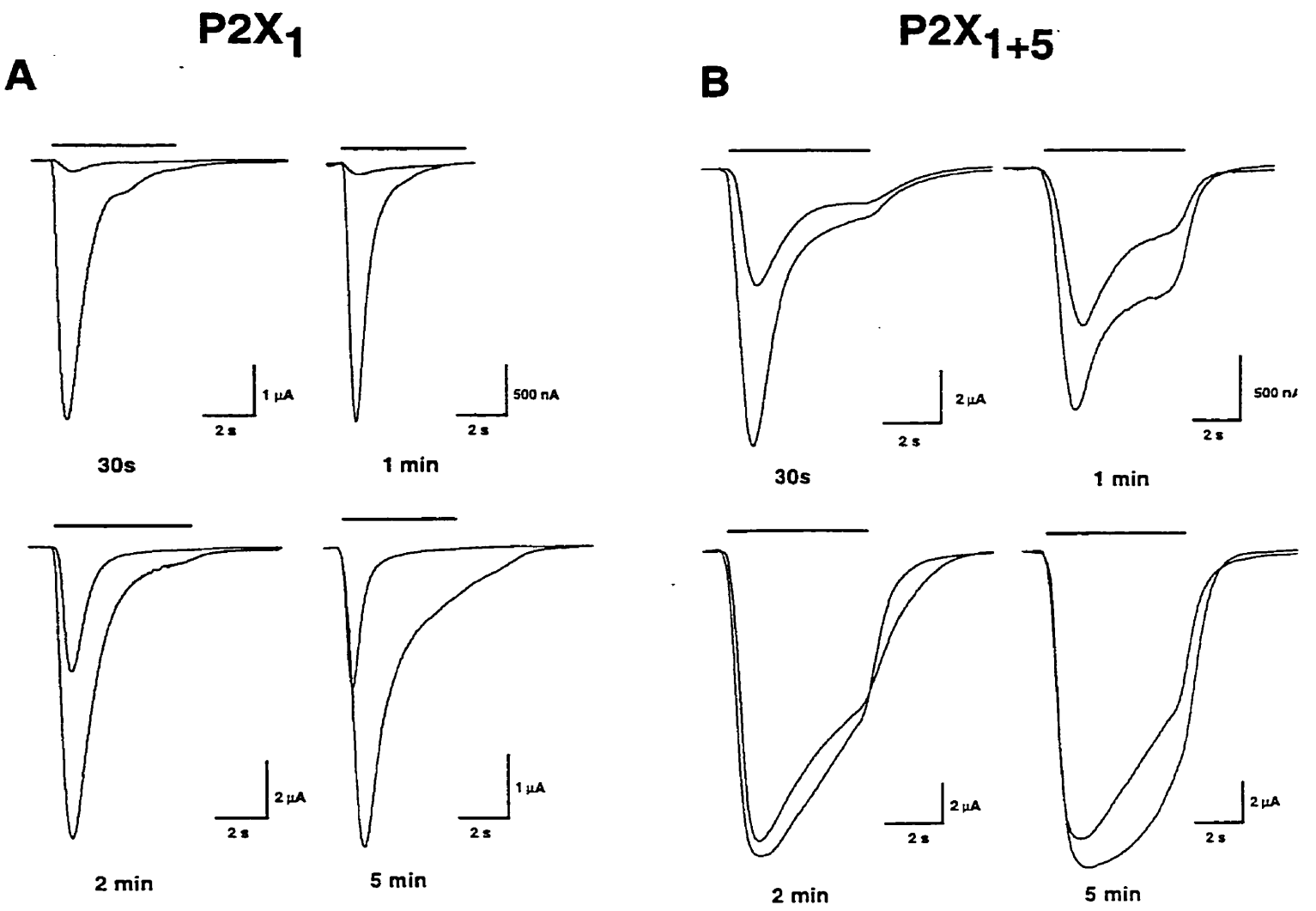
P2X1
P2X1+5
A
B
1 µA
2 s
500 nA
2 s
30s
1 min
2 µA
2 s
500 nA
2 s
30s
1 min
2 µA
2 s
1 µA
2 s
2 min
5 min
2 µA
2 s
2 µA
2 s
2 min
5 min

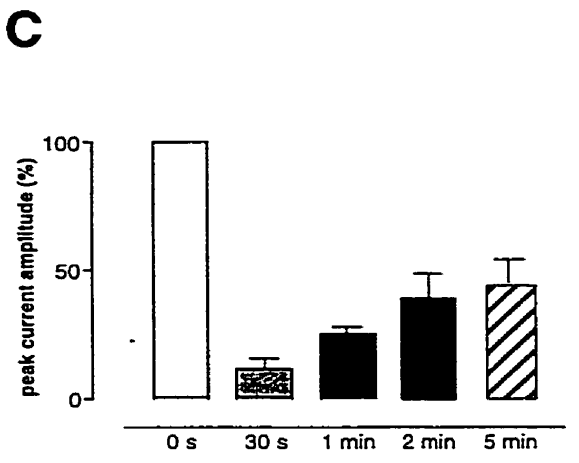
C
peak current amplitude (%)
100
50
0
0 s
30 s
1 min
2 min
5 min

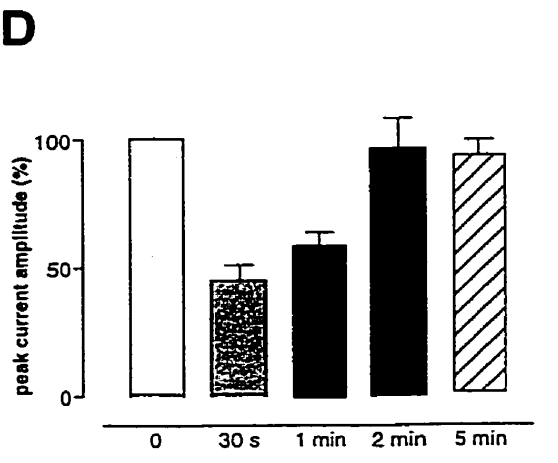
D
peak current amplitude (%)
100
50
0
0
30 s
1 min
2 min
5 min

FIGURE 5.3 $P2X_1$ and $P2X_{1+5}$ receptor sensitivities to purinergic agonists ATP (**A**), αβmATP (**B**), and ADP (**C**). For each agonist concentration-current relationship, average peak currents were normalized to 100 μM ATP responses (average ± SEM from 3-10 oocytes per point). Holding potentials were -50 mV for (**A**), (**B**), and -70 mV for (**C**).

A

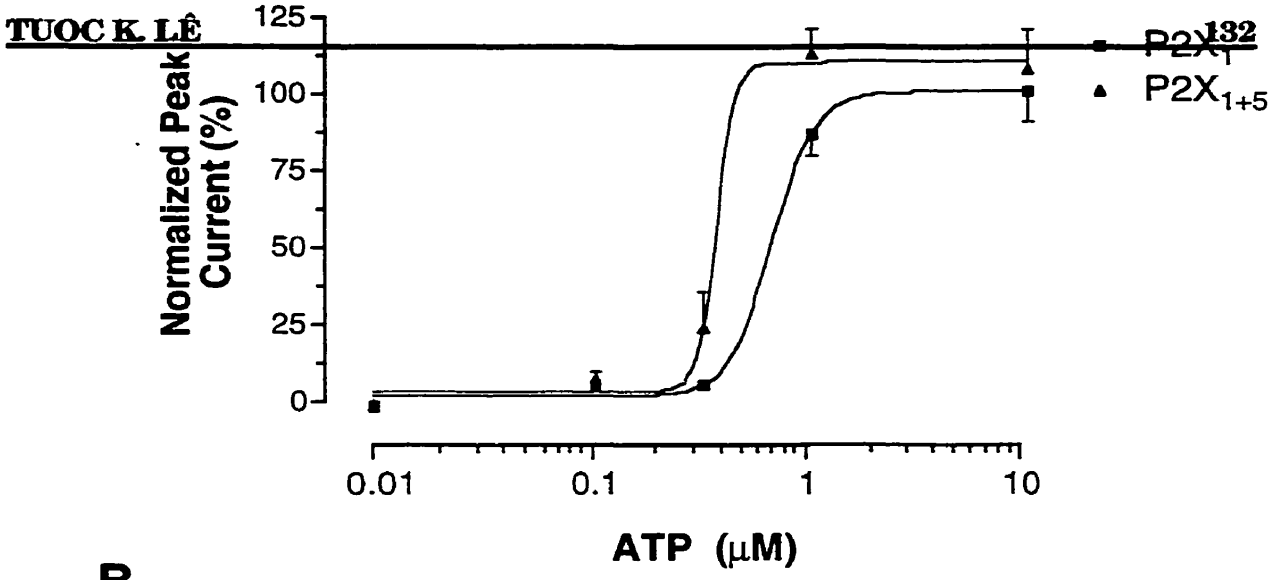
Normalized Peak Current (%)
125
100
75
50
25
0
0.01
0.1
1
10
ATP (μM)
P2X1
P2X1+5

B

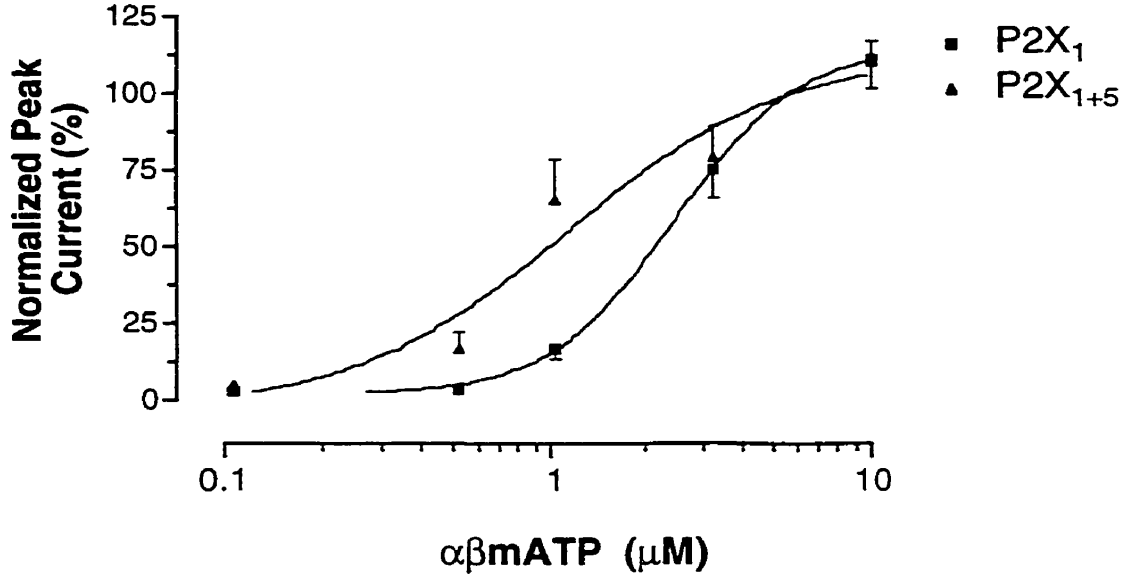
Normalized Peak Current (%)
125
100
75
50
25
0
0.1
1
10
αβmATP (μM)
P2X1
P2X1+5

C

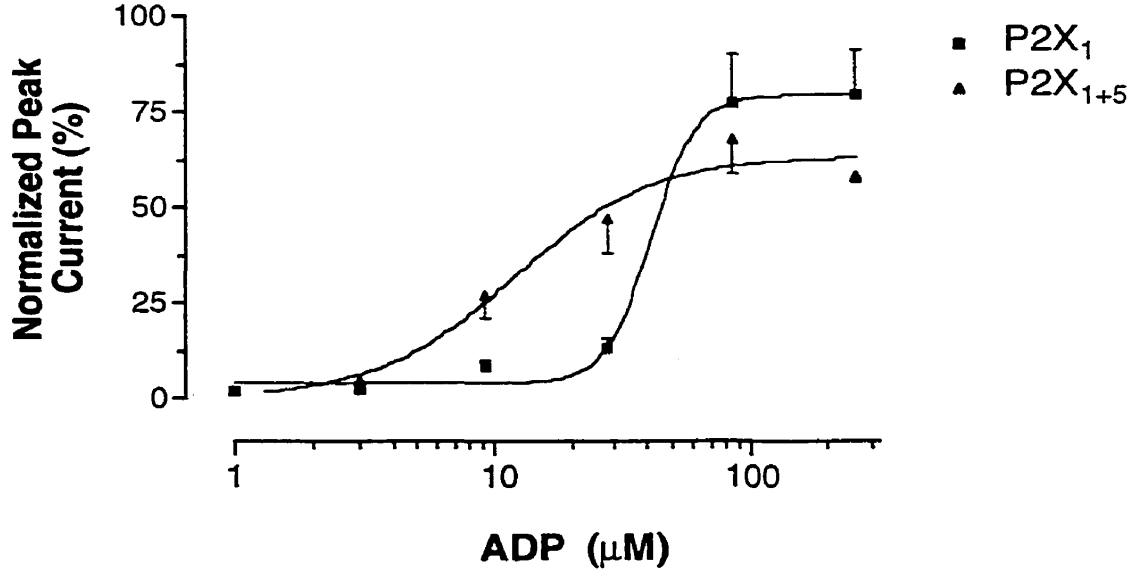
Normalized Peak Current (%)
100
75
50
25
0
1
10
100
ADP (μM)
P2X1
P2X1+5

FIGURE 5.4 Potent blockades of $P2X_1$ and $P2X_{1+5}$ receptor-mediated responses by the antagonist TNP-ATP. (**A**) Representative $P2X_{1+5}$ currents in conditions of inhibitions. (**B**) Sensitivities of $P2X_1$ and $P2X_{1+5}$ responses to TNP-ATP, co-applied with 1 μM αβmATP. Peak currents were normalized to responses elicited by applications of 10 μM αβmATP alone (average ± SEM from 5-8 oocytes per point). Membrane potentials were held at -100 mV.

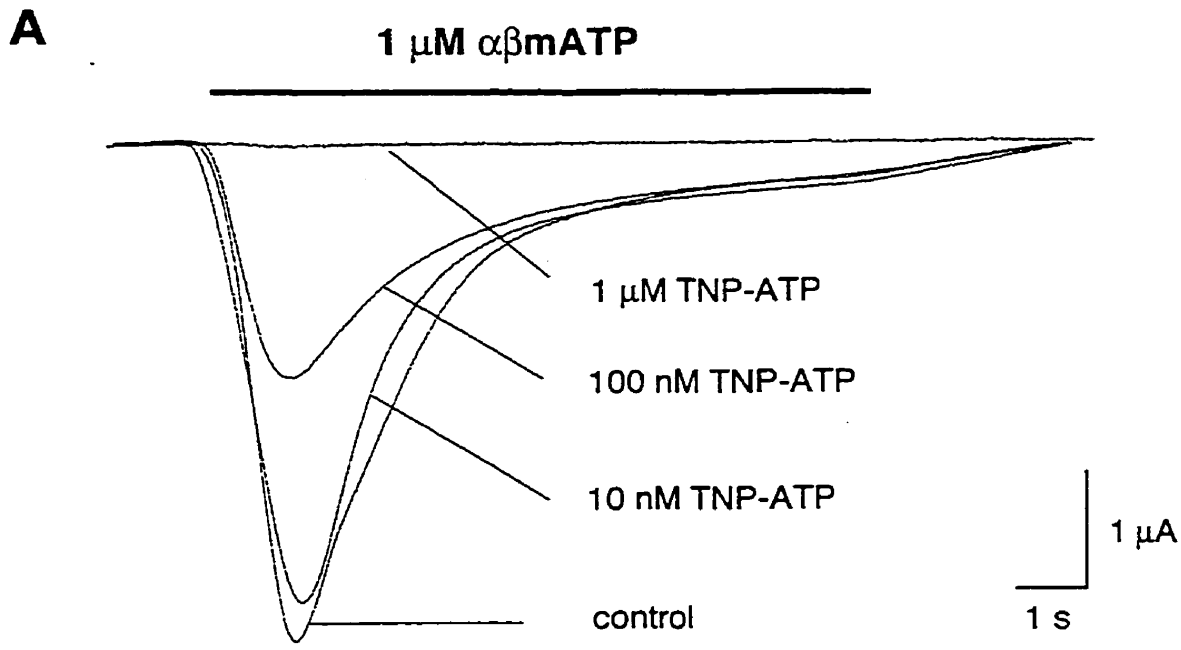
A
1 μM αβmATP
1 μM TNP-ATP
100 nM TNP-ATP
10 nM TNP-ATP
control
1 μA
1 s

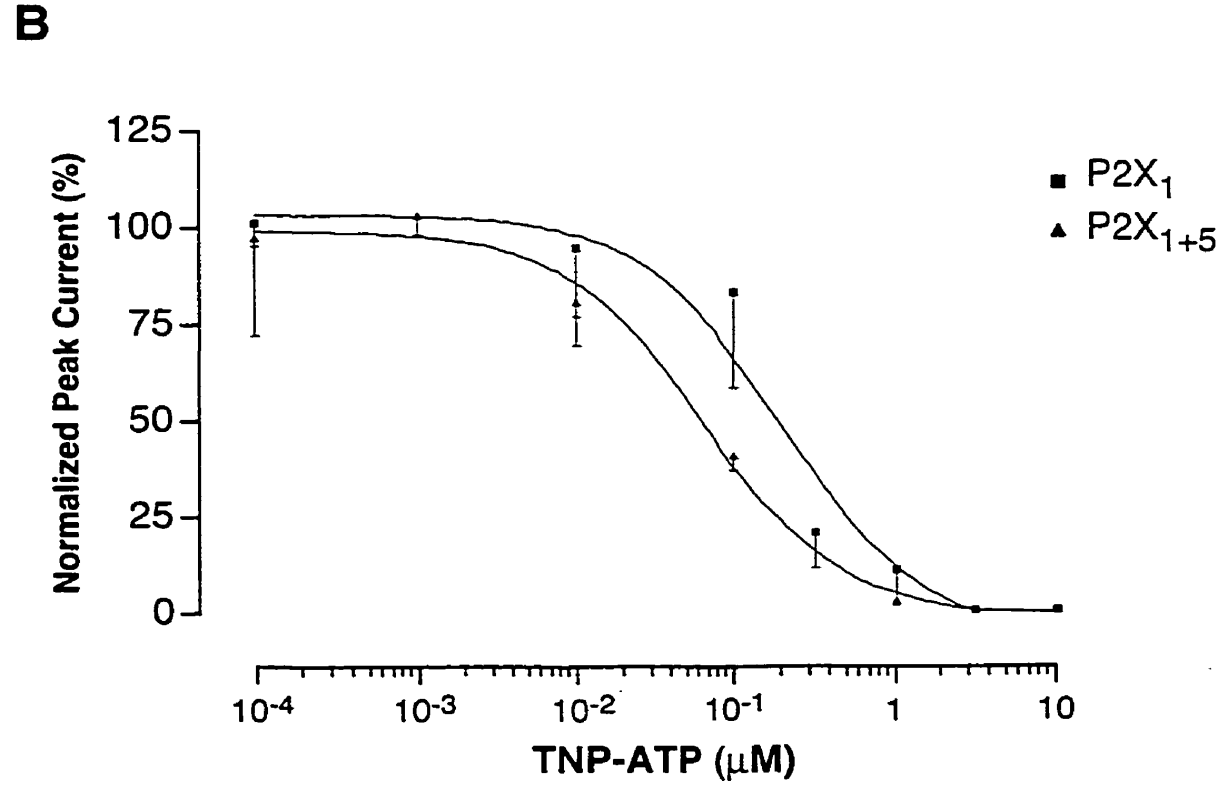
B
Normalized Peak Current (%)
125
100
75
50
25
0
P2X1
P2X1+5
10-4
10-3
10-2
10-1
1
10
TNP-ATP (μM)

FIGURE 5.5 Physical interactions between $P2X_1$ and $P2X_5$ subunits. Solubilized P_{2X} proteins from transiently transfected HEK-293A cells were detected on immunoblots following purifications through His_6-binding Ni-NTA resins. Flag-tagged P_{2X} subunits associated with corresponding His_6-tagged partners were probed with murine M2 (anti-Flag) monoclonal antibodies. Co-purifications as shown are from $P2X_1$-His_6 + $P2X_1$-Flag in lane A (positive controls), $P2X_5$-His_6 + $P2X_5$-Flag in lane B (positive controls), $P2X_5$-His_6 + $P2X_1$-Flag in lane C, and $P2X_1$-His_6 + $P2X_5$-Flag in lane D. Indicated apparent molecular weight markers are in kilodaltons.

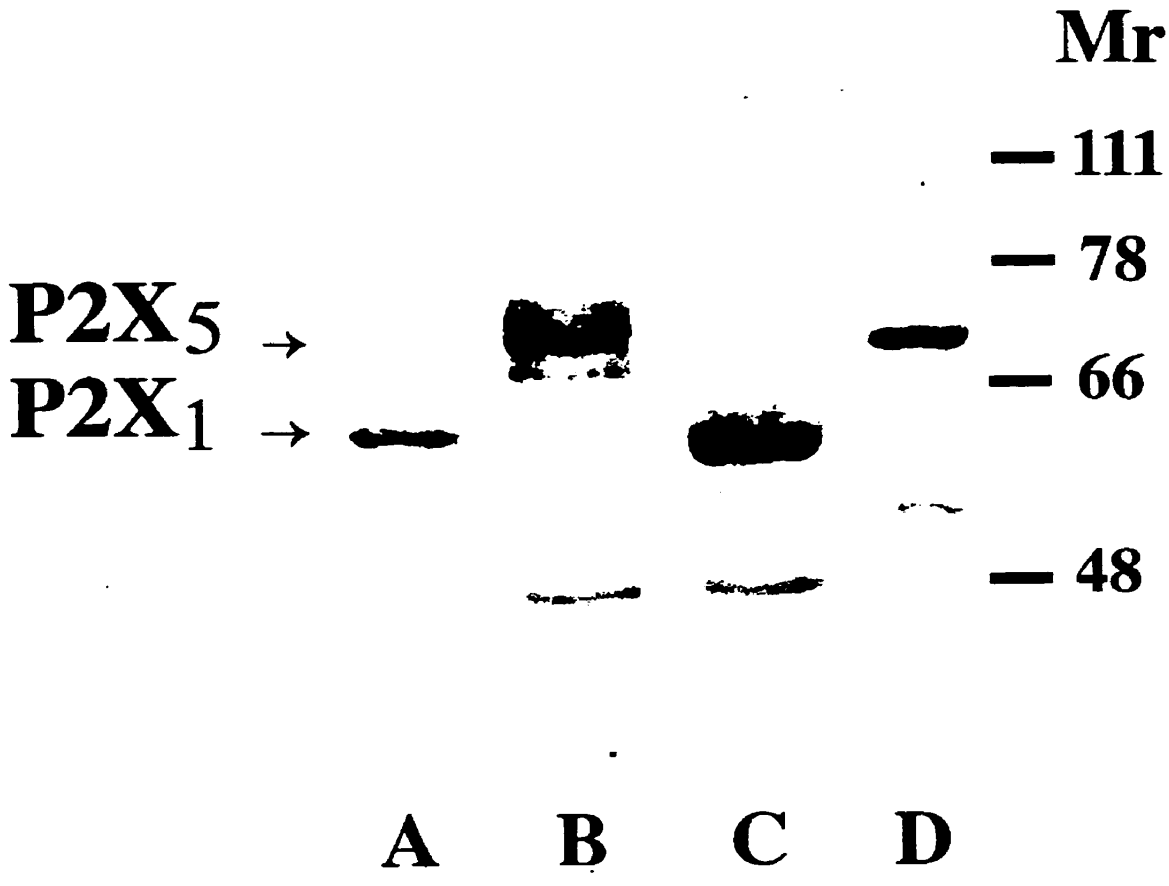
Mr
111
78
66
48
P2X5 →
P2X1 →
A
B
C
D

CHAPTER 6

6.1 RESEARCH RATIONALE

Based upon recent immunocytochemistry reports, ATP-gated P_{2X} ion channels have been shown to be widely expressed within most CNS structures on postsynaptic membranes (Lê *et al.*, 1998a). Similarly, these ionotropic receptors have also been demonstrated to be selectively expressed presynaptically in various central sensory pathways, notably within laminae I and II of the dorsal horn of the spinal cord (Lê *et al.*, 1998a), an anatomical region that processes information from nociceptors.

In agreement with the distribution of ATP-gated channels, it has been recently suggested that P_{2X} receptors might be involved in nociception processing events (Burnstock, 1996), confirmed more directly by the existence of ATP-sensitive pain sensing neurons (Cook *et al.*, 1997). Based upon these observations, the therapeutical value of ATP-gated P_{2X} ion channels in pain treatment could be based on future developments of specific P_{2X} antagonists having potential analgesic actions (Burnstock, 1996).

However, most ATP-gated ion channel structure-function studies have been based upon rodent P_{2X} subunits (Buell *et al.*, 1996b). Further, recent human P_{2X} cloning studies have documented significant functional differences between human and rat P_{2X} homologs (Barnard *et al.*, 1997). Therefore, with these species-specific differences in mind, this cloning project was undertaken in an effort to complete the human P_{2X} gene inventory as well as to discover revealing species-dependent differences in terms of mRNA distribution patterns and functional properties. Henceforth, the whole coding region of rat $P2X_4$ cDNAs, as reported elsewhere by Séguéla *et al.* (1996), was used as a probe to fish out potential human P_{2X} genes represented in public Expressed-Sequence Tags (EST) databases.

6.2 MANUSCRIPT REPRINT

PRIMARY STRUCTURE AND EXPRESSION OF A NATURALLY TRUNCATED HUMAN P_{2X} ATP RECEPTOR SUBUNIT FROM BRAIN AND IMMUNE SYSTEM

KHANH-TUOC LÊ, MICHEL PAQUET, DOMINIQUE NOUEL, KAZIMIERZ BABINSKI AND PHILIPPE SÉGUÉLA. (1997)

FEBS LETTERS **418**: 195-199

ABSTRACT

A novel member of the ionotropic ATP receptor gene family has been identified in human brain. This 422 amino acid-long P_{2X} receptor subunit has 62% sequence identity with rat $P2X_5$. Several characteristic motifs of ATP-gated channels are present in its primary structure, but this $P2X_5$-related subunit displays a single transmembrane domain. Heterologous expression of chimeric subunits containing the C-terminal domain of rat $P2X_5$ leads to the formation of desensitizing functional ATP-gated channels in *Xenopus* oocytes. The developmentally regulated mRNA, found in two splicing variant forms, is expressed at high levels in brain and immune system.

INTRODUCTION

Mammalian P_{2X} receptors belong to a multigene family of non-selective cation channels activated by extracellular ATP. The seven known members of the rat P_{2X} family can be grouped into three functional categories according to their pharmacological profiles and to their properties of desensitization. $P2X_1$ (Valera *et al.*, 1994) and $P2X_3$ (Chen *et al.*, 1995; Lewis *et al.*, 1995) are highly sensitive to α,β-methylene ATP (αβmATP) and desensitize rapidly; $P2X_2$ (Brake *et al.*, 1994), $P2X_5$ (Collo *et al.*, 1996; Garcia-Guzman *et al.*, 1996), and $P2X_7$ (Surprenant *et al.*, 1996) do not respond to αβmATP below 100 μM and do not desensitize; whereas $P2X_4$ (Buell *et al.*, 1996; Séguéla *et al.*, 1996; Soto *et al.*, 1996) and $P2X_6$ (Collo *et al.*, 1996) do not respond to αβmATP, are almost insensitive to co-applied non-competitive antagonists suramin and PPADS, and show moderate desensitization. Despite the fact that high levels of expression of P_{2X} receptors are observed in many central and peripheral tissues, reinforcing the concept of an important role

for ATP in intercellular communication (Buell *et al.*, 1996), much less is known about their human counterparts. Excitatory ATP-gated channels play a specific role in sensory systems (Li and Perl, 1995; Bardoni *et al.*, 1997; Lê *et al.*, 1998), therefore the development of subtype-specific P_{2X} antagonists with analgesic properties should take into account functional differences between mammalian species. The reports on the expression of cloned human P_{2X} orthologs of $P2X_1$ (Valera *et al.*, 1995), $P2X_3$ (Garcia-Guzman *et al.*, 1997), $P2X_4$ (Garcia-Guzman *et al.*, 1997), and $P2X_7$ (Rassendren *et al.*, 1997) emphasized both pharmacological and anatomical specificities that seriously undermine the relevance of our knowledge based on rodent systems for extrapolation to human fast purinergic transmission. In an effort to complete the genetic inventory of human ionotropic ATP receptors, we report here the identification, heterologous expression, and anatomical distribution of a novel member of the human P_{2X} gene family isolated from fetal brain.

MATERIALS AND METHODS

Molecular Cloning and In Vitro Translation

Using the TBLASTN algorithm, virtual screening of the dbEST database (Lennon *et al.*, 1996) with the whole coding region of rat $P2X_4$ subunit led to the identification of human fetal brain EST sequences encoding a novel P_{2X} gene (GenBank Accession numbers T80104 and Z43811). The clone tagged by EST T80104 was sequenced on both strands and was shown to encode a short splicing variant of human P_{2X} subunit related to rat $P2X_5$ ($hP2X_{5R}$) (Fig. 6.1). A longer splicing variant of $hP2X_{5R}$ was detected in RT-PCR from human cerebellum mRNA with exact match primers. The EST clone was enginee-

red to generate the long version of $hP2X_{5R}$ (Fig. 6.1), deposited in Genbank under accession number AF016709. This $hP2X_{5R}$ clone was transferred into the *Hind*III-*Not*I sites of eukaryotic vector pcDNA3 (Invitrogen) for CMV-driven heterologous expression in HEK-293A cells and *Xenopus* oocytes. Supercoiled $hP2X_{5R}$ plasmid was used for *in vitro* translation using the TnT system with T7 RNA polymerase (Promega) and [^{35}S]-cysteine (ICN) according to the manufacturer's specifications.

Construction of Epitope-Tagged $hP2X_{5R}$ Subunits and Immunolocalization

The $hP2X_{5R}$ subunit was epitope-tagged ($hP2X_{5R}$-Flag) to facilitate the immunolocalization of the protein both *in situ* and in Western blots from transfected mammalian cells. The Flag octapeptide, DYKDDDDK (IBI), was inserted by PCR in the C-terminal domain of $hP2X_{5R}$ using an antisense oligonucleotide primer designed for the replacement of its natural stop codon by an artificial in-frame *Xho*I site, TCA*CTCGAG*CAAC-GTGCTCCTGTGGGGCT. Full-length mutant $hP2X_{5R}$ cDNA was amplified in PCR using *Pfu* polymerase (Stratagene), then ligated to a *Xho*I-*Xba*I cassette containing the Flag peptide followed by a stop codon (Mukerji *et al.*, 1996) in the pcDNA3 vector.

For transfection of $hP2X_{5R}$-Flag subunits, HEK-293A cells (ATCC #CRL-1573) were grown in DMEM-10% heat inactivated fetal bovine serum (Wisent, St. Bruno, Quebec) containing penicillin and steptomycin. Freshly plated cells reaching 30-50% confluency were used for transient transfection using the calcium phosphate method on 90 mm dishes with 10 μg supercoiled plasmid/10^6 cells.

For immunofluorescence, transfected HEK-293A cells (48-72 h post-transfection time)

were plated at 50-70% confluency in poly-L-lysine-coated chambers. Adherent cells were washed in PBS and fixed for 20 min at room temperature with 4% paraformaldehyde in 0.1 M phosphate buffer, pH 8.0. After blocking non-specific sites with 2% normal goat serum, fixed cells were incubated with anti-Flag monoclonal antibody (mAb) M2 (10 μg/ml; IBI) for 1 h at room temperature in 0.05 M Tris-saline buffer pH 7.2 containing 0.2% Triton X-100, 5% normal goat serum and 5% dry milk powder. Bound primary antibodies were detected by immunofluorescence after 1 h with Texas red-labeled goat anti-mouse (2 μg/ml) secondary antibodies (ImmunoResearch Labs). For high resolution analysis of $hP2X_{5R}$-Flag subcellular distribution, we used a Zeiss Laserscan Inverted 410 confocal microscope equipped with an argon-krypton laser set at 580 nm for Texas red. Serial images (512 x 512 pixels) acquired as single optical sections were averaged over 32 scans/frame and processed with the Zeiss CLMS software package. For Western blots, transfected cells were lifted in Hank's modified calcium-free medium with 20 mM EDTA, pelleted at low speed and homogenized in 10 volumes of 10 mM HEPES buffer pH 7.4 containing protease inhibitors phenylmethylsulfonyl fluoride (0.2 mM) and benzamidine (1 mM). Lysates were pelleted at 14 000 x *g* for 5 min to remove cell debris before protein assay and crude membrane proteins in supernatants were solubilized with SDS-containing loading buffer. About 150 μg of protein/lane were run on 12% SDS-PAGE, then transferred to nitrocellulose. Immunoprobing was performed with mouse mAb M2 (10 μg/ml) followed by peroxidase-labeled secondary antibodies for visualization by enhanced chemiluminescence (Amersham).

Functional Expression of h-r$P2X_5$ Chimera in Xenopus Oocytes

The domain of $hP2X_{5R}$ containing amino acids 1-318 was fused to the PCR-amplified do-

main corresponding to amino acids 318-455 of $rP2X_5$ using the natural *Bam*HI site of $hP2X_{5R}$ to generate the chimera h-$rP2X_5$. Oocytes surgically removed from mature *Xenopus laevis* frogs were treated for 3 h at room temperature with type II collagenase (Gibco-BRL) in Barth's solution under agitation. Selected stage V-VI oocytes were defolliculated chemically before nuclear micro-injections (Bertrand *et al.*, 1991) of 10 ng of cDNA of $hP2X_{5R}$ or h-$rP2X_5$ chimera in pcDNA3 vector. After 2-5 days of expression at 19 °C in Barth's solution containing 10 μg/ml gentamicin, oocytes were recorded in a two-electrode voltage-clamp configuration using an OC-725B am-plifier (Warner Instruments). Signals were acquired and digitized at 500 Hz using a Macintosh IIci equipped with a A/D card NB-MIO16XL (National Instruments) then traces were post-filtered at 100 Hz in Axograph (Axon Instruments). Agonists dissolved in Ringer's solution containing 115 mM NaCl, 2.5 mM KCl, 1.8 mM $CaCl_2$ in 10 mM HEPES pH 7.4 at room temperature were applied onto oocytes by perfusion in constant flow (12 ml/min).

RT-PCR Detection of $hP2X_{5R}$ mRNA from Human Cerebellum and Lymphocytes

Total RNA from post-mortem adult human cerebellar cortex and adult lymphocytes were isolated using Trizol reagents (Gibco-BRL). Then 5 μg of each RNA was subjected to random-primed reverse-transcription with Superscript (Gibco-BRL). Around 100 ng of RT-cDNA was used as templates for PCR with the following primers, forward, TTCGACTACAAGACCGAGAAGT (P1, see Fig. 6.1-B), and reverse, CTTGACGTCCTTCACATTGT (P2) to amplify the region corresponding to nucleotides 75-671 around the splicing event, as well as forward GAGGCCGAAGACTTCACCAT (P3) and reverse CCTCGTACTTCTTGTCACGG (P4) to detect the expression of a complete second transmembrane domain (M2). Non-RT samples amplified in the same conditions provided the ne-

gative controls. Integrity and representative of RT-cDNA were checked by amplification of $hP2X_7$ subunit message (Rassendren *et al.*, 1997) and $hP2X_4$ message (Garcia-Guzman *et al.*, 1997) with appropriate primers in lymphocytes and in cerebellum, respectively (data not shown).

Distribution of $hP2X_{5R}$ Transcripts in Human Tissues

Known amounts of mRNA blots corresponding to equivalent transcription levels of housekeeping genes from various fetal and adult human tissues (Masterblot, Clontech) were probed with full-length random-primed [^{32}P]-$hP2X_{5R}$ cDNA at high stringency (final elution at 65 °C in 0.3 x SSC buffer). Hybridization signals were quantitated using a Storm phosphorimager and the ImageQuant application (Molecular Dynamics) before substraction of background and normalization of transcription levels.

RESULTS AND DISCUSSION

The longest reading frame of $hP2X_{5R}$ cDNA encodes a protein of 422 amino acids that displays 62% sequence identity with $rP2X_5$ and several unique motifs conserved in all P_{2X} receptor subunits (Fig. 6.1). In the intracellular N-terminal domain, $hP2X_{5R}$ displays a highly conserved threonine residue (Thr^{18}), potentially susceptible to phosphorylation by protein kinase C. In addition, a serine residue (Ser^{12}) is found in a consensus site for phosphorylation by casein kinase II. In the putative extracellular domain of $hP2X_{5R}$, all 10 cysteine, all proline, 91% of glycine, and 75% of lysine residues are present at homologous positions in all P_{2X} subunits, indicating their critical roles in the folding and function of this sensor region. We checked the real position of the predicted

stop codon by *in vitro* translation as well as Western blot assays (Fig. 6.2). The recombinant subunit and its epitope-tagged mutant migrate at a M_r of 49 ± 2 kDa and 51 ± 2 kDa, respectively, in agreement with the calculated MW of 47 kDa for wild-type $hP2X_{5R}$ (Fig. 6.2-B). At least one of the 3 *N*-linked glycosylation consensus sites present in the extracellular domain of $hP2X_{5R}$ is used, according to the difference of M_r (up to 11 kDa) between *in vitro* translated $hP2X_{5R}$ and $hP2X_{5R}$ expressed in transfected HEK-293A cells (Fig. 6.2-B,C). The multiple bands observed in Western blots from transfected cells could be due to the co-expression of several glycosylated forms of $hP2X_{5R}$ (Fig. 6.2-B).

The integrity of the protein was also checked by detection of heterologously expressed epitope-tagged $hP2X_{5R}$ mutants using *in situ* immunofluorescence (Fig. 6.2-A; Fig. 6.3). Analysis of the subcellular localization of $hP2X_{5R}$-Flag in HEK-293A cells using confocal microscopy indicated a correct targeting of the subunit to the plasma membrane (Fig. 6.3), quantitatively similar to the surface distribution of the functional P_{2X} receptors $rP2X_1$-Flag and $rP2X_4$-Flag (Lê *et al.*, 1998). When expressed in *Xenopus* oocytes, homomeric $hP2X_{5R}$ channels do not respond to extracellular ATP applied at concentrations up to 1 mM. However, the chimera h-$rP2X_5$, made of the N-terminal domain of $hP2X_{5R}$ linked to the C-terminal domain of $rP2X_5$, revealed the formation of cationic ATP-gated ion channels (Fig. 6.4). These channels run down rapidly and do not recover fully from desensitization after extensive washing of agonist lasting several minutes in constant perfusion (Fig. 6.4). Therefore, despite the high sequence similarity with non-desensitizing wild-type $rP2X_5$ (62%), this chimeric channel displays a unique functional property not found in any other known homomeric or heteromeric subtypes. These data suggest that kinetics of desensitization of P_{2X} channels are dependent on subtle rules

of complementarity between the N- and the C-terminal halves of the subunits, as has been shown for $P2X_1$ and $P2X_2$ (Werner *et al.*, 1996).

We observed the expression of a splicing variant identified in fetal and adult brain by RT-PCR (Fig. 6.5), differing from the long form of $hP2X_{5R}$ by the absence of a cassette of 24 amino acids, corresponding to the domain Gly^{97}-Glu^{120} (Fig. 6.1). This cassette contains one of the 10 extracellular cysteines, so the expression of this short variant is due to either to some inaccuracy in the intron/exon splicing mechanisms or to some functional regulation. Interestingly, the region including amino acids Ala^{328}-Ala^{349} in $rP2X_5$, corresponding to the pre-M2 region and the outer mouth of M2s in other P_{2X} receptor subunits (Rassendren *et al.*, 1997), is consistently absent in $hP2X_{5R}$ mRNAs from brain and lymphocytes, despite the high sensitivity of the RT-PCR method used and the high levels of expression in both tissues (Fig. 6.6). Furthermore, attempts to detect a variant of $hP2X_{5R}$ with a complete M2 failed in tissues where homologous $rP2X_5$ has been localized by *in situ* hybridization (Collo *et al.*, 1996), like spinal cord and trigeminal sensory ganglia (data not shown).

To assess the anatomical distribution, we measured the relative levels of transcription of the $hP2X_{5R}$ gene in quantitative mRNA dot blots. Hybridization signals from a variety of fetal and adult tissues showed widespread but selective distribution of central and peripheral $hP2X_{5R}$ transcripts (Fig. 6.6). The two systems primarily involved in the processing of extracellular information, i.e., the central nervous system and the immune system, show highest levels of $hP2X_{5R}$ expression. We measured a dramatic developmental down-regulation of $hP2X_{5R}$ mRNAs in the thymus from the fetal to the adult stage (Fig. 6.6) that could be related to the massive apoptosis of immature thymocytes

occurring during negative selection (King and Ashwell, 1994). $P2X_1$ mRNA has been found to be upregulated during the apoptosis of immature thymocytes (Owens *et al.*, 1991) so the distribution of $hP2X_{5R}$ argues strongly for an important role of P_{2X} receptors in clonal deletion of immune cells. With only one transmembrane region, the structure of $hP2X_{5R}$ is reminiscent of tyrosine kinase receptors (Barbacid, 1994). We speculate that $hP2X_{5R}$ could be activated by the binding of an unidentified extracellular ligand or could be involved in the regulation of channel subunit interactions both in the brain and in the immune system.

The $rP2X_5$ is the neuronal subunit with the most limited distribution, so one striking difference between rat and human P_{2X} receptor genes is the high expression of $hP2X_{5R}$ in the brain and in peripheral tissues. The developmental regulation of levels of transcription and the tissue specificity observed in mRNA splicing do not seem compatible with the expression of a processed pseudogene (Maestre *et al.*, 1995). However, it is possible that undetected splicing variants of $hP2X_{5R}$ with two transmembrane domains would form functional human $P2X_5$ channels in homomeric form or assemble in heteromeric complexes in specific cell types. In any case, as has been described in other classes of multimeric integral proteins, i.e., the neurotrophin receptors (Altabef *et al.*, 1997), the steroid receptors (Eide *et al.*, 1996), and voltage-gated K channels (Jiang *et al.*, 1997), the regulatory effect of a dominant negative truncated $hP2X_{5R}$ subunit on human heteromeric ATP-gated channels remains to be investigated.

FIGURE 6.1 Molecular cloning of a novel member of the human P_{2X} ATP gene family, $hP2X_{5R}$. (**A**) Nucleotide sequence and ORF domain. Potential intracellular phosphorylation sites are indicated as well as cysteine residues (bold) and *N*-glycosylation sites (italics) in the putative extracellular domain of the subunit. The spliced domain of 24 amino acids (Gly^{97}-Glu^{120}), absent in the short variant from brain, is boxed. The putative splicing site of missing M2 sequence is indicated by the arrowhead. (**B**) Alignment of human and rat $P2X_5$ amino acid sequences and positions of PCR primers based on $hP2X_{5R}$ primary structure.

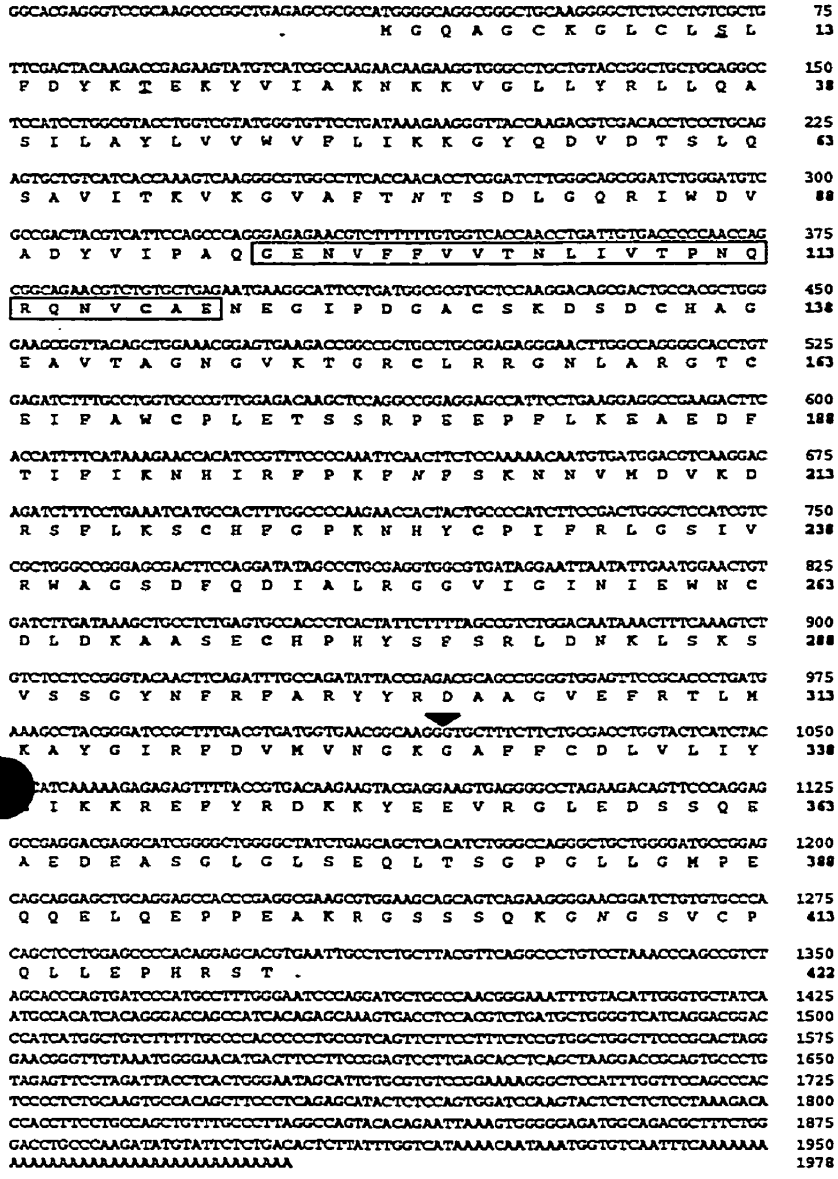

A

B

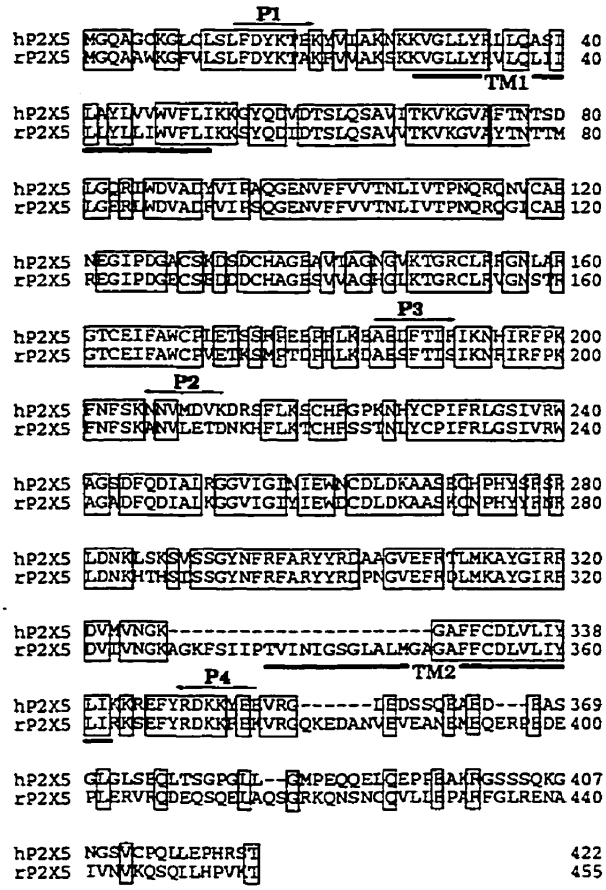

FIGURE 6.2 Heterologous expression and immunodetection of $hP2X_{5R}$ subunits. (**A**) *In vitro* translations of recombinant wild-type (1) and Flag-tagged $hP2X_{5R}$ (2). (**B**) Detections in Western blots of epitope-tagged $hP2X_{5R}$ (1) and rat $P2X_4$ (2) from transfected HEK-293A cells.

A

— 104
— 82

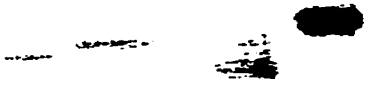

— 48

B C

1 2 1 2

FIGURE 6.3 Subcellular distribution of $hP2X_{5R}$ subunits expressed in HEK-293A cells using confocal microscope immunofluorescence. Arrows indicate the localization of $hP2X_{5R}$ subunits on the plasma membrane.

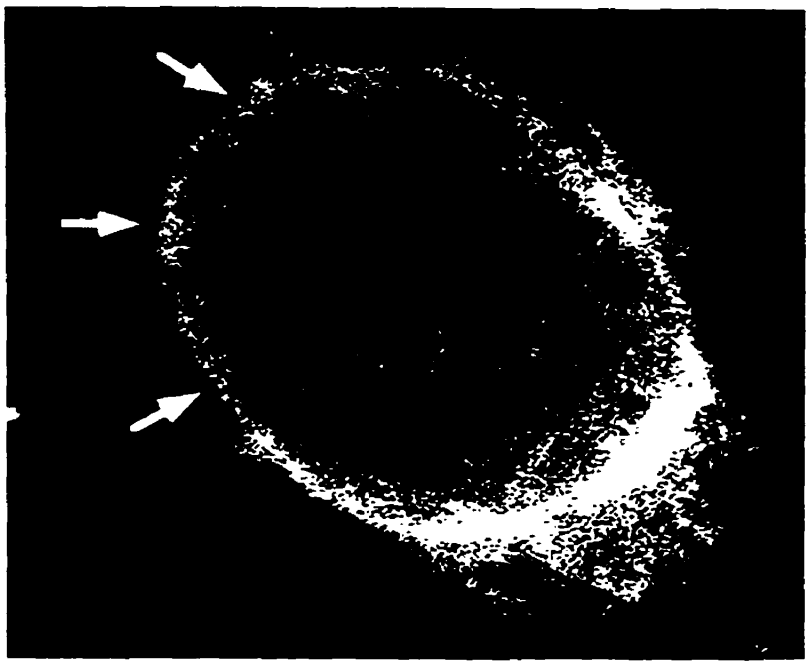

FIGURE 6.4 Functional expression of the chimera h-rP2X$_5$ in *Xenopus* oocytes. Fast and desensitizing inward currents evoked by 100 μM extracellular ATP were recorded after 2-5 days of expressions in two-electrode voltage-clamp configurations (holding potential V_h=-100 mV). Repeated applications of agonists at time t_0 + 500 s or t_0 + 700 s showed profound desensitizations of the chimeric ATP-gated channels.

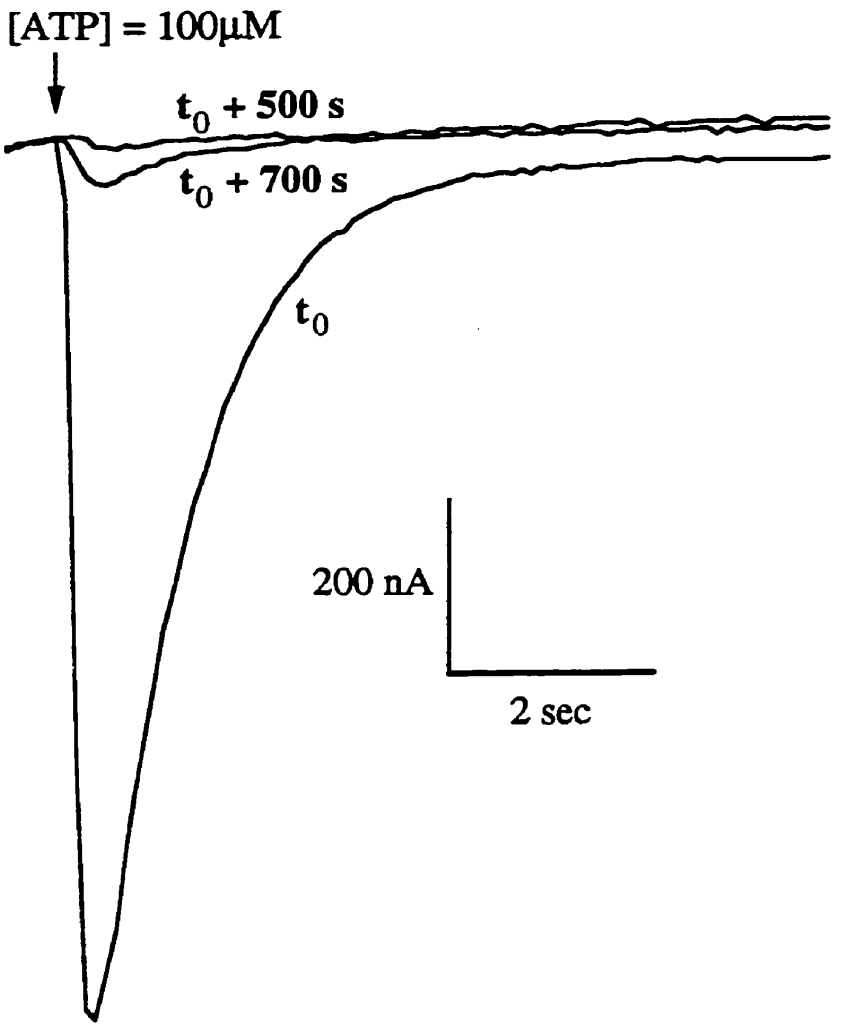
[ATP] = 100μM
t_0 + 500 s
t_0 + 700 s
t_0
200 nA
2 sec

FIGURE 6.5 $hP2X_{5R}$ transcripts are expressed in two alternatively spliced forms in human brain as detected in RT-PCR amplifications (lane 1, primers P1 and P2). The full-length form is predominantly found in lymphocytes (lane 3, primers P1 and P2). Both $hP2X_{5R}$ mRNA populations from brain (lane 2, primers P3 and P4) and lymphocytes (lane 4, primers P3 and P4) encode subunits with a single transmembrane domain.

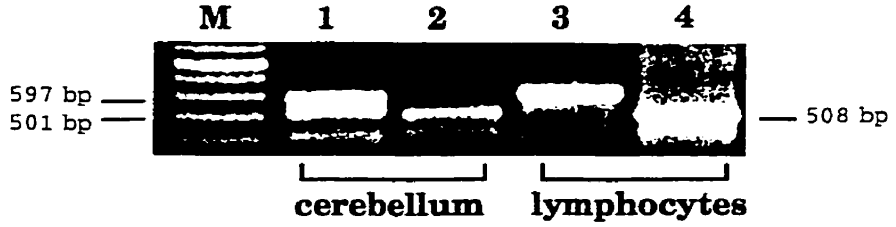
M
1
2
3
4
597 bp
501 bp
508 bp
cerebellum
lymphocytes

FIGURE 6.6 Relative levels of expressions of central and peripheral $hP2X_{5R}$ mRNA in human fetal (shaded bars) and adult tissues using hybridization of a full-length cDNA probe on poly(A)$^+$ RNA blot.

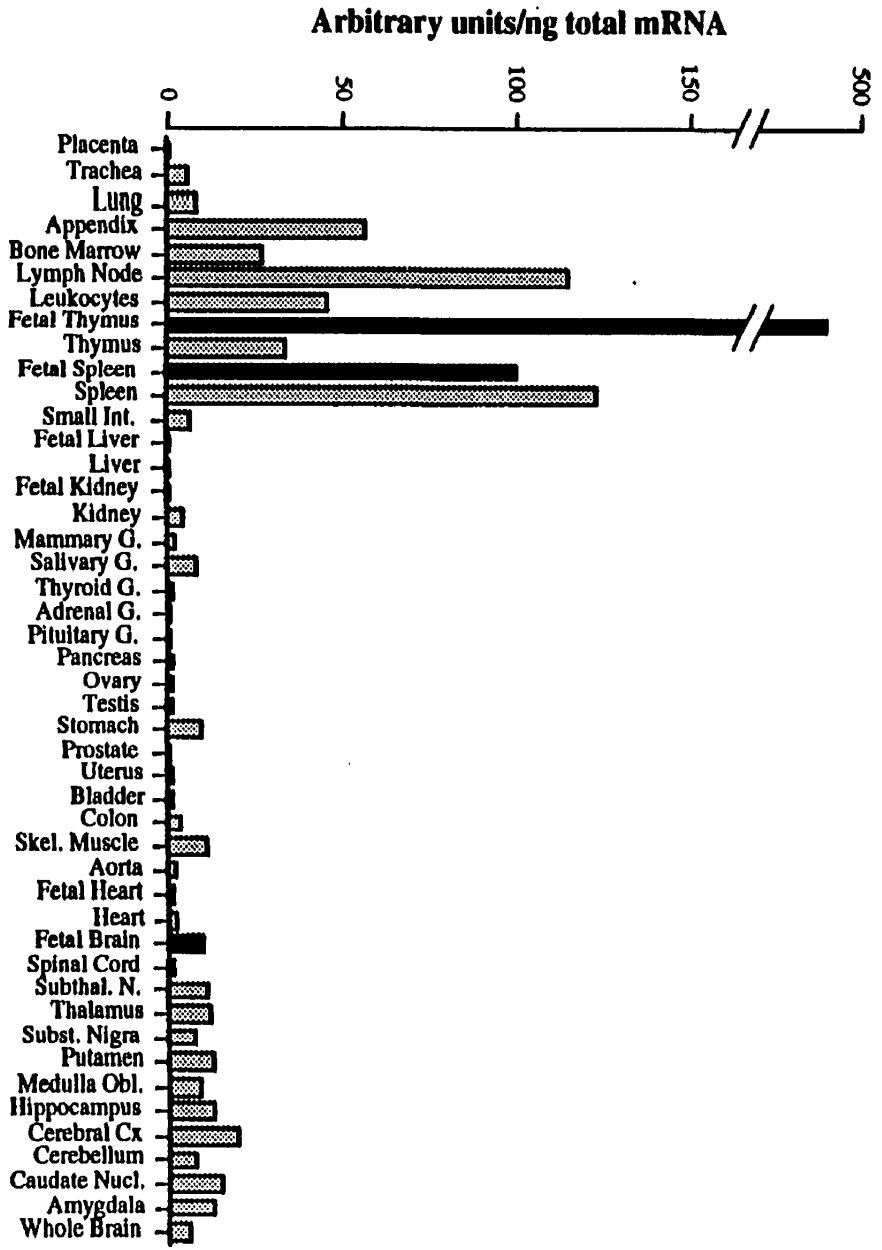
Arbitrary units/ng total mRNA
0
50
100
150
500
Placenta
Trachea
Lung
Appendix
Bone Marrow
Lymph Node
Leukocytes
Fetal Thymus
Thymus
Fetal Spleen
Spleen
Small Int.
Fetal Liver
Liver
Fetal Kidney
Kidney
Mammary G.
Salivary G.
Thyroid G.
Adrenal G.
Pituitary G.
Pancreas
Ovary
Testis
Stomach
Prostate
Uterus
Bladder
Colon
Skel. Muscle
Aorta
Fetal Heart
Heart
Fetal Brain
Spinal Cord
Subthal. N.
Thalamus
Subst. Nigra
Putamen
Medulla Obl.
Hippocampus
Cerebral Cx
Cerebellum
Caudate Nucl.
Amygdala
Whole Brain

CHAPTER 7

GENERAL DISCUSSION

The present Thesis illustrates the use of a multidisciplinary approach based on molecular biology, protein chemistry, and electrophysiology to characterize recombinant ATP-gated P_{2X} cation channels. Our work covers investigations on central P_{2X} immunocytochemistry (Lê *et al.*, 1998a), novel heteromultimeric P_{2X} subunit interactions (Lê *et al.*, 1998b; Lê *et al.*, 1999), and human P_{2X} primary sequence (Lê *et al.*, 1997). These studies might open new avenues such as developments of therapeutical compounds targeting P_{2X} receptors to be pursued in future research programs.

SENSORY PRESYNAPTIC AND WIDESPREAD SOMATODENDRITIC IMMUNOLOCALIZATION OF CENTRAL IONOTROPIC P_{2X} ATP RECEPTORS (Lê *et al.*, 1998a) — Polyclonal anti-$P2X_4$ antibodies, raised against the intracellular C-terminal domain of $P2X_4$ subunits, were affinity-purified and validated through *in situ* immunofluorescence and protein blotting methodologies performed on transiently transfected HEK-293A cells expressing either wild-type $P2X_4$ proteins or various epitope-tagged P_{2X} constructs, namely, C-terminal domain Flag-tagged $P2X_1$ and $P2X_2$ as well as $P2X_4$ mutants. In Western blot, affinity-purified anti-$P2X_4$ antibodies recognized a protein migrating at a relative molecular weight close to 60 kDa from protein homogenates prepared from either heterologous expression systems or brain extracts. On the other hand, both $P2X_1$-Flag and $P2X_2$-Flag were not recognized by anti-$P2X_4$ antibodies, yet, these constructs were detected with monoclonal anti-Flag M2 antibodies. These data validated the subunit specificity of our affinity-purified rabbit polyclonal anti-$P2X_4$ antibodies and they demonstrated that $P2X_4$-containing receptors were widely but variably expressed within various brain regions. Our regional $P2X_4$ protein mapping results from brain homogenates was in good correlation with and extended what has been described previously using *in situ* hybridization data.

Furthermore, cellular $P2X_4$ channel expression patterns were determined by immunocytochemical studies at the light microscope level. First, $P2X_4$ receptor expression profiles within both brain and spinal cord were observed to be widespread thereby corroborating previously reported *in situ* hybridization results regarding $P2X_4$ mRNA distribution patterns (Bo *et al.*, 1995; Buell *et al.*, 1996a; Collo *et al.*, 1996; Séguéla *et al.*, 1996). Second, $P2X_4$ protein immunoreactivity was found to be predominantly on postsynaptic structures thereby demonstrating that fast purinergic neurotransmission can be mediated through natively expressed ATP-gated P_{2X} channels as previously suggested by electrophysiological recordings from various brain loci such as medial habenular neurons (Edwards *et al.*, 1992), hippocampal CA3 subfields (Ross *et al.*, 1998), and cerebellar Purkinje cells (Mateo *et al.*, 1998), spinal cord dorsal horn (Jahr and Jessell, 1983; Bardoni *et al.*, 1997; Gu and MacDermott, 1997), and sensory neurons (Lewis *et al.*, 1995; Khakh *et al.*, 1995; Cook *et al.*, 1997; Gu and MacDermott, 1997; Khakh *et al.*, 1997).

Although widespread postsynaptic $P2X_4$ protein expression patterns were obvious from our immunocytochemical results, yet, $P2X_4$ immunoreactivity was also present on the presynaptic side in discrete brain and spinal cord loci. For instance, presynaptic $P2X_4$-containing receptors were localized in the olfactory bulb thereby strongly suggesting that ATP might be involved in modulatory and/or signaling function in olfaction sensory processing events. Presynaptic $P2X_4$ channel expression was also observed in the dorsal horn of the spinal cord, more specifically in laminae I and II, cell layers known to relay and process various sensory modalities such as nociception. Indeed, P_{2X} receptors have been previously observed to be capable of modulatory functions (Li and Perl, 1995; Gu and MacDermott, 1997). Therefore, our experimental data about $P2X_4$ presy-

naptic protein expression profiles within selective sensory pathways directly strengthen the view that native presynaptic P_{2X} receptors modulate neurotransmission (Li and Perl, 1995) through regulation of neurotransmitter release events (Fu and Poo, 1991; Sperlagh and Vizi, 1991; Sun and Stanley, 1996; Cook *et al.*, 1997; Gu and MacDermott, 1997).

Moreover, other studies have reported the immunolocalization of $P2X_1$ (Vulchanova *et al.*, 1996), $P2X_2$ (Kanjhan *et al.*, 1996; Vulchanova *et al.*, 1996; Vulchanova *et al.*, 1997), $P2X_3$ (Cook *et al.*, 1997; Vulchanova *et al.*, 1997; Bradbury *et al.*, 1998; Vulchanova *et al.*, 1998), and $P2X_7$ (Collo *et al.*, 1997) and these results are corroborated the *in situ* hybridization data (Collo *et al.*, 1996). These studies have also documented presynaptic protein expression of neuronal $P2X_1$ (Vulchanova *et al.*, 1996), $P2X_2$ (Vulchanova *et al.*, 1996; Vulchanova *et al.*, 1997), and $P2X_3$ subunits (Cook *et al.*, 1997; Vulchanova *et al.*, 1997; Bradbury *et al.*, 1998; Vulchanova *et al.*, 1998) in sensory pathways. Taken altogether, all immunocytochemical studies are consistent with the concept of presynaptic P_{2X} localization (Lê *et al.*, 1998a), strongly suggesting that sensory inputs, for instance, olfaction and nociception, could be regulated by presynaptic ATP-gated P_{2X} ion channels. Consistent with this role of neuromodulator of P_{2X} receptors, it has been previously demonstrated that cholinergic presynaptic nerve terminals from chicken ciliary ganglia were exhibiting ionotropic purinergic responses, believed to be of P_{2X} nature, elicited by ATP applications (Sun and Stanley, 1996). Similarly, extracellular ATP has recently been shown to modulate presynaptic glutamate release from DRG axon terminals onto spinal cord neurons in co-culture preparations (Gu and MacDermott, 1997). It has also been reported that ATP enhanced spontaneous acetylcholine releases from developing *Xenopus* neuromuscular synapses (Fu and Poo, 1991). Moreover, ATP has

also been suggested to be directly involved in the potentiation of evoked acetylcholine as well as noradrenaline releases from axon terminals innervating guinea pig ileum muscle strips (Sperlagh and Vizi, 1991).

Although we demonstrated that $P2X_4$ is widely expressed on postsynaptic membranes as well as selectively expressed on nerve terminals in sensory systems, yet, native P_{2X} activity recorded from various brain and spinal cord preparation has been shown to be sensitive to $\alpha\beta$mATP. Strikingly, all central P_{2X} responses recorded from various brain loci have been observed to be sensitive to suramin and/or PPADS blockade (Barnard *et al.*, 1997). Therefore, the problem of the native central P_{2X} subunit composition remains, as yet, to be solved. Accordingly, our second manuscript (Lê *et al.*, 1998b) addressed this issue by documenting a novel P_{2X} channel phenotype characterized by pharmacological profiles corresponding more closely to central P_{2X} responses.

CENTRAL $P2X_4$ AND $P2X_6$ CHANNEL SUBUNITS CO-ASSEMBLE INTO A NOVEL HETEROMERIC ATP RECEPTOR (Lê *et al.*, 1998b) — We used in this study an *in vitro* electrophysiological recording method to assess the association between $P2X_4$ and $P2X_6$ subunits through protein expression time-courses and pharmacological profiles using purinergic agonists and P2 antagonists as well as various co-factors known to modulate P_{2X} channel responses. *Xenopus* oocytes expressing homomultimeric $P2X_4$ or $P2X_6$ channel subunits were compared to those co-expressing both of these predominant and overlapping brain P_{2X} receptor isoforms. We confirmed with direct experimental evidence that $P2X_4$ and $P2X_6$ channel subunits physically interact through the use of an established co-purification assay (Tinker *et al.*, 1996) from mammalian HEK-293A cells co-expressing both subunits.

The most striking observation from this study was the fact that $P2X_{4+6}$ heteromultimeric channels were consistently giving rise to peak current amplitude values, in response to ATP applications, several fold higher than $P2X_4$ homopolymeric receptors after three days of expression. Similarly, recorded αβmATP responses from *Xenopus* oocytes co-expressing $P2X_4$ and $P2X_6$ subunits were significantly larger than those expressing $P2X_4$ channels alone after two days of expression. These observations, coupled to our data on similar potency and efficacy of ATP for $P2X_4$ and $P2X_{4+6}$ phenotypes, strongly suggest that $P2X_4$ and $P2X_6$ subunits assemble into quaternary complexes endowed with more stability than either subtype expressed alone. Consistent with this idea, most ligand-gated as well as voltage-activated ion channels are assembled from heteromultimeric subunit proteins rather than homopolymeric receptors (Green and Millar, 1995).

We then used purinergic agonists as pharmacological tools to further substantiate the existence of $P2X_{4+6}$ channels, notably αβmATP. As opposed to ATP, both αβmATP and 2MeSATP were significantly more potent as well as more efficacious on oocytes co-expressing $P2X_4$ and $P2X_6$ subunits than on those expressing $P2X_4$ receptors alone. The present manuscript therefore provided a novel moderately desensitizing αβmATP-sensitive phenotype mediated by $P2X_{4+6}$ channels. The other two known αβmATP-sensitive phenotypes were the rapidly desensitizing homopolymeric $P2X_1$ (Valera *et al.*, 1994) and $P2X_3$ (Chen *et al.*, 1995; Lewis *et al.*, 1995) and the non-desensitizing heteromultimeric $P2X_{2+3}$ receptors (Lewis *et al.*, 1995; Radford *et al.*, 1997).

Accordingly, native αβmATP-elicited responses previously documented from most central preparations might be in fact mediated by $P2X_{4+6}$ receptor phenotypes within brain

and spinal cord loci lacking $P2X_2$ subunits (Brake *et al.*, 1994; Collo *et al.*, 1996; Kanjhan *et al.*, 1996; Vulchanova *et al.*, 1996; Vulchanova *et al.*, 1997). Further, $P2X_1$ does not seem to be present within the adult rat brain (Valera *et al.*, 1994; Collo *et al.*, 1996; Vulchanova *et al.*, 1996), while $P2X_3$ is only expressed in primary sensory neurons (Chen *et al.*, 1995; Lewis *et al.*, 1995; Collo *et al.*, 1996; Cook *et al.*, 1997; Vulchanova *et al.*, 1997; Bradbury *et al.*, 1998; Vulchanova *et al.*, 1998).

In addition to the medial habenula, the hippocampus, and the cerebellum (Lê *et al.*, 1998b), numerous other central preparations known to express only $P2X_4$ and $P2X_6$ (Collo *et al.*, 1996) have also been observed to respond to αβmATP applications. Hypothalamic neurons from the tuberomammillary nucleus, mainly expressing $P2X_4$ and $P2X_6$ transcripts (Collo *et al.*, 1996), were found to be activated by αβmATP (Furukawa *et al.*, 1994). Second, although it was concluded that observed ionotropic purinergic responses from the hindbrain solitary tract nucleus were mediated by P_{2Y} receptors (Ueno *et al.*, 1992), in hindsight these observations were most likely due to $P2X_{4+6}$ channels. Third, αβmATP has been shown to elicit fast responses from medial vestibular neurons (MVN) (Chessell *et al.*, 1997). Consistent with the presence of $P2X_{4+6}$ heteromultimers presented here, it was concluded that MVN P_{2X} phenotypes must have resulted from channel subunit heteropolymerization with unknown isoform composition (Chessell *et al.*, 1997). Lastly, locus coeruleus neurons also transcribe $P2X_2$ mRNAs in addition to $P2X_4$ and $P2X_6$ transcripts (Collo *et al.*, 1996), yet, these neurons were shown to respond to αβmATP concentrations (Harms *et al.*, 1992; Shen and North, 1993) known to be inactive on homomultimeric $P2X_2$ (Brake *et al.*, 1994) and $P2X_4$ (Bo *et al.*, 1995; Buell *et al.*, 1996a; Séguéla *et al.*, 1996; Soto *et al.*, 1996a; Wang *et al.*, 1996) as well as on $P2X_6$ receptors (Collo *et al.*, 1996; Soto *et al.*, 1996b).

In addition to these supraspinal loci responding to αβmATP applications, spinal cord dorsal horn laminae I to III were shown to be sensitive to this ATP analog, albeit amounting to a small proportion *vis-à-vis* neurons responding to ATP applications (Bardoni *et al.*, 1997). Lamina III was reported to be devoid of any P_{2X} transcripts (Collo *et al.*, 1996). On the other hand, from our results, $P2X_4$ proteins are expressed both post- and presynaptically within lamina II (Lê *et al.*, 1998a). Conversely, $P2X_2$ was shown to be transcribed in lamina II (Collo *et al.*, 1996), however, $P2X_2$ protein expression at this locus remains to be established due to contradictory findings (Vulchanova *et al.*, 1996; Vulchanova *et al.*, 1997). Although $P2X_6$ protein localization data remain, as yet, to be published, the sensitivity to αβmATP in laminae I and II of the spinal cord could be due to $P2X_{4+6}$ receptors.

It has also been reported that a few supraspinal as well as spinal cord preparations did not respond to αβmATP applications, notably neonatal cerebellar Purkinje cells (Mateo *et al.*, 1998) and most neurons in superficial layers within spinal cord dorsal horn neurons (Bardoni *et al.*, 1997). This apparent unresponsiveness to αβmATP in neurons (Bardoni *et al.*, 1997; Mateo *et al.*, 1998) expressing predominantly $P2X_4$ and/or $P2X_6$ (Collo *et al.*, 1996; Lê *et al.*, 1998a), could be explained by a) the weak efficacy of αβmATP in comparision to ATP in eliciting ionotropic responses mediated by hetero-multimeric $P2X_{4+6}$ receptors, based upon our *in vitro* observations from the present study (Lê *et al.*, 1998b) and/or b) the expression of $P2X_4$ homomers or other associations of either $P2X_4$ or $P2X_6$ or $P2X_{4+6}$ with novel subunits, notably $P2X_{2+4+6}$ or $P2X_{4+5+6}$.

P2 antagonists such as suramin, PPADS, and RB-2 were also used to differentiate ho-

mopolymeric $P2X_4$ receptor phenotype from heteromultimeric $P2X_{4+6}$ channel species. Indeed, *Xenopus* oocytes co-expressing $P2X_4$ and $P2X_6$ subunits were found to be significantly more sensitive to suramin, PPADS, and RB-2 blockade than cells expressing $P2X_4$ alone.

Consistent with these data, all central P_{2X} phenotypes, notably from various supraspinal regions known to contain only $P2X_4$ and $P2X_6$ mRNA transcripts and proteins (Collo *et al.*, 1996; Lê *et al.*, 1998a), reported to date have been shown to be blocked by suramin and/or PPADS (Barnard *et al.*, 1997). For instance, medial habenular, hippocampal CA3 subfield, and neonatal Purkinje neurons exhibiting P_{2X} responses were all shown to be antagonized by either suramin or PPADS (Edwards *et al.*, 1992; Mateo *et al.*, 1998; Ross *et al.*, 1998). Similarly, cells from tuberomammillary and solitary tract nuclei as well as MVN neurons mediating ATP-elicited ionotropic responses were also reported to be sensitive to P2 antagonist block (Ueno *et al.*, 1992; Furukawa *et al.*, 1994; Chessell *et al.*, 1997). P2 antagonists cannot be used to infer native P_{2X} subunit composition from locus coeruleus neurons (Harms *et al.*, 1992; Shen and North, 1993) since these cells are known to express $P2X_2$ subunits generating receptors sensitive to suramin, PPADS, and RB-2 (Brake *et al.*, 1994; Buell *et al.*, 1996b).

Another significant contribution from the present study consisted of providing a biochemical assay used to directly demonstrating subunit-dependent interaction bewteen $P2X_4$ and $P2X_6$ subunits. Further, this protein expression system used for co-purification constituted the first mammalian cell assay used for such purposes within the P_{2X} field. Conversely, physical interaction between $P2X_2$ and $P2X_3$ isoforms was demonstrated through a co-immunoprecipitation assay from the invertebrate Sf9 cell expres-

sion system (Radford *et al.*, 1997), which is known for artifacts of protein over-expression giving rise to potentially irrelevant protein complexes (R.A. North, personal communication). So far, we have documented regional, cellular, and subcellular protein localization of a predominant P_{2X} subunit within both brain and spinal cord as well as provided a potential solution bridging apparent discrepancies between native central responses observed in various supraspinal preparations and recombinant receptors. However, P_{2X} channel subunit composition within spinal cord ventral horn cells remain to be established. Spinal motor neurons are known to express predominantly $P2X_2$, $P2X_4$, and $P2X_6$ transcripts as well as $P2X_1$ and $P2X_5$ mRNAs at significant levels (Collo *et al.*, 1996).

FUNCTIONAL AND BIOCHEMICAL EVIDENCE FOR HETEROMERIC ATP-GATED CHANNELS COMPOSED OF $P2X_1$ AND $P2X_5$ SUBUNITS (Lê *et al.*, 1999) — We have reported in this study another heteromultimeric P_{2X} subtype assembled from $P2X_1$ and $P2X_5$ subunits. This conclusion based upon both pharmacological profiles and channel kinetics from *Xenopus laevis* oocytes co-expressing both subunits compared to those expressing either subunit alone, as well as on biochemical assays in transfected HEK-293A cells demonstrating mutual subunit-specific interaction between $P2X_1$ and $P2X_5$ channels. These observations were corroborated by a recent report on the co-assembly between $P2X_1$ and $P2X_5$ subunits where heteromultimeric $P2X_{1+5}$ receptors were shown to display a $P2X_1$-subtype pharmacology ($\alpha\beta$mATP sensitivities) and a $P2X_5$-like channel kinetics (non-desensitizing) from transiently transfected HEK-293 cells (Torres *et al.*, 1998b).

Based upon observed similarities between P_{2X} responses in HEK-293 cells co-expres-

sing $P2X_2$ and $P2X_3$ subnits and nodose neurons, in terms of pharmacological and channel kinetic properties, it was then suggested that these native αβmATP-elicited, yet non-desensitizing responses must have been mediated by heteropolymeric $P2X_{2+3}$ channel complexes since these properties could not be accounted for by either homomultimeric $P2X_2$ or $P2X_3$ subtypes (Lewis *et al.*, 1995). Direct physical association between $P2X_2$ and $P2X_3$ subunits was subsequently reported (Radford *et al.*, 1997). It was also hypothesized that previously documented P_{2X} responses from dorsal root ganglion (DRG) cells (Krishtal *et al.*, 1983; Krishtal *et al.*, 1988; Bean, 1990; Khakh *et al.*, 1995) might have been also mediated by hetero-oligomeric $P2X_{2+3}$ receptors (Lewis *et al.*, 1995; Radford *et al.*, 1997).

Indeed, recent immunocytochemistry data have indicated co-localization of $P2X_2$ and $P2X_3$ subunits within nodose cell bodies as well as their central terminals (Vulchanova *et al.*, 1997). However, a recent study has observed that nodose neurons expressed other P_{2X} subtypes than $P2X_{2+3}$-like subtypes with unknown subunit composition (Thomas *et al.*, 1998). Moreover, DRG neurons have been shown to co-express $P2X_2$ and $P2X_3$ proteins only at their cell bodies but not at their central axon terminals making synapses in the spinal cord (Vulchanova *et al.*, 1997). These observations, coupled to the fact that a) sensory neurons have been reported to transcribe $P2X_1$ and $P2X_5$ mRNAs (Collo *et al.*, 1996) and b) $P2X_1$ subunits have been shown to be expressed presynaptically within the dorsal horn of the spinal cord (Vulchanova *et al.*, 1996) strongly suggested that heteromultimeric $P2X_{1+5}$ receptors studied from *in vitro* assays (Torres *et al.*, 1998b; Lê *et al.*, 1999) might be expressed by central terminals of DRG neurons. Besides $P2X_1$ (Vulchanova *et al.*, 1996) and $P2X_2$ (Vulchanova *et al.*, 1996; Vulchanova *et al.*, 1997) as well as $P2X_3$ (Vulchanova *et al.*, 1997; Bradbury *et al.*,

1998; Vulchanova *et al.*, 1998), $P2X_4$ proteins was also shown to be expressed on the presynaptic side within the dorsal horn of the spinal cord (Lê *et al.*, 1998a), yet, $P2X_4$ subunits have been reported not to interact with either $P2X_1$ (Lewis et al., 1995; Lê *et al.*, 1998b; Torres *et al.*, 1999), $P2X_2$ (Lewis *et al.*, 1995; Torres *et al.*, 1999), or $P2X_3$ subunits (Lewis *et al.*, 1995; Torres *et al.*, 1999) further strengthening the hypothesis in favor of heteropolymeric $P2X_{1+5}$ receptors mediating $P2X_{2+3}$-like phenotypes in nodose cell bodies and central terminals (presynaptic) as well as in DRG processes synapsing onto the dorsal horn of the spinal cord (presynaptic).

Interestingly, it has recently been shown biochemically that $P2X_1$ and $P2X_2$ as well as $P2X_3$ and $P2X_5$ could form heteromultimeric complexes leading to $P2X_{1+2}$ and $P2X_{3+5}$ receptors, respectively (Torres *et al.*, 1999). Conversely to $P2X_{1+5}$ (Torres *et al.*, 1998b; Lê *et al.*, 1999) and $P2X_{2+3}$ channel phenotypes (Lewis *et al.*, 1995), $P2X_{1+2}$ receptors do not give rise to novel functional properties that could not have been accounted for by either homopolymeric subunits (Lewis *et al.*, 1995). On the other hand, functional properties of heteromultimeric $P2X_{3+5}$ channels (Torres *et al.*, 1999) remain to be investigated. TNP-ATP could be used to trace, functionally, the presence of heteromultimeric $P2X_{3+5}$ receptors, assuming that co-assembly between $P2X_3$ and $P2X_5$ subunits would display a $P2X_{2+3}$-like phenotype.

On the same token, TNP-ATP could be used as a potent pharmacological tool, based upon our observations (Lê *et al.*, 1999), to assess whether DRG central terminals, especially those lacking $P2X_2$ and $P2X_3$ protein co-localization (Vulchanova *et al.*, 1997), express $P2X_{1+5}$ receptors natively. The same argument could be used to screen whether motoneurons of the ventral horn of the spinal cord possess $P2X_{1+5}$ channels, since

it has been shown that these two subunits were predominantly transcribed in an overlapping fashion in this population (Collo *et al.*, 1996). Both $P2X_2$ and $P2X_4$ have been shown to be much less sensitive to TNP-ATP block than $P2X_1$, $P2X_3$, $P2X_{2+3}$ (Virginio *et al.*, 1998) or $P2X_{1+5}$ receptors (Lê *et al.*, 1999).

It is clear now, that overlapping presynaptic expression patterns between any given P_{2X} subunits would not necessary warrant co-assembly. The best example is $P2X_3$ and $P2X_4$ (Lewis *et al.*, 1995; Torres *et al.*, 1999) both of which are expressed presynaptically within lamina II of the dorsal horn of the spinal cord (Bradbury *et al.*, 1998; Lê *et al.*, 1998a; Vulchanova *et al.*, 1998). Alternatively, both $P2X_1$ and $P2X_2$ receptors have been reported to display overlapping presynaptic expression profiles (Vulchanova *et al.*, 1996) and they have been shown to interact together biochemically (Torres *et al.*, 1999), yet, their assembly does not generate receptors displaying hybrid functional properties distinct from either homomultimeric $P2X_1$ or $P2X_2$ subunits (Lewis *et al.*, 1995). On the other hand, observed variabilities in P_{2X} responses in terms of TNP-ATP IC_{50} values recorded from nodose cells (Thomas *et al.*, 1998) might be due to heterogeneous populations of homopolymeric as well as heteromultimeric $P2X_{2+3}$ receptors composed of different $P2X_2$ and $P2X_3$ subunit stoichiometries. However, these variable responses to this antagonist have not been observed in HEK-293 cells co-expressing $P2X_2$ and $P2X_3$ isoforms (Virginio *et al.*, 1998) strongly suggesting contributions of other homo- or hetero-oligomeric complexes composed of other P_{2X} subunits besides $P2X_2$ and $P2X_3$ proteins such as $P2X_{1+5}$ (Torres *et al.*, 1998b; Lê *et al.*, 1999).

PRIMARY STRUCTURE AND EXPRESSION OF A NATURALLY TRUNCATED HUMAN P_{2X} ATP RECEPTOR SUBUNIT FROM BRAIN AND IMMUNE SYSTEM (Lê *et al.*, 1997)

— This project was undertaken in an effort to complete the inventory of human P_{2X} gene family members. $rP2X_5$-encoding transcripts have been shown to be the most rare mRNAs among all rP_{2X} subunits, thereby, rendering the cloning of $hP2X_{5R}$ interesting both in terms of species-dependent properties as well as regional distribution differences.

Our most surprising observation has been the predicted primary structure of $hP2X_{5R}$ displaying only one transmembrane domain. Indeed, $hP2X_{5R}$ has been observed to be non-functional in *Xenopus laevis* oocytes despite the fact that this protein is properly targeted to the plasma membrane of transiently transfected HEK-293A cells. Based upon these results, it would be interesting to know if $hP2X_1$ interacts with $hP2X_{5R}$. More specifically, should $hP2X_{1+5R}$, exist then what would be the resultant phenotype(s)? Could $hP2X_{5R}$ act as a natural dominant negative mutant affecting thereby channel function within complexes containing other functional P_{2X} subunits?

Another significant difference between $rP2X_5$ and $hP2X_{5R}$ has been found at the level of the distribution of $hP2X_{5R}$ mRNAs. In other words, as opposed to $rP2X_5$, $hP2X_{5R}$ has been determined to be transcribed both within central nervous as well as in various immune tissues. Similar to the present case whereby transcript distribution has been found to be species-dependent between mammals, $hP2X_m$ (the ortholog of $rP2X_6$) has been reported to be found only within skeletal muscle (Urano *et al.*, 1997) whereas $rP2X_6$ has been documented as having a much more widespread distribution pattern (Collo *et al.*, 1996). In retrospect, it is interesting to note that both $rP2X_5$ and $rP2X_6$ have been hard to characterize in terms of respective functions. More specifically, homomeric $rP2X_5$ receptors gave rise to significantly smaller current amplitudes in com-

parision to other recombinant P_{2X} subunits characterized in either HEK-293 cells (Collo *et al.*, 1996; Torres *et al.*, 1998b) or *Xenopus laevis* oocytes (Lê *et al.*, 1999). Similarly, $rP2X_6$ has been reported to be non-functional from injected oocytes from two independent laboratories (Soto *et al.*, 1996b; Lê *et al.*, 1998b).

And finally as concluding remarks to the present Thesis, fast-acting purinergic synaptic signaling in the CNS is currently well accepted based upon several observations such as a) vesicular co-release of ATP with other well characterized neurotransmitters and b) neuronal P_{2X} protein and mRNA distribution patterns. Therefore, in our quest for understanding the potential physiological roles of ATP-gated P_{2X} channels in global neuronal communication, our results from the present Thesis have significantly contributed to the knowledge of basic biological aspects of P_{2X} receptors, namely their distribution characteristics at the protein level, interactions between subunits in relevant heteromultimeric complexes, and species-dependent biophysical properties as well as dissimilarities in terms of their transcriptional distribution patterns.

Physiological roles of fast-acting purinergic responses have always been difficult to identify due to the lack of specific P_{2X} antagonists. Although TNP-ATP has recently been shown to be an effective blocker at several P_{2X} subtypes, yet, both the sensitivity of adenosine receptors as well as P_{2Y} behaviors to this analog remains to be checked. Involvements of neuronal P_{2X} receptors in selective sensory pathways could be rewarding in terms of significant therapeutical implications such as developments of a novel class of drugs for pain management. Genetic models like P_{2X} receptor knockout mice and/or transgenic animals will be helpful in assessing to what extent P_{2X} channels play a significant role in proprioceptive and nociceptive pathways.

CHAPTER 8

REFERENCES

Altabef M., Garcia M., Varior-Krishnan G., Samarut J. (1997) A truncated RAR alpha co-operates with the v-erbβ oncogene to transform early haematopoietic progenitors *in vitro* and *in vivo*. Oncogene **14**: 1471-1479.

Balachandran C., Bennett M.R. (1996) ATP-activated cationic and anionic conductances in cultured rat hippocampal neurons. *Neuroscience Letters* **204**: 73-76.

Balcar V.J., Li Y., Killinger S., Bennett M.R. (1995) Autoradiography of P_{2X} ATP receptors in the rat brain. *British Journal of Pharmacology* **115**: 302-306.

Barbacid M. (1994) The Trk family of neurotrophin receptors. *Journal of Neurobiology* **25**: 1386-1403.

Bardoni R., Goldstein P.A., Lee C.J., Gu J.G., MacDermott A.B. (1997) ATP P_{2X} receptors mediate fast synaptic transmission in the dorsal horn of the rat spinal cord. *Journal of Neuroscience* **17**: 5297-5304.

Barnard E.A., Simon J., Webb T.E. (1997) Nucleotide receptors in the nervous system — An abundant component using diverse transduction mechanisms. *Molecular Neurobiology* **15**: 103-130.

Bean B.P. (1990) ATP-activated channels in rat and bullfrog sensory neurons — Concentration dependence and kinetics. *Journal of Neuroscience* **10**: 1-10.

Bean B.P., Williams C.A., Ceelen P.W. (1990) ATP-activated channels in rat and bull-

frog sensory neurons — Current-voltage relation and single channel behavior. *Journal of Neuroscience* **10**: 11-19.

Bo X., Burnstock G. (1990) High- and low-affinity binding sites for [^{3}H]-α,β-methylene ATP in rat urinary bladder membranes. *British Journal of Pharmacology* **101**: 291-296.

Bo X., Simon J., Burnstock G., Barnard E.A. (1992) Solubilization and molecular size determination of the P_{2X} purinoceptor from rat vas deferens. *Journal of Biological Chemistry* **267**: 17581-17587.

Bo X., Burnstock G. (1994) Distribution of [^{3}H]α,β-methylene ATP binding sites in rat brain and spinal cord. *NeuroReport* **5**: 1601-1604.

Bo X., Zhang Y., Nassar M., Burnstock G., Schoepfer R. (1995) A P_{2X} purinoceptor cDNA conferring a novel pharmacological profile. *FEBS Letters* **375**: 129-133.

Boarder M.R., Hourani S.M.O. (1998) The regulation of vascular function by P2 receptors — Multiple sites and multiple receptors. *Trends in Pharmacological Sciences* **19**: 99-107.

Bradbury E.J., Burnstock G., McMahon S.B. (1998) The expression of $P2X_3$ purinoreceptors in sensory neurons — Effects of axotomy and glial-derived neurotrophic factor. *Molecular and Cellular Neuroscience* **12**: 256-268.

Brake A.J., Wagenbach M.J., Julius D. (1994) New structural motif for ligand-gated

(Brake and Julius, continued) ion channels defined by an ionotropic ATP receptor. *Nature* **371**: 519-523.

Brake A.J., Julius D. (1996) Signaling by extracellular nucleotides. *Annual Reviews of Cellular and Developmental Biology* **12**: 519-541.

Braun N., Zhu Y., Krieglstein J., Culmsee C., Zimmermann H. (1998) Upregulation of the enzyme chain hydrolyzing extracellular ATP after transient forebrain ischemia in the rat. *Journal of Neuroscience* **18**: 4891-4900.

Buell G., Lewis C., Collo G., North R.A., Surprenant A. (1996a) An antagonist-insensitive P_{2X} receptor expressed in epithelia and brain. *EMBO Journal* **15**: 55-62.

Buell G., Collo G., Rassendren F. (1996b) P_{2X} receptors — An emerging channel family. *European Journal of Neuroscience* **8**: 2221-2228.

Buhl E.H., Otis T.S., Mody I. (1996) Zinc-induced collapse of augmented inhibition by GABA in a temporal lobe epilepsy model. *Nature* **271**: 369-372.

Burnstock G. (1972) Purinergic nerves. *Pharmacological Reviews* **24**: 509-581.

Burnstock G. (1996) A unifying purinergic hypothesis for the initiation of pain. *Lancet* **347**: 1604-1605.

Burnstock G., Kennedy C. (1985) Is there a basis for distinguishing two types of P_2-

(Burnstock and Kennedy, continued; review paper) purinoceptor. *General Pharmacology* **16**: 433-440.

Canessa C.M., Schild L., Buell G., Thorens B., Gautschi I., Horisberger J.-D., Rossier B.C. (1994) Amiloride-sensitive epithelial Na^+ channel is made of three homologous subunits. *Nature* **367**: 463-467.

Chen C.-C., Akopian A.N., Sivilotti L., Colquhoun D., Burnstock G., Wood J.N. (1995) A P_{2X} purinoceptor expressed by a subset of sensory neurons. *Nature* **377**: 428-431.

Chen Z.-P., Lewy A., Lightman S.L. (1994) Activation of specific ATP receptors induces a rapid increase in intracellular calcium ions in rat hypothalamic neurons. *Brain Research* **641**: 249-256.

Chessell I.P., Michel A.D., Humphrey P.P.A. (1997) Functional evidence for multiple purinoceptor subtypes in the rat medial vestibular nucleus. *Neuroscience* **77**: 783-791.

Chow Y.W., Wang H.L. (1998) Functional modulation of $P2X_2$ receptors by cyclic AMP-dependent protein kinase. *Journal of Neurochemistry* **70**: 2606-2612.

Cloues R., Jones S., Brown D.A. (1993) Zn^{2+} potentiates ATP-activated currents in rat sympathetic neurons. *Pflügers Archives* **424**: 152-158.

Collo G., North R.A., Kawashima E., Merlo-Pich E., Neidhart S., Surprenant A.,

Buell G. (1996) Cloning of $P2X_5$ and $P2X_6$ receptors and the distribution and properties of an extended family of ATP-gated ion channels. *Journal of Neuroscience* **16**: 2495-2507.

Collo G., Neidhart S., Kawashima E., Kosco-Vilbois M., North R.A., Buell G. (1997) Tissue distribution of the $P2X_7$ receptor. *Neuropharmacology* **36**: 1277-1283.

Cook S.P., Vulchanova L., Hargreaves K.M., Elde R., McCleskey E.W. (1997) Distinct ATP receptors on pain-sensing and stretch-sensing neurons. *Nature* **387**: 505-508.

Crawford I.L., Connor J.D. (1972) Zinc in maturing rat brain — Hippocampal concentration and localization. *Journal of Neurochemistry* **19**: 1451-1458.

Dalziel H.H., Westfall D.P. (1994) Receptors for adenine nucleotides and nucleosides — Subclassification, distribution, and molecular characterization. *Pharmacological Reviews* **46**: 449-466.

Day T.A., Sibbald J.R., Khanna S. (1993) ATP mediates an excitatory noradrenergic neuron input to supraoptic vasopressin cells. *Brain Research* **607**: 341-344.

DeVries S.H., Baylor D.A. (1993) Synaptic circuitry of the retina and olfactory bulb. *Cell 72/Neuron* **10**: 139-149.

Dowdall M.J., Boyne A.F., Whittaker V.P. (1974) Adenosine triphosphate — A cons-

(Dowdall, Boyne, and Whittaker, continued) tituent of cholinergic synaptic vesicles. *Biochemistry Journal* **140**: 1-12.

Drury A.N., Szent-Györgyi A. (1929) The physiological activity of adenine compounds with special reference to their action upon the mammalian heart. *Journal of Physiology* **68**: 213-237.

Edwards F.A., Gibb A.J., Colquhoun D. (1992) ATP receptor-mediated synaptic currents in the central nervous system. *Nature* **359**: 144-147.

Edwards F.A. (1996) *P2 purinoceptors — localization, function, and transduction mechanisms*. Wiley, Chichester, United Kingdom.

Egan T.M., Haines W.R., Voigt M.M. (1998) A domain contributing to the ion channel of ATP-gated $P2X_2$ receptors identified by the substituted cysteine accessibility method. *Journal of Neuroscience* **18**: 2350-2359.

Eide F.F., Vining E.R., Eide B.L., Zang K., Wang X.Y., Reichardt L.F. (1996) Naturally occuring truncated Trk-B receptors have a dominant inhibitory effects on brain-derived neurotrophic factor signaling. *Journal of Neuroscience* **16**: 3123-3129.

Evans R.J., Derkach V., Surprenant A. (1992) ATP mediates fast synaptic transmission in mammalian neurons. *Nature* **357**: 503-505.

Evans R.J. (1996) Single channel properties of ATP-gated cation channels (P_{2X} recep-

tors) heterologously expressed in Chinese hamster ovary cells. *Neuroscience Letters* **212**: 212-214.

Evans R.J., Lewis C., Virginio C., Lundstrom K., Buell G., Surprenant A., North R.A. (1996) Ionic permeability of, and divalent cation effects on, two ATP-gated cation channels (P_{2X} receptors) expressed in mammalian cells. *Journal of Physiology* **497**: 413-422.

Ferrer-Montiel A.V., Montal M. (1996) Pentameric subunit stoichiometry of a neuronal glutamate receptor. *Proceedings of the National Academy of Sciences* USA **93**: 2741-2744.

Fieber L., Adams D.J. (1991) Adenosine triphosphate-evoked currents in cultured neurons dissociated from rat parasympathetic cardiac ganglia. *Journal of Physiology* **434**: 239-256.

Fredholm B.B., Abbracchio M.P., Burnstock G., Daly J.W., Harden T.K., Jacobson K.A., Leff P., Williams M. (1994) Nomenclature and classification of purinoceptors. *Pharmacological Reviews* **46**: 143-156.

Fröhlich R., Boehm S., Illes P. (1996) Pharmacological characterization of P2 purinoceptor types in rat locus coeruleus neurons. *European Journal of Pharmacology* **315**: 255-261.

Fu W.-M., Poo M.-M. (1991) ATP potentiates spontaneous transmitter release at de-

(Fu and Poo, continued; presynaptic release) veloping neuromuscular synapses. *Neuron* **6**: 837-843.

Funk G.D., Kanjhan R., Walsh C., Lipski J., Comer A.M., Parkis M.A., Housley G.D. (1997) P2 receptor excitation of rodent hypoglossal motoneuron activity *in vitro* and *in vivo* — A molecular physiological analysis. *Journal of Neuroscience* **17**: 6325-6337.

Furukawa K., Ishibashi H., Akaike N. (1994) ATP-induced inward current in neurons freshly dissociated from the tuberomammilary nucleus. *Journal of Neurophysiology* **71**: 868-873.

Fyffe R.E.W., Perl E.R. (1984) Is ATP a central synaptic mediator for certain primary afferent fibers from mammalian brain? *Proceedings of the National Academy of Sciences* USA **81**: 6890-6893.

Galligan J.J., Bertrand P.P. (1994) ATP mediates fast synaptic potentials in enteric neurons. *Journal of Neuroscience* **14**: 7563-7571.

Garcia-Guzman M., Soto F., Laube B., Stühmer W. (1996) Molecular cloning and functional expression of a novel rat heart P_{2X} purinoceptor. *FEBS Letters* **388**: 123-127.

Garcia-Guzman M., Stühmer W., Soto F. (1997a) Molecular characterization and pharmacological properties of the human $P2X_3$ purinoceptor. *Molecular Brain Research* **47**: 59-66.

Garcia-Guzman M., Soto F., Gomez-Hernandez J.M., Lund P.-E., Stühmer W. (1997b) Characterization of recombinant human $P2X_4$ receptor reveals pharmacological differences to the rat homologue. *Molecular Pharmacology* **51**: 109-118.

Green W.N., Millar N.S. (1995) Ion channel assembly. *Trends in Neurosciences* **18**: 280-287.

Gu J.G., MacDermott A.B. (1997) Activation of ATP P_{2X} receptors elicits glutamate release from sensory neuron synapses. *Nature* **389**: 749-753.

Harlow E., Lane D. (1988) *Antibodies — A laboratory Manual.* Cold Spring Harbor Laboratory Press.

Harms L., Finta E.P., Tschöpl M., Illes P. (1992) Depolarization of rat locus coeruleus neurons by adenosine 5'-triphosphate. *Neuroscience* **48**: 941-952.

Hill J.A., Zoli M., Bourgeois J.-P., Changeux J.-P. (1993) Immunocytochemical localization of a neuronal nicotinic receptor — The β2-subunit. *Journal of Neuroscience* **13**: 1551-1568.

Hiruma H., Bourque C.W. (1995) P2 purinoceptor-mediated depolarization of rat supraoptic neurosecretory cells *in vitro*. *Journal of physiology* **489**: 805-811.

Holton F.A., Holton P. (1954) The capillary dilator substances in dry powders of spinal roots — A possible role of ATP in chemical transmission from nerve endings. *Journal of*

(Holton and Holton, continued; purine and neurotransmission) *Physiology* **126**: 124-140.

Inoue K., Koizumi S., Nakazawa K. (1995) Glutamate-evoked release of adenosine 5'-triphosphate causing an increase in intracellular calcium in hippocampal neurons. *NeuroReport* **6**: 437-440.

Jahr C.E., Jessell T.M. (1983) ATP excites a subpopulation of rat dorsal horn neurons. *Nature* **304**: 730-733.

Jiang M., Tseng-Crank J., Tseng G.N. (1997) Suppression of slow-delayed rectifier current by a truncated isoform of K_vLQT1 cloned from normal human heart. *Journal of Biological Chemistry* **272**: 24109-24112.

Jo Y.-H., Schlichter R. (1999) Synaptic corelease of ATP and GABA in cultured spinal neurons. *Nature Neuroscience* **2**: 241-245.

Kanjhan R., Housley G.D., Thorne P.R., Christie D.L., Palmer D.J., Luo L., Ryan A.F. (1996) Localization of ATP-gated ion channels in cerebellum using $P2X_2R$ subunit-specific antisera. *NeuroReport* **7**: 2665-2669.

Kegel B., Braun N., Heine P., Maliszewski C.R., Zimmermann H. (1997) An ecto-ATPase and an ecto-ATP diphosphohydrolase are expressed in rat brain. *Neuropharmacology* **36**: 1189-1200.

Khakh B.S., Humphrey P.P.A., Surprenant A. (1995) Electrophysiological proper-

ties of P_{2X}-purinoceptors in rat superior cervical, nodose and guinea-pig coeliac neurons. *Journal of Physiology* **484**: 385-395.

Khakh B.S., Humphrey P.P.A., Henderson G. (1997) ATP-gated cation channels (P_{2X} purinoceptors) in trigeminal mesencephalic nucleus neurons of the rat. *Journal of Physiology* **498**: 709-715.

Khakh B.S., Bao X.R., Labarca C., Lester H.A. (1999) Neuronal P_{2X} transmitter-gated cation channels change their ion selectivity in seconds. *Nature Neuroscience* **2**: 322-330.

Kidd E.J., Grahames C.B.A., Simon J., Michel A.D., Barnard E.A., Humphrey P.P.A. (1995) Localization of P_{2X} purinoceptor transcripts in the rat nervous system. *Molecular Pharmacology* **48**: 569-573.

Kim M., Yoo O.J., Choe S. (1997) Molecular assembly of the extracellular domain of $P2X_2$, an ATP-gated ion channel. *Biochemical and Biophysical Research Communications* **240**: 618-622.

King L.B., Ashwell J.D. (1994) Thymocyte and T cell apoptosis — Is all cell death created equal. *Thymus* **23**: 209-230.

Koizumi S., Ikeda M., Inoue K., Nakazawa K., Inoue K. (1995) Enhancement by zinc of ATP-evoked dopamine release from rat pheochromocytoma PC12 cells. *Brain Research* **673**: 75-82.

Kraig R.P., Lascola C.D., Caggiano A. (1995) *Glial response to brain ischemia — Neuroglia*. Oxford UP, Oxford, United Kingdom.

Krishtal O.A., Marchenko S.M., Pidoplichko V.I. (1983) Receptor for ATP in the membrane of mammalian sensory neurons. *Neuroscience Letters* **35**: 41-45.

Krishtal O.A., Marchenko S.M., Obukhov A.G., Volkova T.M. (1988) Receptors for ATP in rat sensory neurons — The structure-function relationship for ligands. *British Journal of Pharmacology* **95**: 1057-1062.

Laube B., Kuhse J., Betz H. (1998) Evidence for a tetrameric structure of recombinant NMDA receptors. *Journal of Neuroscience* **18**: 2954-2961.

Lê K.-T., Villeneuve P., Ramjaun A.R., Mukerji J., McPherson P.S., Beaudet A., Séguéla P. (1996) Cellular distribution of $P2X_4$ ATP-gated channels in rat brain and spinal cord. *Society for Neuroscience Abstracts* **22**: 335.

Lê K.-T., Paquet M., Nouel D., Babinski K., Séguéla P. (1997) Primary structure and expression of a naturally truncated human P_{2X} ATP receptor subunit from brain and immune system. *FEBS Letters* **418**: 195-199.

Lê K.-T., Villeneuve P., Ramjaun A.R., Mukerji J., McPherson P.S., Beaudet A., Séguéla P. (1998a) Sensory presynaptic and widespread somatodendritic immunolocalization of central ionotropic P_{2X} ATP receptors. *Neuroscience* **83**: 177-190. ($P2X_4$ protein mapping).

Lê K.-T., Babinski K., Séguéla P. (1998b) Central $P2X_4$ and $P2X_6$ channel subunits co-assemble into a novel heteromeric ATP receptor. *Journal of Neuroscience* **18**: 7152-7159.

Lê K.-T., Boué-Grabot E., Archambault V., Séguéla P. (1999) Functional and biochemical evidence for heteromeric ATP-gated channels composed of $P2X_1$ and $P2X_5$ subunits. *Journal of Biological Chemistry* **274**: 15415-15419.

Lennon G., Auffray C., Polymeropoulos M., Soares M.B. (1996) The I.M.A.G.E. consortium — An integrated molecular analysis of genomes and their expression. *Genomics* **33**: 151-152.

Lewis C., Neidhart S., Holy C., North R.A., Buell G., Surprenant A. (1995) Co-expression of $P2X_2$ and $P2X_3$ receptor subunits can account for ATP-gated currents in sensory neurons. *Nature* **377**: 432-435.

Li C., Peoples R.W., Li Z., Weight F.F. (1993) Zn^{2+} potentiates excitatory action of ATP on mammalian neurons. *Proceedings of the National Academy of Sciences* USA **90**: 8264-8267.

Li C., Peoples R.W., Weight F.F. (1996) Proton potentiation of ATP-gated ion channel responses to ATP and Zn^{2+} in rat nodose ganglion neurons. *Journal of Neurophysiology* **76**: 3048-3058.

Li J., Perl E.R. (1995) ATP modulation of synaptic transmission in the spinal substan-

(Li and Perl, continued; central sensory transmission) tia gelatinosa. *Journal of Neuroscience* **15**: 3357-3365.

Lowry O.H., Rosebrough N.J., Farr A.L., Randall R.J. (1951) Protein measurements with the folin phenol reagents. *Journal of Biological Chemistry* **193**: 265-275.

MacKinnon R. (1995) Pore loops — An emerging theme in ion channel structure. *Neuron* **14**: 889-892.

Maestre J., Tchenio T., Dhellin O., Heidmann T. (1995) mRNA retroposition in human cells — Processed pseudogene formation. *EMBO Journal* **14**: 6333-6338.

Mateo J., Garcia-Lecea M., Miras-Portugal M.T., Castro E. (1998) Ca^{2+} signals mediated by P_{2X}-type purinoceptors in cultured cerebellar Purkinje cells. *Journal of Neuroscience* **18**: 1704-1712.

Michel A.D., Humphrey P.P.A. (1993) Distribution and characterization of [^{3}H]α,β-methylene ATP binding sites in the rat. *Naunyn-Schmiedeberg's Archives of Pharmacology* **348**: 608-617.

Mukerji J., Haghighi A., Séguéla P. (1996) Immunological characterization and transmembrane topology of 5-hydroxytryptamine$_3$ receptors by function epitope tagging. *Journal of Neurochemistry* **66**: 1027-1032.

Nakazawa K., Inoue K., Fujimori K., Takanaka A. (1990) ATP-activated single-

channel currents recorded from cell-free patches of pheochromocytoma PC12 cells. *Neuroscience Letters* **119**: 5-8.

Nicke A., Bäumert H.G., Rettinger J., Eichele A., Lambrecht G., Mutschler E., Schmalzing G. (1998) $P2X_1$ and $P2X_3$ receptors form stable trimers — A novel structural motif of ligand-gated ion channels. *EMBO Journal* **17**: 3016-3028.

North R.A. (1996) Families of ion channels with two hydrophobic segments. *Current Opinion in Cell Biology* **8**: 474-483.

North R.A., Barnard E.A. (1997) Nucleotide receptors. *Current Opinion in Neurobiology* **7**: 346-357.

Novikoff A.B., Novikoff P.M., Quintana N., Davis C. (1972) Diffusion artifacts in 3,3'-diaminobenzidine cytochemistry. *Journal of Histochemistry and Cytochemistry* **20**: 745-749.

Owens G.P., Hahn W.E., Cohen J.J. (1991) Identification of mRNAs associated with programmed cell death in immature thymocytes. *Molecular and Cellular Biology* **11**: 4177-4188.

Palay S.L., Chan-Palay V. (1974) *Cerebellar cortex — Cytology and Organization.* Springer, Berlin.

Paxinos G., Watson C. (1986) *The rat brain in stereotaxic coordinates*. Academic Press,

(Paxinos and Watson, continued; rodent anatomical textbook, immucytochemistry) New York.

Peterson G.L. (1977) A simplification of the protein assay method of Lowry *et al.* which is more generally applicable. *Analytic Biochemistry* **83**: 346-356.

Petrou S., Ugur M., Drummond R.M., Singer J.J., Walsh Jr. J.V. (1997) $P2X_7$ purinoceptor expression in *Xenopus* oocytes is not sufficient to produce a pore-forming P_{2Z}-like phenotype. *FEBS Letters* **411**: 339-345.

Phillis J.W., Wu P.H. (1981) The role of adenosine and its nucleotides in central synaptic transmission. *Progress in Neurobiology* **16**: 187-239.

Pinching A.J., Powell T.P.S. (1971) The neuropil of the glomeruli of the olfactory bulb. *Journal of Cell Science* **9**: 347-377.

Radford K.M., Virginio C., Surprenant A., North R.A., Kawashima E. (1997) Baculovirus expression provides direct evidence for heteromeric assembly of $P2X_2$ and $P2X_3$ receptors. *Journal of Neuroscience* **17**: 6529-6533.

Rassendren F., Buell G., Newbolt A., North R.A., Surprenant A. (1997a) Identification of amino acid residues contributing to the pore of a P_{2X} receptor. *EMBO Journal* **16**: 3446-3454.

Rassendren F., Buell G.N., Virginio C., Collo G., North R.A., Surprenant A.

(1997b) The permeabilizing ATP receptor, $P2X_7$ — Cloning and expression of a human cDNA. *Journal of Biological Chemistry* **272**: 5482-5486.

Reece L.J., Dhanjal S.S., Chung S.H. (1994) Zinc induces hyperexcitability in the hippocampus. *NeuroReport* **5**: 2669-2672.

Robertson S.J., Rae M.G., Rowan E.G., Kennedy C. (1996) Characterization of a P_{2X}-purinoceptor in cultured neurons of the rat dorsal root ganglia. *British Journal of Pharmacology* **118**: 951-956.

Rogers M., Dani J.A. (1995) Comparision of quantitative calcium flux through NMDA, ATP, and ACh receptor channels. *Biophysical Journal* **68**: 501-506.

Rogers S.W., Hughes T.E., Hollmann M., Gasic G.P., Deneris E.S., Heinemann S. (1991) The characterization and localization of the glutamate receptor subunit GluR1 in the rat brain. *Journal of Neuroscience* **11**: 2713-2724.

Rosenmund C., Stern-Bach Y., Stevens C.F. (1998) The tetrameric structure of a glutamate receptor channel. *Science* **280**: 1596-1599.

Ross F.M., Brodie M.J., Stone T.W. (1998) Modulation by adenine nucleotides of epileptiform activity in the CA3 region of rat hippocampal slices. *British Journal of Pharmacology* **123**: 71-80.

Salter M.W., Henry J.L. (1985) Effects of adenosine 5'-monophosphate and adenosine

5'-triphosphate on functionally identified units in the cat spinal dorsal horn — Evidence for a differential effect of adenosine 5'-triphosphate on nociceptive vs non-nociceptive units. *Neuroscience* **15**: 815-825.

Salter M.W., Hicks J.L. (1994) ATP-evoked increases in intracellular calcium in neurons and glia from the dorsal spinal cord. *Journal of Neuroscience* **14**: 1563-1575.

Séguéla P., Wadiche J., Dineley-Miller K., Dani J.A., Patrick J.W. (1993) Molecular cloning, functional expression and distribution of rat brain $\alpha 7$ — A nicotinic cation channel highly permeable to calcium. *Journal of Neuroscience* **13**: 596-604.

Séguéla P., Haghighi A., Soghomonian J.-J., Cooper E. (1996) A novel P_{2x} ATP receptor ion channel with widespread distribution in the brain. *Journal of Neuroscience* **16**: 448-455.

Shen K.-Z., North R.A. (1993) Excitation of rat locus coeruleus neurons by adenosine 5'-triphosphate — Ionic mechanisms and receptor characterization. *Journal of Neuroscience* **13**: 894-899.

Silinsky E.M., Gerzanich V. (1993) On the excitatory effects of ATP and its role as a neurotransmitter in coeliac neurons of the guinea pig. *Journal of Physiology* **464**: 197-212.

Snyder P.M., Cheng C., Prince L.S., Rogers J.C., Welsh M.J. (1998) Electrophysiological and biochemical evidence that DEG/ENaC cation channels are composed of nine

(Snyder, Cheng, Prince, Rogers, and Welsh) subunits. *Journal of Biological Chemistry* **273**: 681-684.

Soto F., Garcia-Guzman M., Gomez-Hernandez J.M., Hollmann M., Karschin C., Stühmer W. (1996a) $P2X_4$ — An ATP-activated ionotropic receptor cloned from rat brain (purinergic receptor). *Proceedings of the National Acadademy of Sciences* USA **93**: 3684-3688.

Soto F., Garcia-Guzman M., Karschin C., Stühmer W. (1996b) Cloning and tissue distribution of a novel P_{2X} receptor from rat brain. *Biochemical and Biophysical Research Communications* **223**: 456-460.

Soto F., Garcia-Guzman M., Stühmer W. (1997) Cloned ligand-gated channels activated by extracellular ATP (P_{2X} receptors). *Journal of Membrane Biology* **160**: 91-100.

Sperlagh B., Vizi E.S. (1991) Effect of presynaptic P2 receptor stimulation on transmitter release. *Journal of Neurochemistry* **56**: 1466-1470.

Stoop R., Surprenant A., North R.A. (1997) Differential sensitivities to pH of ATP-induced currents at four cloned P_{2X} receptors. *Journal of Neurophysiology* **78**: 1837-1840.

Stout J.G., Kirley T.L. (1996) Control of cell membrane ecto-ATPase by oligomerization state — Intermolecular cross-linking modulates ATPase activity. *Biochemistry* **35**: 8289-8298.

Sun X.P., Stanley E.F. (1996) An ATP-activated, ligand-gated ion channel on a cholinergic presynaptic nerve terminal. *Proceedings of the National Academy of Sciences* USA **93**: 1859-1863.

Surprenant A., Rassendren F., Kawashima E., North R.A., Buell G. (1996) The cytolytic P_{2Z} receptor for extracellular ATP identified as a P_{2X} receptor ($P2X_7$). *Science* **272**: 735-738.

Thomas S., Virginio C., North R.A., Surprenant A. (1998) The antagonist trinitrophenyl-ATP reveals co-existence of distinct P_{2X} receptor channels in rat nodose neurons. *Journal of Physiology* **509**: 411-417.

Tinker A., Jan Y.N., Jan L.Y. (1996) Regions responsible for the assembly of inwardly rectifying potassium channels. *Cell* **87**: 857-868.

Torres G.E., Egan T.M., Voigt M.M. (1998a) Topological analysis of the ATP-gated ionotropic $P2X_2$ receptor subunit. *FEBS Letters* **425**: 19-23.

Torres G.E., Haines W.R., Egan T.M., Voigt M.M. (1998b) Co-expression of $P2X_1$ and $P2X_5$ receptor subunits reveals a novel ATP-gated ion channel. *Molecular Pharmacology* **54**: 989-993.

Torres G.E., Egan T.M., Voigt M.M. (1999) Hetero-oligomeric assembly of P_{2X} receptor subunits — Specificities exist with regard to possible partners. *Journal of Biological Chemistry* **274**: 6653-6659.

Tschöpl M., Harms L., Nörenberg W., Illes P. (1992) Excitatory effects of adenosine 5'-triphosphate on rat locus coeruleus neurons. *European Journal of Pharmacology* **213**: 71-77.

Ueno S., Harata N., Inoue K., Akaike N.J. (1992) ATP-gated current in dissociated rat nucleus solitarii neurons. *Journal of Neurophysiology* **68**: 778-785.

Unsworth C.D., Johnson R.G. (1990) Acetylcholine and ATP are co-released from the electromotor nerve terminals of *Narcine brasiliensis* by an exocytotic mechanism. *Proceedings of the National Academy of Sciences* USA **87**: 553-557.

Urano T., Nishimori H., Han H.-J., Furuhata T., Kimura Y., Nakamura Y., Tokino T. (1997) Cloning of $P2X_M$ — A novel human P_{2X} receptor gene regulated by p53. *Cancer Research* **57**: 3281-3287.

Valera S., Hussy N., Evans R.J., Adami N., North R.A., Surprenant A., Buell G. (1994) A new class of ligand-gated ion channel defined by P_{2x} receptor for extracellular ATP. *Nature* **371**: 516-519.

Valera S., Talabot F., Evans R.J., Gos A., Antonarakis S.E., Morris M.A., Buell G.N. (1995) Characterization and chromosomal localization of a human P_{2X} receptor from urinary bladder. *Receptors and Channels* **3**: 283-289.

Vincent P. (1992) Cationic channels sensitive to extracellular ATP in rat lacrimal cells. *Journal of Physiology* **449**: 313-331.

Virginio C., Robertson G., Surprenant A., North R.A. (1998) Trinitrophenyl-substituted nucleotides are potent antagonists selective for $P2X_1$, $P2X_3$, and heteromeric $P2X_{2+3}$ receptors. *Molecular Pharmacology* **53**: 969-973.

Virginio C., MacKenzie A., Rassendren F.A., North R.A., Surprenant A. (1999) Pore dilation of neuronal P_{2X} receptor channels. *Nature Neuroscience* **2**: 315-321.

Vulchanova L., Arvidsson U., Riedl M., Wang J., Buell G., Surprenant A., North R.A., Elde R. (1996) Differential distribution of two ATP-gated ion channels (P_{2X} receptors) determined by immunocytochemistry. *Proceedings of the National Academy of Sciences* USA **93**: 8063-8067.

Vulchanova L., Riedl M.S., Shuster S.J., Buell G., Surprenant A., North R.A., Elde R. (1997) Immunohistochemical study of the $P2X_2$ and $P2X_3$ receptor subunits in rat and monkey sensory neurons and their central terminals. *Neuropharmacology* **36**: 1229-1242.

Vulchanova L., Riedl M.S., Shuster S.J., Stone L.S., Hargreaves K.M., Buell G., Surprenant A., North R.A., Elde R. (1998) $P2X_3$ is expressed by DRG neurons that terminate in inner lamina II. *European Journal of Neuroscience* **10**: 3470-3478.

Walker J.E., Saraste M., Runswick M.J., Gay N.J. (1982) Distantly related sequences in the α- and β-subunits of ATP synthase, myosin, kinases and other ATP-requiring enzymes and a common nucleotide binding fold. *EMBO Journal* **1**: 945-951.

Wang C.-Z., Namba N., Gonoi T., Inagaki N., Seino S. (1996) Cloning and pharmaco-

logical characterization of a fourth P_{2X} receptor subtype widely expressed in brain and peripheral tissues including various endocrine tissues. *Biochemical and Biophysical Research Communications* **220**: 196-202.

Werner P., Seward E.P., Buell G.N., North R.A. (1996) Domains of P_{2X} receptors involved in desensitization. *Proceedings of the National Academy of Sciences* USA **93**: 15485-15490.

Wierasko A., Ehrlich Y.H. (1994) On the role of extracellular ATP in the induction of long-term potentiation in the hippocampus. *Journal of Neurochemistry* **63**: 1731-1737.

Zimmermann H. (1994) Signalling via ATP in the nervous system. *Trends in Neurosciences* **17**: 420-426.

CHAPTER 9

MANUSCRIPT REPRINTS

Pergamon

PII: S0306-4522(97)00365-5

Neuroscience Vol. 83, No. 1, pp. 177–190, 1998
Copyright © 1997 IBRO. Published by Elsevier Science Ltd
Printed in Great Britain. All rights reserved
0306-4522/98 $19.00+0.00

SENSORY PRESYNAPTIC AND WIDESPREAD SOMATODENDRITIC IMMUNOLOCALIZATION OF CENTRAL IONOTROPIC P2X ATP RECEPTORS

K.-T. LÊ, P. VILLENEUVE, A. R. RAMJAUN, P. S. McPHERSON, A. BEAUDET and P. SÉGUÉLA*

Montreal Neurological Institute, McGill University, 3801 University, Montreal, Quebec, Canada H3A 2B4

Abstract—Recent evidence suggests that extracellular ATP plays a neurotransmitter role in the central nervous system. Its fast ionotropic effects are exerted through a family of P2X ATP-gated channels expressed in brain and spinal cord. To determine the physiological significance of central ATP receptors, we have investigated the localization of a major neuronal P2X receptor at the cellular and subcellular levels using affinity-purified antibodies directed against the C-terminal domain of $P2X_4$ subunit. Subunit-specific anti-$P2X_4$ antibodies detected a single band of 57,000±3000 mol. wt in transfected HEK-293 cells and in homogenates from adult rat brain. The strongest expression of central P2X receptors was observed in the olfactory bulb, lateral septum, cerebellum and spinal cord. $P2X_4$ immunoreactivity was also evident in widespread areas including the cerebral cortex, hippocampus, thalamus and brainstem. In all regions examined, P2X receptors were associated with perikarya and dendrites where they were concentrated at the level of afferent synaptic junctions, confirming a direct involvement of postsynaptic ATP-gated channels in fast excitatory purinergic transmission.

Moreover, $P2X_4$-containing purinoceptors were localized in axon terminals in the olfactory bulb and in the substantia gelatinosa of nucleus caudalis of the medulla and dorsal horn of the spinal cord, demonstrating an important selective presynaptic role of ATP in the modulation of neurotransmitter release in central sensory systems. © 1997 IBRO. Published by Elsevier Science Ltd.

Key words: ATP-gated channel, purinergic, nucleotide, olfactory bulb, substantia gelatinosa, spinal cord.

The role of extracellular ATP as a neurotransmitter at neuro-effector and neuro-neuronal synapses in the peripheral nervous system has been convincingly demonstrated (see review in Zimmermann, 1994).[43] Furthermore, a growing body of neurophysiological evidence suggests that ATP is involved in widespread excitatory transmission in the CNS.[12,14–16,20,21,40] Ionotropic peripheral and central effects of extracellular ATP are exerted through a family of P2X purinoceptors.

Seven different genes coding for mammalian central and peripheral P2X ATP receptor subunits have been cloned so far. These genes have distinct but partially overlapping anatomical patterns of transcription that suggest tissue-specific heteromeric assembly of P2X subunits.[24] $P2X_1$ subunits are expressed predominantly in smooth muscle cells.[41] $P2X_2$ mRNA is found in sympathetic and sensory neurons as well as in the pituitary gland.[4] $P2X_3$ is expressed exclusively in sensory neurons,[8,24] while $P2X_5$ is also present in sensory neurons and in a subset of spinal motoneurons.[10,17] The cytolytic $P2X_7$ receptor was found to be expressed in immune cells and in glial cells of central and peripheral nervous system.[39]

In situ hybridization studies have shown that $P2X_4$[3,6,37] and $P2X_6$[10] are the only two members of the P2X gene family to be widely transcribed in the adult CNS and in periphery. Whether recorded in recombinant form in *Xenopus* oocytes[37,38] and transfected HEK-293 cells,[6,10] or natively in cultured epithelial cells from rat maxillary salivary gland,[6] the homomeric forms of these two receptors display a characteristic low sensitivity to the classical purinergic antagonists suramin and pyridoxalphosphate-6-azophenyl-2′,4′-disulphonic acid as well as slow desensitization kinetics. There is still no information available, however, on the cellular and subcellular distribution of these proteins in mammalian CNS. Yet, this information is critical to our understanding of the physiological role of central ATP-gated channels.

Taking advantage of the cloning of neuronal P2X receptors, we have developed subunit-specific polyclonal antibodies directed against $P2X_4$, one major

*To whom correspondence should be addressed.

Abbreviations: DAB, diaminobenzidine; EDTA, ethylenediaminetetra-acetate; GST, glutathione-S-transferase; HEPES, *N*-2-hydroxyethylpiperazine-*N*′-2-ethanesulphonic acid; MBP, maltose-binding protein; NGS, normal goat serum; PCR, polymerase chain reaction; PVDF, polyvinylidene difluoride; SDS-PAGE, sodium dodecyl sulphate-polyacrylamide gel electrophoresis; TBS, Tris-buffered saline.

and widespread component of central P2X receptors. We report here the localization of this receptor-channel subunit at the regional, cellular and ultrastructural level in the adult rat brain and spinal cord. A summary of this work has been presented at the XXVIth Annual Meeting of Society for Neuroscience.[23]

EXPERIMENTAL PROCEDURES

Development and purification of subunit-specific anti-P2X$_4$ antibodies

The cDNA coding for the C-terminal domain of rat P2X$_4$, corresponding to the last 31 amino acids, the stop codon plus the 3' untranslated region, was amplified in polymerase chain reaction (PCR) from a full-length clone[37] using a sense primer (TC*GGATCC*CTCTACTGCATGAA GAAG) containing an artificial BamHI restriction site and a reverse pcDNAI vector primer. The 672 base pair PCR product was double digested with BamHI and EcoRI for subcloning in frame with glutathione-S-transferase (GST) protein in the prokaryotic expression vector pGEX-2T (Pharmacia). The same PCR product was double digested with BamHI and XbaI (a natural site present in P2X$_4$) for subcloning in frame with maltose-binding protein (MBP) in the prokaryotic expression vector pMAL-c2 (New England Biolabs) for affinity purification purpose. The production of GST–P2X$_4$ fusion protein was induced by 0.1 mM isopropyl-β-thiogalactopyranoside in culture and milligrams of the bacterial protein of 32,000 mol. wt were purified directly on preparative sodium dodecyl sulphate–polyacrylamide gel electrophoresis (SDS–PAGE). Excised bands containing 0.2–0.5 mg of GST–P2X$_4$ were mixed with Freund's complete adjuvant to initiate a standard immunization procedure in rabbits.[18] A similar protocol of induction was used to produce a 46,000 mol. wt MBP–P2X$_4$ fusion protein that was separated on 12% SDS–PAGE, blotted and dried on polyvinylidene difluoride (PVDF) membrane. Protein concentrations were estimated by comparison with bovine serum albumin standards in Coomassie Blue staining. IgGs from positive sera pre-selected in western blots were affinity-purified by solid-phase adsorption using MBP–P2X$_4$ on PVDF strips, eluted under acidic conditions (50 mM glycine buffer pH 2.5) prior to rapid neutralization in 2 M Tris buffer pH 8.0 and followed by 16 h dialysis in 0.01 M phosphate buffer pH 7.4 containing 2% sucrose and 1 mM EDTA.

Construction of epitope-tagged P2X receptor subunits

P2X$_1$ and P2X$_4$ receptor subunits were epitope-tagged both to facilitate the localization of the two subunits in heterologous expression systems and to validate the subunit specificity of the immunoreactivity observed with anti-P2X$_4$ polyclonal antibodies. The C-terminal Flag octapeptide DYKDDDDK (IBI) was inserted in mutagenic PCR using oligonucleotide primers designed for the replacement of the natural stop codon of P2X$_1$ (anti-sense TCA*CTCGAGG* GAGGTCCTCATGTTCTCC) and P2X$_4$ subunits (anti-sense TGA*CTCGAGG*CGACACTGGTTCATCTC) by an artificial XhoI site. Full-length mutant P2X subunits cDNAs were amplified in PCR using Pfu polymerase (Stratagene) then ligated in-frame to an XhoI-XbaI cassette containing the Flag peptide followed by a Stop codon,[29] before subcloning in the pcDNAI eukaryotic expression vector (Invitrogen).

Heterologous expression of homomeric P2X receptors in HEK-293 cells

For transfection of epitope-tagged and wild-type P2X subunits in mammalian cells, HEK-293 (ATCC no. CRL1573) were grown in Dulbecco's modified Eagle's medium–10% heat-inactivated fetal bovine serum (Wisent, St Bruno, Quebec) containing penicillin and streptomycin. Freshly plated cells reaching 30–50% confluency were used for transient transfection using the calcium phosphate method on 90 mm dishes with 10 μg supercoiled plasmid DNA/10^6 cells. Heterologous expression of P2X receptor subunits was assayed by immunofluorescence and western blot at 36–48 h of post-transfection time.

Immunolocalization of P2X receptors in transfected HEK-293 cells

After 24–36 h of post-transfection time, HEK-293 cells were plated at 50–70% confluency in poly-lysine-coated chambers. Four hours later, adherent cells were washed in phosphate-buffered saline and fixed for 20 min at room temperature with 4% paraformaldehyde in 0.1 M phosphate buffer, pH 8.0. After blocking non-specific sites with 2% normal goat serum (NGS), fixed cells were incubated with affinity-purified and pre-adsorbed primary antibodies P2X$_4$ (1 μg/ml) or M2 (1 μg/ml) anti-Flag peptide antibodies overnight at 4°C in 0.05 M Tris-saline buffer pH 7.2 containing 0.5% Triton X-100, 5% NGS and 5% dry milk powder. Bound antibodies were detected by immunofluorescence after 1 h incubation with fluorescein isothiocyanate-labelled goat anti-rabbit (1 μg/ml) or Texas Red-labelled goat anti-mouse (2 μg/ml) secondary antibodies (ImmunoResearch Labs).

Western blot of homogenates from transfected cells and rat brain regions

Transfected HEK-293 cells were lifted in Hank's modified calcium-free medium with 20 mM EDTA, pelleted at low speed and homogenized in 10 volumes of 10 mM HEPES buffer pH 7.4 containing the protease inhibitors phenylmethylsulfonylfluoride (0.2 mM) and benzamidine (1 mM). Lysates were pelleted at 14,000 *g* for 5 min to remove cell debris before protein assay. Various brain regions (see Fig. 4) were dissected from an adult rat and homogenized at 1:10 (w:v) in 20 mM HEPES buffer pH 7.4 containing 0.32 M sucrose, 0.83 mM benzamidine, and 0.23 mM phenylmethylsulfonylfluoride using a polytron, then pelleted at 14,000 *g* for 5 min. Protein concentrations in homogenates were determined using the method of Lowry *et al.*[27] as modified by Peterson[33] and equal amounts of protein (150 μg/lane) were run on 10–12% SDS–PAGE, then transferred to nitrocellulose. Depending on the sample, probing was performed with the following primary antibodies: affinity-purified rabbit anti-P2X$_4$ antibodies (2 μg/ml) pre-adsorbed with MBP alone, affinity-purified anti-P2X$_4$ (2 μg/ml) pre-adsorbed with MBP–P2X$_4$ (negative controls) or mouse mAb M2 (1 μg/ml, IBI). Appropriate secondary species-specific peroxidase-labelled antibodies were used for visualization by enhanced chemiluminescence (ECL, Amersham).

Immunocytochemistry in rat brain and spinal cord

Adult male Sprague–Dawley rats (140–180 g, Charles River, Canada) were deeply anaesthetized with sodium pentobarbital (80 mg/kg, i.p.) and perfused transaortically with 375 ml of 2% paraformaldehyde (light microscopy) or with 75 ml of a mixture of 3.75% acrolein and 2% paraformaldehyde followed by 300 ml of 2% paraformaldehyde (for electron microscopy) in 0.1 M phosphate buffer, pH 7.4. Brains and spinal cords were dissected out and postfixed for 1 h by immersion in the same fixative. For light microscopic immunohistochemistry, they were then cryoprotected for 48 h by immersion in a 30% sucrose solution in 0.2 M phosphate buffer pH 7.4 at 4°C, frozen in isopentane at −45°C, and sectioned at a thickness of 30 μm on a freezing microtome. Sections were rinsed in phosphate buffer pH 7.4, and incubated for 30 min in 0.1 M Tris buffer

```
P2X4   LYCMKKKYYYRDKKYKYVEDYEQGLSGEMNQ*
P2X1   LHILPKRHYYKQKKFKYAEDMGPGEGEHDPVATSSTLGLQENMRTS*
P2X2   LTFMNKNKLYSHKKFDKVRTPKHPSSRWPVTLALVLGQIPPPPSH(68 aa)PKGLAQL*
P2X3   LNFLKGADHYKARKFEEVTETTLKGTASTNPVFASDQATVEKQSTDSGAYS*
P2X5   IYLIRKSEFYRDKKFEKVRGQKEDANVEVEANEMEQERP(51 aa)ILHPVKT*
P2X6   LYVDREAGFYWRTKYEEARAPKATTNSA*
P2X7   CEPCAVNEYYYRKKCEPIVEPKPTLKYVSFVDEPHIWMVDQQLLGKSL(167 aa)SGFKYPY*
```

Fig. 1. Alignment of the C-terminal domains of rat P2X ATP-gated channel subunits. The $P2X_4$ domain (amino acids 358–388) targeted for polyclonal anti-fusion protein antibodies production is compared with the corresponding sequences in known members of the P2X gene family. $P2X_1$ channel subunit displays the closest primary structure to $P2X_4$ in this region with 35% homology. Conserved residues in the same relative position in all P2X channel subunits are indicated in bold.

saline, pH 7.4 (TBS) containing 0.03% H_2O_2. For electron microscopic immunocytochemistry, the olfactory bulb, cerebellum and cervical spinal cord were blocked off with a razor blade and serially sectioned at 40 μm thickness on a vibrating microtome (Vibratome). Both frozen and Vibratome sections were then incubated overnight at 4°C in a solution containing 2% NGS, 5% dry milk powder, 0.2% Triton X-100 and 20 μg/ml affinity-purified $P2X_4$ antibodies pre-adsorbed with MBP. Negative control samples were incubated with $P2X_4$ antibodies pre-adsorbed with MBP–$P2X_4$ or with GST–$P2X_4$, with pre-immune serum (1:1000), or in the absence of primary antibodies. All sections were then rinsed in TBS and processed using the avidin–peroxidase–biotin staining method (ABC Elite, Vector Labs). Briefly, they were incubated with 1:100 biotinylated goat anti-rabbit and 1% NGS for 1 h followed by 1:100 avidin–peroxidase complex for an additional hour. Bound peroxidase was visualized by immersion of the sections in 0.01 M Tris buffer, pH 7.6, containing 0.05% 3,3′ diaminobenzidine (DAB), 0.04% nickel chloride and 0.01% H_2O_2. Frozen sections were then mounted on gelatin-coated slides, dehydrated in graded ethanols, defatted in xylene and coverslipped for light microscopic observation.[32] Vibratome-cut sections were postfixed in 2% OsO_4 in 0.1 M phosphate buffer containing 7% dextrose, dehydrated in graded ethanols and embedded in Epon between two acetate sheets. They were then mounted at the tip of Epon blocks and cut at 80 nm thickness on a Reichert ultramicrotome, collected on Formvar-coated copper grids and examined with a JEOL 100CX electron microscope.

RESULTS

Subunit specificity of antibodies directed against rat $P2X_4$

The subunit specificity of affinity-purified $P2X_4$ antibodies was tested on HEK-293 cells transfected with various members of the P2X receptor family. Members of this gene family display low intersubunit homology in the C-terminal domain chosen for the production of $P2X_4$ antibodies (Fig. 1). Since the primary structure of the $P2X_1$ subunit is the closest to that of $P2X_4$ in this region, we expressed epitope-tagged $P2X_1$ subunits in HEK-293 cells to challenge the specificity of our $P2X_4$ antibodies. No immunofluorescence was visible above background level in permeabilized HEK-293 cells expressing Flag-tagged $P2X_1$ (Fig. 2). Flag-tagged $P2X_2$ or the wild-type subunits (data not shown).

In western blots of crude homogenates from transfected cells, $P2X_4$ antibodies and anti-Flag mAb M2 recognized the same major protein band of 57,000±3000 mol. wt (n=4) corresponding to Flag-tagged $P2X_4$ monomers (Fig. 3). $P2X_4$ antibodies detected a major protein band of 56,000±3000 mol. wt (n=4) corresponding to wild-type $P2X_4$ monomers. In keeping with our immunofluorescence results on whole cells, $P2X_4$ antibodies did not bind to homologous $P2X_1$ subunits in homogenates (Fig. 3). An immunoreactive band of 100,000 mol. wt was detectable in homogenates of HEK-293 cells transfected with epitope-tagged $P2X_4$ receptors (Fig. 3). This labelling, observed both with M2 and $P2X_4$ antibodies, likely corresponds to multimers of overexpressed P2X subunits.

In western blots of crude homogenates from multiple regions of the adult rat brain, affinity-purified $P2X_4$ antibodies labelled a single major band of 57,000±3000 mol. wt (n=7) (Fig. 4) in concordance with the size of $P2X_4$ subunits heterogously expressed in HEK-293 cells. The labelling of a single major band demonstrated the monospecificity of our affinity-purified antibodies. $P2X_4$ immunoreactivity was detectable in all brain regions examined. However, relative $P2X_4$ protein levels varied considerably between areas: from very low expression in the striatum to very high expression in the olfactory bulb (Fig. 4).

Light microscopic localization of $P2X_4$ subunits in rat brain and spinal cord

In rat brain sections, $P2X_4$ immunoreactivity was detected with variable intensity throughout the neuraxis. Incubation of control sections with either preimmune serum or with purified serum pre-absorbed with the carboxy-terminal fragment of $P2X_4$ in MBP–$P2X_4$ markedly decreased or completely abolished the immunoreactivity in most regions examined (Fig. 5). Only those regions in which adsorption controls showed a marked decrease in $P2X_4$ signal are considered below.

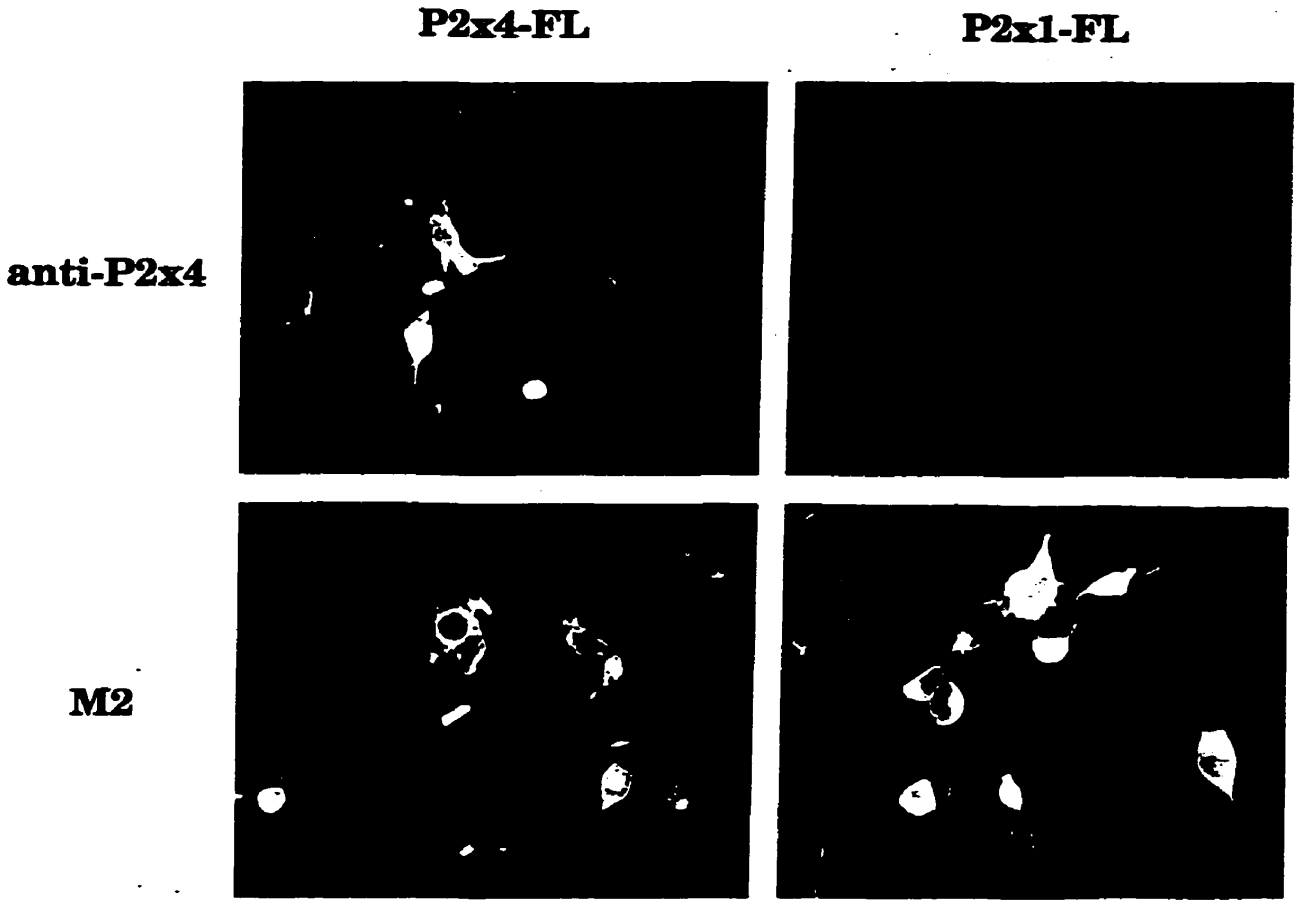

Fig. 2. Subunit-specificity of anti-$P2X_4$ antibodies in transfected HEK-293 cells. By immunofluorescence, affinity-purified anti-$P2X_4$ antibodies detect the expression of Flag-tagged $P2X_4$ subunits ($P2X_4$-FL) but not that of homologous Flag-tagged $P2X_1$ subunits ($P2X_1$-FL). As positive controls, both epitope-tagged $P2X_1$ and $P2X_4$ channel subtypes are visualized with anti-Flag mAb M2.

The most intense $P2X_4$ immunoreactivity in rat brain was detected in the glomerular layer of the olfactory bulb (Figs 5A, 6A) and in the outer layers of the nucleus of the spinal trigeminal tract and dorsal horn of the spinal cord (Fig. 6B). In both of these regions, the labelling was diffusely distributed throughout the neuropil (Fig. 6A, B). In all other brain areas, $P2X_4$ immunostaining was confined to neuronal perikarya and proximal dendrites.

Rostrally, intensely immunoreactive neurons were observed in the mitral cell layer of the olfactory bulb (Fig. 6A). Perikarya and proximal dendrites of tufted cells in the external plexiform layer were much less frequently and only weakly stained.

Moderately immunoreactive pyramidal cells were detected throughout the cerebral cortex. These were particularly numerous in layers II and III (Fig. 7A), but were also scattered throughout layer V. There were no consistent differences in labelling patterns between different cytoarchitectonic areas.

Intensely $P2X_4$-immunopositive neurons were observed in the lateral septal nucleus (Fig. 7B, C). These neurons showed granular staining of the perikaryon extending into proximal dendrites (Fig. 7B). More medially, small, less intensely labelled cells were visible on the midline, within the medial septal nucleus (Fig. 7C). These labelled cells were coextensive ventrally with equally moderately labelled neurons in the vertical limb of the diagonal band of Broca (Fig. 7C). In the caudate–putamen, sparse, lightly immunoreactive spiny type II neurons were visible, most prominently in the ventrolateral segment. No immunoreactive cells were apparent in the nucleus accumbens.

In the hippocampus, a subset of moderately to densely stained neurons were detected throughout the pyramidal layer of the CA1, CA2 and CA3 subfields. As can be seen in Fig. 8, these labelled cells were most numerous in CA2 and at the CA2/CA3 border, as well as at the hilar extremity of CA3. Multiple $P2X_4$-immunoreactive cells were also visible within the granule cell layer of the dentate gyrus. In addition, small, intensely labelled cells were dispersed throughout the hilus as well as in strata oriens and radiatum of the hippocampus.

The reticular, anterodorsal and ventrolateral nuclei of the thalamus exhibited large numbers of

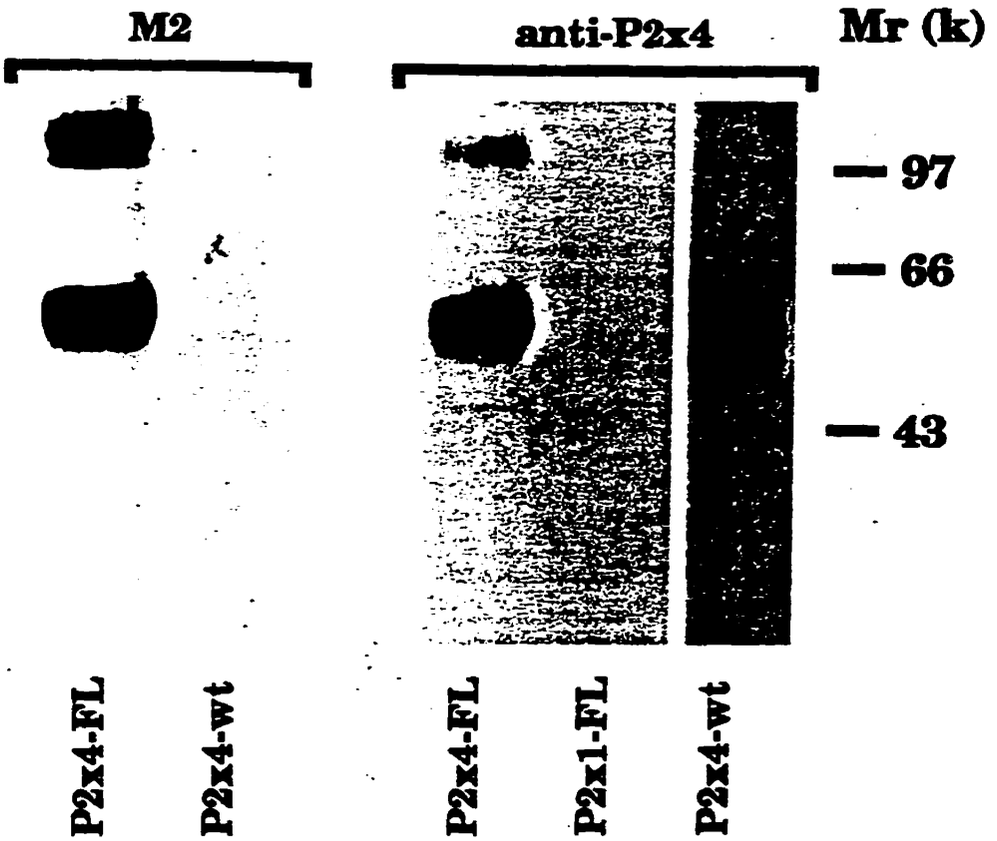

Fig. 3. Western blot of epitope-tagged and wild-type $P2X_4$ channels from homogenates of transiently transfected HEK-293 cells. Both mAb M2 and anti-$P2X_4$ antibodies detect Flag-tagged $P2X_4$ and anti-$P2X_4$ antibodies recognize wild-type $P2X_4$ channel subunit (56,000±3000 mol. wt). The same amount of total proteins (150 μg) has been loaded in each lane. Each sample has been assayed by immunofluorescence after expression with appropriate antibodies for checking the efficiency of the transfection.

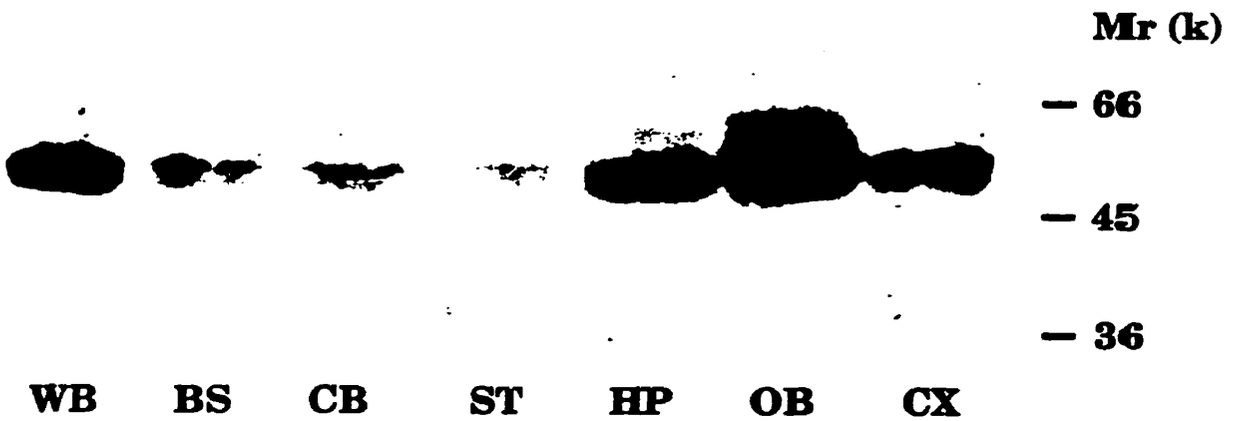

Fig. 4. Western blot of rat brain homogenates from microdissected regions using affinity-purified anti-$P2X_4$ antibodies. The single major band detected displays a mol. wt of 57,000±3000 corresponding to $P2X_4$ monomers in all regions examined. The same amount of total proteins (150 μg) has been loaded in each lane. WB, whole brain; BS, brain stem; CB, cerebellum; ST, striatum; HP, hippocampus; OB, olfactory bulb; CX, cerebral cortex.

moderately immunoreactive nerve cell bodies over relatively high non-specific background labelling.

In the hypothalamus, weakly immunoreactive nerve cell bodies were apparent within the anterior hypothalamic and suprachiasmatic nuclei. In the former, $P2X_4$-immunoreactive cells were sparse and mainly distributed in the lateral segment of the nucleus. In the latter, $P2X_4$-immunoreactive perikarya were more numerous, more intensely immunoreactive, and uniformly distributed throughout the nucleus.

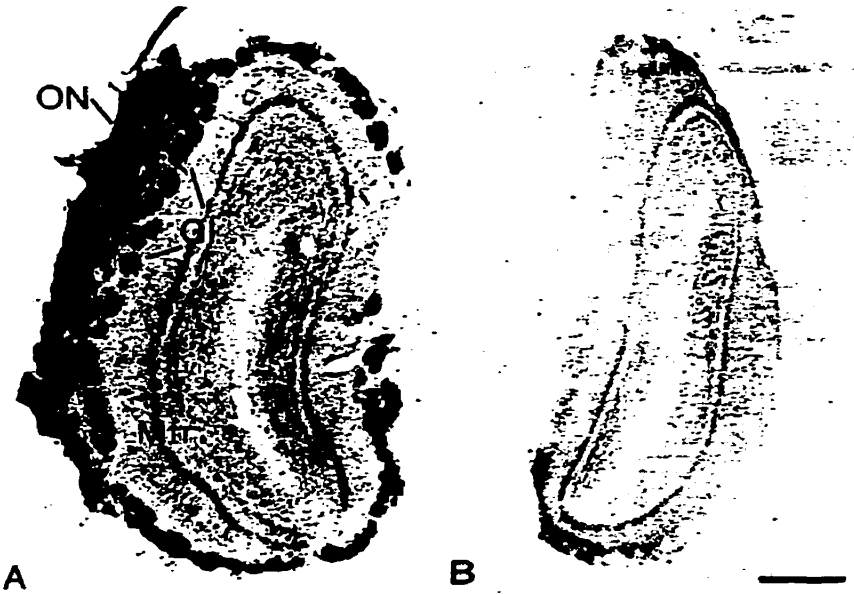

Fig. 5. $P2X_4$ immunoreactivity in rat olfactory bulb before (A) and after (B) pre-adsorption of affinity-purified primary antibodies with an excess of antigen. Immunolabelling in the olfactory nerve layer (ON), glomerular layer (Gl) and mitral cells layer (Mtr) (A) is abolished in sections incubated with pre-adsorbed antibodies (B). Scale bar=500 μm.

Within the brainstem, only a few nuclei showed significant immuno-adsorbable cellular staining. These include the dorsal tegmental and dorsal raphe nuclei of the midbrain and the main sensory nucleus of the trigeminal nerve. Moderate, highly punctate perikaryal staining was also observed in the substantia gelatinosa of the nucleus of the spinal trigeminal tract (nucleus caudalis) and dorsal horn of the spinal cord. These immunolabelled cells often poorly stood out against the intense neuropil staining in their surround (Fig. 6B).

In the cerebellar cortex, Purkinje cells were consistently heavily labelled (Fig. 9A). The immunostaining was most pronounced at the level of their perikarya, where at high magnification it took the form of small intracytoplasmic puncta, but was also observed, albeit more weakly, throughout their dendritic tree (Fig. 9A). Only sparse, weakly immunoreactive neurons, presumably Golgi cells from their size and localization, were detected in the granule cell layer.

Finally, central non-neuronal cells including leptomeningeal cells of the pia mater (Fig. 9B), perivascular cells and some endothelial cells of intraparenchymal blood vessels showed intense $P2X_4$ immunoreactivity.

Electron microscopic localization of $P2X_4$ subunits in the olfactory bulb, cervical spinal cord and cerebellum

In olfactory bulb glomeruli, $P2X_4$ immunoreactivity was evident within both dendrites (not shown) and axon terminals (Fig. 10A). In both structures, the labelling was diffusely distributed throughout the cytoplasm and heavily deposited over synaptic specializations (Fig. 10B). In layers I and II of the dorsal horn of the spinal cord, $P2X_4$ immunoreactivity was detected within neuronal perikarya, dendrites and axon terminals. In perikarya and dendrites, the reaction product was mainly absorbed on the outer surface of mitochondria, microtubules and various vesicular elements (Fig. 10C, D). Heavy DAB deposits were also visible along the plasma membrane, predominently at the level of synaptic junctions (Fig. 10C). In axon terminals, the reaction product was present throughout the cytoplasm and heavily concentrated on the membrane of synaptic vesicles and over synaptic densities (Fig. 10E, F).

In cerebellar cortex, $P2X_4$ immunolabelling was mainly evident over the perikarya and dendrites of Purkinje cells (Fig. 11). In both of these structures, heavy chromogen deposits were apparent along the plasma membrane (Fig. 11B, C) as well as over the membranes of a variety of intracellular organelles including cisterns of rough endoplasmic reticulum (Fig. 11A, C), Golgi saccules and vesicles (Fig. 11A) and mitochondria (Fig. 11A, B). In some instances, plaques of heavy DAB deposits were visible over clusters of endoplasmic reticulum cisternae and Golgi saccules (Fig. 11A) which likely accounted for the intracytoplasmic granularity observed in the light microscope.

DISCUSSION

Affinity-purified $P2X_4$ antibodies detect wild-type $P2X_4$ channel subunits migrating at a mol. wt of 56–57,000 both in heterologous systems and in adult rat brain. The significant difference between the predicted mol. wt of non-glycosylated $P2X_4$ subunit (44,000) and the observed mol. wt strongly suggests

Fig. 6. Distribution of $P2X_4$ immunoreactivity in the olfactory bulb (A) and dorsal horn of the spinal cord (B). (A) Labelling in the olfactory bulb is concentrated over the olfactory nerve layer (ON), glomerular layer (Gl) and individual mitral cells (Mtr). Note that individual glomeruli are not equally densely immunoreactive, and that weakly labelled cells are apparent in the external plexiform layer (EPl). Scale bar=60 μm. (B) $P2X_4$ immunoreactivity in the dorsal horn is concentrated over the outer marginal layer (I) and substantia gelatinosa (II). Only weak labelling is detected over layer III. Scale bar=120 μm.

that the protein is N-glycosylated on several of the six potential glycosylation sites found in the presumed extracellular domain of rat $P2X_4$. A post-translational modification of similar magnitude has been previously reported for the rat $P2X_1$ subunit.[10]

The assessment of the subunit-specificity of our polyclonal $P2X_4$ antibodies rests on convergent structural, biochemical and anatomical data. From a structural point of view, each member of the P2X receptor family has a unique C-terminal domain. A high degree of divergence is observed in this domain even between subunits that have similar functional properties in the homomeric form. As neither $P2X_1$ transcripts[10] nor $P2X_1$ subunits[42] are detected in the adult rat brain, the most likely candidate for cross-reactivity would have been the $P2X_6$ subunit which, like $P2X_4$, is widely expressed in the CNS.[10] However, $P2X_6$ displays a short C-terminal domain that does not share any related sequence with $P2X_4$, making it unlikely to account for the observed immunoreactivity. The immunolabelling of a single major band of the expected size in homogenates from brain regions demonstrates that the set of epitopes recognized by anti-$P2X_4$ antibodies in the C-terminal domain of these ATP-gated channels is unique in the mammalian CNS. Furthermore, the regional

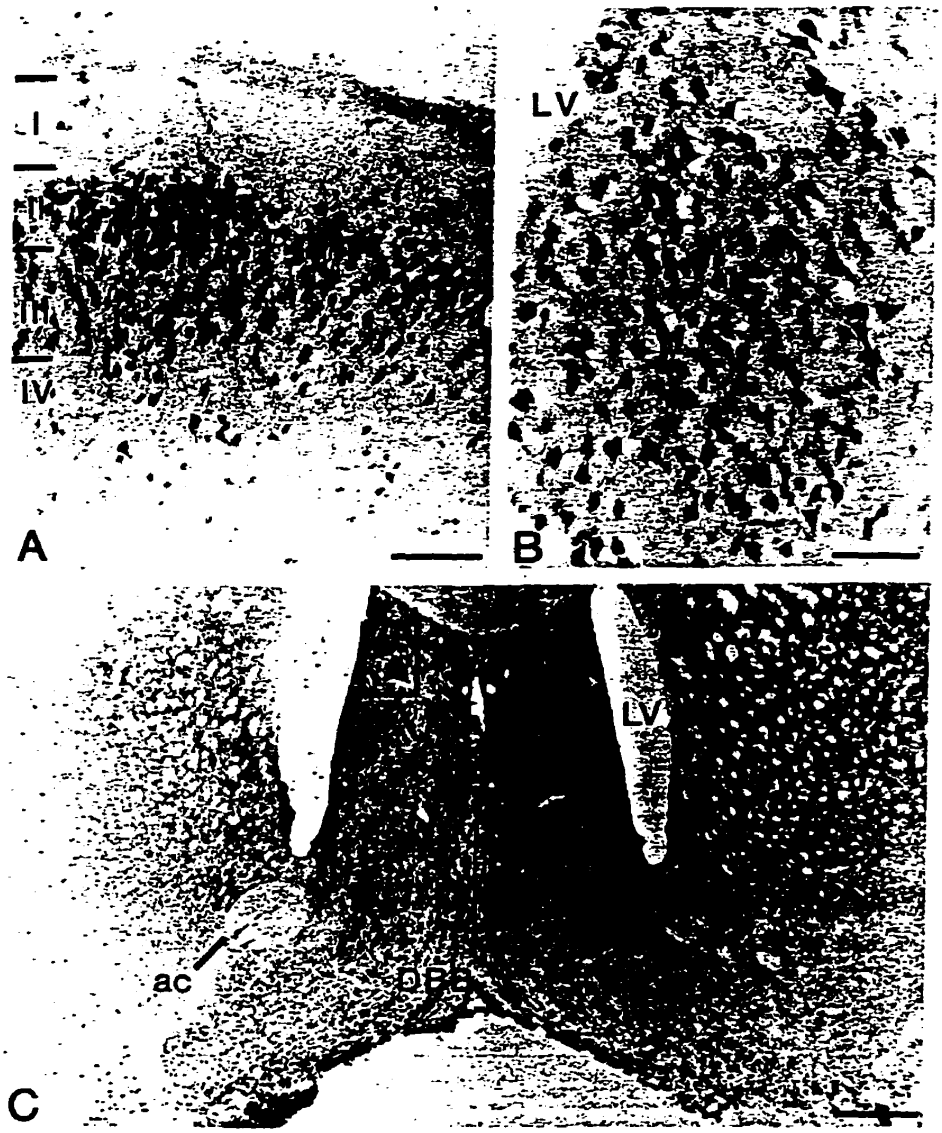

Fig. 7. Distribution of $P2X_4$ receptor subunits in the piriform cortex (A), lateral septum (B) and basal forebrain (C). (A) Moderately to densely labelled pyramidal cells are apparent throughout layers II–III. Scale bar=200 μm. (B) Higher magnification of the framed area in C. Note the heterogeneity of the perikaryal labelling. LV, Lateral ventricle. Scale bar=75 μm. (C) $P2X_4$-immunoreactive cells are visible throughout the lateral septum (LS), medium septum (MS) and diagonal band of Broca (DBB). CPu, caudate putamen; ac, anterior commissure. Scale bar=500 μm.

distribution of $P2X_4$ immunoreactivity in rat brain conforms to the results of earlier *in situ* hybridization studies,[3,6,10,37] confirming the specificity of the signal.

The selective distribution of $P2X_4$ immunoreactivity observed here in the rat CNS is also in good qualitative and quantitative agreement with the results of autoradiography using radiolabelled [^{3}H]α-β-methylene ATP.[1,2,28] However $P2X_4$ and $P2X_6$ subunits generate homomeric receptors insensitive to α-β-methylene ATP. Therefore, the correlation between the $P2X_4$ immunostaining reported here and previous radioligand binding results implies two non-exclusive possibilities: (a) α-β-methylene ATP binds with high-affinity to $P2X_4$ and $P2X_6$ homomeric receptors but is not an agonist because its binding site is not coupled to channel gating; (b) an unidentified central subunit with a similar widespread regional distribution confers α-β-methylene ATP binding and sensitivity to heteromeric channels containing $P2X_4$ and/or $P2X_6$ subunits.

The most intense $P2X_4$ expression in the rat brain was detected in the glomeruli of the olfactory bulb and in the dorsal horn of the spinal cord, two regions in which the immunostaining pervaded the entire neuropil. In olfactory bulb glomeruli, the labelling was found by electron microscopy to be associated with both axonal and dendritic processes. In view of the strong labelling of primary afferent axons observed in the olfactory nerve layer by light

Fig. 8. Immunolocalization of $P2X_4$ receptor subunits in hippocampus. Immunolabelled cells are scattered throughout CA1, CA2 and CA3 subfields of the hippocampus, as well as within the granule cell layer (gc) and hilus (hi) of the dentate gyrus. In the hippocampus, $P2X_4$-immunoreactive cells are mainly found in the pyramidal cell layer (py), of which they nonetheless constitute a subpopulation of interneurons and small pyramidal cells (Insert: arrows). Only sparse immunolabelled cells are evident in strata oriens (or) and radiatum (ra). Scale bar=300 μm. In insert=50 μm.

microscopy, axonal $P2X_4$ immunoreactivity is likely to be mainly associated with primary afferents in the glomeruli. Labelled dendrites presumably belong to either mitral or tufted cells, as both of these have been shown to extend their dendrites within glomeruli.[13,34] This interpretation conforms to the recent demonstration of $P2X_4$ mRNA within these two cell types by *in situ* hybridization.[6]

In the spinal cord, intense $P2X_4$ immunoreactivity was observed by electron and/or light microscopy over neuronal perikarya and axon terminals in the marginal layer and in the substantia gelatinosa of the spinal cord and nucleus caudalis, two areas involved in pain information processing where ATP has been previously shown to modulate synaptic transmission.[26] Whether the axonal $P2X_4$ subunits visualized here by immunohistochemistry are located on primary sensory afferent fibres or are part of local circuits remains to be established. The detection of $P2X_4$ subunit mRNA in sensory neurons of dorsal root ganglia[24] supports the former possibility.

In all other regions of the rat brain, $P2X_4$ immunoreactivity was associated with neuronal perikarya and proximal dendrites, thereby accounting for the good correlation with *in situ* hybridization data. Within $P2X_4$-immunoreactive cells, the bulk of the immunostaining was consistently intracellular, in the form of small intracytoplasmic "hot spots". Such a high proportion of intracellular receptors has been reported for other types of neuronal transmitter-gated channels, including nicotinic acetylcholine receptors[19] and glutamate-gated channels.[36] Electron microscopic observations confirmed the heterogeneity of $P2X_4$ intracytoplasmic labelling and showed that these "hot spots" correspond to stacks of rough endoplasmic reticulum cisterns and to congregated Golgi saccules and vesicles, i.e. to putative sites of synthesis, storage and transport of the ATP receptors.

Dense chromogen deposits were also observed along the outer mitochondrial membrane and microtubules of labelled perikarya and dendrites, as well as over membranes of synaptic vesicles within labelled axon terminals. The interpretation of these labelling patterns should be subject to caution, however, given the reported limitations in the subcellular resolution of DAB cytochemistry.[30]

A major finding of the present ultrastructural investigation is that $P2X_4$ is associated both with intraneuronal perikarya/dendrites and with axon

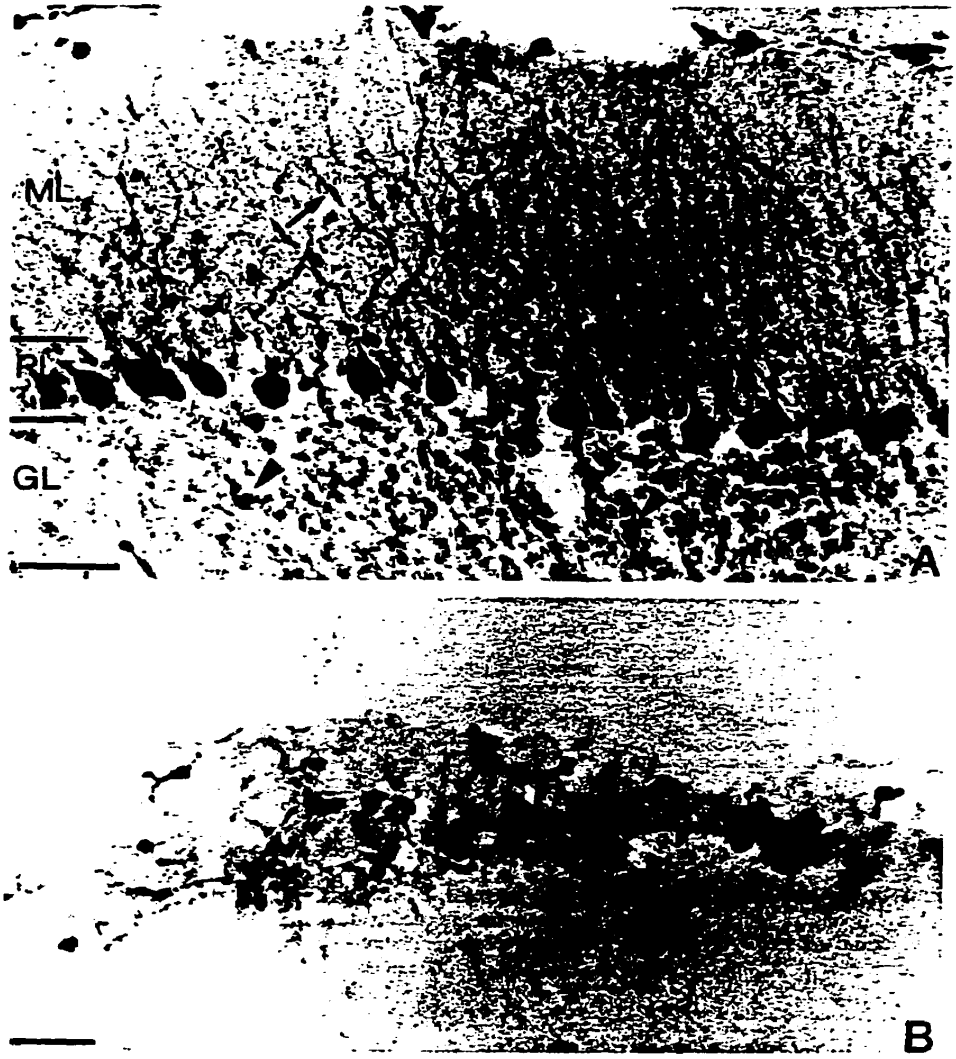

Fig. 9. Distribution of $P2X_4$ immunoreactivity in cerebellar cortex (A) and pia mater (B). (A) In cerebellar cortex, Purkinje cells (PL) are intensely immunoreactive. Partial filling of their dendritic tree is also evident in the molecular layer (ML; arrows). Only sparse, weakly labelled cells are apparent in the granule cell layer (GL). Scale bar=120 μm. (B) In the pia mater, leptomeningeal cells are intensely positive for $P2X_4$ immunoreactivity. Scale bar=40 μm.

terminals, indicating that they mediate both post- and pre-synaptic ATP signalling. In the olfactory bulb and dorsal horn of the spinal cord, this double localization suggests that fast purinergic transmission is involved in both pre- and postsynaptic regulation of olfactory and nociceptive sensory pathways, an interpretation strengthened by the presynaptic localization of $P2X_1$ and $P2X_2$ subtypes in the same areas.[41] This argues strongly in favour of ATP playing a specific modulatory role in sensory information processing through heteromeric $P2X_4$-containing ionotropic receptors.

In other brain areas studied, such as the hippocampus and cerebellar cortex, it appears that ATP mainly plays a postsynaptic neurotransmitter role through $P2X_4$-containing receptors. In the hippocampus, the highest levels of $P2X_4$ immunoreactivity were detected in the pyramidal layer of all CA subfields as well as in granule cells of the dentate gyrus. ATP-induced currents mediated by homomeric $P2X_4$ receptors are potentiated by extracellular zinc.[37,38] This potentiation of fast purinergic responses by zinc, recorded in various preparations,[9,22,25] is a general property of neuronal ATP-gated channels. The hippocampal mossy fibres that synapse on CA3 pyramidal cells contain the highest concentration of releasable zinc in the brain.[11] Therefore, in contrast to the receptors expressed in CA2 where pyramidal cells are not contacted by mossy fibres, the activity of $P2X_4$-containing ATP-gated channels localized on the dendrites of CA3 pyramidal cells and/or interneurons could be regulated by synaptic zinc, the dysfunction of which may have pathological consequences.[7,35]

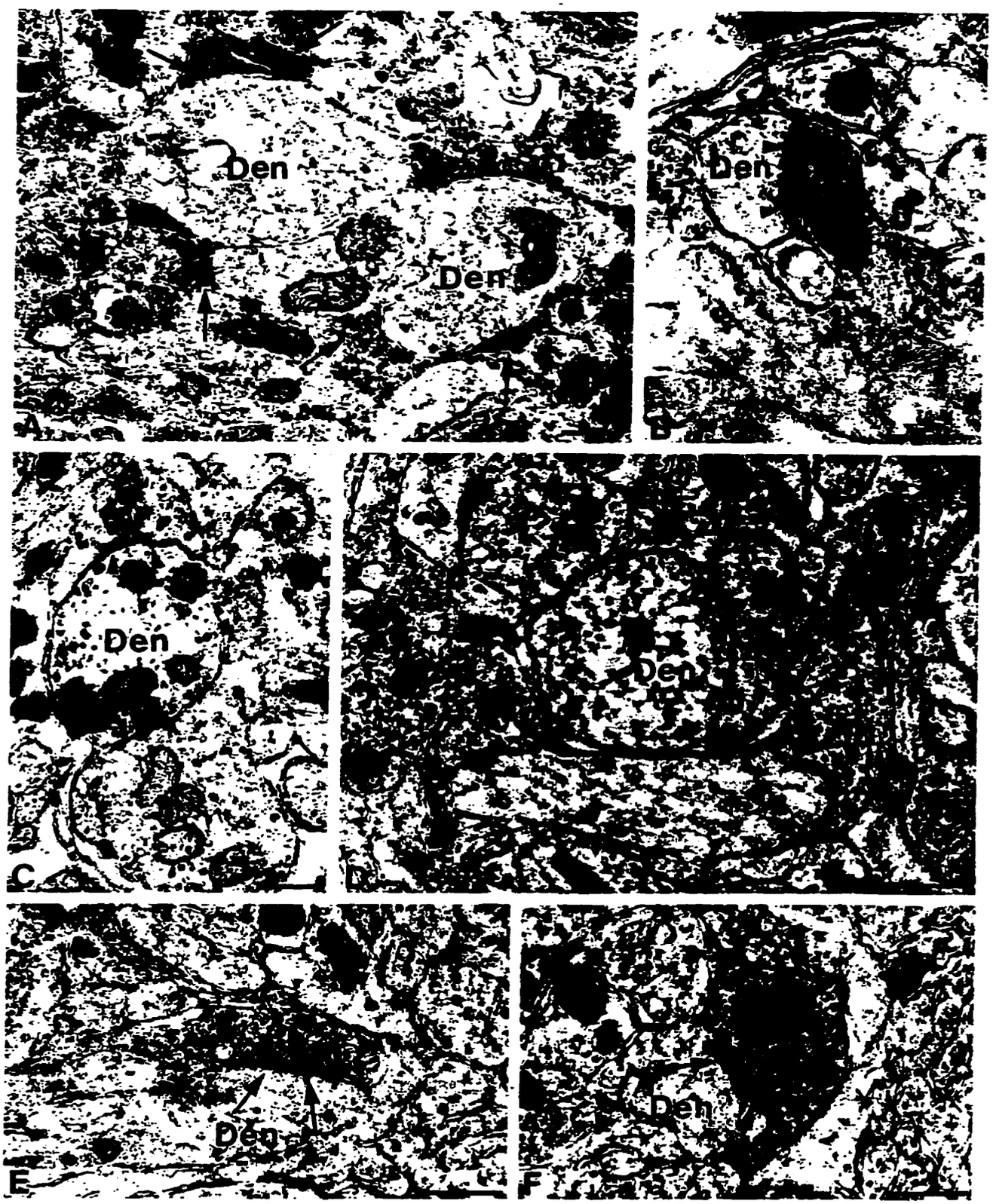

Fig. 10. Fine structural distribution of $P2X_4$ immunoreactivity in olfactory bulb glomeruli (A, B) and substantia gelatinosa of the spinal cord (C–E). (A) Numerous $P2X_4$-immunoreactive axon terminals (arrows) are seen to synapse on immunonegative dendritic trunks (Den). (B) $P2X_4$-immunoreactive axon terminals in synaptic contact with a dendritic branch (Den). Note the heavy chromogen deposits on the membrane of synaptic vesicles as well as at the level of the synaptic specialization (arrowheads). (C, D) $P2X_4$-immunoreactive dendrites (Den) in the substantia gelatinosa of the spinal cord. Dense DAB deposits are apparent at the level of synaptic junctions (arrowheads) as well as over microtubules and the outer membrane of mitochondria. (E, F) $P2X_4$-immunoreactive axon terminals in the substantia gelatinosa. Both terminals show diffuse labelling of their cytoplasm and are seen in asymmetrical synaptic contact (arrows) with unlabelled dendrites (Den). Scale bars=0.5 μm.

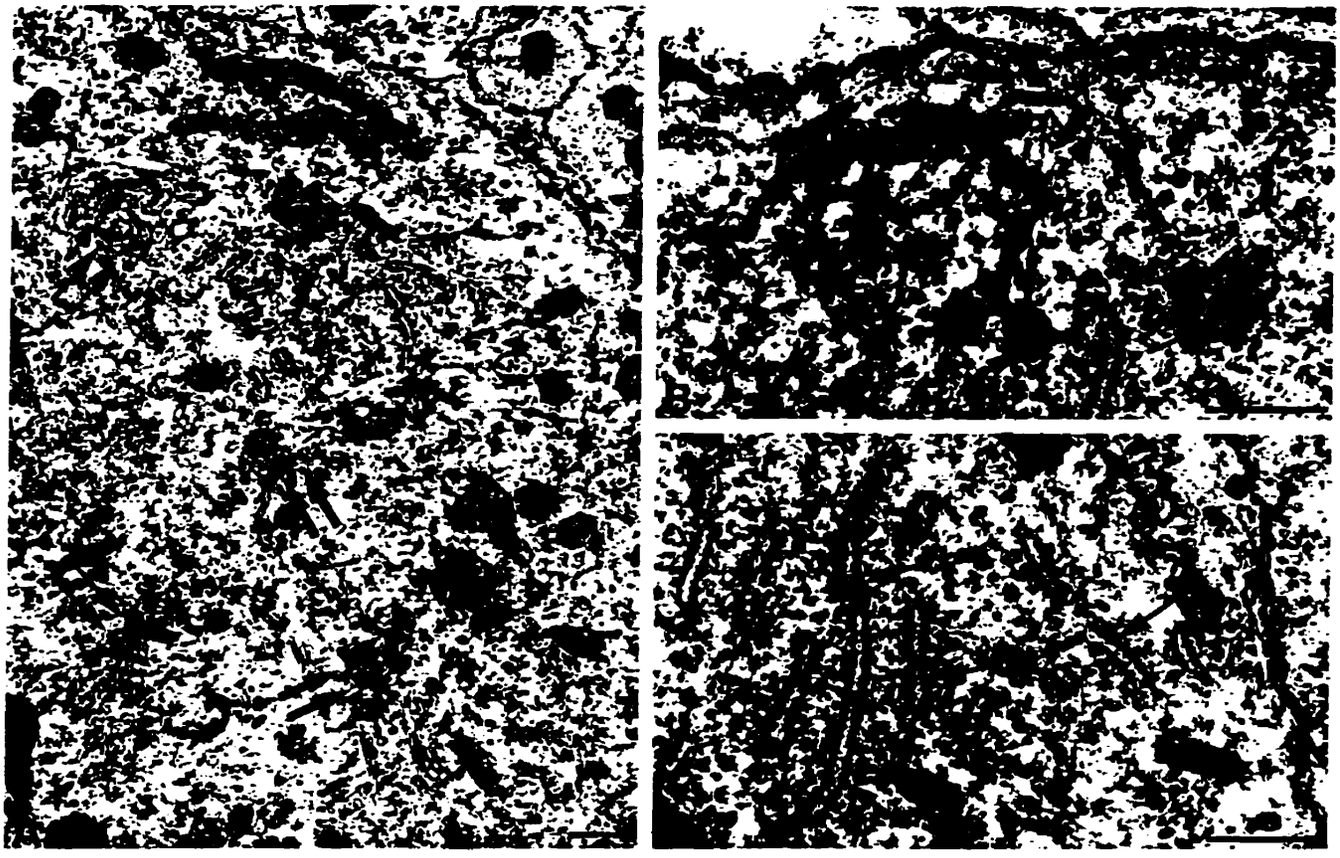

Fig. 11. Electron microscopic localization of $P2X_4$ immunoreactivity in cerebellar cortex. (A–C) $P2X_4$-immunoreactive Purkinje cell perikarya. (A) Plaques of dense chromogen deposits are apparent over cisterns of smooth endoplasmic reticulum (thin arrows) and stacks of Golgi saccules (thick arrows). (B) $P2X_4$ immunoreactivity is evident (arrowheads) as well as on the outer membrane of mitochondria (arrows). (C) $P2X_4$-immunoreactive deposits on cisterns of rough endoplasmic reticulum. Scale bars=0.5 μm.

The cerebellar cortex is the central structure which shows the highest level of $P2X_4$ subunit expression by *in situ* hybridization.[6,37,38] We demonstrate here that $P2X_4$ receptors are associated with both the perikaryal and dendritic membranes of Purkinje cells. The main sources of direct excitatory input to the Purkinje cells are the parallel fibres from granule cells and the climbing fibres from the inferior olivary complex.[31] Thus, our results suggest that ATP may be co-released with excitatory amino acids to control the firing activity of Purkinje cells.

The significant levels of $P2X_4$ receptor expression observed in subpopulations of leptomeningeal cells of the pia mater and perivascular cells suggest an unexpected role for extracellular ATP as a signalling molecule in various vascular-related non-excitable cells through the activation of ionotropic receptors.

CONCLUSION

Fast purinergic currents recorded in response to the activation of P2X channels display a significant primary calcium component due to their high permeability to divalent cations.[5,38] Our ultrastructural data on the presynaptic expression of $P2X_4$ channel subunit indicate that, by increasing intracellular calcium, $P2X_4$-containing ATP receptors may selectively control excitatory synaptic transmission in central sensory systems like the olfactory bulb and the substantia gelatinosa of spinal cord.

Acknowledgements—The authors thank both Mariette Houle and Michel Paquet for expert technical support. This project was funded by grants from MRC-Canada (P.S.M. A.B., P.S.), Quebec Heart and Stroke Foundation (P.S.) and the Savoy Foundation for Epilepsy (P.S.). P.S.M. is an Alfred P. Sloan Research Fellow. K.-T.L. is supported by the Savoy Foundation for Epilepsy.

REFERENCES

1. Balcar V. J., Li Y., Killinger S. and Bennett M. R. (1995) Autoradiography of P2x ATP receptors in the rat brain. *Br. J. Pharmac.* **115**, 302–306.

2. Bo X. and Burnstock G. (1994) Distribution of [^{3}H]α,β-methylene ATP binding sites in rat brain and spinal cord. *NeuroReport* **5**, 1601–1604.
3. Bo X., Zhang Y., Nassar M., Burnstock G. and Schoepfer R. (1995) A P2X purinoceptor cDNA conferring a novel pharmacological profile. *Fedn Eur. biochem. Socs Lett.* **375**, 129–133.
4. Brake A. J., Wagenbach M. J. and Julius D. (1994) New structural motif for ligand-gated ion channels defined by an ionotropic ATP receptor. *Nature* **371**, 519–523.
5. Buell G., Collo G. and Rassendren F. (1996) P2X receptors: an emerging channel family. *Eur. J. Neurosci.* **8**, 2221–2228.
6. Buell G., Lewis C., Collo G., North R. A. and Surprenant A. (1996) An antagonist-insensitive P2X receptor expressed in epithelia and brain. *Eur. molec. Biol. Org. J.* **15**, 55–62.
7. Buhl E. H., Otis T. S. and Mody I. (1996) Zinc-induced collapse of augmented inhibition by GABA in a temporal lobe epilepsy model. *Nature* **271**, 369–372.
8. Chen C., Akopian A. N., Sivilotti L., Colquhoun D., Burnstock G. and Wood J. N. (1995) A P2X receptor expressed by a subset of sensory neurons. *Nature* **377**, 428–430.
9. Cloues R., Jones S. and Brown D. A. (1993) Zn^{2+} potentiates ATP-activated currents in rat sympathetic neurons. *Pflügers Arch.* **424**, 152–158.
10. Collo G., North R. A., Kawashima E., Merlo-Pich E., Neidhart S., Surprenant A. and Buell G. (1996) Cloning of P2X5 and P2X6 receptors, and the distribution and properties of an extended family of ATP-gated ion channels. *J. Neurosci.* **16**, 2495–2507.
11. Crawford I. L. and Connor J. D. (1972) Zinc in maturing rat brain: hippocampal concentration and localization. *J. Neurochem.* **19**, 1451–1458.
12. Day T. A., Sibbald J. R. and Khanna S. (1993) ATP mediates an excitatory noradrenergic neuron input to supraoptic vasopressin cells. *Brain Res.* **607**, 341–344.
13. DeVries S. H. and Baylor D. A. (1993) Synaptic circuitry of the retina and olfactory bulb. *Cell 72/Neuron* **10**, 139–149.
14. Edwards F. A., Gibb A. J. and Colquhoun D. (1992) ATP receptor-mediated synaptic currents in the central nervous system. *Nature* **359**, 144–147.
15. Furukawa K., Ishibashi H. and Akaike N. (1994) ATP-induced inward current in neurons freshly dissociated from the tuberomammilary nucleus. *J. Neurophysiol.* **71**, 868–873.
16. Fyffe R. E. W. and Perl E. R. (1984) Is ATP a central synaptic mediator for certain primary afferent fibers from mammalian brain? *Proc. natn. Acad. Sci. U.S.A.* **81**, 6890–6893.
17. Garcia-Guzman M., Soto F., Laube B. and Stühmer W. (1996) Molecular cloning and functional expression of a novel rat heart P2X purinoceptor. *Fedn Eur. biochem. Socs Lett.* **388**, 123–127.
18. Harlow E. and Lane D. (1988) *Antibodies: A Laboratory Manual*. Cold Spring Harbor Laboratory Press.
19. Hill J. A., Zoli M., Bourgeois J.-P. and Changeux J.-P. (1993) Immunocytochemical localization of a neuronal nicotinic receptor: the β2-subunit. *J. Neurosci.* **13**, 1551–1568.
20. Hiruma H. and Bourque C. W. (1995) P2 purinoceptor-mediated depolarization of rat supraoptic neurosecretory cells *in vitro*. *J. Physiol.* **489**, 805–811.
21. Jahr C. E. and Jessell T. M. (1983) ATP excites a subpopulation of rat dorsal horn neurones. *Nature* **304**, 730–733.
22. Koizumi S., Ikeda M., Inoue K., Nakazawa K. and Inoue K. (1995) Enhancement by zinc of ATP-evoked dopamine release from rat pheochromocytoma PC12 cells. *Brain Res.* **673**, 75–82.
23. Lê K.-T., Villeneuve P., Ramjaun A., Mukerji J., McPherson P., Beaudet A. and Séguéla P. (1996) Cellular distribution of $P2X_4$ ATP-gated channels in rat brain and spinal cord. *Soc. Neurosci. Abstr.* **22**, 335.
24. Lewis C., Neidhart S., Holy C., North R. A., Buell G. and Surprenant A. (1995) Heteropolymerization of P2X receptor subunits can account for ATP-gated currents in sensory neurons. *Nature* **377**, 432–435.
25. Li C., Peoples R. W., Li Z. and Weight F. F. (1993) Zn^{2+} potentiates excitatory action of ATP on mammalian neurons. *Proc. natn. Acad. Sci. U.S.A.* **90**, 8264–8267.
26. Li J. and Perl E. R. (1995) ATP modulation of synaptic transmission in the spinal substantia gelatinosa. *J. Neurosci.* **15**, 3347–3365.
27. Lowry O. H., Rosebrough N. J., Farr A. L. and Randall R. J. (1951) Protein measurements with the folin phenol reagent. *J. biol. Chem.* **193**, 265–275.
28. Michel A. D. and Humphrey P. P. A. (1993) Distribution and characterization of [^{3}H]α,β-methylene ATP binding sites in the rat. *Naunyn-Schmiedebergs Arch. Pharmac.* **348**, 608–617.
29. Mukerji J., Haghighi A. and Séguéla P. (1996) Immunological characterization and transmembrane topology of 5-hydroxytryptamine$_3$ receptors by functional epitope tagging. *J. Neurochem.* **66**, 1027–1032.
30. Novikoff A. B., Novikoff P. M., Quintana N. and Davis C. (1972) Diffusion artifacts in 3,3′-diaminobenzidine cytochemistry. *J. Histochem. Cytochem.* **20**, 745–749.
31. Palay S. L. and Chan-Palay V. (1974) *Cerebellar Cortex. Cytology and Organization*. Springer, Berlin.
32. Paxinos G. and Watson C. (1986) *The Rat Brain in Stereotaxic Coordinates*. Academic, New York.
33. Peterson G. L. (1977) A simplification of the protein assay method of Lowry *et al.* which is more generally applicable. *Analyt. Biochem.* **83**, 346–356.
34. Pinching A. J. and Powell T. P. S. (1971) The neuropil of the glomeruli of the olfactory bulb. *J. Cell Sci.* **9**, 347–377.
35. Reece L. J., Dhanjal S. S. and Chung S. H. (1994) Zinc induces hyperexcitability in the hippocampus. *NeuroReport* **5**, 2669–2672.
36. Rogers S. W., Hughes T. E., Hollmann M., Gasic G. P., Deneris E. S. and Heinemann S. (1991) The characterization and localization of the glutamate receptor subunit GluR1 in the rat brain. *J. Neurosci.* **11**, 2713–2724.
37. Séguéla P., Haghighi A., Soghomonian J.-J. and Cooper E. (1996) A novel neuronal P2x ATP receptor ion channel with widespread distribution in the brain. *J. Neurosci.* **16**, 448–455.
38. Soto F., Garcia-Guzman M., Gomez-Hernandez J. M., Hollmann M., Karschin C. and Stühmer W. (1996) P2X4: an ATP-activated ionotropic receptor cloned from rat brain. *Proc. natn. Acad. Sci. U.S.A.* **93**, 3684–3688.
39. Surprenant A., Rassendren F., Kawashima E., North R. A. and Buell G. (1996) The cytolytic P2z receptor for extracellular ATP identified as a P2X receptor ($P2X_7$). *Science* **272**, 735–738.

40. Ueno S., Harata N., Inoue K. and Akaike N. J. (1992) ATP-gated current in dissociated rat nucleus solitarii neurons. *J. Neurophysiol.* **68**, 778–785.
41. Valera S., Hussy N., Evans R. J., Adami N., North R. A., Surprenant A. and Buell G. (1994) A new class of ligand-gated ion channel defined by P_{2x} receptor for extracellular ATP. *Nature* **371**, 516–519.
42. Vulchanova L., Arvidsson U., Riedl M., Wang J., Buell G., Surprenant A., North R. A. and Elde R. (1996) Differential distribution of two ATP-gated ion channels (P2X receptors) determined by immunocytochemistry. *Proc. natn. Acad. Sci. U.S.A.* **93**, 8063–8067.
43. Zimmermann H. (1994) Signalling via ATP in the nervous system. *Trends Neurosci.* **17**, 420–426.

(*Accepted* 16 *July* 1997)

Central $P2X_4$ and $P2X_6$ Channel Subunits Coassemble into a Novel Heteromeric ATP Receptor

Khanh-Tuoc Lê, Kazimierz Babinski, and Philippe Séguéla

Cell Biology of Excitable Tissue Group, Montreal Neurological Institute, McGill University, Montreal, Quebec, Canada H3A 2B4

Ionotropic ATP receptors are widely expressed in mammalian CNS. Despite extensive functional characterization of neuronal homomeric P2X receptors in heterologous expression systems, the subunit composition of native central P2X ATP-gated channels remains to be elucidated. $P2X_4$ and $P2X_6$ are major central subunits with highly overlapping mRNA distribution at both regional and cellular levels. When expressed alone in *Xenopus* oocytes, $P2X_6$ subunits do not assemble into surface receptors responsive to ATP applications. On the other hand, $P2X_4$ subunits assemble into bona fide ATP-gated channels, slowly desensitizing and weakly sensitive to the partial agonist α,β-methylene ATP and to noncompetitive antagonists suramin and pyridoxal-5-phosphate-6-azophenyl-2′,4′-disulfonic acid. We demonstrate here that the coexpression of $P2X_4$ and $P2X_6$ subunits in *Xenopus* oocytes leads to the generation of a novel pharmacological phenotype of ionotropic ATP receptors. Heteromeric $P2X_{4+6}$ receptors are activated by low-micromolar α,β-methylene ATP (EC_{50} = 12 μM) and are blocked by suramin and by Reactive Blue 2, which has the property, at low concentrations, to potentiate homomeric $P2X_4$ receptors. The assembly of $P2X_4$ with $P2X_6$ subunits results from subunit-dependent interactions, as shown by their specific copurification from HEK-293 cells transiently transfected with various epitope-tagged P2X channel subunits. Our data strongly suggest that the numerous cases of neuronal colocalizations of $P2X_4$ and $P2X_6$ subunits observed in mammalian CNS reflect the native expression of heteromeric $P2X_{4+6}$ channels with unique functional properties.

Key words: purinoceptor; nucleotide; transmitter-gated cation channel; α,β methylene ATP; suramin; PPADS

Fast purinergic neurotransmission is mediated by nonselective cation channels gated by extracellular ATP. These transduction proteins, designated P2X receptors, constitute a distinct class of neurotransmitter-gated channels on the basis of their primary cDNA sequences and their predicted transmembrane protein topology. Currently, seven mammalian P2X genes have been identified with either expression or homology cloning assays (Buell et al., 1996). Among the neuronal P2X receptors, only $P2X_4$ and $P2X_6$ isoforms are predominantly expressed in the adult rat brain in which they show an overlapping pattern of regional and cellular distribution at the mRNA level (Collo et al., 1996). Homomeric rat $P2X_4$ receptors expressed in HEK-293A cells or *Xenopus laevis* oocytes and homomeric $P2X_6$ receptors silent in oocytes (Soto et al., 1996) but functional in HEK-293A cells (Collo et al., 1996) are weakly responsive to α,β-methylene ATP ($\alpha\beta$mATP) and to P2 antagonists suramin and pyridoxal-5-phosphate-6-azophenyl-2′,4′-disulfonic acid (PPADS) (North and Barnard, 1997). Yet, native ionotropic purinergic responses from rat medial habenula, cerebellum, and hippocampus were blocked by P2 antagonists, and most native ATP receptors are activated by $\alpha\beta$mATP (Edwards et al., 1992; Mateo et al., 1998; Ross et al., 1998). Moreover, high-affinity [^{3}H]$\alpha\beta$mATP autoradiographic binding sites have been localized in specific but widespread regions within the brain and spinal cord (Bo and Burnstock, 1994; Michel and Humphrey, 1994; Balcar et al., 1995). Discrepancies between pharmacological profiles of heterologously expressed homo-oligomeric P2X subunits and electrophysiological recordings from neuronal preparations likely reflect the existence of native heteromeric phenotypes of P2X receptors in peripheral nervous system as well as the CNS. Indeed, one such hybrid P2X phenotype was recorded in sensory neurons (Khakh et al., 1995; Lewis et al., 1995) and has been proposed to result from the association between coexpressed $P2X_2$ and $P2X_3$ subunits (Chen et al., 1995; Lewis et al., 1995; Radford et al., 1997). We describe in this report a novel P2X heteromeric receptor containing central $P2X_4$ and $P2X_6$ subunits. This phenotype of ATP-gated channel is endowed with a unique pharmacology characterized by increased sensitivities to $\alpha\beta$mATP, 2-methylthio-ATP (2MeSATP), suramin, PPADS, and Reactive Blue 2 (RB-2) in *Xenopus* oocytes.

MATERIALS AND METHODS

Molecular biology. Wild-type full-length $P2X_6$ subunit cDNA was obtained by RT-PCR using adult rat spinal cord RT-cDNA template, Expand DNA polymerase (Boehringer Mannheim, Indianapolis, IN), and exact match primers based on published primary sequences (Collo et al., 1996; Soto et al., 1996). Construction of $P2X_1$-Flag and $P2X_4$-Flag was reported previously (Lê et al., 1998). To generate epitope-tagged $P2X_6$-Flag and $P2X_4$-$(His)_6$ subunits, an *Xho*I–*Xba*I cassette containing an in-frame His_6 epitope followed by an artificial stop codon was grafted to the full-length *Hin*dIII–*Xho*I $P2X_4$ construct. The $P2X_4$-$(His)_6$ mutant was then subcloned directionally into the *Hin*dIII and *Xba*I sites of pcDNAI vector (Invitrogen, San Diego, CA) for cytomegalovirus-driven heterologous expression in mammalian cells and *Xenopus laevis* oocytes. Epitope-tagged and RT-PCR constructs were subjected to dideoxy sequencing either manually with Sequenase (Upstate Biotechnology,

Received April 6, 1998; revised June 22, 1998; accepted July 6, 1998.

K-T.L. holds a PhD studentship from the Savoy Foundation for Epilepsy; K.B. is a Medical Research Council-PMAC-Astra postdoctoral Fellow; and P.S. is a junior Scholar from the Fonds de la Recherche en Santé du Québec. We thank the Medical Research Council of Canada, the Fondation des Maladies du Coeur du Québec, and the Astra Research Center in Montreal for their operating support, as well as Michel Paquet for expert technical assistance.

Correspondence should be addressed to Dr. Philippe Séguéla, Cell Biology of Excitable Tissue Group, Montreal Neurological Institute, 3801 University Avenue, Room 778, Montreal, Quebec, Canada H3A 2B4.

Copyright © 1998 Society for Neuroscience 0270-6474/98/187152-08$05.00/0

Lake Placid, NY) or with an ALF DNA sequencer (Pharmacia, Piscataway, NJ).

Cell culture and protein chemistry. For cDNA transfections of epitope-tagged and wild-type P2X subunits into mammalian cells, HEK-293A cells (CRL 1573; American Type Culture Collection, Rockville, MD) were cultured in DMEM and 10% heat-inactivated fetal bovine serum (FBS) (Wisent, St-Bruno, Quebec, Canada) containing penicillin and streptomycin. Freshly plated cells reaching 30–50% confluency were used for transient cDNA transfections with the calcium phosphate method on 90 mm cell culture dishes (Falcon) with 10 μg of supercoiled plasmid cDNA/10^6 cells (Lê et al., 1998). For Western blots, transfected HEK-293A cells were lifted in Hank's modified calcium-free medium with 20 mM EDTA, pelleted at low centrifugation, and homogenized in 10 volumes of 10 mM HEPES buffer, pH 7.4, containing protease inhibitors phenylmethylsulfonyl fluoride (0.2 mM) and benzamidine (1 mM). Cell lysates were pelleted at 14,000 × *g* for 5 min, and membrane proteins in supernatants were solubilized with SDS-containing loading buffer. Approximately 150 μg of protein/lane were run on 12% SDS-PAGE and then transferred to nitrocellulose. Immunoprobing was performed with mouse mAb M2 (1 μg/ml, IBI) followed by peroxidase-labeled anti-mouse secondary antibodies for visualization by enhanced chemiluminescence (Amersham, Oakville, Ontario, Canada). Copurification of associated P2X subunits was performed as previously described for IRK channels (Tinker et al., 1996) with minor modifications. Cell lysates were solubilized with 5% Triton X-100 for 2 hr at 4°C. Unsolubilized materials were pelleted at 10,000 × *g*, and supernatants were incubated with 50 μl of 50% slurry of equilibrated Ni-NTA-Resin (Qiagen, Hilden, Germany) for 2 hr at 4°C. Nickel beads were then washed six times in TBS containing 25 mM imidazole and 1% Triton X-100. Bound proteins were eluted from Ni-NTA resin with 500 mM imidazole, diluted 1:1 (v/v) with SDS-containing loading buffer, and warmed for 10 min at 37°C. Samples were then loaded onto a 12% SDS-PAGE, transferred to nitrocellulose, and analyzed in Western blot using chemiluminescence as above.

Electrophysiology. For electrophysiological recordings in oocytes, ovary lobes were surgically removed from *Xenopus laevis* frogs anesthetized with Tricaine (Sigma, St. Louis, MO) and treated for 3 hr at room temperature with type II collagenase (Life Technologies, Gaithersburg, MD) in calcium-free Barth's solution under vigorous agitations. Stage V–VI oocytes were then defolliculated chemically before nuclear microinjections of 5–10 ng of cDNA coding for each P2X channel subunit. After 2–5 d of incubation at 19°C in Barth's solution containing 1.8 mM calcium chloride ($CaCl_2$) and 10 μg/ml gentamicin, P2X currents were recorded in a two-electrode voltage-clamp configuration using an OC-725B amplifier (Warner Institute). Signals were low-pass-filtered at 1 kHz, acquired at 500 Hz using a Macintosh IIci equipped with an NB-MIO-16XL analog-to-digital card (National Instruments). Traces were postfiltered at 100 Hz in Axograph (Axon Instruments). Agonists, antagonists, and cofactors (zinc chloride, pH 6.5 and 8.0) were dissolved in Ringer's solution containing (in mM): 115 NaCl, 2.5 KCl, and 1.8 $CaCl_2$ in 10 HEPES, pH 7.4 standard at room temperature, and applied on oocytes at a constant flow rate of 12 ml/min. Dose–response curves and EC_{50} values were derived from fittings for the sigmoidal equation of Hill using Prism 2.0 software (Graphpad Software, San Diego, CA).

Statistical analysis. All comparisons involving two variances were performed with Fisher's *F* values (variance homogeneity requirements) and with Student's *t* tests for two unpaired groups. Two-tailed statistical thresholds, for both Fisher's *F* and Student's *t* critical values, were set at $p < 0.05$.

RESULTS

Functional impact of $P2X_6$ subunit expression on ATP-induced currents

In response to 100 μM ATP, *Xenopus* oocytes microinjected with a mix of $P2X_4$ and $P2X_6$ cDNAs (1:1 molar ratio) gave rise to currents with kinetic profiles similar to those observed with oocytes expressing $P2X_4$ alone (Fig. 1*A*). $P2X_6$ by itself appeared to be silent in *Xenopus* oocytes, because no current was detected during ATP applications (Fig. 1*A*), in agreement with what has been reported previously (Soto et al., 1996). Comparison of peak current amplitudes after 3 d of expression revealed, however, that currents from cells coexpressing $P2X_4$ and $P2X_6$ subunits were reproducibly and significantly smaller than currents from cells expressing only $P2X_4$ receptors (Fig. 1*A,B*), suggesting the possibility that the $P2X_6$ channel subunit can heteropolymerize with other members of the P2X family. We coexpressed $P2X_6$ together with $P2X_1$ (Valera et al., 1994) or with $P2X_2$ (Brake et al., 1994). In response to 100 μM ATP, there were no differences between peak currents recorded from oocytes coexpressing $P2X_1$ and $P2X_6$ and those expressing $P2X_1$ alone (Fig. 1*C*) after 3 d of expression. Similarly, we did not observe any functional impact of $P2X_6$ on the expression of $P2X_2$ under the same experimental conditions (Fig. 1*D*), eliminating the possibility of a general inhibitory effect of $P2X_6$ on protein synthesis or on translocation. Thus these data indicate either that the subunit-specific interaction between $P2X_4$ and $P2X_6$ isoforms generates a heteromeric $P2X_{4+6}$ receptor, or that $P2X_6$ subunits exert a specific inhibitory function on $P2X_4$ receptor expression. If $P2X_{4+6}$ heteromers are expressed, smaller peak currents could result from a lower affinity for ATP or a smaller single conductance in comparison with homomeric $P2X_4$ channels. Alternatively, smaller ATP responses at day 3 could simply reflect a slower kinetics of receptor expression.

To further characterize a time-dependent effect, we studied the time course of expression, daily recording peak currents in response to 100 μM ATP from oocytes expressing either $P2X_4$ and $P2X_6$ cDNAs or $P2X_4$ cDNA alone. Figure 2 demonstrates that ATP receptors in oocytes coexpressing $P2X_4$ and $P2X_6$ subunits, compared with $P2X_4$ alone, needed a longer time to reach the same levels of ATP-induced currents. However, between days 2 and 5 after injection, there was a dramatic sevenfold increase in peak current amplitudes in oocytes coexpressing $P2X_4$ and $P2X_6$ subunits (Fig. 2*A*). This profile is in striking contrast with the time course of $P2X_4$ expression that slowly decayed over the same period (Fig. 2*B*).

Agonist sensitivity profile of $P2X_{4+6}$ heteromeric receptors

No significant difference was detected between the EC_{50} values derived from ATP dose–response profiles of $P2X_{4+6}$ (6.3 ± 0.9 μM) channel phenotype and homomeric $P2X_4$ (4.2 ± 1.1 μM) receptors (Fig. 3*A*) expressed in oocytes. However, the partial agonist 2MeSATP had EC_{50} values of 7.67 ± 1.01 and 26 ± 1.8 μM for $P2X_{4+6}$ and $P2X_4$ receptors, respectively, a statistically significant difference (Fig. 3*B*). Even more striking, in response to 100 μM αβmATP on day 3 after injection, oocytes expressing $P2X_{4+6}$ heteromeric channels gave rise to peak current amplitudes of 0.7 ± 0.13 μA compared with 0.12 ± 0.02 μA only from oocytes expressing $P2X_4$ homomeric receptors, in marked contrast with the situation observed in response to ATP (compare Figs. 4A, 1*B*). The αβmATP EC_{50} values were found to be 12 ± 2 μM for $P2X_{4+6}$ and 55 ± 2 μM for $P2X_4$ channel phenotypes (Fig. 4*B*). Therefore, αβmATP shows more potency and has a higher affinity on $P2X_{4+6}$ receptors than on $P2X_4$ receptors. These different sensitivities to 2MeSATP and αβmATP constitute more experimental evidence for a functional association between $P2X_4$ and $P2X_6$ subunits coexpressed in *Xenopus* oocytes.

Sensitivity of $P2X_{4+6}$ receptors to suramin, PPADS, and RB-2

It is widely recognized that neither $P2X_4$ nor $P2X_6$ homomeric receptors (in HEK-293 cells) are completely blocked by suramin or PPADS up to 100 μM without preincubation (Buell et al., 1996; Collo et al., 1996). In response to 100 μM ATP and 10 μM suramin coapplications without preincubation, oocytes expressing $P2X_{4+6}$

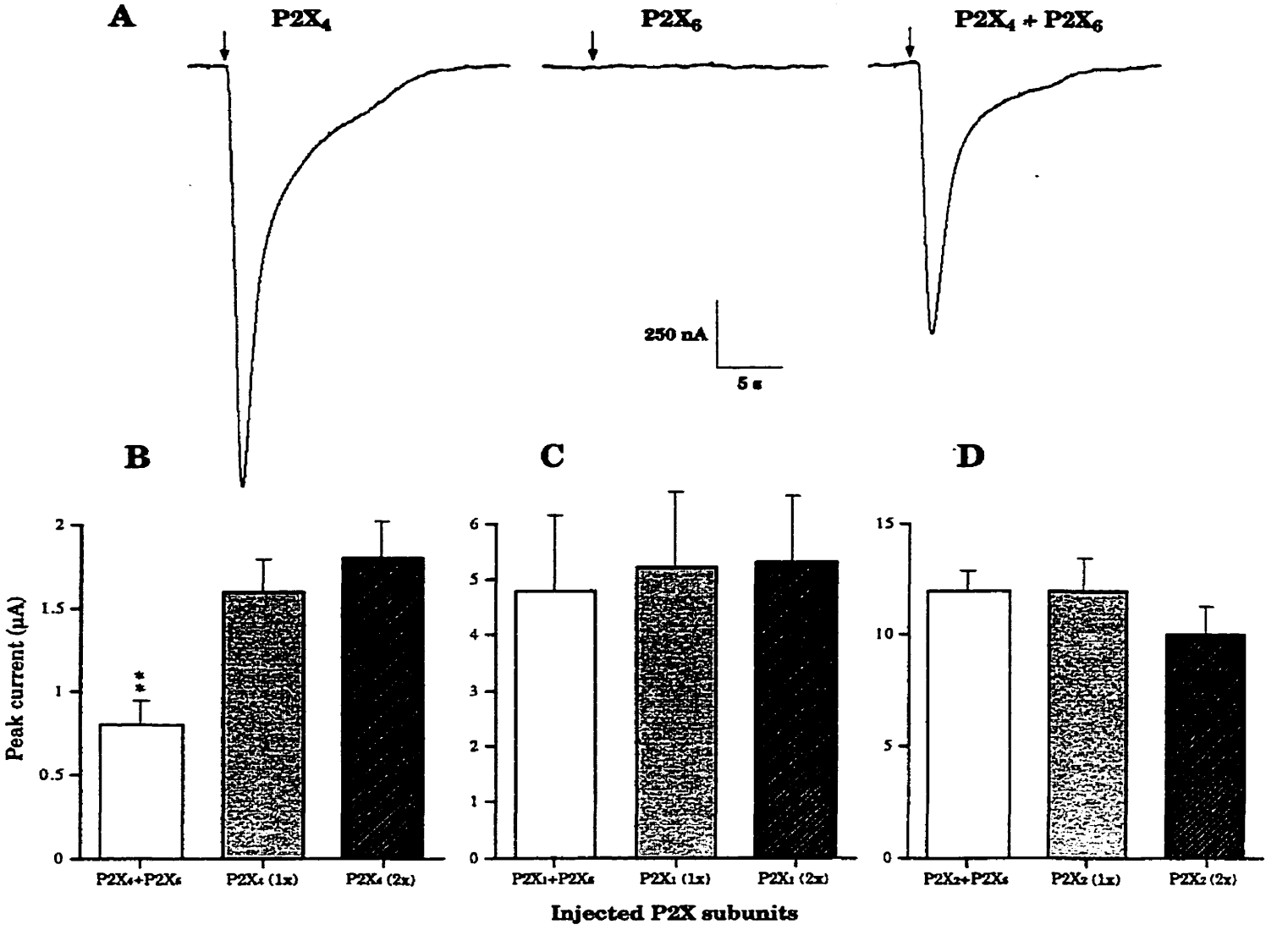

Figure 1. Representative heteromeric $P2X_{4+6}$ channel current phenotype at day 3. *A*, ATP-induced currents after heterologous expression of $P2X_4$, $P2X_6$, and $P2X_4$ + $P2X_6$ (1:1 molar ratio) subunits recorded 3 d after corresponding cDNA nuclear microinjections in *Xenopus* oocytes. *Arrows* indicate beginnings of ATP applications (10 sec). *B*, $P2X_4$-dependent functional impact of $P2X_6$ on ATP-induced response ($P2X_4$ expressed alone; *1x*, 5 ng of cDNA; *2x*, 10 ng). *C*, $P2X_1$ receptor ($P2X_1$; *1x*, 5 ng; *2x*, 10 ng) functional expression is unaffected by coexpressed $P2X_6$ subunits. *D*, $P2X_2$-mediated ($P2X_2$; *1x*, 5 ng; *2x*, 10 ng) ATP-induced peak current amplitudes are unchanged in the presence of $P2X_6$ subunits. (Averages ± SEM from 3 to 15 oocytes in 2–4 independent experiments; double asterisks denote significant difference; $p < 0.01$).

gave rise to residual currents of 61 ± 3% (Fig. 5) of the response to 100 μM ATP (100%). Under the same experimental conditions, oocytes expressing $P2X_4$ receptors alone were almost unaffected (93 ± 3%; Fig. 5). We have also found that 10 μM PPADS coapplied with 100 μM ATP gave rise to peak current amplitudes of 83 ± 7 and 103 ± 6% for $P2X_{4+6}$ and $P2X_4$ receptor phenotypes, respectively (Fig. 5*B*), but we did not find any significant difference between this 17% inhibition on $P2X_{4+6}$ and no effect on $P2X_4$. We have also investigated the effects of RB-2 by coapplying 10 μM of the antagonist with 100 μM ATP: oocytes expressing $P2X_{4+6}$ receptor phenotypes were characterized by residual peak currents of 60 ± 9% compared with potentiated peak currents of 123 ± 18% from oocytes expressing $P2X_4$ receptors alone (Fig. 5*A*). Preincubation of the cell with antagonist during 1 min before coapplication with ATP resulted in even more dramatic phenotypical differences between $P2X_4$ and $P2X_{4+6}$ for suramin (23% blockade vs 41%) and PPADS (19% blockade vs 38%) (Fig. 5*B*). Furthermore, in conditions of preincubation, 10 μM RB-2 blocked $P2X_{4+6}$ heteromeric channels by up to 26% but increased $P2X_4$ response by >45% (Fig. 5*B*). A potentiating effect of RB-2 on $P2X_4$ homomeric receptors has been reported in oocytes, albeit to a smaller extent (Bo et al., 1995).

Sensitivity of $P2X_{4+6}$ receptors to coagonists zinc ions and protons

We have reported previously that 10 μM extracellular zinc ions coapplied with 10 μM ATP potentiated $P2X_4$ peak currents by almost twofold (Séguéla et al., 1996). In addition, it has also been shown that the sensitivity to ATP of homomeric $P2X_4$ channels is modulated by external pH: pH <7 inhibits ATP responses, whereas pH >8 has no significant effects (Stoop et al., 1997). Therefore, we checked whether these coagonists applied with ATP could discriminate between $P2X_{4+6}$ and $P2X_4$ receptor phenotypes. In response to 10 μM zinc ions and 10 μM ATP

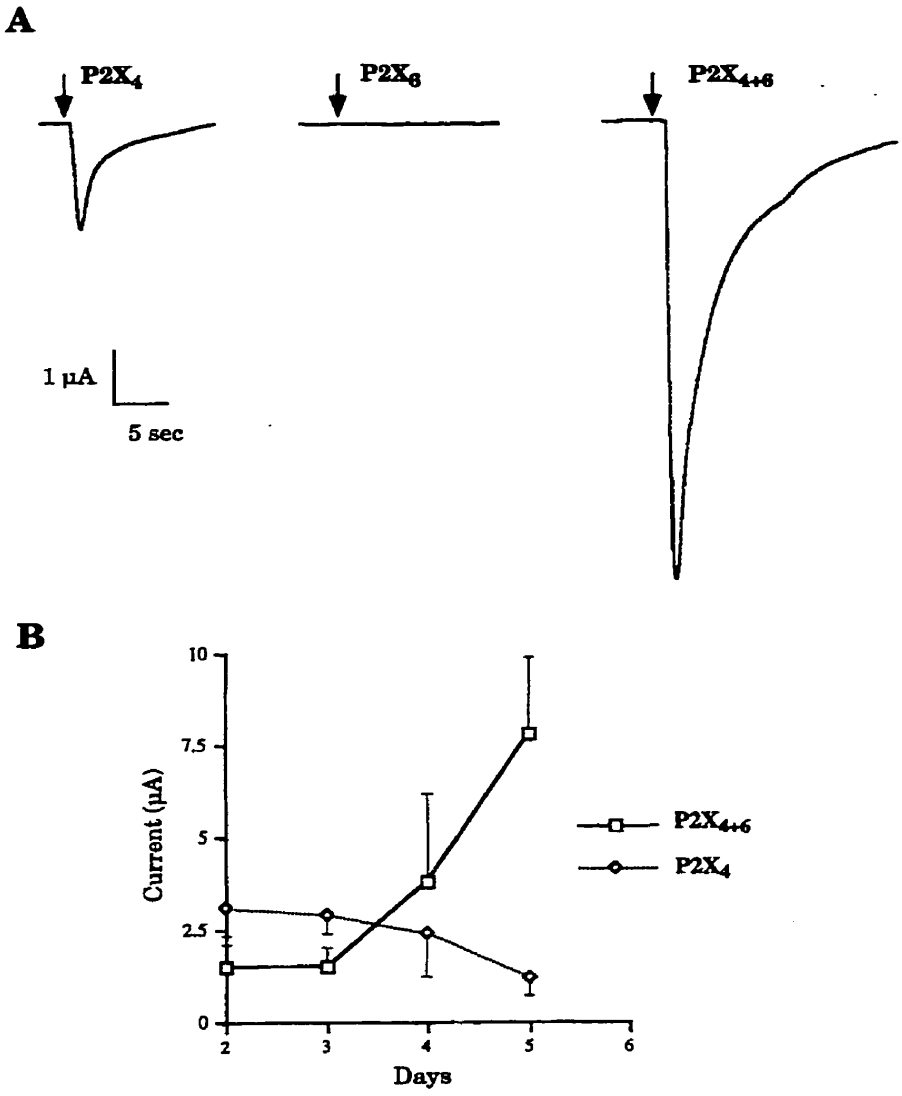

Figure 2. *A*, Potentiation of ATP response represented by $P2X_{4+6}$ channel current phenotype at day 5. *Arrows* indicate beginnings of ATP applications (10 sec). *B*, Time course of heteromeric $P2X_{4+6}$ expression. Kinetics of appearance of functional ATP receptors on plasma membranes is strikingly different in oocytes coinjected with $P2X_4$ and $P2X_6$ subunits compared with those injected with $P2X_4$ subunits (averages ± SEM from 3 to 15 oocytes in 2–8 independent experiments).

coapplications, there were no significant differences between potentiating factors of 1.8 ± 0.19 and 1.8 ± 0.21 for $P2X_{4+6}$ heteromeric channels and $P2X_4$ homomeric receptors, respectively (Fig. 6*A*). There was also no significant difference between these two receptor phenotypes with respect to ATP (20 μM) applied at pH 6.5. In both cases, residual peak current amplitudes were 46 ± 4% of control values measured at pH 7.4 (Fig. 6*B*). When 20 μM ATP was applied at pH 8.0, it elicited peak currents of 121 ± 4 and 106 ± 4% for $P2X_{4+6}$ heteromers and $P2X_4$ homomers, respectively (Fig. 6*C*). Thus, contrary to αβmATP, 2MeSATP, and antagonists suramin, PPADS, and RB-2, cofactors zinc and protons did not discriminate between $P2X_{4+6}$ and $P2X_4$ receptors on a pharmacological basis.

Subunit-specific association of $P2X_4$ with $P2X_6$ subunits

Before testing their biochemical interaction, the expression of Flag-tagged $P2X_1$, $P2X_4$, and $P2X_6$ subunit proteins in transiently transfected HEK-293A cells was confirmed by immunoblot of total membrane proteins (Fig. 7*A*, *lanes 1–6*). Homogenates from HEK-293A cells transiently cotransfected with cDNA templates encoding $P2X_4$-$(His)_6$ and either $P2X_1$-Flag, $P2X_4$-Flag, or $P2X_6$-Flag constructs were analyzed for copurification. After solid-phase binding of $P2X_4$-$(His)_6$ proteins on poly His-binding resin, we detected the coprecipitation of $P2X_4$-Flag subunits, confirming that $P2X_4$ subunits interacted between themselves to generate a homomultimeric complex (positive controls, Fig. 7*B*, *lane 1*). Coexpression of $P2X_4$-$(His)_6$ with $P2X_6$-Flag subunits gave a positive band corresponding to the expected size of $P2X_6$ (51 kDa; Fig. 7*B*, *lane 3*), demonstrating directly for the first time that $P2X_4$ and $P2X_6$ subunits do physically interact in a multimeric complex. Coexpression of $P2X_4$-$(His)_6$ with $P2X_1$-Flag subunits did not give any signal when probed with anti-Flag M2 antibodies after purification, confirming that $P2X_4$ and $P2X_1$ subunits do not heteropolymerize (Fig. 7*B*, *lane 5*). All control coexpressions including wild-type $P2X_4$ (lacking the poly-His motif) cotransfected with Flag-tagged $P2X_4$, $P2X_6$, or $P2X_1$ subunits were negative after purification on poly His-binding resin (Fig. 7*B*, *lanes 2, 4, 6*).

DISCUSSION

Functional identification of $P2X_{4+6}$ heteromeric receptors

In the present study, we first observed an apparent inhibition of $P2X_6$ subunits on ATP-induced currents in oocytes expressing $P2X_4$ subunits (Fig. 1*B*). However, neither ATP-induced currents

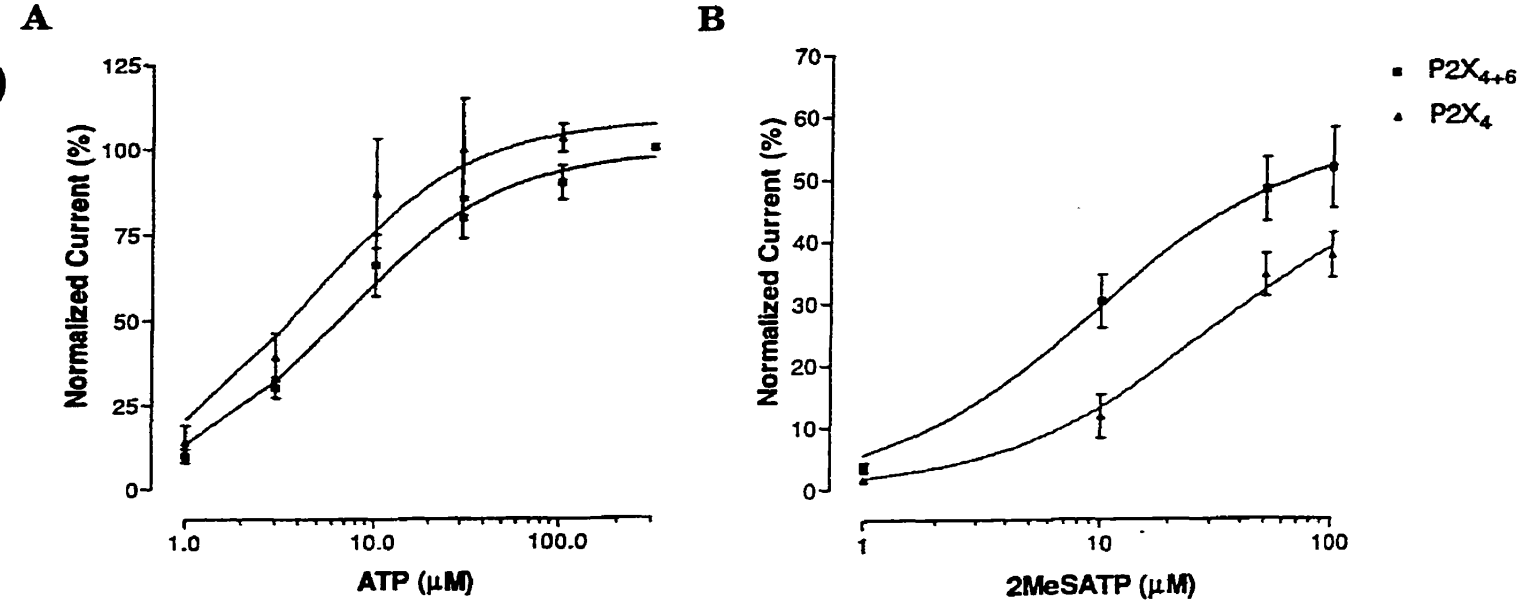

Figure 3. Sensitivity of $P2X_{4+6}$ receptors to the agonists ATP and 2MeSATP. *A*, Similar ATP dose–response profile between heteromeric $P2X_{4+6}$ channels and homomeric $P2X_4$ receptors in *Xenopus* oocytes. *B*, Heteromeric $P2X_{4+6}$ receptors showed increased sensitivity to 2MeSATP compared with $P2X_4$ receptors. Values are normalized to the response to 300 μM ATP (averages ± SEM from 3 to 7 oocytes per point in 2 independent experiments).

mediated by $P2X_1$ subunits (Fig. 1*C*) nor currents mediated by $P2X_2$ subunits (Fig. 1*D*) were affected, strongly suggesting that $P2X_4$ and $P2X_6$ isoforms associate together, in a subunit-specific manner, into a novel heteromeric P2X channel. Functional $P2X_{4+6}$ protein assembly and/or plasma membrane channel targeting appeared to be on a different time scale compared with $P2X_4$ receptors. Indeed, in response to 100 μM ATP, $P2X_{4+6}$ heteromultimers gave rise to increasing peak currents even after 5 d of expression (Fig. 2*A*), whereas $P2X_4$ homopolymers yielded decreasing peak current amplitudes under identical conditions (Fig. 2*B*). We did not find any difference between the EC_{50} values of ATP for both homomeric and heteromeric receptor isoforms (Fig. 4*A*), so we concluded that the apparent inhibitory effect of $P2X_6$ on $P2X_4$ recorded 3 d after injection was mainly attributed to a slower expression of $P2X_{4+6}$ receptors on the cell surface, assuming similar channel conductance. These findings constituted our first set of experimental evidence demonstrating a heteropolymerization between $P2X_4$ and $P2X_6$ subunits. It has been noticed previously that $P2X_6$ subunits and channels express poorly in HEK-293A cells (Collo et al., 1996) and are silent to ATP in the *Xenopus* oocyte expression system (Soto et al., 1996), as observed here. However, maximal ATP-induced peak currents were significantly larger at day 5 in the case of $P2X_{4+6}$ channels than in the case of $P2X_4$ alone (Fig. 2*A*). This situation is reminiscent of epithelial sodium-selective channels, belonging to another family of two-transmembrane-domain cation channels, whereby a fully functional channel requires the heteropolymerization of α subunits with β and γ subunits, both inactive when expressed alone (Canessa et al., 1994).

Unique pharmacological profile of $P2X_{4+6}$ heteromeric receptors

We made the assumption that the association between $P2X_4$ and $P2X_6$ subunits should be reflected in some unique aspects of the pharmacological profile of the resulting heteromeric receptor. Although $P2X_4$ seemed the dominant subunit for the sensitivity to ATP in the heteromers, we observed a statistical difference between EC_{50} values of 2MeSATP for $P2X_{4+6}$ heteromeric channels and $P2X_4$ receptors (Fig. 4*B*). Furthermore, in response to 100 μM αβmATP applications, oocytes coexpressing $P2X_4$ and $P2X_6$ subunits gave rise to larger maximal peak currents than oocytes expressing $P2X_4$ isoforms alone (Fig. 3*A*), despite slower kinetics of expression. Indeed, we measured a lower EC_{50} of αβmATP for $P2X_{4+6}$ than for $P2X_4$ channel species (Fig. 3*B*). Therefore, in addition to opposite protein expression profiles between $P2X_{4+6}$ and $P2X_4$ channels, these observations strongly indicate that $P2X_4$ and $P2X_6$ subunits generate a novel receptor phenotype characterized by a unique agonist profile, namely increased 2MeSATP and αβmATP sensitivity. Moreover, these data provide for the first time experimental evidence for moderately desensitizing αβmATP-activated ionotropic responses.

Furthermore, we probed the sensitivity of $P2X_{4+6}$ heteromers to P2 antagonists suramin, PPADS, and RB-2 coapplied with ATP. We found that suramin significantly blocked $P2X_{4+6}$ activity without inhibiting significantly $P2X_4$ homomeric receptors (Fig. 5*A*); 10 μM suramin coapplied with 100 μM ATP decreased $P2X_{4+6}$ heteromeric receptor peak current amplitudes by up to 40% compared with 7% for $P2X_4$ homomeric channels. Coapplied PPADS inhibited $P2X_{4+6}$ weakly, although it had no measurable effects on oocytes expressing $P2X_4$ subunits alone (Fig. 5*A*). After preincubation, low concentrations of RB-2 provided the most dramatic differential effect by inhibiting $P2X_{4+6}$ heteromers while potentiating $P2X_4$ channel activity (Fig. 5*B*). Suramin and RB-2 would thus be useful pharmacological tools to investigate the expression of native $P2X_{4+6}$ heteromers in αβmATP-sensitive neuronal preparations.

Biochemical evidence of $P2X_{4+6}$ heteropolymers

We demonstrated direct interactions between the two predominant brain $P2X_4$ and $P2X_6$ isoforms through the use of an established copurification assay (Tinker et al., 1996). Based on our coprecipitation results with epitope-tagged subunits in nondenaturing conditions, $P2X_4$ associates with $P2X_6$ subunits (Fig. 7*B*). In *Xenopus* oocytes, this heteropolymerization underlies the spe-

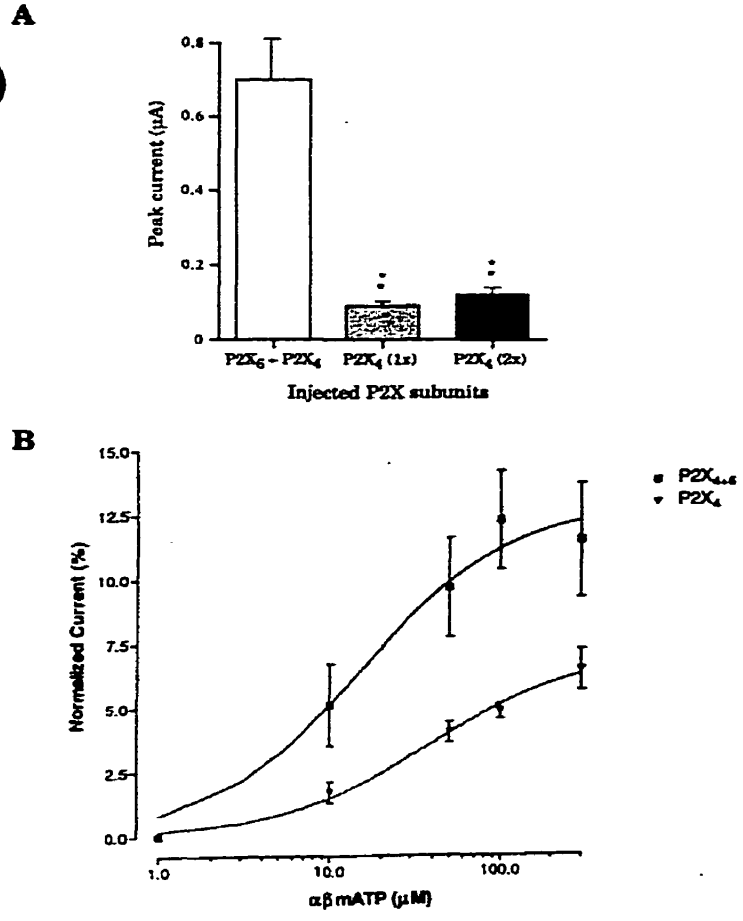

Figure 4. Sensitivity of $P2X_{4+6}$ receptors to the agonist αβmATP. *A*, Differential αβmATP responsiveness measured in peak current amplitudes between *Xenopus* oocytes expressing either $P2X_{4+6}$ channels or $P2X_4$ at day 3 after injection; see Figure 1*B* for comparison of ATP-induced peak currents. *B*, Normalized dose–response curves of $P2X_{4+6}$ and $P2X_4$ receptor species for αβmATP. Values are normalized to the response to 100 μM ATP; *double asterisks* denote significant difference; $p < 0.01$ (averages ± SEM from 5 to 8 oocytes per point in 2 independent experiments).

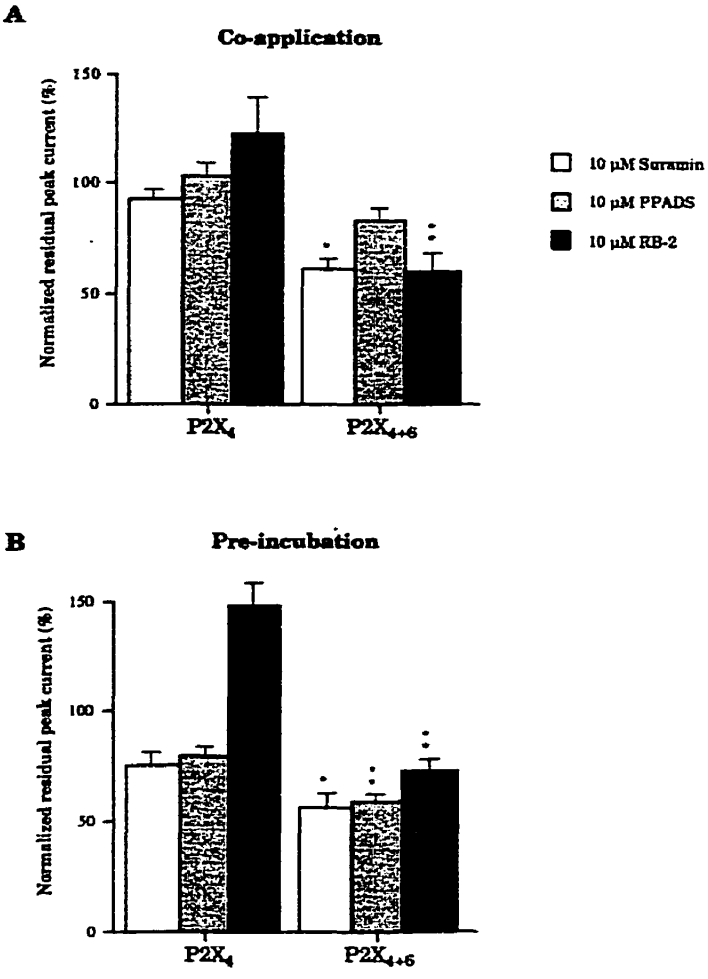

Figure 5. Sensitivity of $P2X_{4+6}$ to P2X antagonists. Suramin, PPADS, and RB-2 were tested for their blocking properties on heteromeric $P2X_{4+6}$ channels and on homomeric $P2X_4$ receptors. Antagonists were coapplied with ATP (*A*) or preincubated before coapplication (*B*). Note that $P2X_{4+6}$ receptors are inhibited, whereas $P2X_4$ receptors are potentiated by 10 μM RB-2. Values are normalized to the response to ATP only (averages ± SEM from 5 oocytes per experiment; *single* and *double asterisks* denote significant difference; $p < 0.05$ and $p < 0.01$, respectively).

cific pharmacological and electrophysiological phenotype of a novel heteromeric channel distinct from either $P2X_4$ or $P2X_6$ homomeric receptors. On the other hand, $P2X_4$ and $P2X_1$ subunits did not seem to interact significantly with each other (Fig. 7*B*). Furthermore, the absence of obvious phenotypical differences between oocytes coexpressing $P2X_6$ + $P2X_1$ and $P2X_1$ subunits alone (Fig. 1*C*), or between $P2X_6$ + $P2X_2$ and $P2X_2$ homomers (Fig. 1*D*), indicate that structural determinants of association between $P2X_4$ and $P2X_6$ isoforms are subunit-dependent. A similar biochemical approach using copurification of $P2X_4$ with chimeric subunits based on $P2X_6$ and $P2X_1$ structures could lead to the identification of the domain(s) involved in specific heteropolymerization.

Functional correlates of native $P2X_{4+6}$ heteromers

Purinergic responses from CA3 neurons in rat hippocampal slices have been shown recently to be activated by αβmATP and inhibited by suramin but not by PPADS (Ross et al., 1998). Based on *in situ* hybridization results (Collo et al., 1996), $P2X_4$ and $P2X_6$ are the only P2X subunits expressed at significant levels in adult rat hippocampus, namely in CA1–CA4 hippocampal subfields

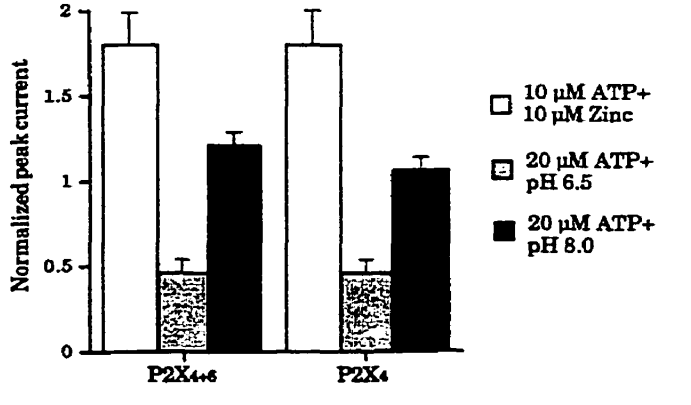

Figure 6. Sensitivity of $P2X_{4+6}$ to the extracellular cofactors zinc ions and pH. Extracellular Zn^{2+}, pH 6.5 and 8.0, coapplied with ATP, did not allow differentiation between $P2X_{4+6}$ and $P2X_4$ receptors. Values are normalized to the response to ATP only (averages ± SEM from 4 oocytes per experiment).

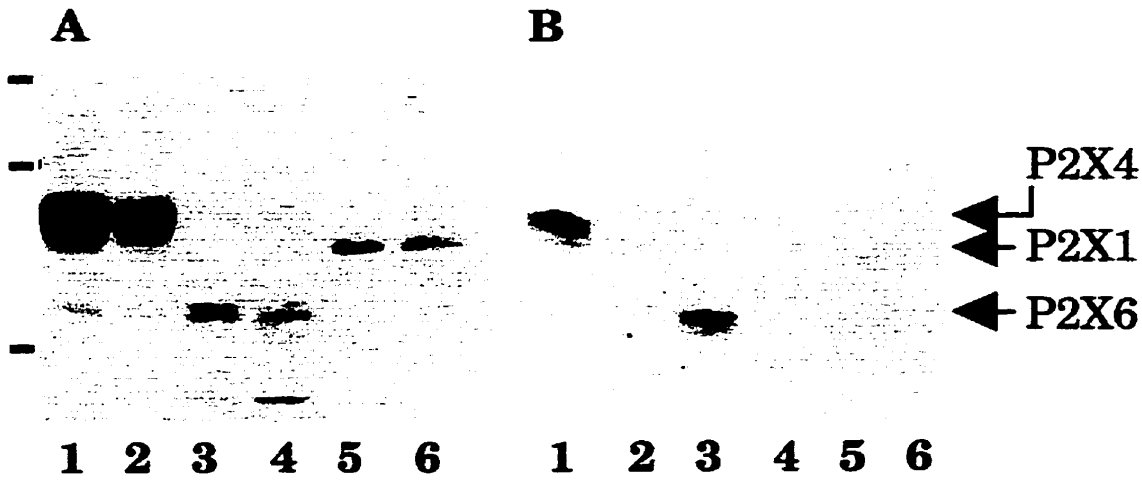

Figure 7. Subunit specificity of $P2X_4$ and $P2X_6$ heteropolymerization. *A*, Immunoblot of Flag-tagged $P2X_1$, $P2X_4$, and $P2X_6$ subunits probed with anti-Flag M2 monoclonal antibodies in total membrane proteins from transiently transfected HEK-293A cells. *B*, From the same samples, immunoblot of Flag-tagged $P2X_1$, $P2X_4$, and $P2X_6$ subunits probed with M2 antibodies after copurification through $P2X_4$-$(His)_6$ subunits. Molecular weight markers (in *A*): 104, 82, and 48 kDa. Cotransfections: *lane 1*, $P2X_4$-$(His)_6$ + $P2X_4$-Flag; *lane 2*, $P2X_4$-wt + $P2X_4$-Flag; *lane 3*, $P2X_4$-$(His)_6$ + $P2X_6$-Flag; *lane 4*, $P2X_4$-wt + $P2X_6$-Flag; *lane 5*, $P2X_4$-$(His)_6$ + $P2X_1$-Flag; *lane 6*, $P2X_4$-wt + $P2X_1$-Flag.

and in the dentate gyrus. Thus, our functional data obtained from recombinant receptors are in close agreement with this native phenotype and suggest that the sensitivities to $\alpha\beta$mATP and to suramin of rat CA3 neurons might be mediated through native $P2X_{4+6}$ heteromeric channels.

Neonatal rat cerebellar Purkinje cells have been characterized as having purinergic receptors with a $P2X_2$-like pharmacological profile in eliciting extracellular calcium influxes (Mateo et al., 1998). This conclusion rested on $\alpha\beta$mATP insensitivity, the potency ratio of ATP to 2MeSATP, as well as suramin and PPADS blockade after preincubation. However, on recombinant $P2X_{4+6}$ receptors, the concentration of $\alpha\beta$mATP used by Mateo et al. (1998) (50 μM) was ~10% as efficacious as 50 μM ATP in eliciting ionotropic responses, so $\alpha\beta$mATP-mediated intracellular calcium increases could have remained undetected and consequently interpreted as $\alpha\beta$mATP unresponsiveness. The developmental regulation of expression levels of neuronal P2X genes in cerebellum is not established so far. Adult rat Purkinje neurons are known to transcribe $P2X_4$ and $P2X_6$ mRNA (Collo et al., 1996) and have been shown to translate high levels of $P2X_4$ subunits (Lê et al., 1998), whereby $P2X_2$ mRNAs (Collo et al., 1996) or subunits (Vulchanova et al., 1996) were reported previously to be absent (Kanjhan et al., 1996). It is also possible that native P2X receptors in neonatal Purkinje cells are composed of three subunits, namely $P2X_2$, $P2X_4$, and $P2X_6$, assembled in a heteromeric complex in which $P2X_2$ is pharmacologically dominant. We have recorded in oocytes purinergic currents mediated by $P2X_{4+6}$ heteromeric channels that were significantly more sensitive to the agonists $\alpha\beta$mATP and 2MeSATP, as well as to the antagonist suramin compared with $P2X_4$ homomeric receptors. So it is likely that the moderately desensitizing $\alpha\beta$mATP-activated and suramin-sensitive postsynaptic purinergic responses recorded from medial habenula (Edwards et al., 1992) could be accounted for by the expression of postsynaptic $P2X_{4+6}$ receptors, because *in situ* hybridization results demonstrate the exclusive presence of $P2X_4$ and $P2X_6$ transcripts in this region (Collo et al., 1996). The widespread distribution of high-affinity [^{3}H]$\alpha\beta$mATP binding sites within the rat CNS (Bo and Burnstock, 1994; Michel and Humphrey, 1994; Balcar et al., 1995) appears to correlate with *in situ* hybridization data on $P2X_4$ and $P2X_6$ mRNA distributions (Collo et al., 1996; Séguéla et al., 1996) as well as with the immunocytochemical localization of $P2X_4$ protein (Lê et al., 1998). This neuroanatomical evidence strongly suggests that the $P2X_{4+6}$ channel phenotype might be present in most rat brain and spinal cord regions. Moreover, we have shown that the $P2X_4$ subunit is a major presynaptic purinoceptor component in laminae I and II of spinal cord and in olfactory glomeruli (Lê et al., 1998), two regions in which $P2X_6$ is also expressed (Collo et al., 1996). Therefore, the heteromeric $P2X_{4+6}$ ATP-gated cation channel could play a significant role in the regulation of excitatory transmitter release in central sensory synapses.

REFERENCES

Balcar VJ, Li Y, Killinger S, Bennett MR (1995) Autoradiography of P2X ATP receptors in the rat brain. Br J Pharmacol 115:302–306.

Bo X, Burnstock G (1994) Distribution of [^{3}H]α,β-methylene ATP binding sites in rat brain and spinal cord. NeuroReport 5:1601–1604.

Bo X, Zhang Y, Nassar M, Burnstock G, Schoepfer R (1995) A P2X purinoceptor cDNA conferring a novel pharmacological profile. FEBS Lett 375:129–133.

Brake AJ, Wagenbach MJ, Julius D (1994) New structural motif for ligand-gated ion channels defined by an ionotropic ATP receptor. Nature 371:519–523.

Buell G, Collo G, Rassendren F (1996) P2X receptors: an emerging channel family. Eur J Neurosci 8:2221–2228.

Canessa CM, Schild L, Buell G, Thorens B, Gautschi I, Horisberger J-D, Rossier BC (1994) Amiloride-sensitive epithelial Na^+ channel is made of three homologous subunits. Nature 367:463–467.

Chen C-C, Akopian AN, Sivilotti L, Colquhoun D, Burnstock G, Wood JN (1995) A P2X purinoceptor expressed by a subset of sensory neurons. Nature 377:428–431.

Collo G, North RA, Kawashima E, Merlo-Pich E, Neidhart S, Surprenant A, Buell G (1996) Cloning of $P2X_5$ and $P2X_6$ receptors and the distribution and properties of an extended family of ATP-gated ion channels. J Neurosci 16:2495–2507.

Edwards FA, Gibb AJ, Colquhoun D (1992) ATP receptor-mediated synaptic currents in the CNS. Nature 359:144–147.

Kanjhan R, Housley GD, Thorne PR, Christie DL, Palmer DJ, Luo L, Ryan AF (1996) Localization of ATP-gated ion channels in cerebellum using $P2X_{2R}$ subunit-specific antisera. NeuroReport 7:2665–2669.

Khakh BS, Humphrey PPA, Surprenant A (1995) Electrophysiological properties of P2X-purinoceptors in rat superior cervical, nodose, and guinea pig coeliac neurones. J Physiol (Lond) 484:385–395.

Lê K-T, Villeneuve P, Ramjaun AR, McPherson PS, Beaudet A, Séguéla P (1998) Sensory presynaptic and widespread somatodendritic immunolocalization of central ionotropic P2X ATP receptors. Neuroscience 83:177–190.

Lewis C, Neidhart S, Holy C, North RA, Buell G, Surprenant A (1995) Coexpression of $P2_X2$ and $P2X_3$ receptor subunits can account for ATP-gated currents in sensory neurons. Nature 377:432–435.

Mateo J, Garcia-Lecea M, Miras-Portugal MT, Castro E (1998) Ca^{2+} signals mediated by P2X-type purinoceptors in cultured cerebellar Purkinje cells. J Neurosci 18:1704–1712.

Michel AD, Humphrey PPA (1994) Distribution and characterization of [^{3}H]α,β-methylene ATP binding sites in the rat. Naunyn- Schmiedebergs Arch Pharmacol 348:608–617.

North RA, Barnard EA (1997) Nucleotide receptors. Curr Opin Neurobiol 7:346–357.

Radford KM, Virginio C, Surprenant A, North RA, Kawashima E (1997) Baculovirus expression provides direct evidence for heteromeric assembly of $P2X_2$ and $P2X_3$ receptors. J Neurosci 17:6529–6533.

Ross FM, Brodie MJ, Stone TW (1998) Modulation by adenine nucleotides of epileptiform activity in the CA3 region of rat hippocampal slices. Br J Pharmacol 123:71–80.

Séguéla P, Haghighi A, Soghomonian JJ, Cooper E (1996) A novel neuronal P2X ATP receptor ion channel with widespread distribution in the brain. J Neurosci 16:448–455.

Soto F, Garcia-Guzman M, Karschin C, Stühmer W (1996) Cloning and tissue distribution of a novel P2X receptor from rat brain. Biochem Biophys Res Commun 223:456–460.

Stoop R, Surprenant A, North RA (1997) Differential sensitivities to pH of ATP-induced currents at four cloned P2X receptors. J Neurophysiol 78:1837–1840.

Tinker A, Jan YN, Jan LY (1996) Regions responsible for the assembly of inwardly rectifying potassium channels. Cell 87:857–868.

Valera S, Hussy N, Evans RJ, Adami N, North RA, Surprenant A, Buell G (1994) A new class of ligand-gated ion channel defined by P2X receptor for extracellular ATP. Nature 371:516–519.

Vulchanova L, Arvidsson U, Riedl M, Wang J, Buell G, Surprenant A, North RA, Elde R (1996) Differential distribution of two ATP-gated ion channels (P2X receptors) determined by immunocytochemistry. Proc Natl Acad Sci USA 93:8063–8067.

THE JOURNAL OF BIOLOGICAL CHEMISTRY
Vol. 274, No. 22, Issue of May 28, pp. 15415–15419, 1999
Printed in U.S.A.
© 1999 by The American Society for Biochemistry and Molecular Biology, Inc.

Functional and Biochemical Evidence for Heteromeric ATP-gated Channels Composed of $P2X_1$ and $P2X_5$ Subunits*

(Received for publication, January 26, 1999)

Khanh-Tuoc Lê‡§, Éric Boué-Grabot‡¶, Vincent Archambault, and Philippe Séguéla‖

From the Department of Neurology and Neurosurgery, Cell Biology of Excitable Tissue Group, Montreal Neurological Institute, McGill University, Montreal, Quebec H3A 2B4 Canada

The mammalian P2X receptor gene family encodes two-transmembrane domain nonselective cation channels gated by extracellular ATP. Anatomical localization data obtained by *in situ* hybridization and immunocytochemistry have shown that neuronal P2X subunits are expressed in specific but overlapping distribution patterns. Therefore, the native ionotropic ATP receptors diversity most likely arises from interactions between different P2X subunits that generate hetero-multimers phenotypically distinct from homomeric channels. Rat $P2X_1$ and $P2X_5$ mRNAs are localized within common subsets of peripheral and central sensory neurons as well as spinal motoneurons. The present study demonstrates a functional association between $P2X_1$ and $P2X_5$ subunits giving rise to hybrid ATP-gated channels endowed with the pharmacology of $P2X_1$ and the kinetics of $P2X_5$. When expressed in *Xenopus* oocytes, hetero-oligomeric $P2X_{1+5}$ ATP receptors were characterized by slowly desensitizing currents highly sensitive to the agonist α,β-methylene ATP (EC_{50} = 1.1 μM) and to the antagonist trinitrophenyl ATP (IC_{50} = 64 nM), observed with neither $P2X_1$ nor $P2X_5$ alone. Direct physical evidence for $P2X_{1+5}$ co-assembly was provided by reciprocal subunit-specific co-purifications between epitope-tagged $P2X_1$ and $P2X_5$ subunits transfected in HEK-293A cells.

Ionotropic ATP receptors constitute a unique class of neurotransmitter-gated ion channels generated from the assembly of P2X subunits having two transmembrane-spanning domains and a protein architecture similar to the one of the amiloride-sensitive sodium channels (1, 2). Functional characterization studies of the seven mammalian cloned P2X subunits heterologously expressed as homomeric channels allowed to classify them in three groups according to their properties of desensitization and to their sensitivity to the agonist α,β-methylene ATP ($\alpha\beta$m-ATP)[1]: (i) rapidly desensitizing and $\alpha\beta$m-ATP-sensitive receptors including $P2X_1$ and $P2X_3$ (3–5), (ii) moderately desensitizing and $\alpha\beta$m-ATP-insensitive receptors including $P2X_4$ and $P2X_6$ (6–12), and (iii) nondesensitizing as well as $\alpha\beta$m-ATP-insensitive receptors including $P2X_2$, $P2X_5$, and $P2X_7$ (11–14). Results from Northern blots and *in situ* hybridization data (11) have indicated that the six neuronal P2X subunits genes are transcribed in specific but overlapping populations in the central and peripheral nervous system (1, 11). This strongly suggests that neuronal P2X subunits belonging to different functional groups might co-assemble into hetero-multimeric channels.

All P2X subunits have been detected in peripheral sensory ganglia, reinforcing the view that synaptically or lytically released ATP could play an important signaling role in sensory pathways (1, 11, 15). Rat $P2X_3$ subunits have been reported to be exclusively expressed in small to medium-sized isolectin B4-positive nociceptive neurons in nodose, trigeminal, and dorsal root ganglia (4, 5, 15). A significant proportion of sensory neurons are thought to express hetero-oligomeric $P2X_{2+3}$ receptors based on their sustained response to $\alpha\beta$m-ATP applications (5). However, recent immunocytochemistry results have demonstrated that $P2X_2$ and $P2X_3$ subunits in rat dorsal root ganglia are rarely co-localized at the level of central primary afferents in the dorsal horn of the spinal cord, despite their high degree of co-localization in somata, indicating different subunit-specific subcellular targetings (16). Altogether, these data suggest that physiologically relevant associations of neuronal P2X subunits, giving rise to phenotypes that are not mediated by the previously described $P2X_{2+3}$ (5, 17) or $P2X_{4+6}$ (18) receptors, remain to be discovered.

Rat $P2X_5$ subunits mRNAs have the most restricted distribution in the P2X family, but in *situ* hybridization studies have indicated that $P2X_1$ and $P2X_5$ mRNAs are co-localized in primary sensory neurons as well as within subsets of large motoneurons in the ventral horn of the spinal cord (1, 11). We report here the characterization of a novel heteromeric P2X receptor with hybrid properties generated by co-expression and co-assembly of $P2X_1$ with $P2X_5$ subunits in *Xenopus laevis* oocytes and transfected HEK-293A cells, further strengthening arguments for a diversity of native ATP-gated channels and purinergic phenotypes in mammalian neurons.

EXPERIMENTAL PROCEDURES

Molecular Biology—Full-length wild-type rat $P2X_1$ and $P2X_5$ cDNAs were obtained through polymerase chain reaction amplification using A10 smooth muscle cells (ATCC No. CRL 1476) and adult rat spinal cord reverse transcribed-cDNA templates, respectively. Reactions were performed with exact match oligonucleotide primers based upon published primary sequences (3, 11, 12) using *Pfu* DNA polymerase (Stratagene) to minimize artifactual mutations. Epitope-tagged P2X subunits with carboxyl-terminal hexahistidine motif (His_6) or Flag peptide were constructed as reported previously (18). Briefly, an *XhoI-XbaI* stuffer cassette containing in-frame Flag or His_6 epitopes followed by an artificial stop codon was ligated to $P2X_1$ and $P2X_5$ cDNAs previously mutated to replace their natural stop codon with a *XhoI* restriction site. $P2X_1$-Flag, $P2X_1$-His_6, $P2X_5$-Flag, and $P2X_5$-His_6 were then subcloned

* This work was supported by the Medical Research Council of Canada and the Fondation des Maladies du Coeur du Québec. The costs of publication of this article were defrayed in part by the payment of page charges. This article must therefore be hereby marked "*advertisement*" in accordance with 18 U.S.C. Section 1734 solely to indicate this fact.

‡ These authors contributed equally to this work.

§ Present address: Dept. of Cellular and Molecular Physiology, Boyer Center for Molecular Medicine, Yale University School of Medicine, New Haven, CT 06536.

¶ Recipient of a Postdoctoral Fellowship from the Fondation pour la Recherche Médicale (France).

‖ Junior Scholar from the Fonds de la Recherche en Santé du Québec. To whom correspondence should be addressed: Montreal Neurological Institute, 3801 University, Montreal, Quebec H3A 2B4, Canada. Tel.: 514-398-5029; Fax: 514-398-8106; E-mail: mips@musica.mcgill.ca.

[1] The abbreviations used are: $\alpha\beta$m-ATP, α,β-methylene ATP; His_6, hexahistidine; TNP-ATP, trinitrophenyl-ATP; NTA, nitrilotriacetic acid.

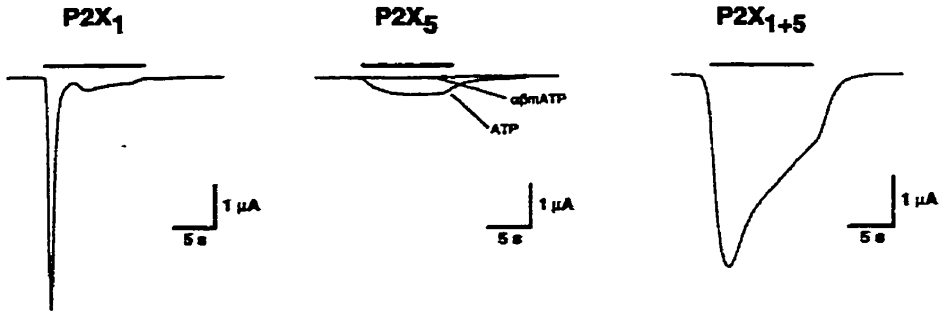

FIG. 1. **Co-expression of $P2X_1$ with $P2X_5$ ($P2X_{1+5}$) yields a slowly desensitizing current that is activated by αβm-ATP.** Whole-cell currents were recorded from oocytes after nuclear injections with $P2X_1$ cDNA alone, $P2X_5$ cDNA alone, and $P2X_1$ + $P2X_5$ cDNAs ($P2X_{1+5}$) on prolonged applications of 50 μM αβm-ATP. Fast desensitization of the αβm-ATP-induced current occurs in oocytes expressing $P2X_1$ alone but not in oocytes expressing $P2X_1$ and $P2X_5$ together. $P2X_5$-expressing oocytes showed weak currents to 50 μM ATP and no detectable response to 50 μM αβm-ATP. Oocytes were voltage-clamped at V_h = −100 mV. *Bars* represent the durations of agonist applications.

directionally into the *Hin*dIII-*Xba*I sites of pcDNAI vector (Invitrogen, San Diego, CA) compatible with CMV-driven heterologous expression in HEK-293A cells and *Xenopus laevis* oocytes. RT-PCR products as well as mutant epitope-tagged subunits were subjected to automatic dideoxy sequencing (Sheldon Biotechnology Center, Montreal).

Cell Culture and Protein Chemistry—cDNA transfections of epitope-tagged P2X subunits were performed in mammalian cells. HEK-293A cells (ATCC No. CRL 1573) were cultured in Dulbecco's modified Eagle's medium and 10% heat-inactivated fetal bovine serum (Wisent, St. Bruno, Canada) containing penicillin and streptomycin. Cells reaching 30–50% confluency were used for transient cDNA transfections with the calcium phosphate method with 10 μg of supercoiled plasmid cDNA per 10^6 cells. Transfected HEK-293A cells used for Western blots were then lifted in Hanks' modified calcium-free medium with 20 mM EDTA, pelleted at low centrifugation, and homogenized in 10 volumes of 10 mM HEPES buffer and 0.3 M sucrose, pH 7.40, containing protease inhibitors phenylmethylsulfonyl fluoride (0.2 mM) and benzamidine (1 mM). Membranes from cell lysates were solubilized with 1% Triton X-100 (Sigma) for 2 h at 4 °C and pelleted at 14000 × *g* for 5 min, and remaining membrane proteins within supernatants were used for Western blots. Solubilized proteins were incubated with 25 μl of equilibrated Ni-NTA resin (Qiagen, Hilden, Germany) for 2 h at 4 °C under agitation. Then Ni-NTA beads were washed six times in Tris-buffered saline containing 25 mM imidazole and 1% Triton X-100. Bound proteins were eluted from His_6-binding resin with 500 mM imidazole, diluted 1:1 (v/v) with SDS-containing loading buffer. Samples were then loaded onto 10–12% SDS-PAGE and transferred to nitrocellulose. Immunostainings were performed with M2 murine monoclonal antibodies (10 μg/ml) (Sigma) or chicken anti-Flag polyclonal antibodies (1:200) (Aves) followed by incubations with corresponding species-specific peroxidase-labeled secondary antibodies (1:5000–1:20,000) for visualization by enhanced chemiluminescence (Amersham Pharmacia Biotech).

Electrophysiology—Electrophysiological recordings were performed in *Xenopus* oocytes. Ovary lobes were surgically retrieved from *X. laevis* frogs under deep tricaine (Sigma) anesthesia. Oocyte-containing lobes were then treated for 3 h at room temperature with type II collagenase (Life Technologies, Gaithersburg, MD) in calcium-free Barth's solution under vigorous agitations. Stage V–VI oocytes were then chemically defolliculated before nuclear micro-injections of 5–10 ng of cDNA coding for each P2X channel subunit. Following 2–5 days of incubation at 19 °C in Barth's solution containing 1.8 mM calcium chloride and 10 μg/ml gentamicin (Sigma), elicited P2X currents were recorded in two-electrode voltage-clamp configuration using an OC-725B amplifier (Warner Instruments). Responsive signals were low pass filtered at 1 kHz, acquired at 500 Hz using a Macintosh IIci computer equipped with an NB-MIO-16XL analog-to-digital card (National Instruments). Recorded traces were post-filtered at 100 Hz in Axograph (Axon Instruments). Agonists, antagonists, and P2X co-factors (10 μM zinc chloride, pH 6.40 and pH 8.40) were prepared at room temperature in Ringer's perfusion solution containing 115 mM NaCl, 2.5 mM KCl, 1.8 mM $CaCl_2$, and 10 mM HEPES buffered at pH 7.40. Solutions were perfused onto oocytes at a constant flow rate of 10–12 ml/min. Dose-response curves were fitted to the Hill sigmoidal equation, and EC_{50} as well as IC_{50} values were determined using the software Prism 2.0 (Graphpad Software, San Diego, CA).

RESULTS AND DISCUSSION

To assess the presence of $P2X_{1+5}$ heteromers in *Xenopus* oocytes co-injected with both subunits, we tested the expression of inward currents during prolonged applications (5–10 s) of 50 μM αβm-ATP, exploiting the fact that homomeric $P2X_5$ ATP-gated channels are almost insensitive to this agonist when applied at concentrations below 100 μM (Fig. 1) (11, 12). Whereas homomeric $P2X_1$ receptors desensitize strongly in the first seconds of agonist application, a slowly desensitizing response induced by 50 μM αβm-ATP was observed in oocytes co-injected with $P2X_1$ and $P2X_5$ subunits at a 1:1 cDNA molar ratio (Fig. 1). This hybrid phenotype was the unambiguous trademark of the expression of heteromeric $P2X_{1+5}$ receptors. Oocytes expressing $P2X_{1+5}$ receptors showed robust 50 μM αβm-ATP-induced whole-cell currents with amplitudes in the range of 3–15 μA at V_h = −50 mV after 2–5 days of post-injection time, similar to currents recorded from oocytes expressing $P2X_1$ alone (Fig. 1).

$P2X_{1+5}$ receptors slowly desensitized during agonist application but showed complete recovery in 2 min (Fig. 2), a noticeable difference with homomeric $P2X_5$ receptors that do not desensitize in heterologous systems (Fig. 1) (11, 12). However, $P2X_{1+5}$ receptors (Fig. 2, *B* and *D*) recovered significantly faster than $P2X_1$ receptors, the latter recovering less than 50% of their initial response after 5 min of washout (Fig. 2, *A* and *C*). We noticed slight differences in the rate of desensitization of $P2X_{1+5}$ receptors between oocytes (Fig. 2). These variations of phenotype could be because of the expression of populations of heteromeric channels with different stoichiometries, a cell-dependant variable that is not controlled in these experiments of co-injection. The kinetic properties of $P2X_2$ receptors have been shown to be modulated by protein kinase A activity (19). Thus it is possible that inter-individual differences in the levels of endogenous kinase activity present in oocytes could have some impact on the properties of desensitization of $P2X_{1+5}$ receptors. Furthermore, the correlation between the number of $P2X_5$ subunits and the kinetic properties of the oligomeric complex, which has been reported to be a trimer for homomeric $P2X_1$ channels (20), is not yet known.

$P2X_{1+5}$ receptors were challenged with ATP, αβm-ATP, and ADP at various concentrations for comparison with the pharmacology of homomeric $P2X_1$ and $P2X_5$ receptors. We measured EC_{50} values for $P2X_{1+5}$ heteromers of 0.4 ± 0.2 μM for ATP, 1.1 ± 0.6 μM for αβm-ATP and 13 ± 4 μM for ADP (Fig. 3). These EC_{50} values were not significantly different from those obtained with homomeric $P2X_1$ receptors in the same experimental conditions: 0.7 ± 0.1 μM for ATP, 2.4 ± 1 μM for αβm-ATP, and 47 ± 9 μM for ADP (Fig. 3), in good agreement

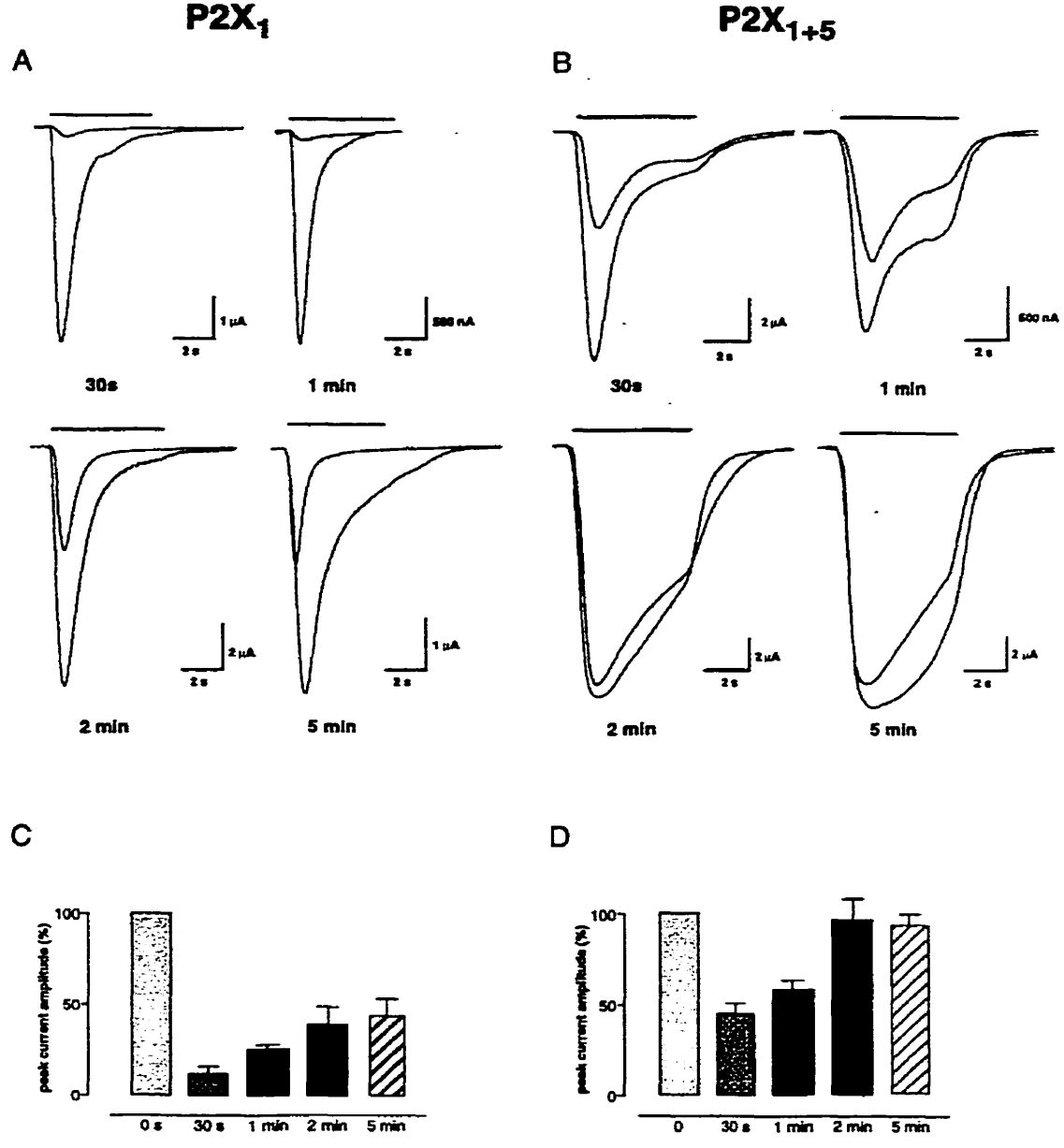

FIG. 2. **Comparison of recovery rate from desensitization between homomeric $P2X_1$ and heteromeric $P2X_{1+5}$ receptors.** Shown are superimposed whole-cell currents recorded from individual oocytes expressing $P2X_1$ (*A*) or $P2X_{1+5}$ receptors (*B*) during two applications of αβm-ATP separated by different time intervals as indicated. 5-s applications of αβm-ATP at 1 μM for $P2X_1$ and 10 μM for $P2X_{1+5}$ were recorded at holding potentials of −100 mV. Shown are mean peak currents evoked by repeated applications of αβm-ATP on $P2X_1$ (*C*) and $P2X_{1+5}$ receptors (*D*). Currents were normalized to the value of the first response ($t = 0$) in the same oocyte ($n = 5$).

with previously published data (3). Differences in the apparent Hill coefficient n_H (cooperativity index) of ADP activation between $P2X_1$ ($n_H = 4.9 \pm 2.3$) and $P2X_{1+5}$ ($n_H = 1.6 \pm 0.8$) (Fig. 3*C*) could be because of the fact that we record from a heterogeneous population of $P2X_1$-containing receptors with varying stoichiometries. The amplitudes of peak currents from $P2X_5$-expressing oocytes were too small to carry out complete dose-response curve experiments with these agonists (Fig. 1). No significant differences were observed between $P2X_{1+5}$ and $P2X_1$ receptors during co-applications of extracellular zinc ions (10 μM), protons (pH 6.4), or alkaline solutions (pH 8.4) with sub-saturating concentrations of ATP (0.1 μM) (data not shown). Our results suggest that $P2X_1$ subunits confer their high αβm-ATP sensitivity to the $P2X_{1+5}$ heteromers. Another specific pharmacological property of $P2X_1$ subunits, the potent inhibitory effect of trinitrophenyl-ATP (TNP-ATP) (20), is observed in the heteromeric receptors (Fig. 4*A*). In conditions of co-application of TNP-application of TNP-ATP and αβm-ATP without pre-incubation, we measured an IC_{50} of 64 ± 14 nM on $P2X_{1+5}$ and 200 ± 120 nM on homomeric $P2X_1$receptors (Fig. 4*B*). This subunit association is therefore reminiscent of the association between $P2X_2$ and $P2X_3$ in which $P2X_3$ is the pharmacologically dominant component both for αβm-ATP sensitivity (5, 17) and blockade by TNP-ATP (21, 22).

To demonstrate direct associations between $P2X_1$ and $P2X_5$ subunits that underlie their assembly in hybrid heteromers, we assayed their physical interaction by co-purification of epitope-tagged subunits in transfected HEK-293A cells. Purification of $P2X_5$-His_6 on nickel-binding resin in nondenaturing conditions (see "Experimental Procedures" for details) allowed the detection of co-transfected $P2X_1$-Flag in Western blots (Fig. 5, *lane C*). Reciprocally, $P2X_1$-His_6 was shown to co-assemble with $P2X_5$-Flag (Fig. 5, *lane D*). Positive controls included pseudo-homomeric receptors composed of $P2X_1$-His_6 + $P2X_1$-Flag or

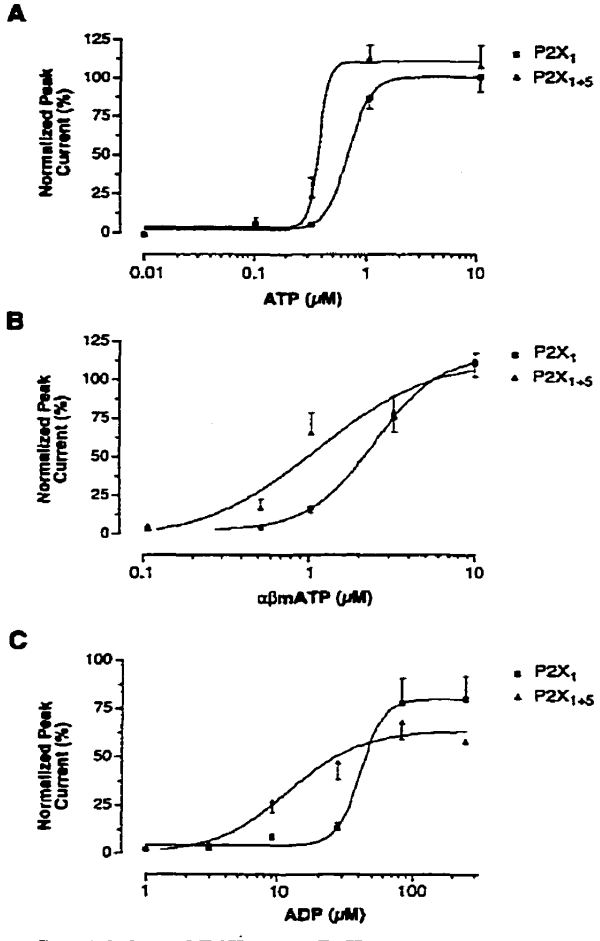

FIG. 3. **Sensitivity of $P2X_1$ and $P2X_{1+5}$ receptors to the purinergic agonists ATP (*A*), αβm-ATP (*B*), and ADP (*C*).** For each agonist concentration-current relationship, mean peak currents were normalized to the response to 100 μM ATP (mean ± S.E. from 3 to 10 oocytes per point). Holding potentials were −50 mV (*A* and *B*) and −70 mV (*C*).

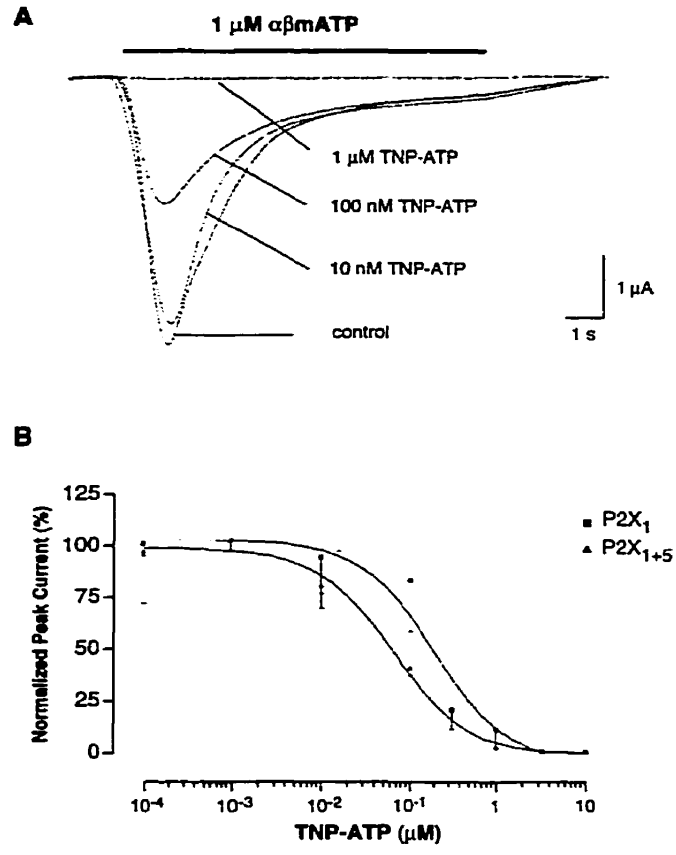

FIG. 4. **Potent blockade of $P2X_1$ and $P2X_{1+5}$ receptors-mediated responses by the antagonist TNP-ATP.** *A*, representative $P2X_{1+5}$ currents in conditions of inhibition. *B*, sensitivity of $P2X_1$ and $P2X_{1+5}$ responses to TNP-ATP, co-applied with 1 μM αβm-ATP. Peak currents were normalized to the response elicited by application of 10 μM αβm-ATP alone (mean ± S.E. from 5 to 8 oocytes per point). Membrane potentials were held at −100 mV.

$P2X_5$-His_6 + $P2X_5$-Flag (Fig. 5, *lanes A* and *B*). Technical controls of transfections with one P2X subunit only or with sham-transfected HEK-293A cells were negative (data not shown).

Peripheral sensory neurons have been reported to express ATP-gated channels with a slow rate of desensitization and a high sensitivity to αβm-ATP characterized by EC_{50} in the low micromolar range (Ref. 5, and references therein). This sensory phenotype was thought to be exclusively accounted for by the co-assembly of $P2X_2$ and $P2X_3$ subunits into heteromeric $P2X_{2+3}$ receptors (5, 17). Alternatively, we propose from our results that slowly desensitizing and αβm-ATP-elicited responses could be mediated by hybrid $P2X_{1+5}$ heteromeric receptors endowed with the pharmacology of $P2X_1$ and the kinetics of $P2X_5$. Our data suggest to use TNP-ATP as a specific antagonist of $P2X_1$-containing ATP-gated channels. In spinal motoneurons where $P2X_3$ is absent, complete blockade of slowly desensitizing P2X responses by 1 μM TNP-ATP would indicate the expression of $P2X_{1+5}$ heteromeric channels.

Using subunit-specific polyclonal antibodies, Vulchanova *et al.* (23) described a strong $P2X_1$ immunoreactivity in the laminae I-II of spinal cord, corresponding to presynaptic labeling of central axon terminals from dorsal root ganglia sensory neurons. As $P2X_2$ and $P2X_3$ subunits do not appear to co-assemble in heteromeric channels in these primary afferents (16), a presynaptic localization of $P2X_{1+5}$ receptors would provide sensory axon terminals with high sensitivity to ATP and slowly

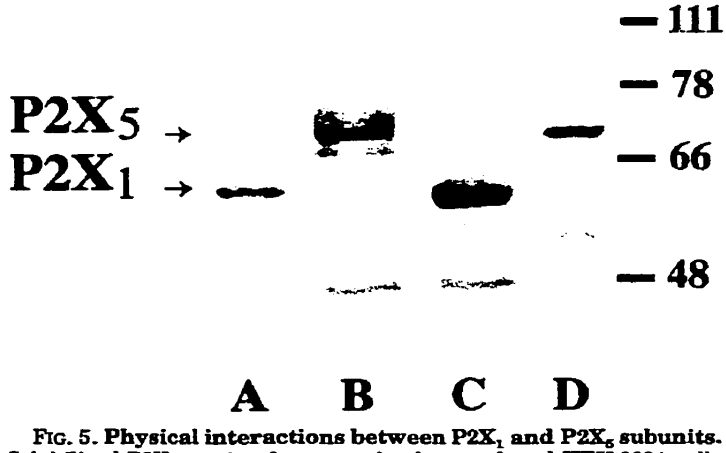

FIG. 5. **Physical interactions between $P2X_1$ and $P2X_5$ subunits.** Solubilized P2X proteins from transiently transfected HEK-293A cells were detected on immunoblots after purification using His_6-binding Ni^{++}-NTA resin. P2X subunits associated with corresponding His_6-tagged partners were probed with anti-Flag antibodies. Co-purifications shown are: $P2X_1$-His_6 + $P2X_1$-Flag in *lane A* (positive control), $P2X_5$-His_6 + $P2X_5$-Flag in *lane B* (positive control), $P2X_5$-His_6 + $P2X_1$-Flag in *lane C*, and $P2X_1$-His_6 + $P2X_5$-Flag in *lane D*. Molecular weight markers are indicated in kilodaltons.

desensitizing voltage-independent calcium entry that could play a modulatory role in the release of central neurotransmitters glutamate or substance P (24). The effects of presynaptic $P2X_{1+5}$ receptors on the release of sensory transmitters can now be experimentally challenged with application of the blocker TNP-ATP at low concentrations.

In the central nervous system, an important role for purines in motor systems is deduced both from the distribution of several P2X subunits mRNA within cranial and spinal motor nuclei (11) and from the powerful cellular effects of extracellular ATP on motor outflow (25). More specifically, a subset of large projection motoneurons in lamina IX of rat spinal cord has been characterized by the co-expression of $P2X_1$ and $P2X_5$ subunits (11). We propose from their functional properties that highly agonist-sensitive $P2X_{1+5}$ receptors might provide a specific excitatory function to the motor control by allowing a sustained entry of extracellular calcium within motoneurons in response to minute amounts of released ATP.

Acknowledgment—We gratefully acknowledge Kazimierz Babinski for the cloning of the rat $P2X_5$ receptor subunit.

REFERENCES

1. Buell, G., Collo, G., and Rassendren, F. (1996) *Eur. J. Neurosci.* **8**, 2221–2228
2. North, R. A., and Barnard, E. A. (1997) *Curr. Opin. Neurobiol.* **7**, 346–357
3. Valera, S., Hussy, N., Evans, R. J., Adami, N., North, R. A., Surprenant, A., and Buell, G. (1994) *Nature* **371**, 516–519
4. Chen, C.-C., Akopian, A. N., Sivilotti, L., Colquhoun, D., Burnstock, G., and Wood, J. N. (1995) *Nature* **377**, 428–431
5. Lewis, C., Neidhart, S., Holy, C., North, R. A., Buell, G., and Surprenant, A. (1995) *Nature* **377**, 432–435
6. Bo, X., Zhang, Y., Nassar, M., Burnstock, G., and Schoepfer, R. (1995) *FEBS Lett.* **375**, 129–133
7. Buell, G. Lewis, C. Collo, G. North, R. A., and Surprenant, A. (1996) *EMBO J.* **15**, 55–62
8. Séguéla, P., Haghighi, A., Soghomonian, J.-J., and Cooper, E. (1996) *J. Neurosci.* **1**, 448–455
9. Soto, F., Garcia-Guzman, M., Gomez-Hernandez, M. J., Hollmann, M., Karschin, C., and Stuhmer, W. (1996) *Proc. Natl. Acad. Sci. U. S. A.* **93**, 3684–3688
10. Wang, C., Namba, N., Gonoi, T., Inagaki, K., and Seino, S. (1996) *Biochem. Biophys. Res. Commun.* **230**, 8063–8067
11. Collo, G., North, R. A., Kawashima, E., Merlo-Pich, E., Neidhart, S., Surprenant, A., and Buell, G. (1996) *J. Neurosci.* **16**, 2495–2507
12. Garcia-Guzman, M., Soto, F., Laube, B., and Stuhmer, W. (1996) *FEBS Lett.* **388**, 123–127
13. Brake, A. J., Wagenbach, M. J., and Julius, D. (1994) *Nature* **371**, 519–523
14. Surprenant, A., Rassendren, F., Kawashima, E., North, R. A., and Buell, G. (1996) *Science* **272**, 735–738
15. Cook, S. P., Vulchanova, L., Hargreaves, K. M., Elde, R., and McCleskey, E. W. (1997) *Nature* **387**, 505–508
16. Vulchanova, L., Riedl, M. S., Shuster, S. J., Buell, G., Surprenant, A., North, R. A., and Elde, R. (1997) *Neuropharmacology* **36**, 1229–1242
17. Radford, K. M., Virginio, C., Surprenant, A., North, R. A., and Kawashima, E. (1997) *J. Neurosci.* **17**, 6529–6533
18. Lê, K.-T., Babinski, K., and Séguéla, P. (1998) *J. Neurosci.* **18**, 7152–7159
19. Chow, Y.-W., and Wang, H.-L. (1998) *J. Neurochem.* **70**, 2606–2612
20. Nicke, A., Bäumert, H. G., Rettinger, J. Eichele, A., Lambrecht, G., Mutschler, E., and Schmalzing, G. (1998) *EMBO J.* **17**, 3016–3028
21. Virginio, C., Robertson, G., Surprenant, A., and North, R. A. (1998) *Mol. Pharmacol.* **53**, 969–973
22. Thomas, S., Virginio, C., North R. A., and Surprenant, A. (1998) *J. Physiol.* **509**, 411–417
23. Vulchanova, L., Arvidsson, U., Rield, M., Wang, J., Buell, G. N., Surprenant, A., North, R. A., and Elde, R. (1996) *Proc. Natl. Acad. Sci. U. S. A.* **93**, 8063–8067
24. Gu, J. G., and MacDermott, A. B. (1997) *Nature* **389**, 749–753
25. Funk, G. D., Kanjhan, R., Walsh, C., Lipski, J., Comer, A. M., Parkis, M. A., and Housley, G. D. (1997) *J. Neurosci.* **17**, 6325–6337

Primary structure and expression of a naturally truncated human P2X ATP receptor subunit from brain and immune system

Khanh-Tuoc Lê[1], Michel Paquet[1], Dominique Nouel, Kazimierz Babinski, Philippe Séguéla*

Cell Biology of Excitable Tissue Group, Montreal Neurological Institute, McGill University, 3801 University, Montreal, Que. H3A 2B4, Canada

Received 2 October 1997; revised version received 23 October 1997

Abstract **A novel member of the ionotropic ATP receptor gene family has been identified in human brain. This 422 amino acid long P2X receptor subunit has 62% sequence identity with rat $P2X_5$. Several characteristic motifs of ATP-gated channels are present in its primary structure, but this $P2X_5$-related subunit displays a single transmembrane domain. Heterologous expression of chimeric subunits containing the C-terminal domain of rat $P2X_5$ leads to the formation of desensitizing functional ATP-gated channels in *Xenopus* oocytes. The developmentally regulated mRNA, found in two splicing variant forms, is expressed at high levels in brain and immune system.**

© 1997 Federation of European Biochemical Societies.

Key words: Transmitter-gated channel; Purinoceptor; Nucleotide; Lymphocyte; Cerebellum

1. Introduction

Mammalian P2X receptors belong to a multigene family of non-selective cation channels activated by extracellular ATP. The seven known members of the rat P2X family can be grouped into three functional categories according to their pharmacological profiles and to their properties of desensitization. $P2X_1$ [1] and $P2X_3$ [2,3] are highly sensitive to α,β-methylene-ATP (αβmATP) and desensitize rapidly; $P2X_2$ [4], $P2X_5$ [5,6] and $P2X_7$ [7] do not respond to αβmATP below 100 μM and do not desensitize, whereas $P2X_4$ [8–10] and $P2X_6$ [5] do not respond to αβmATP, are almost insensitive to co-applied non-competitive antagonists suramin and PPADS, and show moderate desensitization. Despite the fact that high levels of expression of P2X receptors are observed in many central and peripheral tissues, reinforcing the concept of an important role for ATP in intercellular communication [11], much less is known about their human counterparts. Excitatory ATP-gated channels play a specific role in sensory systems [12–14], therefore the development of subtype-specific P2X antagonists with analgesic properties should take into account functional differences between mammalian species. The reports on the expression of cloned human P2X orthologs of $P2X_1$ [15], $P2X_3$ [16], $P2X_4$ [17] and $P2X_7$ [18] emphasized both pharmacological and anatomical specificities that seriously undermine the relevance of our knowledge based on rodent systems for extrapolation to human fast purinergic transmission. In an effort to complete the genetic inventory of human ionotropic ATP receptors, we report here the identification, heterologous expression and anatomical distribution of a novel member of the human P2X gene family isolated from fetal brain.

2. Materials and methods

2.1. Molecular cloning and in vitro translation

Using the TBLASTN algorithm, virtual screening of the dbEST database [19] with the whole coding region of rat $P2X_4$ subunit led to the identification of human fetal brain EST sequences encoding a novel P2X gene (GenBank accession numbers T80104 and Z43811). The clone tagged by EST T80104 was sequenced on both strands and was shown to encode a short splicing variant of human P2X subunit related to rat $P2X_5$: $hP2X_{5R}$ (Fig. 1). A longer splicing variant of $hP2X_{5R}$ was detected in RT-PCR from human cerebellum mRNA with exact match primers. The EST clone was engineered to generate the long version of $hP2X_{5R}$ (Fig. 1), deposited in Genbank under accession number AF016709. This $hP2X_{5R}$ clone was transferred into the *Hin*dIII-*Not*I sites of eukaryotic vector pcDNA3 (Invitrogen) for CMV-driven heterologous expression in HEK-293 cells and *Xenopus* oocytes. Supercoiled $hP2X_{5R}$ plasmid was used for in vitro translation using the TnT system with T7 RNA polymerase (Promega) and [^{35}S]cysteine (ICN) according to the manufacturer's specifications.

2.2. Construction of epitope-tagged $hP2X_{5R}$ subunits and immunolocalization

$hP2X_{5R}$ subunit was epitope-tagged ($hP2X_{5R}$-FL) to facilitate the immunolocalization of the protein both in situ and in Western blot from transfected mammalian cells. The Flag octapeptide DYKDDDDK (IBI) was inserted by PCR in the C-terminal domain of $hP2X_{5R}$ using an antisense oligonucleotide primer designed for the replacement of its natural stop codon by an artificial in-frame *Xho*I site (TCACTCGAGCAACGTGCTCCTGTGGGGCT). Full-length mutant $hP2X_{5R}$ cDNA was amplified in PCR using *Pfu* polymerase (Stratagene), then ligated to an *Xho*I-*Xba*I cassette containing the Flag peptide followed by a stop codon [20] in the pcDNA3 vector.

For transfection of $hP2X_{5R}$-FL subunits, HEK-293 cells (ATCC CRL1573) were grown in DMEM-10% heat-inactivated fetal bovine serum (Wisent, St Bruno, Quebec) containing penicillin and streptomycin. Freshly plated cells reaching 30–50% confluence were used for transient transfection using the calcium phosphate method on 90 mm dishes with 10 μg supercoiled plasmid/10^6 cells.

For immunofluorescence, transfected HEK-293 cells (48–72 h post-transfection time) were plated at 50–70% confluence in poly-lysine-coated chambers. Adherent cells were washed in PBS and fixed for 20 min at room temperature with 4% paraformaldehyde in 0.1 M phosphate buffer, pH 8.0. After blocking non-specific sites with 2% normal goat serum, fixed cells were incubated with anti-Flag monoclonal antibody (mAb) M2 (1 μg/ml, IBI) for 1 h at room temperature in 0.05 M Tris-saline buffer pH 7.2 containing 0.2% Triton X-100, 5% normal goat serum and 5% dry milk powder. Bound primary antibodies were detected by immunofluorescence after 1 h incubation with Texas red-labeled goat anti-mouse (2 μg/ml) secondary antibodies (ImmunoResearch Labs).

For high resolution analysis of $hP2X_{5R}$-FL subcellular distribution, we used a Zeiss Laserscan Inverted 410 confocal microscope equipped with an argon-krypton laser set at 580 nm for Texas red. Serial images (512×512 pixels) acquired as single optical sections were averaged over 32 scans/frame and processed with the Zeiss CLMS software package.

For Western blots, transfected cells were lifted in Hanks' modified

*Corresponding author. Fax: (1) (514) 398-8106.
E-mail: mips@musica.mcgill.ca

[1]These authors contributed equally to this work.

0014-5793/97/$17.00 © 1997 Federation of European Biochemical Societies. All rights reserved.
PII S0014-5793(97)01380-X

calcium-free medium with 20 mM EDTA, pelleted at low speed and homogenized in 10 volumes of 10 mM HEPES buffer pH 7.4 containing the protease inhibitors phenylmethylsulfonyl fluoride (0.2 mM) and benzamidine (1 mM). Lysates were pelleted at 14000×*g* for 5 min to remove cell debris before protein assay and crude membrane proteins in supernatants were solubilized with SDS-containing loading buffer. About 150 μg of protein/lane were run on 12% SDS-PAGE, then transferred to nitrocellulose. Immunoprobing was performed with mouse mAb M2 (1 μg/ml) followed by peroxidase-labeled secondary antibodies for visualization by enhanced chemiluminescence (Amersham).

2.3. Functional expression of h-rP2X$_5$ chimera in Xenopus oocytes

The domain of hP2X$_{5R}$ containing amino acids 1–318 was fused to the PCR-amplified domain corresponding to amino acids 318–455 of rat P2X5 using the natural *Bam*HI site of hP2X$_{5R}$ to generate the chimera h-rP2X$_5$. Oocytes surgically removed from mature *Xenopus laevis* frogs were treated for 2 h at room temperature with type II collagenase (Gibco-BRL) in Barth's solution under agitation. Selected stage IV–V oocytes were defolliculated manually before nuclear microinjection [21] of 10 ng cDNA of hP2X$_5$ or h-rP2X$_5$ chimera in pcDNA3 vector. After 2–4 days of expression at 19°C in Barth's solution containing 10 μg/ml gentamicin, oocytes were recorded in two-electrode voltage-clamp configuration using a OC-725B amplifier (Warner Inst.). Signals were acquired and digitized at 500 Hz using a Macintosh IIci equipped with an A/D card NB-MIO16XL (National Instruments) then traces were post-filtered at 100 Hz in Axograph (Axon Instruments). Agonists dissolved in Ringer's solution containing 115 mM NaCl, 2.5 mM KCl, 1.8 mM $CaCl_2$ in 10 mM HEPES pH 7.4 at room temperature were applied on oocytes by perfusion in constant flow (10 ml/min).

2.4. RT-PCR detection of hP2X$_{5R}$ mRNA from human cerebellum and lymphocytes

Total RNA from post-mortem adult human cerebellar cortex and adult lymphocytes were isolated using Trizol reagent (Gibco-BRL). Then 5 μg of each RNA was subjected to random-primed reverse-transcription with Superscript (Gibco-BRL). Around 100 ng of RT-cDNA was used as template for PCR with the following primers: forward TTCGACTACAAGACCGAGAAGT (P1, see Fig. 1B) and

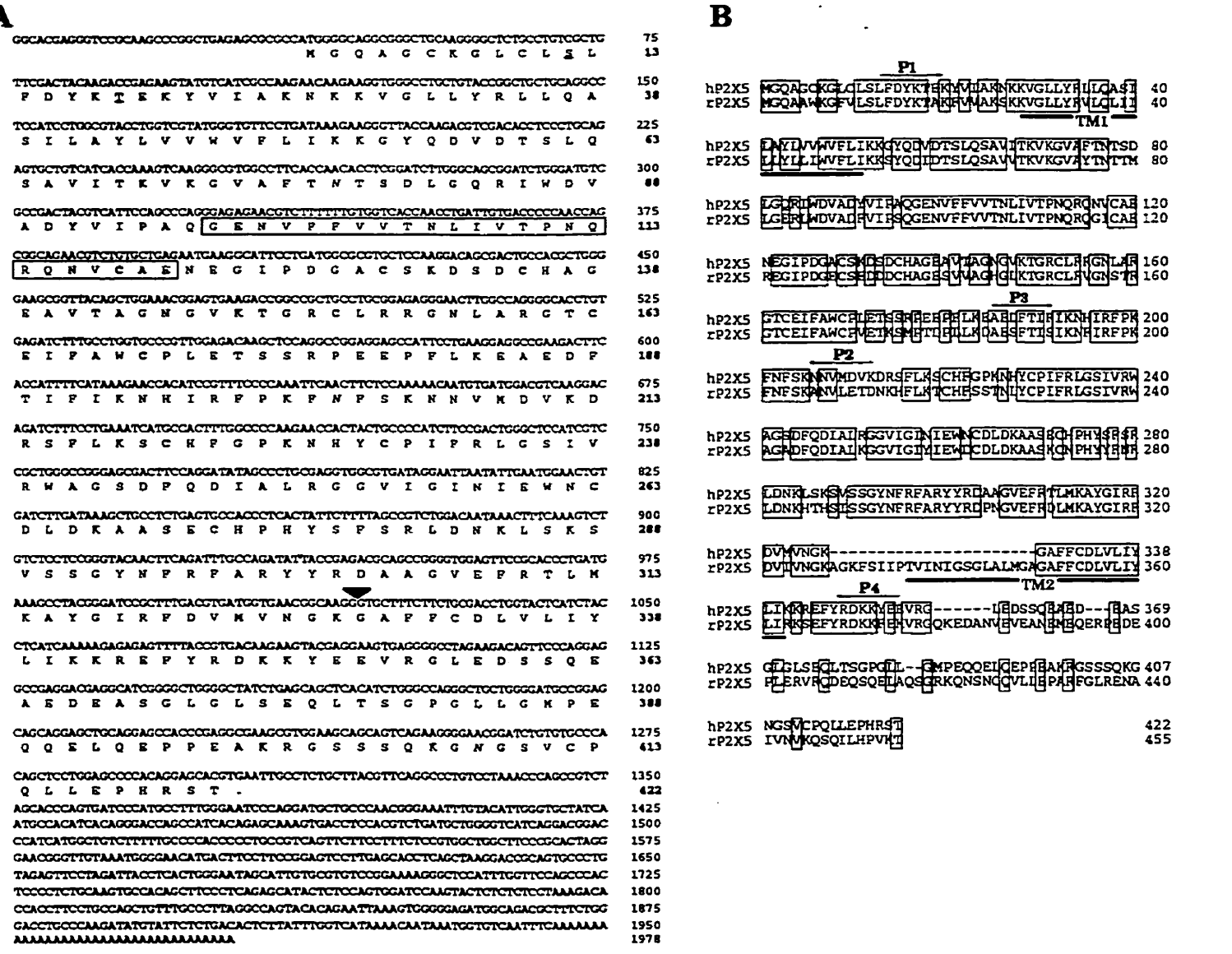

Fig. 1. Molecular cloning of a novel member of the human P2X ATP gene family: hP2X$_{5R}$. A: Nucleotide sequence and ORF domain. Potential intracellular phosphorylation sites are indicated, as well as cysteine residues (bold) and *N*-glycosylation sites (italics) in the putative extracellular domain of the subunit. The spliced domain of 24 amino acids (Gly^{97}–Glu^{120}), absent in the short variant from brain, is boxed. The putative splicing site of missing TM2 sequence is indicated by the arrowhead. B: Alignment of human and rat P2X$_5$ amino acid sequences and positions of PCR primers based on hP2X$_{5R}$ primary structure.

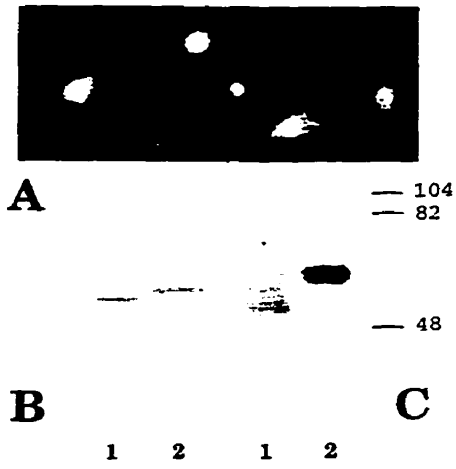

Fig. 2. Heterologous expression and immunodetection of $hP2X_{5R}$ subunits. A: In vitro translation of recombinant wild-type (1) and Flag-tagged $hP2X_{5R}$ (2). B: Detection in Western blot of epitope-tagged $hP2X_{5R}$ (1) and rat $P2X_4$ (2) from transfected HEK-293 cells.

reverse CTTGACGTCCTTCACATTGT (P2) to amplify the region corresponding to nucleotides 75–671 around the splicing event, as well as forward GAGGCCGAAGACTTCACCAT (P3) and reverse CCTCGTACTTCTTGTCACGG (P4) to detect the expression of a complete second transmembrane domain (TM2). Non-RT samples amplified in the same conditions provided the negative controls. Integrity and representativity of RT-cDNA were checked by amplification of human $P2X_7$ subunit message [18] and human $P2X_4$ message [17] with appropriate primers in lymphocytes and in cerebellum, respectively (data not shown).

2.5. Distribution of $hP2X_{5R}$ transcripts in human tissues

Known amounts of mRNA blots corresponding to equivalent transcription levels of housekeeping genes from various fetal and adult human tissues (Masterblot, Clontech) were probed with full-length random-primed [^{32}P]$hP2X_{5R}$ cDNA at high stringency (final elution at 65°C in 0.3×SSC buffer). Hybridization signals were quantitated using a Storm phosphorimager and the ImageQuant application (Molecular Dynamics) before subtraction of background and normalization of transcription levels.

3. Results and discussion

The longest reading frame of $hP2X_{5R}$ cDNA encodes a protein of 422 amino acids that displays 62% sequence identity with rat $P2X_5$ and several unique motifs conserved in all P2X receptor subunits (Fig. 1). In the intracellular N-terminal domain, $hP2X_{5R}$ displays an highly conserved threonine residue (Thr^{18}), potentially susceptible to phosphorylation by protein kinase C. In addition, a serine residue (Ser^{12}) is found in a consensus site for phosphorylation by casein kinase II. In the putative extracellular domain of $hP2X_{5R}$, all 10 cysteine, all proline, 91% of glycine and 75% of lysine residues are present at homologous positions in all P2X subunits, indicating their critical roles in the folding and function of this sensor region. We checked the real position of the predicted stop codon by in vitro translation as well as Western blot (Fig. 2). The recombinant subunit and its epitope-tagged mutant migrate at a M_r of 49±2 kDa and 51±2 kDa, respectively, in agreement with the calculated MW of 47 kDa for wild-type $hP2X_{5R}$ (Fig. 2B). At least one of the 3 *N*-linked glycosylation consensus sites present in the extracellular domain of $hP2X_{5R}$ is used, according to the difference of M_r (up to 11 kDa) between in vitro translated $hP2X_{5R}$ and $hP2X_{5R}$ expressed in transfected HEK-293 cells (Fig. 2B,C). The multiple bands observed in Western blot from transfected cells could be due to the co-expression of several glycosylated forms of $hP2X_{5R}$ (Fig. 2B).

The integrity of the protein was also checked by detection of heterologously expressed epitope-tagged $hP2X_{5R}$ mutants using in situ immunofluorescence (Fig. 2AFig. 3). Analysis of the subcellular localization of $hP2X_{5R}$-FL in HEK-293 cells using confocal microscopy indicated a correct targeting of the subunit to the plasma membrane (Fig. 3), quantitatively similar to the surface distribution of the functional P2X receptors rat $P2X_1$-FL and rat $P2X_4$-FL [14]. When expressed in *Xenopus* oocytes, homomeric $hP2X_5$ channels do not respond to extracellular ATP applied at concentrations up to 1 mM. However, the chimera h-r$P2X_5$, made of the N-terminal domain of $hP2X_5$ linked to the C-terminal domain of rat $P2X_5$, revealed the formation of cationic ATP-gated ion channels (Fig. 4). These channels run down rapidly and do not recover fully from desensitization after extensive washing of agonist lasting several minutes in constant perfusion (Fig. 4). There-

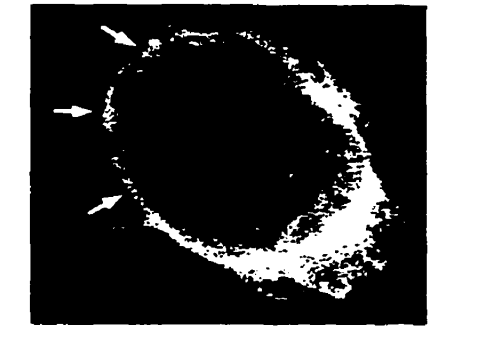

Fig. 3. Subcellular distribution of $hP2X_{5R}$ subunits expressed in HEK-293 cells using confocal microcope immunofluorescence. Arrows indicate the localization of $hP2X_{5R}$ subunits on the plasma membrane.

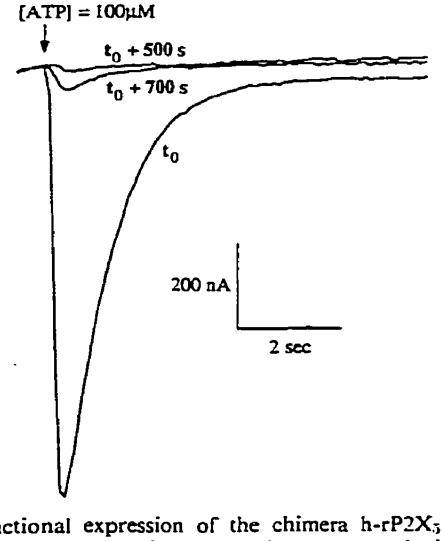

Fig. 4. Functional expression of the chimera h-r$P2X_5$ in *Xenopus* oocytes. Fast and desensitizing inward currents evoked by 100 μM extracellular ATP were recorded after 2–4 days of expression in two-electrode voltage-clamp configuration (holding potential $v_h = -100$ mV). Repeated applications of agonist at time to +500 s or to +700 s showed profound desensitization of the chimeric ATP-gated channels.

fore, despite the high sequence similarity with non-desensitizing wild-type rat $P2X_5$ (62%), this chimeric channel displays a unique functional property not found in any other known homomeric or heteromeric subtypes. These data suggest that the kinetics of desensitization of P2X channels is dependent on subtle rules of complementarity between the N-terminal and the C-terminal halves of the subunits, as has been shown for $P2X_1$ and $P2X_2$ [23].

We observed the expression of a splicing variant identified in fetal and adult brain by RT-PCR (Fig. 5), differing from the long form of $hP2X_{5R}$ by the absence of a cassette of 24 amino acids, corresponding to the domain Gly^{97}–Glu^{120} (Fig. 1). This cassette contains one of the 10 extracellular cysteines, so the expression of this short variant is due either to some inaccuracy in the intron/exon splicing mechanisms or to some functional regulation. Interestingly, the region including amino acids Ala^{328}–Ala^{349} in rat $P2X_5$, corresponding to the pre-TM2 region and the outer mouth of TM2 in P2X receptor subunits [22], is consistently absent in $hP2X_{5R}$ mRNA from brain and from lymphocytes, despite the high sensitivity of the RT-PCR method used and the high levels of expression in both tissues (Fig. 6). Furthermore, attempts to detect a variant of $hP2X_{5R}$ with a complete TM2 failed in tissues where homologous rat $P2X_5$ has been localized by in situ hybridization [5], like spinal cord and trigeminal sensory ganglia (data not shown).

To assess the anatomical distribution, we measured the relative levels of transcription of the $hP2X_{5R}$ gene in quantitative mRNA dot blot. Hybridization signals from a variety of fetal and adult tissues showed widespread but selective distribution of central and peripheral $hP2X_{5R}$ transcripts (Fig. 6). The two systems primarily involved in the processing of extracellular information, i.e. the central nervous system and the immune system, show the highest levels of $hP2X_{5R}$ expression. We measured a dramatic developmental down-regulation of $hP2X_{5R}$ mRNA in the thymus from the fetal to the adult stage (Fig. 6) that could be related to the massive apoptosis of immature thymocytes occurring during negative selection [24]. $P2X_1$ mRNA has been found to be upregulated during the apoptosis of immature thymocytes [25] so the distribution of $hP2X_5$ argues strongly for an important role of P2X receptors in clonal deletion of immune cells. With only one transmembrane region, the structure of $hP2X_{5R}$ is reminiscent of tyrosine kinase receptors [26]. We speculate that $hP2X_{5R}$ could be activated by the binding of an unidentified extracellular ligand or could be involved in the regulation of channel subunit interactions both in the brain and in the immune system.

The rat $P2X_5$ is the neuronal subunit with the most limited

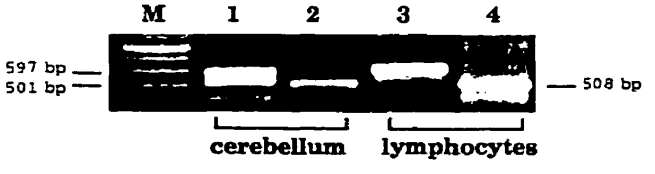

Fig. 5. The $hP2X_{5R}$ transcripts are expressed in two alternatively spliced forms in human brain as detected in RT-PCR amplification (1, primers P1+P2). The full-length form is predominantly found in lymphocytes (3, primers P1+P2). Both $hP2X_{5R}$ mRNA populations from brain (2, primers P3+P4) and lymphocytes (4, primers P3+P4) encode subunits with a single transmembrane domain.

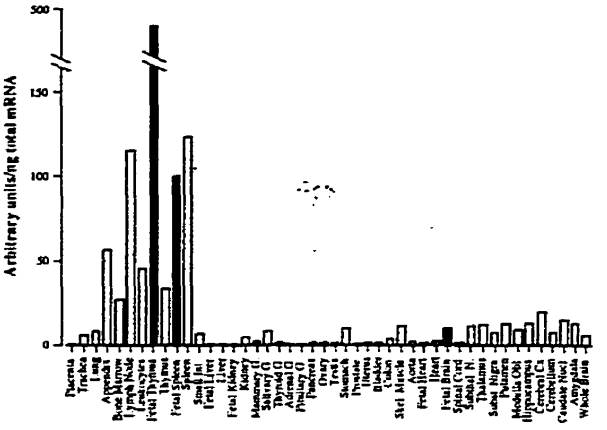

Fig. 6. Relative levels of expression of central and peripheral $hP2X_{5R}$ mRNA in human fetal (shaded bars) and adult tissues using hybridization of a full-length cDNA probe on poly(A)$^+$ RNA blot.

distribution, so one striking difference between rat and human P2X receptor genes is the high expression of $hP2X_{5R}$ in the brain and in peripheral tissues. The developmental regulation of levels of transcription and the tissue specificity observed in mRNA splicing do not seem compatible with the expression of a processed pseudogene [27]. However, it is possible that undetected splicing variants of $hP2X_{5R}$ with two transmembrane domains would form functional human $P2X_5$ channels in homomeric form or assemble in heteromeric complexes in specific cell types. In any case, as has been described in other classes of multimeric integral proteins, i.e. the neurotrophin receptors [28], the steroid receptors [29] and voltage-gated K channels [30], the regulatory effect of a dominant negative truncated $hP2X_{5R}$ subunit on human heteromeric ATP-gated channels remains to be investigated.

Acknowledgements: The authors thank Dr. E. Hamel (Montreal Neurological Institute, McGill University) for the availability of human post-mortem brain tissues, and Dr. G.I. Bell (HHMI-University of Chicago) for sharing unpublished data. Operating support was provided by the Council of Medical Research of Canada, the Heart and Stroke Foundation of Quebec, the Savoy Foundation for Epilepsy and the Astra Research Center in Montreal. K.-T.L. is a fellow of the Savoy Foundation. K.B. is a MRC-PMAC-Astra postdoctoral fellow. P.S. is a junior Scholar of the Fonds de la Recherche en Santé du Québec.

References

[1] Valera, S., Hussy, N., Evans, R.J., Adami, N., North, R.A., Surprenant, A. and Buell, G. (1994) Nature 371, 516–519.
[2] Chen, C., Akopian, A.N., Sivilotti, L., Colquhoun, D., Burnstock, G. and Wood, J.N. (1995) Nature 377, 428–430.
[3] Lewis, C., Neidhart, S., Holy, C., North, R.A., Buell, G. and Surprenant, A. (1995) Nature 377, 432–435.
[4] Brake, A.J., Wagenbach, M.J. and Julius, D. (1994) Nature 371, 519–523.
[5] Collo, G., North, R.A., Kawashima, E., Merlo-Pich, E., Neidhart, S., Surprenant, A. and Buell, G. (1996) J. Neurosci. 16, 2495–2507.
[6] Garcia-Guzman, M., Soto, F., Laube, B. and Stühmer, W. (1996) FEBS Lett. 388, 123–127.
[7] Surprenant, A., Rassendren, F., Kawashima, E., North, R.A. and Buell, G. (1996) Science 272, 735–738.
[8] Buell, G., Lewis, C., Collo, G., North, R.A. and Surprenant, A. (1996) EMBO J. 15, 55–62.

[9] Séguéla, P., Haghighi, A., Soghomonian, J.-J. and Cooper, E. (1996) J. Neurosci. 16, 448–455.
[10] Soto, F., Garcia-Guzman, M., Gomez-Hernandez, J.M., Hollmann, M., Karshin, C. and Stühmer, W. (1996) Proc. Natl. Acad. Sci. USA 93, 3684–3688.
[11] Buell, G., Collo, G. and Rassendren, F. (1996) Eur. J. Neurosci. 8, 2221–2228.
[12] Li, J. and Perl, E.R. (1995) J. Neurosci. 15, 3347–3365.
[13] Bardoni, R., Goldstein, P.A., Lee, C.J., Gu, J.G. and MacDermott, A.B. (1997) J. Neurosci. 17, 5297–5304.
[14] Lê, K.-T., Villeneuve, P., Ramjaun, A., McPherson, P.S., Beaudet, A. and Séguéla, P. (1997) Neuroscience (in press).
[15] Valera, S., Talabot, F., Evans, R.J., Gos, A., Antonarakis, S.E., Morris, M.A. and Buell, G. (1995) Receptors Channels 3, 283–289.
[16] Garcia-Guzman, M., Stühmer, W. and Soto, F. (1997) Mol. Brain Res. 47, 59–66.
[17] Garcia-Guzman, M., Soto, F., Gomez-Hernandez, J.M., Lund, P.-E. and Stühmer, W. (1997) Mol. Pharmacol. 51, 109–118.
[18] Rassendren, F., Buell, G., Virginio, C., Collo, G., North, R.A. and Surprenant, A. (1997) J. Biol. Chem. 272, 5482–5486.
[19] Lennon, G., Auffray, C., Polymeropoulos, M. and Soares, M.B. (1996) Genomics 33, 151–152.
[20] Mukerji, J., Haghighi, A. and Séguéla, P. (1996) J. Neurochem. 66, 1027–1032.
[21] Bertrand, D., Cooper, E., Valera, S., Rungger D. and Ballivet, M. (1991) in: Methods in Neurosciences (Conn, M.P., Ed.), pp. 174–193, Academic Press, New York.
[22] Rassendren, F., Buell, G., Newbolt, A., North, R.A. and Surprenant, A. (1997) EMBO J. 13, 3446–3454.
[23] Werner, P., Seward, E., Buell, G. and North, R.A. (1996) Proc. Natl. Acad. Sci. USA 93, 15485–15490.
[24] King, L.B. and Ashwell, J.D. (1994) Thymus 23, 209–230.
[25] Owens, G.P., Hahn, E.E. and Cohen, J.J. (1991) Mol. Cell. Biol. 11, 4177–4188.
[26] Barbacid, M. (1994) J. Neurobiol. 25, 1386–1403.
[27] Maestre, J., Tchenio, T., Dhellin, O. and Heidmann, T. (1995) EMBO J. 14, 6333–6338.
[28] Altabef, M., Garcia, M., Variorkrishnan, G. and Samarut, J. (1997) Oncogene 14, 1471–1479.
[29] Eide, F.F., Vining, E.R., Eide, B.L., Zang, K., Wang, X.Y. and Reichardt, L.F. (1996) J. Neurosci. 16, 3123–3129.
[30] Jiang, M., Tseng-Crank, J. and Tseng, G.-N. (1997) J. Biol. Chem. 272, 24109–24112.

Journal of Neurochemistry
Lippincott Williams & Wilkins, Philadelphia
© 1999 International Society for Neurochemistry

Molecular Cloning and Regional Distribution of a Human Proton Receptor Subunit with Biphasic Functional Properties

Kazimierz Babinski, Khanh-Tuoc Lê, and Philippe Séguéla

Cell Biology of Excitable Tissue Group, Montreal Neurological Institute, McGill University, Montreal, Quebec, Canada

Abstract: Small changes of extracellular pH activate depolarizing inward currents in most nociceptive neurons. It has been recently proposed that acid sensitivity of sensory as well as central neurons is mediated by a family of proton-gated cation channels structurally related to *Caenorhabditis elegans* degenerins and mammalian epithelial sodium channels. We describe here the molecular cloning of a novel human proton receptor, hASIC3, a 531-amino acid-long subunit homologous to rat DRASIC. Expression of homomeric hASIC3 channels in *Xenopus* oocytes generated biphasic inward currents elicited at pH <5, providing the first functional evidence of a human proton-gated ion channel. Contrary to the DRASIC current phenotype, the fast desensitizing early component and the slow sustained late component differed both by their cationic selectivity and by their response to the antagonist amiloride, but not by their pH sensitivity (pH_{50} = 3.66 vs. 3.82). Using RT-PCR and mRNA blot hybridization, we detected hASIC3 mRNA in sensory ganglia, brain, and many internal tissues including lung and testis, so hASIC3 gene expression was not restricted to peripheral sensory neurons. These functional and anatomical data strongly suggest that hASIC3 plays a major role in persistent proton-induced currents occurring in physiological and pathological conditions of pH changes, likely through a tissue-specific heteropolymerization with other members of the proton-gated channel family. **Key Words:** Proton-gated channel—Degenerin—Amiloride—Trigeminal sensory neurons—Pain—*Xenopus* oocytes.
J. Neurochem. **72,** 51–57 (1999).

Acid sensing is a specific kind of chemoreception that plays a critical role in the detection of nociceptive pH imbalances occurring in conditions of cramps, trauma, inflammation, and hypoxia (Lindahl, 1974). In mammals, a population of small-diameter primary sensory neurons in the dorsal root ganglia and trigeminal ganglia express specialized pH-sensitive surface receptors activated by increase of extracellular proton concentration (Bevan and Yeats, 1991). Native electrophysiological responses of sensory neurons to applications of pH 5.8–6.5 are characterized by a fast desensitizing inward current followed by a slow sustained current (Krishtal and Pidoplichko, 1981). Clarifying the native molecular composition of proton sensors in human sensory neurons will be an important step in the rational development of a novel class of analgesics. A family of genes coding for neuronal proton-gated channels subunits has been discovered recently (Garcia-Anoveros et al., 1997; Waldmann et al., 1997*a,b*). Heterologously expressed amiloride-sensitive homomeric rat acid-sensing ion channel (ASIC) (Waldmann et al., 1997*b*) responds to small pH changes by a fast desensitizing sodium-selective current, whereas mammalian degenerin 1 (MDEG1) (Waldmann et al., 1996) and dorsal root ganglia ASIC (DRASIC) (Waldmann et al., 1997*a*) require drastic pH changes to gate desensitizing and biphasic currents, respectively. ASIC and MDEG1 can associate together to generate a heteromeric channel activated at low pH (<5) with unique kinetics and ionic selectivities (Bassilana et al., 1997). A neuronal splicing variant of MDEG1 was shown to modulate DRASIC biophysical properties by heteromeric association (Lingueglia et al., 1997). These proton-gated channels share a putative two-transmembrane domain topology and colocalization in small-diameter capsaicin-sensitive sensory neurons with P2X ATP-gated channels (North, 1997). From their sequence, they belong to an expanding gene superfamily including mammalian epithelial sodium channels (Canessa et al., 1994*a,b*), pickpocket (PPK) and ripped pocket (RPK) subunits from *Drosophila* (Adams et al., 1998), degenerins of *Caenorhabditis elegans* (Corey and Garcia-Anoveros, 1996), and the FMRFamide-gated channel of *Helix aspersa* (Lingueglia et al., 1995). Despite their potential importance in monitoring pH changes in CNS and sensory pathways, human proton receptor genes have not yet been functionally characterized. We report here for the first time the heterologous expression of a human proton-gated channel, as well as significant interspecies differences observed both in functional properties and in regional distribution of acid sensors.

Received May 22, 1998; revised manuscript received August 3, 1998; accepted August 6, 1998.

Address correspondence and reprint requests to Dr. P. Séguéla at Montreal Neurological Institute, 3801 University, Rm. 778, Montreal, Quebec, Canada H3A 2B4.

Abbreviations used: ASIC, acid-sensing ion channel; DRASIC, dorsal root ganglia ASIC; MDEG1, mammalian degenerin 1.

MATERIALS AND METHODS

Molecular cloning

Using the tblastn algorithm, virtual screening of the dbEST database of NCBI (Lennon et al., 1996) with probes corresponding to the protein motif LXFPAVTLCNXNXXRXS, conserved in all known members of the degenerin/ENaC/ASIC family, led to the identification of human EST sequences encoding a novel member of the proton sensor gene family (GenBank accession nos. AA449579 and AA429417). The clone tagged by 5′ EST AA449579 and by 3′ EST AA449322 from a total fetus cDNA library was sequenced on both strands, using walking primers and an ALF DNA sequencer (Pharmacia-LKB). Full-length hASIC3 was subcloned directionally into unique *Eco*RI and *Not*I sites of eukaryotic vector pcDNA3 (Invitrogen) for cytomegalovirus promoter-driven heterologous expression in *Xenopus* oocytes.

Electrophysiology in *Xenopus* oocytes

Oocytes surgically removed from adult *Xenopus laevis* were treated for 2 h at room temperature with type II collagenase (GibcoBRL) in Barth's solution under constant agitation. Selected oocytes at stage IV–V were defolliculated manually before nuclear microinjections (Bertrand et al., 1991) of 5 ng of hASIC3 in pcDNA3 vector. After 2–4 days of expression at 19°C in Barth's solution containing 50 μg/ml gentamicin, currents were recorded in the two-electrode voltage-clamp configuration, using an OC-725B amplifier (Warner Instruments). Whole-cell currents were acquired and digitized at 500 Hz on a Macintosh IIci computer with an A/D NB-MIO16XL interface (National Instruments), then recorded traces were postfiltered at 100 Hz in an Axograph (Axon Instruments). Agonist, amiloride, and wash solutions were prepared in a modified Ringer's solution containing 115 m*M* NaCl, 2.5 m*M* KCl, and 1.8 m*M* $CaCl_2$ in 5–20 m*M* HEPES (Sigma) buffer adjusted with NaOH or HCl at pH 2–8 and applied on oocytes by constant perfusion (10–12 ml/min) at room temperature. Mean ± SEM values corresponded to measurements from a minimum of five oocytes.

RT-PCR and mRNA dot-blot hybridization

Total RNA from postmortem samples of normal human trigeminal ganglia were isolated by using TriZOL reagent (GibcoBRL), then 1 μg was subjected to random-primed reverse transcription using Superscript (GibcoBRL). Around 100 ng of RT-cDNA was used as template for PCR with Expand DNA polymerase (Boehringer-Mannheim). Specific hASIC3 primers TCAGTGGCCACCTTCCTCTA (forward) and ACAGTCCAGCAGCATGTCATC (reverse) were used to amplify the region corresponding to nucleotides 175–513 (see Fig. 1A). After initial template denaturation for 2 min at 94°C, thermal cycles consisted of 45 s at 94°C, 45 s at 55°C, and 2 min at 72°C for 30 cycles. Molecular identity and homogeneity of PCR products were checked by sizing and specific restriction patterns. Initial sample loading was checked by coamplification of glyceraldehyde-3-phosphate dehydrogenase housekeeping mRNA. RNA samples not subjected to reverse transcription but PCR-amplified in identical conditions provided our negative controls.

Known amounts of human poly(A)$^+$ RNA (89–514 ng), isolated from various fetal and adult normal tissues and normalized for the transcription levels of several housekeeping genes (Clontech), were dot-blotted and probed with the ^{32}P-labeled *Eco*RI–*Xba*I fragment of hASIC3 cDNA at high stringency (final elution at 65°C in 0.3 × saline–sodium citrate buffer for 10 min). After exposure for 16 h, hybridization signals were acquired and quantitated by using a Storm phosphorimager (Molecular Dynamics), and then analyzed in densitometry with ImageQuant software (Molecular Dynamics).

Data analysis

All data are expressed as mean ± SEM values and represent results of experiments done in triplicate on at least three separate oocyte preparations. Statistical methods consisted of two-tailed *t* tests and regression analysis available with the PRISM software package (GraphPad, San Diego, CA, U.S.A.). Nonlinear regression on *I/V* curves used the Boltzman equation, whereas dose–response curves were fitted with the four-parameter logistic equation. Multiple comparison of sigmoidal curves was evaluated by the partial *F* test, using ALLFIT software (De Léan et al., 1978).

RESULTS

Primary structure of hASIC3 channel subunit

Sequence analysis of the 1.7-kb-long hASIC3 poly(A)$^+$ mRNA revealed an open reading frame encoding 531 amino acids (Fig. 1A), with initiation of translation at the proximal Met codon located at nucleotide position 22. The predicted molecular mass of 59 kDa for the immature protein was confirmed by in vitro translation (data not shown). According to the current topological model based on primary structure analysis and biochemical tests, a large domain of 365 amino acids faces the extracellular side of the plasma membrane (Canessa et al., 1994*a*,*b*). In this extracellular domain, a total of 15 cysteine residues are highly conserved in the ASIC family, with the exception of Cys^{267} being absent in human BNaC1 (hASIC2) only. Two potential sites for Asn-linked glycosylation, Asn^{175} and Asn^{398}, are located in this cysteine-rich loop. Consensus sites for phosphorylation by casein kinase II (Ser^{5}) and by protein kinase C (Ser^{39}, Ser^{478}, Ser^{493}, and Ser^{521}) are found in the intracellular N-terminal domain of hASIC3 as well as in the intracellular C-terminal domain (Fig. 1A). The hASIC3 subunit displays 83% of identity with rat DRASIC subunit at the amino acid level, 48% with human BNaC2 (hASIC1) and 47% with BNaC1 (hASIC2) (Fig. 1B). Therefore, hASIC3 belongs to the proton-gated channel family, itself a branch of the degenerin/ENaC/FMRFamide-gated channel phylogenetic tree (Fig. 1C).

Functional and pharmacological properties of homomeric hASIC3 channels

When heterologously expressed in *Xenopus* oocytes, hASIC3 subunits assemble into functional homomeric channels activated by low extracellular pH (Fig. 2A). Rapid changes of extracellular pH (Fig. 2B and C) revealed a biphasic response. This unique phenotype was characterized by a fast and rapidly desensitizing current followed by a slow and sustained current that returned to baseline only on return to physiological pH. The relative amplitude of the fast current appeared dependent on the slope of the pH gradient applied (Fig. 2A and C). However, we found the pH sensitivity of the two hASIC3-mediated currents to be almost identical with a pH_{50} of

A

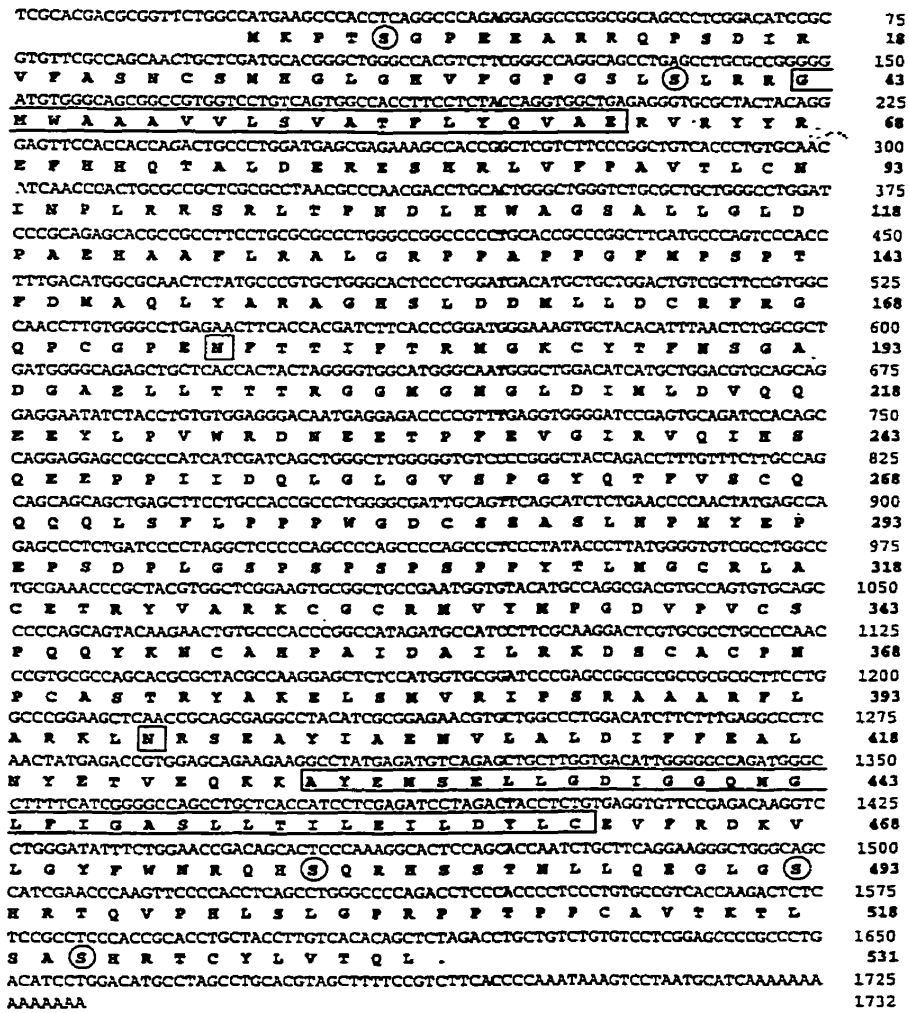

B

	hASIC2	hASIC1	α	β	γ	δ	
hASIC3	47.9	46.6	17.3	15.4	16.6	14.9	hASIC3
hASIC2		64.5	15.2	17.2	16.4	15.0	hASIC2
hASIC1			13.1	17.0	16.9	15.0	hASIC1
α				26.7	29.1	33.4	α
β					31.4	22.6	β
γ						21.8	γ

C

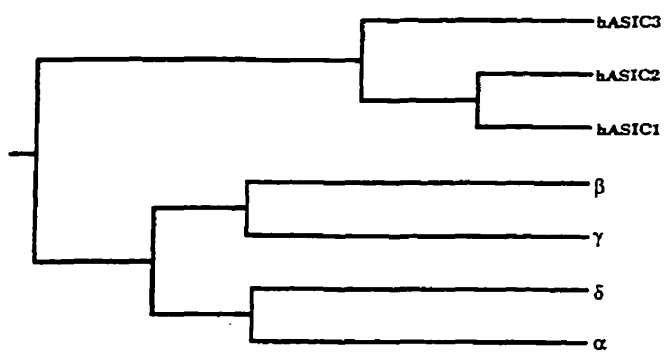

FIG. 1. Nucleotide and predicted amino acid sequence of hASIC3 cDNA (**A**), deposited in GenBank database under the accession no. AF057711. Two stretches of 20–34 amino acids corresponding to potential transmembrane domains, identified in Kyte–Doolittle hydrophobicity plot, are highlighted. Consensus phosphorylation sites in intracellular domains and *N*-glycosylation sites in extracellular domain are indicated by circled and boxed residues, respectively. Homology (%) of hASIC3 (**B**) and phylogenetic relationships (**C**) with known members of the human ASIC/ENaC family. The protein dendrogram was generated by using UPGMA algorithm (Geneworks 2.5.1, Oxford Molecular Group).

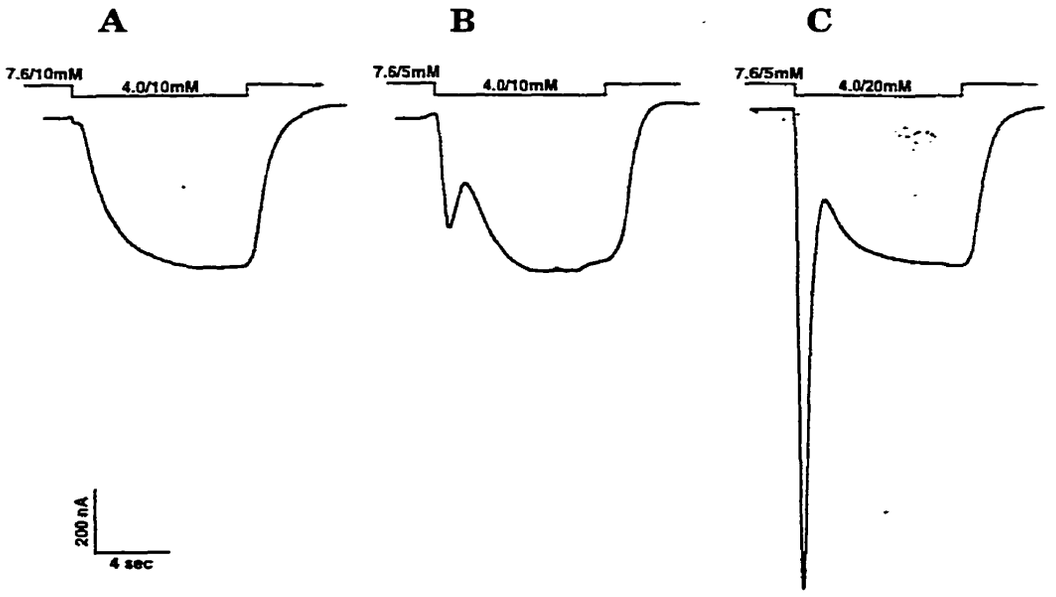

FIG. 2. Biphasic current phenotype of homomeric hASIC3 channels; effects of increasing rates of pH change. Oocytes were clamped at −70 mV and continuously perfused with Ringer's buffer containing 10 m*M* HEPES at pH 7.6. pH was then dropped to 4.0 for 10 s with increasing pH gradients obtained by raising the buffer capacity differential between control and test buffers: **A:** pH 7.6–4.0 in 10 m*M* HEPES. **B:** pH 7.6 in 5 m*M* to pH 4.0 in 10 m*M* HEPES. **C:** pH 7.6 in 5 m*M* to pH 4.0 in 20 m*M* HEPES. Controls done with the test buffers at pH 7.6 did not activate the hASIC3 channel. Oocytes injected with injection buffer alone showed no inward currents. The amplitude of the early but not the late component, and thus the ratio of early to late peak currents, appears to be very sensitive to the speed at which the pH drops from normal to acid pH values.

3.66 ± 0.06 (fast) vs. 3.82 ± 0.04 (slow) (Fig. 3). The positive cooperativity reflected in the dose–response curve profile, n_{Hfast} = 1.57 ± 0.3 and n_{Hslow} = 1.55 ± 0.17, indicated that at least two protonations on two subunits are required to gate the cation channel. To study possible differences of ionic selectivity between fast and slow components, we performed a current–voltage relationship at pH 4.0 in normal Ringer. The peak amplitude of the fast component displayed some voltage dependence from its slight inward rectification, whereas the slow and sustained component was ohmic in the range from −70 to + 70 mV (Fig. 4B). Furthermore, although both reversal potentials were greater than 30 mV as expected for channels conducting mainly sodium, we measured a ΔE_{rev} = +15 ± 3.2 mV ($p < 0.01$) between the fast (+32.9 ± 4.4 mV) and the slow component (+48.2 ± 4.8 mV) (Fig. 4A and B). These two phases of proton-induced hASIC3 current differed also by their sensitivity to the antagonist amiloride. Coapplication of 100 μ*M* amiloride with pH 4.0 under conditions of biphasic response demonstrated a more efficient blockade of the fast (62.8 ± 6.5%) than of the slow current (28.7 ± 4.6%) by amiloride (Fig. 5A and B).

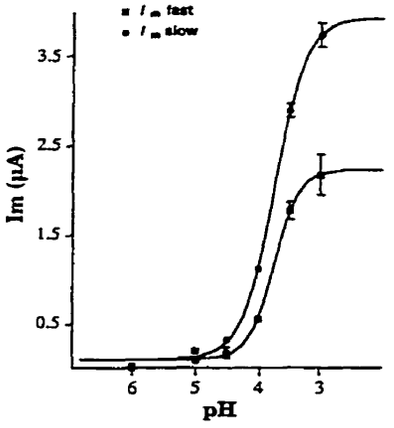

FIG. 3. Dose–response curves of pH activation of hASIC3 currents. Dose–response curves were constructed in 20 m*M* HEPES buffered at different pH values from 6.0 to 3.0. Peak currents of fast and slow currents were analyzed with the four-parameter logistic equation and the partial *F* test for statistical comparison. Each point represents mean ± SEM from this typical experiment. Apart from the maximal response, no other significant difference was observed between both curves.

Central and peripheral distribution of hASIC3 gene expression

As a rough index of anatomical distribution and mRNA abundance, we noticed several cDNAs encoding hASIC3 in total fetus and testis cDNA libraries represented in the dbEST database. Results obtained in RNA hybridization at high stringency confirmed that the hASIC3 gene is transcribed in a wide spectrum of internal organs as well as in the CNS (Fig. 6). In the adult stage, hASIC3 transcripts were detected in lung, lymph nodes, kidney, pituitary, heart, and testis as well as in brain and spinal cord. A developmental up-regulation of hASIC3 gene expression was apparent when comparing fetal vs. adult mRNA levels in lung and kidney (Fig. 6).

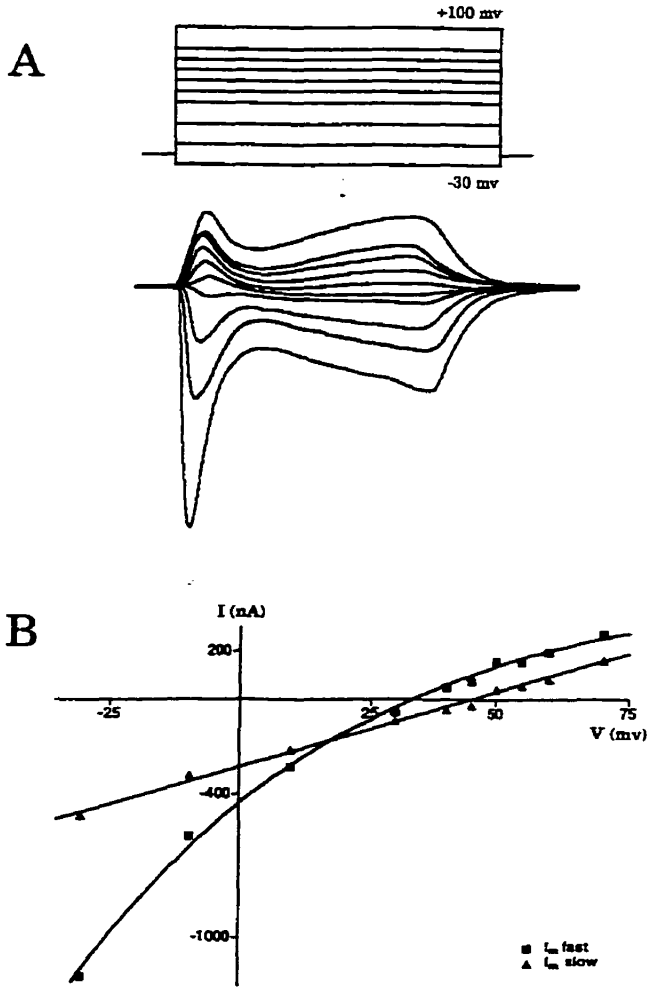

FIG. 4. Current–voltage (*I/V*) relationship of the fast and slow hASIC3 currents. Recordings were done in Ringer's buffer containing (m*M*) NaCl 115, KCl 2.5, $CaCl_2$ 1.8, and HEPES 5, pH 7.6. The *I/V* relationship was established by measuring peak currents of both fast and slow responses to pH 4.0 (applied 1 s after voltage step) at different membrane potentials, after subtracting background currents recorded without pH applications (**A**). Peak current values were plotted (**B**) and reversal potential estimated from linear (slow current) and nonlinear (fast current) regression analysis. A and B represent a typical experiment where reversal potentials were 33.4 and 44.8 mV, respectively, for the fast and slow currents.

Thus, hASIC3 subunit expression is not restricted exclusively to sensory ganglia as is its rat homologue DRASIC, explaining our decision to use a chronological nomenclature that is distribution independent. The potentially important function of noninactivating proton-gated channels in nociceptive sensory neurons was nevertheless confirmed by the detection of high levels of ASIC3 mRNA in adult human trigeminal ganglia, using RT-PCR (Fig. 7).

DISCUSSION

We report in the present study the characterization of a novel central member of the human degenerin/ENaC channel family, genetically identical to hTNaC isolated from human testis (Ishibashi and Marumo, 1998). Significant homologies found both in extracellular and in transmembrane domains of the predicted hASIC3 subunit with known proton-gated channels were substantiated by our electrophysiological data showing activation of the homomeric channel by changes of extracellular pH. In contrast to rat ASIC, which responds to slight external acidification, a drastic pH decrease (pH_{50} ~4) was required to activate hASIC3 channels when heterologously expressed in *Xenopus* oocytes.

Despite a strong conservation of primary structure, the hASIC3 channel displayed several interesting differences of properties with its rodent homologue DRASIC. Two potential regulatory protein kinase C sites found in hASIC3 sequence are conserved in DRASIC (Ser^{39} and Ser^{521}), so the functional impact of phosphorylation of these domains will be worth investigating in the context of heterologous sensitization of nociceptive response by

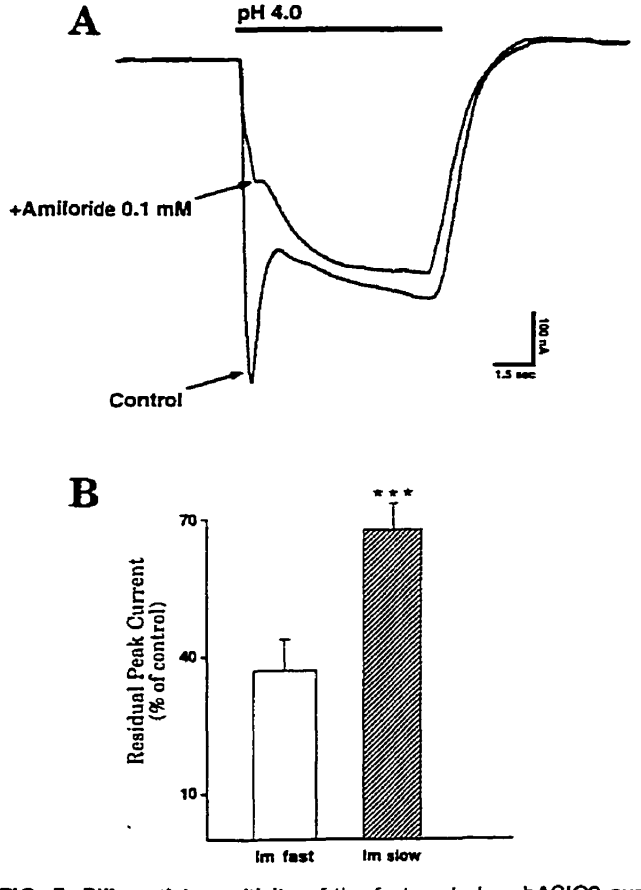

FIG. 5. Differential sensitivity of the fast and slow hASIC3 currents to amiloride. hASIC3 currents were activated by pH 4.0 in the presence and absence of 100 μM amiloride (**A**). Inhibition by amiloride was much stronger on the fast than the sustained current. **B:** Data are mean ± SEM values (n = 17) of residual peak currents during amiloride application for the fast (37.2 ± 6.4%) and sustained (72.0 ± 3.8%) components expressed as percentages of controls. Statistical significance was evaluated by unpaired two-tailed *t* test (***$p < 0.001$).

= 1.32) (Konnerth et al., 1987; Bevan and Yeats, 1991); (2) if most capsaicin-sensitive sensory neurons display biphasic pH responses, some display either the fast or the slow component (Krishtal and Pidoplichko, 1981; Bevan and Yeats, 1991); and (3) the two phases appear to be differentially regulated by nerve growth factor in primary cultured sensory neurons (Bevan and Winter, 1995). The ionic selectivity favoring sodium over potassium ions and the low sensitivity to pH of hASIC3 suggest that it is associated with other ASICs or non-ASIC partners in sensory neurons to generate a native heteromeric channel with emergent phenotype not predicted from the properties of each individual component. Indeed, Lingueglia and colleagues (1997) reported that DRASIC could associate with silent MDEG2, a splicing variant of MDEG, to produce a proton sensor poorly sensitive to pH but endowed with a weak cation selectivity closer to the properties of the native current. Alternatively, it is also possible that posttranslational modifications of proton sensor subtypes composed of known subunits could explain the nonselective and sustained ionotropic responses elicited by small pH changes in mammalian sensory neurons.

Acknowledgment: We thank Dr. E. Hamel (Montreal Neurological Institute, McGill University) for the availability of postmortem human trigeminal ganglia. We also gratefully acknowledge the Astra Research Center in Montreal, the Medical Research Council of Canada (MRC), the Savoy Foundation for Epilepsy (SFE), the T2C2 Group, as well as the Fondation des Maladies du Coeur du Québec for their operating support. K.B. is an MRC-Astra postdoctoral Fellow, K.-T.L. holds a PhD studentship from the SFE, and P.S. is a junior Scholar from the Fonds de la Recherche en Santé du Québec.

REFERENCES

Adams C. M., Anderson M. G., Motto D. G., Price M. P., Johnson W. A., and Welsh M. J. (1998) Ripped pocket and pickpocket, novel *Drosophila* DEG/ENaC subunits expressed in early development and in mechanosensory neurons. *J. Cell Biol.* **140,** 143–152.

Bassilana F., Champigny G., Waldmann R., de Weille J. R., Heurteaux C., and Lazdunski M. (1997) The acid-sensitive ionic channel subunit ASIC and the mammalian degenerin MDEG form a heteromultimeric H^+-gated Na^+ channel with novel properties. *J. Biol. Chem.* **272,** 28819–28822.

Bertrand D., Cooper E., Valera S., Rungger D., and Ballivet M. (1991) Electrophysiology of neuronal nicotinic acetylcholine receptors expressed in *Xenopus* oocytes following nuclear injection of genes or cDNAs, in *Methods in Neurosciences* (Conn M. P., ed), pp. 174–193. Academic Press, San Diego.

Bevan S. and Winter J. (1995) Nerve growth factor (NGF) differentially regulates the chemosensitivity of adult rat cultured sensory neurons. *J. Neurosci.* **15,** 4918–4926.

Bevan S. and Yeats J. (1991) Protons activate a cation conductance in a subpopulation of rat dorsal root ganglion neurones. *J. Physiol. (Lond.)* **433,** 145–161.

Canessa C. M., Merillat A. M., and Rossier B. C. (1994*a*) Membrane topology of the epithelial sodium channel in intact cells. *Am. J. Physiol.* **267,** C1682–C1690.

Canessa C. M., Schild L., Buell G., Thorens B., Gautschi I., Horisberger J.-D., and Rossier B. C. (1994*b*) Amiloride-sensitive epithelial Na^+ channel is made of three homologous subunits. *Nature* **367,** 463–467.

Corey D. P. and Garcia-Anoveros J. (1996) Mechanosensation and the DEG/ENaC ion channels. *Science* **273,** 323–324.

Coscoy S., Lingueglia E., Lazdunski M., and Barbry P. (1998) The Phe-Met-Arg-Phe-amide-activated sodium channel is a tetramer. *J. Biol. Chem.* **273,** 8317–8322.

De Léan A., Munson P. J., and Rodbard D. (1978) Simultaneous analysis of families of sigmoidal curves: application to bioassay, radioligand assay, and physiological dose-response curves. *Am. J. Physiol.* **235,** E97–E102.

Dray A. and Perkins M. (1993) Bradykinin and inflammatory pain. *Trends Neurosci.* **16,** 99–104.

Firsov D., Gautschi I., Merillat A.-M., Rossier B. C., and Schild L. (1998) The heterotetrameric architecture of the epithelial sodium channel (ENaC). *EMBO J.* **17,** 344–352.

Garcia-Anoveros J., Derfler B., Neville-Golden J., Hyman B. T., and Corey D. P. (1997) BNaCl and BNaC2 constitute a new family of human neuronal sodium channels related to degenerins and epithelial sodium channels. *Proc. Natl. Acad. Sci. USA* **94,** 1459–1464.

Ishibashi K. and Marumo F. (1998) Molecular cloning of a DEG/ENaC sodium channel from human testis. *Biochem. Biophys. Res. Commun.* **245,** 589–593.

Kleyman T. R. and Cragoe E. J. (1988) Amiloride and its analogs as tools in the study of ion transport. *J. Membr. Biol.* **105,** 1–21.

Konnerth A., Lux H. D., and Morad M. (1987) Proton-induced transformation of calcium channel in chick dorsal root ganglion cells. *J. Physiol. (Lond.)* **386,** 603–633.

Krishtal O. A. and Pidoplichko V. I. (1981) A receptor for protons in the membrane of sensory neurons may participate in nociception. *Neuroscience* **6,** 2599–2601.

Krishtal O. A., Osipchuk Y. V., Shelest T. N., and Smirnoff S. V. (1987) Rapid extracellular pH transients related to synaptic transmission in rat hippocampal slices. *Brain Res.* **436,** 352–356.

Lennon G., Auffray C., Polymeropoulos M., and Soares M. B. (1996) The I.M.A.G.E. consortium: an integrated molecular analysis of genomes and their expression. *Genomics* **33,** 151–152.

Lindahl O. (1974) Pain—a general chemical explanation. *Adv. Neurol.* **4,** 45–47.

Lingueglia E., Champigny G., Lazdunski M., and Barbry P. (1995) Cloning of the amiloride-sensitive FMRFamide peptide-gated sodium channel. *Nature* **378,** 730–733.

Lingueglia E., de Weille J. R., Bassilana F., Heurteaux C., Sakai H., Waldmann R., and Lazdunski M. (1997) A modulatory subunit of acid sensing ion channels in brain and dorsal root ganglion cells. *J. Biol. Chem.* **272,** 29778–29783.

North R. A. (1997) Families of ion channels with two hydrophobic segments. *Curr. Opin. Cell Biol.* **8,** 474–483.

Price M. P., Snyder P. M., and Welsh M. J. (1996) Cloning and expression of a novel human brain Na^+ channel. *J. Biol. Chem.* **271,** 7879–7882.

Snyder P. M., Cheng C., Prince L. S., Rogers J. C., and Welsh M. J. (1998) Electrophysiological and biochemical evidence that DEG/ENaC cation channels are composed of nine subunits. *J. Biol. Chem.* **273,** 681–684.

Tavernarakis N., Shreffler W., Wang S., and Driscoll M. (1997) *unc-8*, a DEG/ENaC family member, encodes a subunit of a candidate mechanically gated channel that modulates *C. elegans* locomotion. *Neuron* **18,** 107–119.

Waldmann R., Champigny G., Voilley N., Lauritzen I., and Lazdunski M. (1996) The mammalian degenerin MDEG, an amiloride-sensitive cation channel activated by mutations causing neurodegeneration in *Caenorhabditis elegans*. *J. Biol. Chem.* **271,** 10433–10436.

Waldmann R., Bassilana F., de Weille J., Champigny G., Heurteaux C., and Lazdunski M. (1997*a*) Molecular cloning of a non-inactivating proton-gated Na^+ channel specific for sensory neurons. *J. Biol. Chem.* **272,** 20975–20978.

Waldmann R., Champigny G., Bassilana F., Heurteaux C., and Lazdunski M. (1997*b*) A proton-gated cation channel involved in acid-sensing. *Nature* **386,** 173–177.